UNIWERSYTET JAGIELLOŃSKI
W KRAKOWIE

Instytut Nauk Geologicznych

Analiza sedymentologiczna wybranych utworów formacji ropianieckiej (górna kreda – paleocen) jednostki skolskiej

Piotr Łapcik

Rozprawa doktorska
wykonana pod opieką
prof. dr hab. Alfreda Uchmana
w Zakładzie Geodynamiki i Geologii Środowiskowej

Kraków 2018

Spis treści

Podziękowania

Serdecznie dziękuję mojemu promotorowi prof. dr hab. A. Uchmanowi za wieloletnie wsparcie, poświęcony czas oraz pomoc, którą okazał w przeciągu całości trwania moich studiów doktoranckich. Jego liczne pomysły, uwagi oraz spostrzeżenia pozwoliły nakreślić tematykę badań oraz zachować swobodę w trakcie realizowania pracy badawczej.

Chciałbym wyrazić wdzięczność dla Instytutu Nauk Geologicznych, Uniwersytetu Jagiellońskiego za sfinansowanie moich badań oraz za przyjazne i komfortowe warunki pracy.

Chcę złożyć ogromne podziękowania dla mojej rodziny i bliskich, którzy wspierali mnie przez wszystkie lata studiów doktoranckich. Szczególne podziękowania pragnę złożyć moim rodzicom Janowi i Reginie oraz mojej siostrze Ilonie. Bez nich nie udało by mi się rozpocząć wspaniałej przygody z geologią.

Pragnę złożyć podziękowania wszystkich osobom które miały wkład w niniejszą rozprawę doktorską, a których ze względu na ich ilość nie sposób wymienić z imienia i nazwiska.

Piotr Łapcik

Streszczenie

Niniejsza rozprawa doktorska dotyczy detalicznej analizy sedymentologicznej oraz facjalnej wybranych profili utworów górnokredowo-paleoceńskiej formacji z Ropianki (płaszczowina skolska, Karpaty). Badania objęły dwie sukcesje osadowe usytuowane w bardziej zewnętrznej części płaszczowiny skolskiej, pierwotnie w bardziej proksymalnej części systemu depozycyjnego (Łapcik, 2018, w druku) oraz jedną usytuowaną bliżej osi basenu (Łapcik, 2017). Głównym celem prezentowanego zbioru publikacji jest detaliczna charakterystyka pionowej sukcesji głębokomorskich facji osadowych w badanych profilach wraz z ich interpretacją subśrodowisk ich systemu depozycyjnego. Wraz z interpretacją mechanizmów depozycji przeprowadzano interpretację rozwoju środowiska depozycji w kontekście stratygrafii dynamicznej dla dwóch badanych sukcesji (Łapcik, 2017, w druku). Ponadto, zgromadzone dane zostały opracowane statystycznie a dla najbardziej miąższej, ponad 400 m sukcesji Huciska Jawornickiego, została wykonana analiza modalnych przejść facji metodą włożonych łańcuchów Markova (Łapcik, w druku).

Otrzymane wyniki wskazują na dużą różnorodność głębokomorskich facji osadowych w poszczególnych profilach. Analiza sedymentologiczna wielu litologicznie podobnych utworów wskazuje na zróżnicowane mechanizmy depozycji. Oprócz pospolitych utworów prądów zawiesinowych o wysokiej i niskiej gęstości, kohezyjnych i niekohezyjnych spływów rumoszu oraz utworów hemipelagicznych i pelagicznych wykazano obecność utworów sugerujących genezę z prądów hybrydowych (tzw. „slurry flows" *sensu* Lowe i Guy, 2000), prądów hiperpiknalnych oraz trakcyjnych (np. prądów konturowych lub głębokomorskich prądów pływowych). W badanych sukcesjach osadowych po raz pierwszy wyróżniono asocjacje facjalne zinterpretowane jako osady gromadzone w elementach architektury dna basenu, takich jak głębokomorskie kanały, loby depozycyjne, czy wały przykorytowe, a także jako osady równi basenowej, osady międzylobowe, osady glifów krewasowych oraz osady skłonu basenu.

Opisane zmiany facjalne różnej rangi świadczą o dynamice środowiska depozycji. W badanych sukcesjach zaobserwowane zmiany sięgają od lokalnej lateralnej migracji i agradacji wybranych elementów architektury dna po progradację i retrogradację całego systemu depozycyjnego. Nie jest wykluczone, że pionowe zmiany facjalne wyższego rzędu są powiązane z niektórymi zmianami eustatycznymi jakie miały miejsce w kampanie–paleocenie. Mimo to, depozycja kontrolowana tektoniczne wydaje się być dominującym czynnikiem w basenie fliszowym. Oszacowano, że dystans między bardziej dystalnym środowiskiem nieskanalizowanych lobów depozycyjnych w okolicy Słonnego (Łapcik, 2017) a relatywnie proksymalnymi kanałami i lobami w Hucisku Jawornickim i Manasterzu (Łapcik, 2018) wynosił pierwotnie ~25–35 km. Sukcesja Huciska Jawornickiego posiada najpełniejszy zapis sedymentacji na obszarze przejściowym dla migrujących stref depozycji z opisanymi elementami architektury dna basenu.

Silikoklastyczne źródło materiału zawierające sporą ilość detrytusu roślinnego jest prawdopodobnie powiązane ze środowiskiem deltowym lub paralicznym. By dostarczyć odpowiednio dużą ilość materiału piaszczystego do uformowania wyróżnionych kanałów i lobów depozycyjnych, źródło powinny stanowić delty usytuowane przy krawędzi skłonu

basenu. Margliste osady występujące z różną częstotliwością pochodzą z okresowo funkcjonującego węglanowego źródła, prawdopodobnie usytuowanego na szelfie. Źródło węglanowe musiało współwystępować w bliskim sąsiedztwie źródła klastycznego, co jest dodatkowo podkreślone obecnością detrytusu roślinnego w marglach.

Dotychczas panował pogląd o dystrybucji materiału równoległe do osi basenu skolskiego (Książkiewicz, 1962; Bromowicz, 1974; Kotlarczyk, 1978). Proponowaną alternatywą wynikającą z prezentowanych danych jest uformowanie się piaszczystego pasa wzdłuż osi wąskiego basenu poprzez scalenie fartuchów lub stożków rozłożonych wzdłuż skłonu, w fazie ich maksymalnej ekspansji. Jednocześnie opisywane ciała osadowe mogły być częściowo rotowane podążając za zwiększającą się lokalnie przestrzenią akomodacyjną oraz progradując zgodnie z nachyleniem osi basenu.

Summary

This doctoral dissertation concerns a detailed sedimentological and facies analysis of the selected sections of the Upper Cretaceous–Paleocene Ropianka Formation (Skole Nappe, Carpathians). The study area includes two sedimentary successions located in the more external part of the Skole Nappe, which refers to primarily more proximal part of the depositional system (Łapcik, 2018, in press), and one located closer to its basin axis (Łapcik, 2017). The main purpose of the presented collection of publications is the detailed characterization of the vertical succession of deep-water sedimentary facies in the studied sections along with their interpretive attribution to the specific sub-environments of the depositional system. An interpretation of depositional environment development in the context of dynamic stratigraphy was carried out for the two sedimentary successions (Łapcik, 2017, in press). In addition, the collected data were elaborated statistically and for the thickest, the over 400 m-thick Hucisko Jawornickie succession, the analysis of facies transition trend by means of the embedded Markov chain method (Łapcik, in press) was conducted.

The results obtained show a wide variety of deep-water sedimentary facies in the individual sections. A more detailed sedimentological analysis of numerous lithologically similar deposits implies various mechanisms of deposition. In addition to abundant deposits of high- and low-density turbidity currents, cohesive and non-cohesive debris flow, hemipelagites and pelagites, deposits suggesting genesis from hybrid currents (so-called 'slurry flows' *sensu* Lowe & Guy, 2000) are present, as well as deposits of hyperpycnal and traction currents (e.g., contour currents or deep-sea tidal currents). In the studied sedimentary successions, the facies associations which deposits accumulated in architectural elements, such as distributary channels, depositional lobes, channel levees, and as basin plain deposits, interlobe deposits, crevasse splays, and slope deposits, were distinguished for the first time.

The described facial changes of various magnitudes testify to the dynamics of depositional environment. In the studied successions, the observed changes range from local lateral migration and aggradation of architectural elements to the progradation and retrogradation of the entire depositional system. Eustatic influences are likely, but difficult to ascertain with poor biostratigraphic data. It was estimated that the distance between the more distant environment of the unchannelized depositional lobes in the Słonne area (Łapcik, 2017) and the relatively proximal channels and lobes at Hucisko Jawornickie and Manasterz (Łapcik, 2018) was originally ~25-35 km. The Hucisko Jawornickie succession displays the most complete record of sedimentation in the transitional area for migrating zones of deposition referred to the described architectural elements.

A siliciclastic source containing a high contribution of plant detritus is probably related to some deltas or paralic environments. To provide sufficient amount of sandy material to formation of the distinguished channels and depositional lobes, the source should be referred to deltas located along the margin of the basin slope. Marly deposits occurring at different frequencies come from a periodically active carbonate source, probably located on the shelf. The carbonate source have had to coexist in close proximity to the clastic one; this is emphasized by the presence of plant detritus in the marlstone.

Until now, the view on the distribution of sedimentary material distribution parallel to the axis of the Skole Basin prevailed (Książkiewicz, 1962, Bromowicz, 1974, Kotlarczyk, 1978). The proposed alternative resulting from the presented data is the formation of a sandy belt along the axis of the narrow basin by merging of aprons or fans which spread along the slope in the phase of their maximum expansion. At the same time, the described sedimentary bodies could be partially rotated in response to increase in local accommodation space and to progradation, according to the inclination of the basin axis.

Spis publikacji stanowiących spójny tematycznie zbiór

1. Łapcik, P., 2017. Facies heterogeneity of a deep-sea depositional lobe complex: case study from the Słonne section of Skole Nappe, Polish Outer Carpathians. *Annales Societatis Geologorum Poloniae*, 87: 301–324. [Opublikowana].

2. Łapcik, P., 2018. Sedimentary processes and architecture of Upper Cretaceous deep-sea channel deposits: a case from the Skole Nappe, Polish Outer Carpathians. *Geologica Carpathica*, 69: 71–88. [Opublikowana].

3. Łapcik, P., (in press). Facies anatomy of a progradational submarine channelized lobe complex: semi-quantitative analysis of the Ropianka Formation (Campanian–Paleocene) in Hucisko Jawornickie section, Skole Nappe, Polish Carpathians. *Acta Geologica Polonica.* [W druku]. DOI: 10.1515/agp-2018-0026

1. Wprowadzenie

Polskie Karpaty fliszowe są obiektem badań geologicznych od XIX w. na terenach dawnej Galicji. Z biegiem czasu głównym ośrodkiem badań nad polskimi Karpatami stał się Kraków, gdzie narodziła się polska szkoła geologiczna, której tradycja badań jest kontynuowana do dziś. Do połowy XX w. badania te skupiały się na zagadnieniach tektonicznych, stratygraficznych, paleontologicznych, surowcowych (ze szczególnym uwzględnieniem złóż ropy naftowej) oraz na kartowaniu geologicznym. Znacznie mniej uwagi poświęcano sedymentologicznemu aspektowi utworów karpackich i aż do końca lat 40-tych wiedza na temat mechanizmów oraz środowiska depozycji utworów karpackich była bardzo ograniczona.

Dzięki pionierskim pracom oraz innowacyjnemu podejściu prof. M. Książkiewicza oraz jego uczniów z tzw. krakowskiej szkoły sedymentologicznej (m.in. S. Dżułyńskiego, K. Birkenmajera, A. Radomskiego, L. Koszarskiego, K. Żytki, A. Ślączki, R. Unruga), sposób postrzegania Karpat uległ całkowitej zmianie. Książkiewicz jako pierwszy zasugerował depozycję karpackich utworów fliszowych w warunkach głębokomorskich, uwzględniając przy tym osuwiska podmorskie oraz redepozycję skamieniałości z płytszych stref. Badania geologów krakowskiej szkoły sedymentologicznej nad utworami karpackimi stanowią kolebkę dla zrozumienia mechanizmów depozycji w głębokomorskim środowisku. Dzięki dostarczeniu obszernych ilości danych terenowych ustanowili oni podwaliny pod powszechnie stosowaną dzisiaj koncepcję prądów zawiesinowych (Książkiewicz, 1948; Kuenen i Migliorini, 1950). Co więcej, w karpackim fliszu opisano piaskowce zlepieńcowate, których nie dało się wytłumaczyć modelem formowania się typowych turbidytów. Powstała w ten sposób idea fluksoturbidytów (Dżułyński et al., 1959; Unrug, 1963; Leszczyński, 1981, 1986, 1989), która z czasem ustąpiła modelowi prądów zawiesinowych o wysokiej gęstości, zaprezentowanemu przez Lowe'a (1982). W Karpatach prowadzono również pionierskie badania sedymentologiczne na temat podmorskich spływów mułowych (Bukowy, 1957a). Równie ważnym elementem są badania S. Dżułyńskiego na polu sedymentologii eksperymentalnej i struktur sedymentacyjnych, głównie hieroglifów oraz struktur deformacyjnych. Prace Dżułyńskiego pozwoliły wnieść badania sedymentologiczne na nowy poziom i rozsławić krakowską szkołę sedymentologiczną (np. Dżułyński i Kotlarczyk, 1962; Dżułyński i Sanders, 1962; Dżułyński i Walton, 1965). W polskich Karpatach powstał pierwszy atlas przedstawiający szeroko zakrojone pomiary kierunków paleotransportu, rozmieszczenie i architekturę facji oraz analizę paleogeografii i pochodzenia materiału egzotycznego (Książkiewicz, 1962) oraz późniejsza pionierska analiza batymetryczna basenów karpackich (Książkiewicz, 1975). Dodatkowo, nie sposób nie wspomnieć o dokonaniach na polu analizy skamieniałości śladowych (Książkiewicz, 1977) czy o ustanowieniu modelu tektonicznego polskich Karpat (Książkiewicz, 1972), który w dużej mierze pozostaje aktualny aż do dzisiaj. Tak szeroko zakrojone badania pozwoliły na rozpowszechnienie opracowanej metodologii badań oraz myśli naukowej poza granice Polski oraz owocną współpracę międzynarodową.

W późniejszych latach wykonano liczne wiercenia na terenie Polski, wnoszące wiele istotnych informacji na temat budowy Karpat. Prowadzono prace opisujące facje sedymentacyjne oraz interpretowano je w kontekście ciągle poznawanych mechanizmów depozycji. Mimo to, słaby stan odsłonięć oraz często ich niewielka skala, połączone z silnymi deformacjami tektonicznymi znacząco utrudniły dokładniejsze rozpoznanie środowiska depozycji oraz architektury subbasenów karpackich. W międzyczasie bardzo silnie rozwinęły się badania nad facjami oraz architekturą kopalnych jak i współczesnych basenów głębokomorskich na całym świecie (np. Mutti i Normark, 1987). Badania te wykazały dużą różnorodność facji osadowych oraz modeli sedymentacji głębokomorskiej, dając podstawy do nowego spojrzenia na Karpaty. Pomimo opracowania wielu modeli głębokomorskiej sedymentacji (np. Normark 1970, 1978, 1987; Mutti i Ricci Lucchi, 1972; Walker, 1978; Pickering et al., 1986; 1989; Mutti i Normark, 1987; Shanmugam i Moiola, 1991; Ghibaudo, 1992; Stow i Mayall, 2000) część formacji nie daje się nimi opisać, gdyż wykazują one unikatową architekturę oraz zespoły facjalne. W związku z tym konieczne wydaje się indywidualne podejście do każdej badanej sukcesji osadowej. Także w odniesieniu do Karpat powstały prace wyróżniające poszczególne elementy środowiska depozycji (tzw. elementy architektury basenu) w wybranych częściach głównych jednostek tektonicznych polskich Karpat (np. Unrug, 1963; Leszczyński, 1981; Słomka, 1986, 1995; Bromowicz i Górniak, 1988; Kotlarczyk i Leśniak, 1990; Bilan, 2001; Słomka i Słomka, 2001; Leszczyński i Malata, 2002; Stadnik, 2007, 2009a, b; Warchoł, 2007; Leszczyński et. al., 2012; Kędzierski i Leszczyński, 2013; Strzeboński, 2015; Siemińska et al., 2018) jak i prace poza granicami Polski (np. Janočko, 2001; Janočko i Jacko, 2001; Teťák, 2008, 2010; Prekopová i Janočko, 2009; Stanová et al., 2009 Dirnerová et al., 2012; Dirnerová i Janočko, 2014). Mimo tego, wiedza na temat rozkładu asocjacji facjalnych składających się na wybrane elementy architektury dna w subbasenach karpackich pozostaje mocno ograniczona. W kontekście podobnych badań istotna jest pół-ilościowa charakterystyka facji i zespołów facjalnych często podparta metodami statystycznymi. Dają one podstawę do szerszych interpretacji historii sedymentacji i ewolucji basenów jak i podstawę do analizy porównawczej z innymi systemami depozycyjnymi. Tego typu badania są przedmiotem niniejszej rozprawy doktorskiej.

Spośród głównych jednostek tektonicznych polskich Karpat, płaszczowina skolska stanowi najbardziej zewnętrzną część wysuniętą ku północy. Zawiera ona mezozoiczne i kenozoiczne utwory rozpoczynające się hoterywskimi mułowcami z Bełwina, które stopniowo przechodzą w łupki spaskie o wieku od późnego hoterywu do wczesnego cenomanu (Gucik, 1963). W obrębie łupków spaskich wyróżniono piaskowce z Kuźminy które zostały nawiercone w najgłębszym karpackim otworze Kuźmina-1 (Żytko, 1989). Powyżej znajduje się cenomańska formacja łupków radiolariowych z Dołhego, której facjalne odpowiedniki są obecne we wszystkich płaszczowinach polskich Karpat (formacja z Barnasiówki; Bąk et al., 2001). Wraz z początkiem turonu rozpoczyna się sedymentacja fliszowa formacji z Ropianki, gdzie utwory margliste występujące w dolnych częściach ogniw z Cisowej, Wiaru oraz Leszczyn, stopniowo przechodzą w sedymentację silikoklastyczną (Kotlarczyk, 1978). Epizod sedymentacji formacji z Ropianki kończy się w paleocenie ogniwem z Woli Korzenieckiej (Kotlarczyk, 1978). Powyżej formacji z Ropianki znajduje się paleoceńsko-eoceńska formacja łupków pstrych oraz wyżejległa eoceńska

formacja hieroglifowa (Rajchel, 1990), których odpowiedniki facjalne mogą być również śledzone w pozostałych basenach karpackich. Oligoceńska formacja menilitowa jest oddzielona od formacji hieroglifowej przez tzw. margle globigerynowe będące karpacki horyzontem korelacyjnym występującym we wszystkich jednostkach tektonicznych (Leszczyński, 1997). Najwyższą pozycje w profilu płaszczowiny skolskiej zajmuje formacja krośnieńska (warstwy krośnieńskie), której utwory interpretowane są jako molasa powstała w trakcie fałdowania Karpat (Kotlarczyk, 1988).

Pierwsze badania geologiczne formacji z Ropianki sięgają końca XIX wieku, kiedy stworzono podstawy schematów litostratygraficznych (np. Tietze, 1883; Hilber,1885). Późniejsze prace skupiały się głównie na litostratygrafii (np. Chlebowski et al., 1937; Wdowiarz, 1949; Bromowicz, 1974; Kotlarczyk, 1978, 1988; Rajchel, 1989; Malata, 1996, 2001), paleogeografii oraz badaniach proweniencji materiału (np. Bukowy, 1957b; Bukowy i Geroch, 1957; Książkiewicz, 1962; Kotlarczyk i Śliwowa, 1963; Nowak, 1963; Skulich, 1986; Salata i Uchman, 2013; Salata, 2014; Łapcik et al., 2016), analizie mikroskamieniałości (np. Jednorowska, 1957; Geroch et al., 1979; Leszczyński et al., 1995; Gedl, 1999; Gasiński i Uchman, 2009, 2011; Gasiński et al., 2013; Kędzierski i Leszczyński, 2013; Kędzierski et al., 2015), ze znacznie mniejszym udziałem badań sedymentologicznych (Bukowy, 1957a; Burzewski, 1966; Bromowicz, 1974; Dżułyński et al., 1979; Geroch et al., 1979; Kotlarczyk, 1988; Leszczyński et al., 1995; Łapcik et al., 2016). Uwagi na temat sedymentacji formacji z Ropianki były raczej pobocznym elementem prac kartograficznych (np. Kotlarczyk, 1978; Malata, 2001). Większość cytowanych prac sedymentologicznych powstała w czasach, gdy badania sedymentologiczne nad utworami głębokomorskimi były o wiele mniej zaawansowane niż obecnie. Zgromadzone dane na temat głębokomorskich systemów depozycyjnych z całego świata pozwoliły rozwinąć koncepcję elementów architektonicznych podmorskich stożków oraz lepiej zrozumieć genezę zróżnicowanych zespołów facjalnych które je budują (np. Pickering et al., 1995; Clark i Pickering, 1996; Sprague et al., 2005; Mutti et al., 2009; Prélat et al., 2009; McHargue et al., 2011; Mulder, 2011; Shanmugam, 2016a). Ta różnorodność wskazuje na unikatowość warunków sedymentacji w każdym basenie. Aktualnie wiedza sedymentologiczna o formacji z Ropianki ogranicza się do informacji o głębokomorskim charakterze jej środowiska depozycji, rozkładzie kierunków paleotransportu i występowaniu osadów zdeponowanych przez szeroko rozumiane prądy gęstościowe oraz ruchy masowe. Dotychczasowy stan wiedzy nie pozwala jednoznacznie ustalić miejsca formacji z Ropianki w proponowanych w literaturze modelach sedymentacji głębokomorskiej oraz przeprowadzić szczegółowego porównania z innymi formacjami głębokomorskimi. Wciąż jest brak dokładniejszych informacji o rozkładzie facji osadowych w basenie skolskim, mechanizmach ich depozycji oraz znaczeniu dla lokalnej architektury basenu. Niejasna pozostaje przestrzenna i czasowa relacja facji oraz asocjacji facjalnych stanowiących klucz do zrozumienia historii ewolucji basenu skolskiego.

Zbiór artykułów prezentowanych w niniejsze rozprawie doktorskiej stanowi pierwsze szczegółowe opracowanie sedymentologiczne oraz facjalne dla trzech wybranych sukcesji osadowych formacji z Ropianki. Badane profile znajdują się w brzeżnej oraz środkowej części płaszczowiny skolskiej. Prezentowane prace po raz pierwszy wyróżniają elementy architektury basenu, to jest głębokomorskie kanały, wały przykorytowe, loby depozycyjne,

osady międzylobowe, osady równi basenowej oraz osady skłonu basenu (Łapcik, 2017, 2018, w druku). Pionowe zmiany w następstwie asocjacji facjalnych w obrębie wymienionych elementów architektury wskazują na obecność czynników różnego rzędu, które kontrolowały lokalne zmiany sedymentacji oraz powodowały zmiany w basenie na szerszą skalę. W prezentowanych pracach wymieniono obecność utworów o różnorodnych mechanizmach depozycji, które często pozostają niejednoznaczne. Wyniki badań przedstawione w sposób pół-ilościowy stanowią podstawę do dalszych, szerzej zakrojonych badań sedymentologicznych i analizy facji w płaszczowinie skolskiej. Dopiero szersza analiza sedymentologiczna oraz facjalna może dać informacje na temat historii formowania się basenu, wzajemnych relacji między elementami architektury, sposobu dystrybucji materiału osadowego oraz dać lepsze zrozumienie czynników wewnątrz- i pozabasenowych na formowanie się formacji z Ropianki.

2. Wyniki

Publikacja 1: Facies heterogeneity of a deep-sea depositional lobe complex: case study from the Słonne section of Skole Nappe, Polish Outer Carpathians. *Annales Societatis Geologorum Poloniae*, 87: 301–324.

Publikacja 1 dotyczy analizy facjalnej fragmentu sukcesji osadowej formacji z Ropianki o miąższości ponad 140 m (fig. 2), odsłaniającej się w skarpie lewego brzegu Sanu w okolicy miejscowości Słonne (fig. 1). Sukcesja ta została detalicznie sprofilowana, ze szczególnym uwzględnieniem tekstur i pierwotnych struktur sedymentacyjnych (fig. 3). Celem pracy jest: (1) wyróżnienie i scharakteryzowanie facji osadowych oraz przypisanie ich interpretacyjnie do wybranego środowiska depozycji; oraz (2) przeanalizowanie zmian zespołów facjalnych w pionowej sukcesji osadowej, jako zapisu bocznej migracji lobów depozycyjnych. Z profilu pobrano 80 prób piaskowca do analizy wielkości ziarna metodą sitową. Dodatkowo, z 11 prób wykonano płytki cienkie, które poddano późniejszej statystycznej analizie wielkości ziarna techniką zliczania najdłuższych osi ziaren oraz obserwacjom mikrofacji i składu mineralnego. W terenie wykonano 377 pomiarów podatności magnetycznej, głównie dla masywnych piaskowców w 20-centymetrowych interwałach by wykazać możliwe a makroskopowo nierozpoznawalne trendy zmiany uziarnienia osadu. Pobrano sześć prób mułowca w celu określenia biostratygraficznego wieku badanych osadów dzięki mikropaleontologicznej analizie zespołów otwornic.

W badanej sukcesji osadowej zdominowanej piaskowcem wyróżniono, scharakteryzowano oraz zinterpretowano sześć facji osadowych (figs. 3, 4). Wyróżnione facje zinterpretowano jako osady prądów zawiesinowych o wysokiej oraz niskiej gęstości (facje F1, F2 i F4) *sensu* Lowe (1982) o różnej objętości, post-turbidytowe osady hemipelagiczne i pelagiczne deponowane w pobliżu lizokliny (facja F3; Bouma, 1962; Mutti i Ricci Lucchi, 1975; Stow i Shanmugam, 1980; Pickering et al., 1986), osady piaszczystych spływów rumoszu (facja F5; Breien et al., 2010; Strzeboński, 2015) oraz osady marglistych prądów zawiesinowych o niskiej gęstości (facja F6; Flügel, 2010).

Dodatkowe badania podatności magnetycznej zakładały, że masywne piaskowce zdeponowane przez turbulentne spływy mogą wykazywać subtelne, makroskopowo nierozpoznawalne drobnienie ziarna ku stropowi ławicy oraz wzrost zawartości mułu, w przeciwieństwie do masywnych piaskowców zdeponowanych przez nieturbulentne spływy. Wyniki analizy nie okazały się pomocne przy rozpoznawaniu mody depozycji oraz rozróżnianiu debrytów od turbidytów.

Badany profil podzielono na kilkumetrowe pakiety o specyficznej kompozycji facjalnej oraz charakterystyce statystycznej budujących je piaskowców (średnia, mediana oraz wariancja miąższości ławic piaskowców, piaskowcowe netto/brutto), wyróżniając cztery typy asocjacji facjalnych (tabela 1). W oparciu o dużą ilość tabularnych (płaskich w skali odsłonięcia) ławic piaskowca, dominującym, stopniowym przejściu facji bez wyraźnych głębokich wcięć erozyjnych i oznak kanalizacji, wyróżnione asocjacje facjalne zostały zinterpretowane jako morfodynamiczne strefy lobów depozycyjnych (Mutti i Ricci Lucchi, 1972; Shanmugam i Moiola, 1988, 1991; Pickering et al., 1995; Mulder, 2011; Shanmugam,

2016a). Asocjacje facjalne reprezentują odpowiednio: oś lobu, bok lobu, skraj lobu oraz osady międzylobowe lub dystalny skraj lobu (Mutti i Normark, 1987; Pickering et al., 1995; Shanmugam i Moiola, 1991; Stow i Mayall, 2000; Deptuck et al., 2008; Prélat et al., 2009; Mulder, 2011; Grundvåg et al., 2014; Marini et al., 2015).

Analiza mikropaleontologiczna najlepiej zachowanych zespołów otwornic z dwóch prób, pozwoliła określić wiek badanych osadów na przedział kampan–mastrycht i przyporządkować badaną sukcesję osadową do ogniwa z Wiaru (fig. 2). Jest to dodatkowo podparte podobieństwem litologicznym do opisanego przez Rajchla (1989) stratygraficznego kompleksu I, wyróżnionego w okolicy badanego profilu. Zaobserwowane zespoły otwornic wskazują na sedymentację poniżej lizokliny. Jednak, występowanie otwornic z wapiennym cementem jak *Dorothia crassa* sugeruje okresowe zmiany głębokości powyżej lizokliny, która w późnej kredzie mogła być około ~50% płycej niż dzisiaj (Lyle, 2003; Rea i Lyle, 2005).

Badany profil został zinterpretowany w kontekście stratygrafii dynamicznej, gdzie wyróżnione asocjacje facjalne reprezentują różne strefy morfodynamiczne lobu tworząc sukcesję sześciu nakładających się lobów (fig. 11D). Stopniowe, pionowe przejścia bezpośrednio przylegających do siebie asocjacji facjalnych reprezentujących wybrane strefy lobu (fig. 11A) przypisano do jego lateralnej migracji poprzez przesuwanie się wewnątrzlobowej osi spływu dostarczającej osad (fig. 11B). Zmiany pionowe w profilu obejmujące następstwo niesąsiadujących ze sobą asocjacji facjalnych w zaproponowanym modelu lobu (fig. 11A) oraz pojawienie się asocjacji międzylobowej zinterpretowano jako całościowe boczne przesunięcie się lobu z powodu agradacji oraz zmiany pozycji kanału zasilającego (fig. 11C).

Nie można wykluczyć że część pakietów zdominowanych mułowcem (zinterpretowanych jako dystalny skraj lobu) mogło powstać na skutek podniesienia się relatywnego poziomu morza wraz ze spadkiem ilości dostarczanego materiału w trakcie cofania się systemu depozycyjnego. W przedziale czasu obejmującym kampan–mastrycht miały miejsce 4 duże (>75 m), 4 średnie (25–75 m) oraz 5 pomniejszych (<25 m) eustatycznych zmian poziomu morza (Snedden i Liu, 2010). Pomimo aktywności tektonicznej w basenie skolskim nie jest wykluczone, że przynajmniej większe zmiany eustatyczne miały wpływ na sedymentację oraz, że grubsze międzylobowe pakiety odpowiadają transgresywnym osadom skraju lobu.

Udokumentowane przez Bromowicza (1974) kierunki paleotransportu w basenie skolskim są głównie z północy oraz północnego zachodu i tylko najstarsze osady formacji w południowo-wschodniej części płaszczowiny w Polsce były transportowane ze wschodu i południowego wschodu. Wyniki niniejszych badań poddają w wątpliwość wcześniejsze sugestie o rozprowadzaniu piaszczystego osadów wzdłuż osi basenu. Zazębiające się loby w kompleksie lobowym Słonnego w fazie ich maksymalnej ekspansji w wąskim basenie mogły dać fałszywe wrażenie wąskich piaszczystych centrów depozycji równoległych do osi basenu. Południowy trend tworzących się lobów mógł zostać przekrzywiony ku wschodowi/lub zachodowi w wąskim basenie, zależnie od lokalnej przestrzeni akomodacyjnej na dnie. Nie oznacza to jednak, że dystrybucja osadu przebiegała wzdłuż osi basenu.

Piaszczyste osady Słonnego charakteryzują się dużą ilością uwęglonego detrytusu roślinnego. Może to sugerować deltowe lub paraliczne zasilanie dla badanej części basenu skolskiego. Głęboko wcięte kaniony lub podmorskie doliny zasilające basen skolski powinny

rozpoczynać się w pobliżu delt, z których również mogły być inicjowane spływy hiperpiknalne, co sugerują niektóre ławice facji F1. Fluktuacje zasilania silikoklastycznego oraz węglanowego wskazują na współwystępowanie fluwio-deltowego oraz węglanowego źródła. Ich zazębianie może być podkreślone przez margle zawierające detrytus roślinny (fig. 9D). Relatywnie mały i rzadki udział facji margli (facje F6) sugeruje, że węglanowe źródło jedynie okazyjnie zasilało badany obszar. Może to wskazywać na epizodyczną produkcję węglanową na wąskim szelfie basenu, być może spowodowaną eustatycznymi zmianami poziomu morza (Snedden i Liu, 2010).

Publikacja 2: Sedimentary processes and architecture of Upper Cretaceous deep-sea channel deposits: a case from the Skole Nappe, Polish Outer Carpathians. *Geologica Carpathica*, 69: 71–88.

Publikacja 2 skupia się na charakterystyce facji osadowych oraz ukazaniu architektury piaszczystego profilu formacji z Ropianki, odsłaniającego się w kamieniołomie w Manasterzu (fig. 1). W terenie pobrano 50 prób do analizy wielkości ziarna metodą sitową by rozróżnić osady spływów turbulentnych i nieturbulentnych. Pomierzono orientację dłuższych osi dla 103 klastów mułowych i marglistych by określić potencjalny kierunek paleotransportu badanych utworów. Dodatkowo, badania terenowe objęły profilowanie dwóch pobliskich sukcesji osadowych formacji z Ropianki (profil Manasterz Rzeki oraz profil Manasterz) zlokalizowanych na północny zachód od kamieniołomu w Manasterzu (fig. 1). Dla każdego odsłonięcia profilu Manasterz Rzeki podano procentową zawartość wyróżnionych litologii, bazującą na ilości oraz miąższości ławic (fig. 3).

Najbardziej szczegółowo zbadanym profilem jest kamieniołom w Manasterzu, gdzie odsłania się w pełni piaszczysta sukcesja formacji z Ropianki o miąższości ponad 30 m. W profilu wyróżniono dwie facje osadowe obejmujące makroskopowo bezstrukturalne lub uziarnione frakcjonalnie piaskowce zdeponowane przez prądy zawiesinowe o wysokiej gęstości (facja 1; Lowe, 1982) oraz fację masywnych, zamulonych piaskowców z licznymi klastami śródformacyjnymi (facja 2), interpretowanych jako piaszczyste debryty (cf. Shanmugam, 2006; Strzeboński, 2015). W profilu znajduje się pakiet szarych i sinym mułowców oraz margli o miąższości 1,8 m i nieokreślonym lateralnym zasięgu (fig 4). Litologie budujące tą warstwę zostały zinterpretowane jako osady niskogęstościowych mułowych prądów zawiesinowych oraz pelagicznych i hemipelagicznych mułowców, jednak całość prawdopodobnie reprezentuje duży olistolit stanowiący część debrytu lub osuwiska.

Na podstawie dużej zawartości piasku, występowania grubych ławic bezstrukturalnych i uziarnionych frakcjonalnie piaskowców, relatywnie dużej zawartości grubego materiału klastycznego, powszechnej amalgamacji oraz licznych klastów i struktur erozyjnych, profil kamieniołomu w Manasterzu został zinterpretowany jako wypełnienie głębokomorskiego kanału (cf. Mutti i Normark, 1987; Shanmugam i Moiola, 1988; Mayall et al., 2006; McHargue et al., 2011; Hubbard et al., 2014). Powszechne powierzchnie amalgamacji oraz przeławicanie turbidytów z debrytami sugeruje wieloetapowy proces wypełniania kanału charakteryzującego się powtarzającym się przejściem od depozycji debrytu, przez jego erozję i pozostawieniu bruku, aż do wypełniania kanału przez bezstrukturalne i uziarnione frakcjonalnie piaski. W profilu wyróżniono debryty z licznymi klastami (facies 2), występujące w spągu poszczególnych elementów kanału, przykryte turbidytowym wypełnieniem. W kamieniołomie rozpoznano 3 debrytowe elementy oraz 5 turbidytowych wypełnień (fig. 4). Nie można jednak wykluczyć, że najmłodsze turbidytowe wypełnienie reprezentuje dwa oddzielne elementy rozdzielone przez słabo odsłonięty debryt (fig. 4). Miąższości poszczególnych elementów wahają się od 2,5 do 8 m lub do 13 m w najmłodszej części reprezentowanej jako pojedynczy, nierozdzielony element.

Relatywnie miąższa sukcesja amalgamowanych piaskowców w kamieniołomie w Manasterzu może reprezentować obszar w pobliżu osiowej części kanału, gdzie był

akumulowany najgrubszy materiał. Agradacja miąższej sukcesji piaszczystej, sugeruje jej przynależność do wypełnienia kanału lub kompleksu kanałowego, gdzie tempo agradacji przewyższało lateralną migrację. Podobnie, agradujący kanał nie powinien się uformować bez jednoczesnej agradacji otaczających go wałów. Stosunkowo niewielka zawartość mułu w turbidytowych piaskowcach w kamieniołomie w Manasterzu (fig. 6) może być związana z przelewaniem się przez wał stropowej, bogatej w muł części prądu zawiesinowego lub niedepozycją i przemieszczeniem się mułowej części spływu w dół systemu. Co więcej, osady kanału w Manasterzu wykazują niemal całkowity brak detrytusu roślinnego oraz węgla będącego powszechnym składnikiem nie tylko w formacji z Ropianki ale i młodszych osadów jednostki skolskiej. Sugeruje to zdeponowanie wspomnianego, stosunkowo łatwo transportowanego materiału w bardziej dystalnej części systemu, na przykład w lobach depozycyjnych, takich jak w profilu Słonne.

Bazując na podobnej pozycji stratygraficznej górnej części profilu Manasterza oszacowano wyklinowywania się facji osi kanału ku północnemu zachodowi na dystans nie większy niż 800 m (fig. 1). To boczne przejście sugeruje, że średnio i cienkoławicowy flisz w górnej części profilu Manasterza reprezentuje facje krawędzi kanału lub wału w odniesieniu do profilu z kamieniołomu (figs. 1, 2). Brak odsłonięć z podobnymi osadami ku wschodowi sugeruje, że szerokość kanału nie powinna przekraczać kilkuset metrów. Potencjalne lateralne przejście z facji osi kanału do facji krawędzi kanału lub wału pozwala na spekulacje o krętości kanału. W przeciwnym razie facja osi lub pozaosiowa kanału powinna znajdować się również w stropowej części profilu Manasterza. Stąd, facje kanałowe obecne w kamieniołomie w Manasterzu powinny zmienić swój bieg ku północy lub zachodowi by ominąć przypuszczalny obszar wału. Mimo to, brak jest innych istotnych przesłanek, jak na przykład boczne pakiety akrecyjne (Bouma i Coleman. 1985; Mutti i Normark. 1991; Abreu et al., 2003; Janočko et al., 2013) potwierdzających krętość kanału w Manasterzu.

Opisywane kierunki paleotransportu w osadach formacji z Ropianki są zorientowane z północnego zachodu, północy i północnego wschodu z dominacją kierunków z północnego zachodu w pobliżu obszaru badań (Książkiewicz, 1962; Bromowicz, 1974). Słabe wskaźniki paleotransportu z kamieniołomu w Manasterzu obejmujące orientację struktur erozyjnych, pomiary dłuższych osi klastów oraz imbrykację również wskazują na kierunek północno-zachodni. Tym niemniej kierunki transportu w głębokomorskich kanałach mogą być zróżnicowane i rzadko są jednokierunkowe. Kotlarczyk i Leśniak (1990) zaproponowali łańcucką strefę kanałową depozycji materiału piaszczystego zorientowaną podłużnie do skłonu basenu dla osadów oligoceńskich. Podobny kierunek transportu w osadach kanałowych Manasterza może sugerować że wspomniana strefa była już aktywna w późnej kredzie.

Występujące piaszczyste mułowce oraz piaskowce mułowe z klastami (margle z Węgierki) poniżej kanału z kamieniołomu w Manasterzu, wskazują na to, że kanał Manasterza został uformowany na podłożu z powszechnymi debrytami, które mogły stanowić morfologiczne ograniczenie (obwałowanie) dla inicjalnej strefy kanałowej. Margle z Węgierki oraz gruboławicowe piaskowce ogniwa z Leszczyn znane są ze wzajemnego przeławicania (Wdowiarz, 1949; Burzewski, 1966; Kotlarczyk, 1978, 1988). Nie jest jasne czy piaskowce z kamieniołomu w Manasterzu są usytuowane jedynie w stropie margli z Węgierki, czy również graniczą z nimi obocznie lub są przez nie przykryte. Niektóre debryty w kamieniołomie w

Manasterzu zawierają duże głazy o litologii podobnej do margli z Węgierki, co może sugerować że margle z Węgierki mogły być odsłaniane w kanałach.

Za Gardnerem et. al. (2003), osady w kamieniołomie w Manasterzu wykazują cechy fazy wypełniania dla kanału zlokalizowanego w dolnym skłonie lub przy podstawie skłonu, co zgadza się z proksymalnym usytuowaniem obszaru badań. Cała sukcesja profili okolic Manasterza jest interpretowana jako przejście pozaosiowych stref lobów lub kanałów oraz otaczających ich osadów międzykanałowych ogniwa z Wiaru (profile Manasterz Rzeki i Manasterz) w kanałowe osady kamieniołomu w Manasterzu wcinające się w debryty margli z Węgierki należących do ogniwa z Leszczyn (górna część profilu Manasterz).

Publikacja 3: Semi-quantitative analysis of the late Cretaceous–Palaeogene succession of deep-sea channel-lobe complex: case study from the Hucisko Jawornickie section, Skole Nappe, Polish Outer Carpathians. *Acta Geologica Polonica*. [In press].

Trzeci artykuł dotyczy analizy sedymentologicznej ponad 400-m sukcesji osadowej ogniwa z Wiaru oraz ogniwa z Leszczyn (kampan–paleocen), która odsłania się w okolicy Huciska Jawornickiego (figs. 1, 3). Celem detalicznego profilowania było (1) wyróżnienie oraz pół-ilościowa charakterystyka asocjacji facjalnych wraz z określeniem ich subśrodowisk depozycyjnych; (2) przeprowadzenie statystycznej analizy metodą włożonych łańcuchów Markova dla mody pionowych przejść facjalnych i ich późniejsza interpretacja jako mechanizmów depozycji dla każdej asocjacji facjalnej; oraz (3) analiza pionowych zmian asocjacji facjalnych w sukcesji osadowej jako hipotetyczny zapis progradacji kompleksu kanałowo–lobowego u podstawy skłonu na starszą generację kompleksu kanałowo–lobowego, z późniejszym etapem progradacji skłonu basenu.

W przedstawionym profilu wyróżniono siedem facji osadowych. Wyróżnione facje zostały zinterpretowane jako: utwory zdeponowane przez prądy zawiesinowe o wysokiej oraz niskiej gęstości (facja F1 oraz F2) *sensu* Lowe (1982), utwory uformowane przez tzw. prądy hybrydowe (tzw. „slurry flows") mające cechy ruchu laminarnego i turbulentnego (facja F1 i F2) *sensu* Lowe i Guy (2000), utwory zdeponowane przez niekohezyjne (facja F3) oraz kohezyjne spływy rumoszu (facja F7), mułowce pelagiczne oraz hemipelagiczne (facja F4), margle o genezie turbidytowej z możliwym współwystępowaniem margli zdeponowanych przez prądy konturowe oraz margli hemipelagicznych (facja F5) oraz heterolity (facja F6) o niejasnej genezie z prądów trakcyjnych, w tym prądów zawiesinowych i możliwym występowaniu konturytów oraz utworów zdeponowanych przez głębokomorskie prądy pływowe (Dykstra, 2012).

Na podstawie kompozycji, mediany, wariancji, średniej miąższości ławic oraz stosunku piaskowców netto/brutto wyróżniono 6 asocjacji facjalnych reprezentujących głębokomorskie subśrodowiska depozycyjne (tabela 1). Asocjacje facjalną z największym udziałem piaskowców oraz zlepieńców z trendem ławic cieniejących ku górze, drobniejącym ku górze ziarnie oraz powszechną amalgamacją zinterpretowano jako utwory wypełniające kanały zasilające. Druga w kolejności pod względem udziału piaskowców asocjacja facjalna z wyraźnie drobniejszym ziarnem, cieńszymi ławicami, rzadszą amalgamacją, zdominowana tabularnymi ławicami (w skali odsłonięcia) została zinterpretowana jako utwory lobów depozycyjnych w pobliżu ujścia kanału. Asocjacje facjalne ze znacząco mniejszym udziałem piaskowców zostały odpowiednio uznane za wały przykorytowe oraz utwory równi międzylobowej lub dystalne części lobów. Dodatkowo wyróżniono asocjację facjalną wypełnienia krewas z większym udziałem prądów zawiesinowych o wysokiej gęstości oraz większą miąższością ławic piaskowców niż w wałach przykorytowych oraz piaszczyste glify krewasowe formujące się na równi międzylobowej. Dla każdej asocjacji facjalnej wykonano statystyczną analizę pionowych przejść facji metodą włożonych łańcuchów Markova (figs. 6, 7, 8, 9, 10) wraz z interpretacją prawdopodobnych procesów depozycyjnych występujących w danym subśrodowisku.

Sukcesję osadową Huciska Jawornickiego zinterpretowano w kontekście stratygrafii dynamicznej (fig. 12), jako progradację kompleksu kanałowo-lobowego u podstawy skłonu na starszą generacją kompleksu kanałowo-lobowego. Słabo odsłoniętą, najmłodszą część profilu z częstymi debrytami reprezentuje etap progradacji utworów skłonu basenu zakończonego przejściem do paleoceńsko-eoceńskiej formacji łupków pstrych (fig. 2). W profilu wyróżniono dwa typy pionowych zmian sukcesji osadowej. Zmiany pierwszego typu to lokalne zmiany spowodowane autogeniczną, lateralną migracją i agradacją lobów depozycyjnych oraz wielopiętrowych kanałów. Są one reprezentowane przez stopniowe pionowe zmiany facjalne w poszczególnych segmentach profilu Huciska Jawornickiego. Zmiany drugiego typu odzwierciedlają migrację całego systemu depozycyjnego i nawiązują do przejścia sukcesji osadowej Huciska Jawornickiego od międzylobowej równi basenowej z glifami krewasowymi, przez progradujące loby depozycyjne z ich kanałami zasilającymi w stropie aż do profili z licznymi osuwiskami i debrytami interpretowanych jako progradacja skłonu basenu. Nie jest wykluczone, że pionowe zmiany drugiego typu w profilu Huciska Jawornickiego są powiązane z niektórymi zmianami eustatycznymi jakie miały miejsce w późnej kredzie–paleocenie (Snedden i Liu 2010). Jednak, brak dowodów biostratygraficznych pozwalających na korelację z krzywą eustatyczną. Depozycja kontrolowana głównie tektoniczne w basenie fliszowym wydaje się bardziej prawdopodobna.

Oszacowano, że dystans między bardziej dystalnym środowiskiem nieskanalizowanych lobów depozycyjnych w okolicy Słonnego (Łapcik, 2017) a relatywnie proksymalnymi kanałami i lobami w Hucisku Jawornickim i Manasterzu (Łapcik, 2018) wynosił pierwotnie ~25–35 km. W przypadku poprawności tych założeń można implikować przesuwanie się w stronę basenu nieskanalizowanej dolnej i środkowej strefy lobów depozycyjnych, skanalizowanej górnej strefy lobów depozycyjnych oraz osadów skłonu basenu na dystans nie większy niż 35–40 km dla każdej strefy (fig. 13). W tym modelu sukcesja Huciska Jawornickiego stanowi strefę przejściową dla kolejnych progradujących elementów architektury basenu.

Kierunki paleotransportu podane w dotychczasowej literaturze są pozbawione kontekstu facji w których były dokonywane pomiary (Książkiewicz, 1962; Bromowicz, 1974). Rozrzut kierunków transportu w lobach depozycyjnych i głębokomorskich kanałach może przekroczyć 180°. W takim przypadku, piaszczysty pas zorientowany równolegle do osi basenu skolskiego może odpowiadać serii małych piaszczystych fartuchów wzdłuż skłonu basenu zamiast reprezentować system osiowego zasilania basenu jak sugerowano dotychczas (Książkiewicz, 1962; Bromowicz, 1974; Kotlarczyk, 1978).

Utwory w Hucisku Jawornickim zawierają relatywnie dużo uwęglonej sieczki roślinnej. Podobny materiał często jest powiązany z deltowym lub paralicznym źródłem zasilania, gdzie jego dystrybucja następuje poprzez wąskie doliny wcięte w skłon basenu (fig. 12). Współwystępowanie relatywnie częstych ławic margli w profilu wskazuje na okresową sedymentację węglanową na obrzeżającym basen od północy wąskim szelfie i wpływ utworów redeponowanych na skłon i jego pobliże. Wpływ sedymentacji węglanowej wyraźnie zanika w głąb basenu, co zaznacza się niewielkim udziałem margli w profilu kompleksu lobowego w okolicy Słonnego (Łapcik, 2017).

3. Wnioski

1. Różnorodność mechanizmów depozycji które uformowały utwory formacji z Ropianki jest bezpośrednim odzwierciedleniem heterogeniczności facji osadowych wyróżnionych w prezentowanych artykułach. Większość facji współwystępuje we wszystkich badanych profilach w zmiennym udziale ilościowym i objętościowym. Badania wykazały, że pomimo makroskopowego podobieństwa utworów, wiele z nich może mieć różną genezę. W takim przypadku detaliczna analiza sedymentologiczna pozwala na rozróżnienie mechanizmów depozycji. Utwory formacji z Ropianki na badanym obszarze zostały zdeponowane przez prądy zawiesinowe o niskiej i wysokiej gęstości (np. Bouma, 1962; Lowe, 1982; Talling et al., 2012), kohezyjne i niekohezyjne spływy rumoszu (Strzeboński, 2015; Shanmugam, 2016b) oraz prądy hybrydowe (tzw. „slurry flows" *sensu* Lowe i Guy, 2000) mające cechy ruchu laminarnego i turbulentnego. W przypadku utworów o relatywnie dużym udziale detrytusu roślinnego, uformowanych przez długotrwałe fluktuujące spływy, prawdopodobna jest geneza z prądów hiperpiknalnych (Mulder et al., 2001, 2002, 2003; Porębski i Warchoł, 2006). Dodatkowo, w formacji z Ropianki powszechnie występują utwory hemipelagiczne oraz pelagiczne. Warto zaznaczyć że sposób depozycji niektórych opisanych facji (np. heterolity) wciąż pozostaje niejednoznaczny, wskazując na potencjalne występowanie prądów trakcyjnych (np. prądów konturowych lub głębokomorskich prądów pływowych) na dnie basenu skolskiego. W świetle prezentowanych danych, różnorodność mechanizmów depozycji występujących w formacji z Ropianki jest znacznie większa niż opisano we wcześniejszej literaturze.

2. W prezentowanych artykułach po raz pierwszy scharakteryzowano oraz wyróżniono asocjacje facjalne, które składają się na elementy architektury dna basenu skolskiego dla formacji z Ropianki. Przedstawienie danych pół-ilościowych uwypukla różnorodność facji osadowych oraz ich wzajemny udział w elementach architektury dna zależnie od miejsca w basenie jak i typu ciała osadowego. W badanym obszarze opisano głębokomorskie kanały, loby depozycyjne, wały przykorytowe, osady równi basenu, osady międzylobowe, glify krewasowe oraz osady skłonu basenu. Podobne ciała osadowe są typowe dla znanych głębokomorskich basenów a ich rozmiar jest porównywalny z szacunkami w prezentowanymi artykułach. Opisane ciała osadowe stanowiąc hierarchiczną strukturę na dnie basenu, ostatecznie składają się na kompleksy kanałowo-lobowe, które stanowią najwyższą rangę wyróżnionych elementów architektury w obrębie formacji z Ropianki.

3. Duża ilość detrytusu roślinnego występująca powszechnie w piaskowcach sugeruje wpływ środowisk deltowych lub paralicznych na źródło zasilania w badanej części basenu skolskiego. By dostarczyć odpowiednią ilość materiału piaszczystego do uformowania wyróżnionych kanałów i lobów depozycyjnych, źródło powinny stanowić delty usytuowane przy krawędzi skłonu basenu. Większa ilość materiału piaszczystego w basenie skolskim prawdopodobnie była dystrybuowana kanionami lub dolinami wciętymi w skłon basenu, które przechwytywały materiał redeponowany z płytszych stref. Dodatkowym wskaźnikiem na

redepozycję materiału z płytszych stref jest występowanie skamieniałości makrofauny w utworach kanałowych Manasterza oraz powszechny materiał egzotyczny w górnej części formacji z Ropianki. Niestety szansa na odnalezienie pełniejszych przekrojów kanionów lub wciętych dolin jest niewielka ze względu na słaby stopień odsłonięcia formacji z Ropianki. Jedyną przesłanką na ich występowanie jest obecność klastów dolnokredowych czarnych mułowców w kampańskich utworach formacji z Ropianki, świadczących o głębokiej erozji starszych osadów w tamtym czasie (Kotlarczyk, 1988).

4. W utworach formacji z Ropianki wyraźnie zaznacza się obecność margli, których ilość zmienia się w poszczególnych profilach oraz generalnie spada w stronę osi basenu. Takie osady pochodzą z okresowo funkcjonującego węglanowego źródła, prawdopodobnie usytuowanego na wąskim szelfie. Źródło węglanowe musiało współwystępować w bliskim sąsiedztwie źródła klastycznego. Jest to dodatkowo podkreślone obecnością detrytusu roślinnego w marglach. Osad węglanowy redeponowany z płytszych stref, głównie w formie prądów zawiesinowych, miał relatywnie mały zasięg i był deponowany głównie na skłonie basenu i w jego okolicy (profile Manasterza i Huciska Jawornickiego). Jedynie lokalnie i w niewielkich ilościach materiał węglanowy docierał w głąb basenu (profil Słonne) co potwierdza wcześniejsze spostrzeżenia Kotlarczyka (1978, 1988).

5. Analiza sukcesji osadowych prezentowanych profili ukazuje zmienną dynamikę środowiska depozycji. Utwory formacji z Ropianki w badanym obszarze stanowią zapis zmieniającego się środowiska podmorskiego stożka usytuowanego w pobliżu skłonu lub na dnie basenu. Depozycja zachodziła na głębokościach batialnych, głównie ponad lokalną lizokliną w obszarze proksymalnym (profile Manasterza i Huciska Jawornickiego) oraz poniżej lokalnej lizokliny na obszarze dystalnym (profil Słonne). Jest to prawdopodobnie bezpośrednim odzwierciedleniem pogłębiania się basenu w stronę jego osi.

W badanych profilach wyróżniono dwa typy pionowych zmian sukcesji osadowej. Zmiany pierwszego typu to zmiany lokalne spowodowane autogeniczną, lateralną migracją i agradacją lobów depozycyjnych oraz kanałów. W profilu są one reprezentowane przez pionowe zmiany facjalne, które obejmują stopniowe przejścia pomiędzy asocjacjami facjalnymi graniczącymi ze sobą w prezentowanych modelach. Zmiany wyższej hierarchii odzwierciedlają migrację wszystkich stref w badanej części systemu depozycyjnego, obejmując progradację i retrogradację lobów depozycyjnych wraz z ich kanałami zasilającymi. Jest to najlepiej widoczne w profilu Huciska Jawornickiego, gdzie jest zapisane przejście od międzylobowej równi basenowej z glifami krewasowymi, przez progradujące loby depozycyjne z ich kanałami zasilającymi w stropie aż do profili z licznymi osuwiskami i debrytami interpretowanymi jako progradacja skłonu basenu. Z prezentowanych artykułów wyraźnie wynika, że w obrębie basenu może mieć miejsce depozycja różnorodnych facji jednocześnie. Taki model depozycji w basenie skolskim tłumaczy wcześniejsze problemy z utworzeniem jednolitego podziału litostratygraficznego oraz występowanie licznych, bezpośrednio niekorelujących się ze sobą miąższych ciał piaszczystych w różnych częściach płaszczowiny (Kotlarczyk, 1978). W tym kontekście aktualny schemat litostratygraficzny (w tym chronohoryzonty zaproponowane przez Kotlarczyka, 1978) może mieć ograniczone

zastosowanie nie dając możliwości bardziej precyzyjnej korelacji utworów w skali basenu, ponieważ nie uwzględnia on dynamiki środowiska depozycji z formującymi się różnorodnymi ciałami osadowymi.

Nie jest wykluczone, że pionowe zmiany facjalne wyższego rzędu są powiązane z niektórymi zmianami eustatycznymi jakie miały miejsce w kampanie–paleogenie. Pomniejszymi przesłankami na wpływ eustatycznych zmian poziomu morza na depozycję są: występowanie grubszych mułowych pakietów sugerujących spadek dostawy materiału detrytycznego przy rosnącym poziomie morza, okresowy wzrost i spadek aktywności węglanowego źródła, współwystępowanie wapnistych i niewapnistych pakietów mułowych oraz obecność otwornicy z wapiennym cementem (*Dorothia crassa*) w relatywnie dystalnym profilu w Słonnem, deponowanym głównie poniżej lokalnej lizokliny. Wciąż pozostaje brak dowodów biostratygraficznych pozwalających na korelację z krzywą eustatyczną. Mimo to, depozycja kontrolowana tektoniczne wydaje się być dominującym czynnikiem w basenie fliszowym. Dalsze badania koncentrujące się na detalicznej analizie zmian facjalnych połączonych z szeroko zakrojonymi badaniami biostratygraficznymi mogą dać wiele istotnych informacji na temat historii formowania się formacji z Ropianki oraz zaktualizować obecnie stosowany podział litostratygraficzny zaproponowany przez Kotlarczyka (1978).

6. Oszacowano że dystans między bardziej dystalnym środowiskiem nieskanalizowanych lobów depozycyjnych w okolicy Słonnego (Łapcik, 2017) a relatywnie proksymalnymi kanałami i lobami w Hucisku Jawornickim i Manasterzu (Łapcik, 2018) wynosił pierwotnie ~25–35 km. W przypadku poprawności tych założeń można implikować przesuwanie się w stronę basenu nieskanalizowanych, dolnej i środkowej stref lobów depozycyjnych, skanalizowanej górnej strefy lobów depozycyjnych oraz osadów skłonu basenu na odległość nie większą niż 35–40 km dla każdej z tych stref. W zaprezentowanym modelu sukcesja Huciska Jawornickiego stanowi strefę przejściową dla kolejnych, migrujących elementów architektury basenu.

7. Kierunki paleotransportu dotychczas podane w literaturze (Książkiewicz, 1962; Bromowicz, 1974) zwykle są pozbawione kontekstu facji w których były dokonywane pomiary. Rozrzut kierunków transportu w poszczególnych elementach architektury może być bardzo zróżnicowany. Na przykład w lobach depozycyjnych i głębokomorskich kanałach może on przekroczyć 180°. Dlatego dotychczasowe założenie o dystrybucji materiału klastycznego równolegle do osi basenu skolskiego (Książkiewicz, 1962; Bromowicz, 1974; Kotlarczyk, 1978) można poddać w wątpliwość. Proponowaną alternatywą wynikającą z prezentowanych prac jest uformowanie się piaszczystej strefy wzdłuż osi basenu poprzez scalenie fartuchów lub stożków rozłożonych wzdłuż skłonu, w fazie ich maksymalnej ekspansji. Jednocześnie, opisywane ciała osadowe mogły być częściowo rotowane podążając za przestrzenią akomodacyjną oraz progradując zgodnie z nachyleniem osi basenu. Jest to wyraźna przesłanka do tego aby dalsze badania kierunków transportu prowadzić w kontekście facji osadowych w których będą wykonywane pomiary.

Niezależnie od kierunku transportu materiału w badanym obszarze zaobserwowano podobieństwo między formacja z Ropianki a formacją menilitową w rozmieszczeniu facji z

dużą zawartością piaskowców. Niewykluczone, że oligoceńska architektura basenu skolskiego opisana przez Kotlarczyka i Leśniaka (1990) została odziedziczona po turońsko-paleoceńskiej sedymentacji.

4. Bibliografia

Abreu, V., Sullivan, M., Pirmez, C. & Mohrig, D., 2003. Lateral accretion packages (LAPs): an important reservoir element in deep water sinuous channels. *Marine Petroleum Geology*, 20: 631–648.

Bąk, K., Bąk, M. & Paul, Z., 2001. Barnasiówka Radiolarian Shale Formation – a new lithostratigraphic unit in the Upper Cenomanian–lowermost Turonian of the Polish Outer Carpathians (Silesian Series). *Annales Societatis Geologorum Poloniae*, 71: 75–103.

Bilan, W., 2001. Development and sedimentary environment of the Chwaniów calcareous sandstones within southern part of the Skole Unit. *Geologia*, 27: 7–21. [In Polish, with English summary.]

Bouma, A. H., 1962. *Sedimentology of Some Flysch Deposits: A Graphic Approach to Facies Interpretation*. Elsevier, Amsterdam, 168 pp.

Bouma, A. H. & Coleman, J. M., 1985. Mississippi fan, Leg 96 program and principal results. In: Bouma, A. H., Normark, W. R. & Barnes. N. E. (eds), *Submarine Fans and Related Turbidite Systems*. Springer Verlag, New York, pp. 247–252.

Breien, H., De Blasio, F. V., Elverhøi, A., Nystruen, J. P. & Harbitz, C. B., 2010. Transport mechanisms of sand in deep-marine environments – insights based on laboratory experiments. *Journal of Sedimentary Research*, 80: 975–990.

Bromowicz, J., 1974. Facial variability and lithological character of Inoceramian Beds of the Skole-Nappe between Rzeszów and Przemyśl. *Prace Geologiczne*, 84: 1–83. [In Polish, with English summary.]

Bromowicz, J. & Górniak, K., 1988. Lithology and sedimentation of the Łącko Marls in the eastern part of the Magura Nappe, Flysch Carpathians, Poland. *Annales Societatis Geologorum Poloniae*, 58: 385–421. [In Polish, with English summary.]

Bukowy, S., 1957a. Remarks on the sedimentation of the Babica Clays. *Rocznik Polskiego Towarzystwa Geologicznego*, 26: 147–155. [In Polish, with English summary.]

Bukowy, S., 1957b. Węgiel kamienny w Karpatach brzeżnych. *Przegląd Geologiczny*, 5: 577–578. [In Polish.]

Bukowy, S. & Geroch, S., 1957. On the age of exotic conglomerates at Kruhel Wielki near Przemyśl (Carpathians). *Rocznik Polskiego Towarzystwa Geologicznego,* 26: 297–329. [In Polish, with English summary.]

Burzewski, J., 1966. Les marnes à Baculithes sur le fond de la lithostratigraphie des à Inocérames dans les Carpathes de skibas". *Zeszyty Naukowe AGH, Geologia*, 7: 89–115. [In Polish, with French summary.]

Chlebowski, T., Obtułowicz, J. & Wdowiarz, J., 1937. Carte géologique des Karpathes Occidentales dans les environs de Rzeszów, Tyczyn et Ropczyce. *Kosmos A*, 62: 669–683.

Clark, J. D. & Pickering, K. T., 1996. Architectural elements and growth patterns of submarine channels: application to hydrocarbon exploration. *American Association of Petroleum Geologists Bulletin*, 80: 194–220.

Deptuck, M. E., Piper, D. J. W., Savoye, B. & Gervais, A., 2008. Dimensions and architecture of Late Pleistocene submarine lobes off the northern margin of East Corsica. *Sedimentology*, 55: 869–898.

Dirnerová, D. & Janočko, J., 2014. Sole structures as a tool for depositional environment interpretation; a case study from the Oligocene Cergowa Sandstone, Dukla Unit (Outer Carpathians, Slovakia). *Geological Quarterly*, 58: 41–50.

Dirnerová, D., Prekopová, M. & Janočko, J., 2012. Sedimentary record of the Dukla Basin (Outer Carpathians, Slovakia and Poland) and its implications for basin evolution. *Geological Quarterly*, 56: 547–560.

Dykstra, M., 2012. Deep-water tidal sedimentology. In: Davis, R. A. & Dalrymple, R. W. (eds), *Principles of Tidal Sedimentology.* Springer, Berlin, pp. 371–396.

Dżułyński, S. & Kotlarczyk, J., 1962. O pogrzęźniętych pręgach falistych (riplemarkach) (On load-casted ripples). *Rocznik Polskiego Towarzystwa Geologicznego*, 32: 147–160. [In Polish, with English summary.]

Dżułyński, S., Kotlarczyk, J. & Ney, R., 1979. Podmorskie ruchy masowe w basenie skolskim. In: Kotlarczyk, J. (ed.), *Poziomy z olistostromami w Karpatach przemyskich. Materiały Terenowej Naukowej Konferencji w Przemyślu: Stratygrafa formacji z Ropianki (fm)*. Powielarnia AGH, Przemyśl, pp. 17–27. [In Polish.]

Dżułyński, S., Książkiewicz, M. & Kuenen, Ph. H., 1959. Turbidites in flysch of the Polish Carpathian Mountains. *Geological Society of America Bulletin*, 70: 1089–1118.

Dżułyński, S. & Sanders, J. E., 1962. Current marks on firm mud bottoms. *Transaction of the Connecticut Academy of Arts and Sciences*, 42: 57–96.

Dżułyński, S. & Walton, E. K., 1965. *Sedimentary Features of Flysch and Greywackes*. Elsevier, Amsterdam, 274 pp.

Flügel, E., 2010. *Microfacies of Carbonate Rocks. Analysis, Interpretation and Application*. Springer, Berlin, 984 pp.

Gardner, M. H., Borer, J. M., Melick, J. J., Mavilla, N., Dechesne, M. & Wagerle, R. N., 2003. Stratigraphic process-response model for submarine channels and related features from studies of Permian Brushy Canyon outcrops, West Texas. *Marine Petroleum Geology*, 20: 757–787.

Gasiński, M. A. & Uchman, A., 2009. Latest Maastrichtian foraminiferal assemblages from the Husów region (Skole Nappe, Outer Carpathians, Poland). *Geologica Carpathica*, 60: 283–294.

Gasiński, M. A. & Uchman, A., 2011. The Cretaceous–Paleogene boundary in turbiditic deposits identified to the bed: a case study from the Skole Nappe (Outer Carpathians, southern Poland). *Geologica Carpathica,* 62: 333–343.

Gasiński M. A., Olshtynska, A. & Uchman, A., 2013. Late Maastrichtian foraminiferids and diatoms from the Polish Carpathians (Ropianka Formation, Skole Nappe): a case study from the Chmielnik-Grabówka composite section. *Acta Geologica Polonica*, 63: 515–525.

Gedl, E., 1999. Lower Cretaceous palynomorphs from the Skole Nappe (Outer Carpathians, Poland). *Geologica Carpathica,* 50: 75–90.

Geroch, S., Krysowska-Iwaszkiewicz, M., Michalik, M., Prochazka, K., Radomski, A., Radwański, Z., Unrug, Z., Unrug, R. & Wieczorek, J., 1979: Sedimentation of

Węgierka Marls (Late Senonian, Polish Flysch Carpathians). *Annales Societatis Geologorum Poloniae*, 49: 105–134. [In Polish, with English summary.]

Ghibaudo, G., 1992. Subaqueous sediment gravity flow deposits, practical criteria for their field description and classification. *Sedimentology*, 39, 423–454.

Grundvåg, S. A., Johannessen, E. P., Hansen, W. H. & Plink-Björklund, P., 2014. Depositional architecture and evolution of progradationally stacked lobe complexes in the Eocene Central Basin of Spitsbergen. *Sedimentology*, 61: 535–569.

Gucik, S., 1963. Profile of the Lower Cretaceous from Bełwin in the Przemyśl Carpathians. *Kwartalnik Geologiczny*, 7, 257–268. [In Polish with English summary.]

Hilber, V., 1885. Randtheil der Karpathen bei Dębica, Ropczyce und Łańcut. *Jahrbuch Kaiserlich-Königlichen Geologischen Reichsanstalt,* 35: 407–428.

Hubbard, S. T., Covault, J. A., Fildani, A. & Romans, B. R., 2014. Sediment transfer and deposition in slope channels: Deciphering the record of enigmatic deep-sea processes from outcrop. *Geological Society of America Bulletin*, 126: 857–871.

Janočko, J., 2001. Turbiditic sedimentary fill of the Central-Carpathian Paleogene Basin. *GeoLines*, 13: 68.

Janočko, J. & Jacko, S., 2001. Turbidite deposit systems of the Central-Carpathian Paleogene Basin. *GeoLines*, 13: 133–140.

Janočko, M., Nemec, W., Henriksen, S. & Warchoł, M., 2013. The diversity of deep-water sinous channel belts and slope valley-fill complexes. *Marine Petroleum Geology*, 41: 7–34.

Jednorowska, A., 1957. On the microfauna of the Inoceramus Beds within the "Skiba" region in the vicinity of Słonne and Wara. *Acta Geologica Polonica*, 7: 303–320. [In Polish, with English summary.]

Kędzierski, M., Gasiński, M. A. & Uchman, A., 2015. Last occurrence of Abathomphalus mayaroensis (Bolli) foraminiferid index of the Cretaceous–Paleogene boundary: the calcareous nannofossil proof. *Geologica Carpathica*, 66: 181–195.

Kędzierski, M. & Leszczyński, S., 2013. A paleoceanographic model for the Late Campanian–Early Maastrichtian sedimentation in the Polish Carpathian Flysch basin based on nannofossils. *Marine Micropaleontology*, 102: 34–50.

Kotlarczyk, J., 1978. Stratigraphy of the Ropianka Formation or of Inoceramian beds in the Skole Unit of the Flysch Carpathians. *Prace Geologiczne*, 108: 1–75. [In Polish, with English summary.]

Kotlarczyk, J., 1988. *Przewodnik LIX Zjazdu PTG w Przemyślu*. Wydawnictwa AGH, Kraków, 298 pp. [In Polish.]

Kotlarczyk, J. & Leśniak, T., 1990. *Lower Part of the Menilite Formation and Related Futoma Diatomite Member in the Skole Unit of the Polish Carpathians*. Instytut Geologii i Surowców Mineralnych AGH, Wydawnictwo Akademii Górniczo-Hutniczej, Kraków, 74 pp. [In Polish, with English summary.]

Kotlarczyk, J. & Śliwowa, M., 1963. On knowledge of the productive Carboniferous formations in the substratum of the eastern part of the Polish Carpathians. *Przegląd Geologiczny*, 11: 268–272. [In Polish, with English summary.]

Książkiewicz, M., 1948. Current bedding in Carpathian Flysch. *Rocznik Polskiego Towarzystwa Geologicznego*, 17: 137–152. [In Polish, with English summary.]

Książkiewicz, M., 1962. *Geological Atlas of Poland. Stratigraphic and Facial Problems. Cretaceous and Early Tertiary in the Polish External Carpathians, 13*. Wydawnictwa Geologiczne, Warszawa. [In Polish, with English summary.]

Książkiewicz, M., 1972. Karpaty. In: *Budowa geologiczna Polski, 4. Tektonika Volume 3*, Wydawnictwa Geologiczne, Warszawa, 228 pp. [In Polish.]

Książkiewicz, M., 1975. Bathymetry of the Carpathian Flysch Basin. *Acta Geologica Polonica*, 25: 309–367.

Książkiewicz, M., 1977. Trace Fossils in the Flysch of the Polish Carpathians. *Palaeontologia Polonica*, 36: 1–208.

Kuenen, P. H. & Migliorini, C. I., 1950. Turbidity currents as a cause of graded bedding. *Journal of Geology*, 58: 91–127.

Leszczyński, S., 1981. Piaskowce ciężkowickie jednostki śląskiej w Karpatach: studium sedymentacji głębokowodnej osadów gruboklastycznych. *Annales Societatis Geologorum Poloniae*, 51: 435–502. [In Polish, with English abstract.]

Leszczyński, S., 1986. Depositional processes of fluxoturbidites on example of the Ciężkowice Sandstone, Polish Carpathians. In: 7th *European Regional Meeting Excursion Guidebook. Ossolineum, Wrocław*, pp. 113–121 & 131–135.

Leszczyński, S., 1989. Characteristics and origin of fluxoturbidites from the Carpathian flysch (Cretaceous–Palaeogene), south Poland. *Annales Societatis Geologorum Poloniae*, 59: 351–382.

Leszczyński, S., 1997. Origin of the Sub-Menilite Globigerina Marl (Eocene–Oligocene transition) in the Polish Outer Carpathians. *Annales Societatis Geologorum Poloniae*, 67: 367–427.

Leszczyński, S. & Malata, E., 2002. Sedimentary conditions in the Siary Zone of the Magura Basin (Carpathians) in the Late Eocene–Early Oligocene. *Annales Societatis Geologorum Poloniae*, 72: 201–239.

Leszczyński, S., Kołodziej, B., Bassi, D., Malata, E. & Gasiński, M. A., 2012. Origin and resedimentation of rhodoliths in the Late Paleocene flysch of the Polish Outer Carpathians. *Facies*, 58: 367–387.

Leszczyński, S., Malik, K. & Kędzierski, M., 1995. New data on lithofacies and stratigraphy of the siliceous and fucoid marl of the Skole Nappe (Cretaceous, Polish Carpathians). *Annales Societatis Geologorum Poloniae*, 65: 43–62. [in Polish, with English summary.]

Lowe, D. R., 1982. Sediment gravity flows, 2. Depositional models with special reference to high density turbidity currents. *Journal of Sedimentary Petrology*, 52: 279–298.

Lowe, D.R. & Guy, M., 2000. Slurry-flow deposits in the Britannia Formation (Lower Cretaceous), North Sea: a new perspective on the turbidity current and debris flow problem. *Sedimentology*, 47: 31–70.

Lyle, M. W., 2003. Neogene carbonate burial in the Pacific Ocean. *Paleoceanography*, 18: PA1059.

Łapcik, P. 2017. Facies heterogeneity of a deep-sea depositional lobe complex: case study from the Słonne section of Skole Nappe, Polish Outer Carpathians. *Annales Societatis Geologorum Poloniae*, 87, 301–324.

Łapcik, P., 2018. Sedimentary processes and architecture of Upper Cretaceous deep-sea channel deposits: a case from the Skole Nappe, Polish Outer Carpathians. *Geologica Carpathica*, 69: 71–88.

Łapcik, P. (in press). Facies anatomy of a progradational submarine channelized lobe complex: semi-quantitative analysis of the Ropianka Formation (Campanian–Paleocene) in Hucisko Jawornickie section, Skole Nappe, Polish Carpathians. *Acta Geologica Polonica*.

Łapcik, P., Kowal-Kasprzyk, J. & Uchman, A., 2016. Deep-sea mass-flow sediments and their exotic blocks from the Ropianka Formation (Campanian–Paleocene) in the Skole Nappe: a case study of the Wola Rafałowska section (SE Poland). *Geological Quarterly*, 60: 301–316.

Malata, T., 1996. Analysis of standard lithostratigraphic nomenclature and proposal of division for Skole unit in the Polish Flysch Carpathians. *Geological Quarterly*, 40: 543–554.

Malata, T., 2001, Jednostka skolska na E od Rzeszowa. *Posiedzenia Naukowe Państwowego Instytutu Geologii*, 57: 60–63. [In Polish.]

Marini, M., Salvatore, M., Ravnås, R. & Moscatelli, M., 2015. A comparative study of confned vs. semi-confned turbidite lobes from the Lower Messinian Laga Basin (Central Apennines, Italy): Implications for assessment of reservoir architecture. *Marine and Petroleum Geology*, 63: 142–165.

Mayall, M., Jones, E. & Casey, M., 2006. Turbidite channel reservoirs – Key elements in facies prediction and effective development. *Marine Petroleum Geology*, 23: 821–841.

McHargue, T., Prycz, M. J., Sullivan, M. D., Clark, J. D., Fildani, A., Romans, B. W., Covault, J. A., Levy, M., Posamentier, H. W. & Drinkwater, N. J., 2011. Architecture of turbidite channel systems on the continental slope: Patterns and predictions. *Marine Petroleum Geology*, 28: 728–743.

Mulder, T., 2011. Gravity processes and deposits on continental slope, rise and abyssal plains. In: Hüeneke, H. & Mulder, T. (eds), *Deep-Sea Sediments. Developments in Sedimentology*, 63: 25–148.

Mulder, T., Migeon, S., Savoye, B. & Faugères, J. C., 2001. Inversely-graded turbidite sequences in the deep Mediterranean. A record of deposits by flood-generated turbidity currents. *Geo-Marine Letters*, 21: 86–93.

Mulder, T., Migeon, S., Savoye, B. & Faugères, J. C., 2002. Inversely-graded turbidite sequences in the deep Mediterranean. A record of deposits by flood-generated turbidity currents. Reply. *Geo-Marine Letters*, 22: 112–120.

Mulder, T., Syvitski, J. P. M., Migeon, S., Faugères, J. C. & Savoye, B., 2003. Marine hyperpycnal flows: initiation, behavior and related deposits. A review. *Marine and Petroleum Geology*, 20: 861–882.

Mutti, E. & Ricci Lucchi, F., 1975. Turbidite facies and facies association. In: Mutti, E., Parea, G. C., Ricci Lucchi, F., Sagri, M., Zanzucchi, G., Ghibaudo, G. & Iaccarino, S. (eds), *Example of Turbidite Facies Associations from Selected Formations of Northern Apennines. 9th International Sedimentological Congress*. International Association of Sedimentologists, Nice, France, pp. 21–36.

Mutti, E., Bernoulli, D., Ricci Lucchi, F., Tineterri, R., 2009. Turbidites and turbidity currents from Alpine 'flysch' to the exploration of continental margins. *Sedimentology,* 56: 267–318.

Mutti, E. & Normark, W. R., 1987. Comparing examples of modern and ancient turbidite systems: problems and concepts. In: Leggett, J. K. & Zuffa, G. G. (eds), *Marine Clastic Sedimentology*. Graham and Trotman, London, pp. 1–38.

Mutti, E. & Normark, W. R., 1991. An Integrated Approach to the Study of Turbidite Systems. In: Weimer, P. & Link, M. H (eds), *Seismic Facies and Sedimentary Processes of Submarine Fans and Turbidite Systems*. Springer, New York, 75–106.

Mutti, E. & Ricci Lucchi, F., 1972. Turbidites of the Northern Apennines, introduction to facies analysis (English translation by T. H., Nilsen, 1978). *International Geology Review,* 20: 125–166.

Mutti, E. & Ricci Lucchi, F., 1972. Turbidites of the Northern Apennines, introduction to facies analysis (English translation by T. H., Nilsen, 1978). *International Geology Review*, 20: 125–166.

Normark, W. R., 1970. Growth patterns of deep sea fans. *American Association of Petroleum Geologists Bulletin*, 54: 2170–2195.

Normark, W. R., 1978. Fan valleys, channels, and depositional lobes on modern submarine fans, characters for recognition of sandy turbidite environments. *American Association of Petroleum Geologists Bulletin*, 62: 912–931.

Normark, W.R., 1987. Depositional models from modern submarine fans and ancient turbidites, interpretation differences or different animals. In: Gorsline, D. S. (ed.), *Depositional Systems in Active Margin Basins*. SEPM Pacific Section, pp. 25–37.

Nowak, W., 1963. Wstępne wyniki badań egzotyków warstw inoceramowych serii skolskiej z niektórych stanowisk Karpat przemyskich i birczańskich. *Geological Quarter*ly, 7: 421–430. [in Polish, with English summary.]

Pickering, K. T., Stow, D., Watson, M. & Hiscott, R., 1986. Deepwater facies, processes and models: A review and classifcation scheme for modern and ancient sediments. *Earth-Science Reviews*, 23: 75–174.

Pickering, K. T., Hiscott, R. N. & Hein, F. J., 1989. *Deep Marine Environments: Clastic Sedimentation and Tectonics*. Unwin Hyman, London, 416 pp.

Pickering, K. T., Hiscott, R. N., Kenyon, N. H., Ricci Lucchi, F. & Smith, R. D. A., 1995. *Atlas of Deep Water Environments: Architectural Style in Turbidite Systems*. Chapman and Hall, London, 334 pp.

Porębski, S. J. & Warchoł, M., 2006. Hyperpycnal flows and deltaic clinoforms – implications for sedimentological interpretations of Late Middle Miocene fill in the Carpathian Foredeep Basin. *Przegląd Geologiczny*, 54: 421–429. [In Polish, with English summary.]

Prekopová, M. & Janočko, J., 2009. Quantitative approach in environmental interpretations of deep-marine sediments (Dukla Unit, Western Carpathian Flysch Zone). *Geologica Carpathica*, 60: 485–494.

Prélat, A., Hodgson, D. M. & Flint, S. S., 2009. Evolution, architecture and hierarchy of distributary deep-water deposits: a high-resolution outcrop investigation from the Permian Karoo Basin, South Africa. *Sedimentology*, 56: 2132–2154.

Rajchel, J., 1989. The geological structure of the San Valley in the Dynów-Dubiecko region. *Biuletyn Państwowego Instytutu Geologicznego*, 361: 11–53. [In Polish, with English summary.]

Rajchel, J., 1990. Lithostratigraphy of the Upper Palaeocene and Eocene sediments from the Skole Unit. *Zeszyty Naukowe AGH 1369, Geologia*, 48: 1–112. [In Polish, with English summary.]

Rea, D. K. & Lyle, M. W., 2005. Paleogene calcite compensation depth in the eastern subtropical Pacific: answers and questions. *Paleoceanography*, 20: PA1012.

Salata, D. & Uchman, A., 2013. Conventional and high-resolution heavy mineral analyses applied to flysch deposits: comparative provenance studies of the Ropianka (Upper Cretaceous–Paleocene) and Menilite (Oligocene) formations (Skole Nappe, Polish Carpathians). *Geological Quarterly*, 57: 649–664.

Salata, D., 2014. Detrital tourmaline as an indicator of source rock lithology: an example from the Ropianka and Menilite formations (Skole Nappe, Polish Flysch Carpathians). *Geological Quarterly*, 58: 19–30.

Shanmugam, G., 2006. Deep-water processes and facies models: Implications for sandstone petroleum reservoirs. Handbook of Petroleum Exploration and Production, 5. Elsevier, Amsterdam, 476 pp.

Shanmugam, G., 2016a. Submarine fans: A critical retrospective (1950-2015). *Journal of Palaeogeography*, 5: 2–76.

Shanmugam, G. 2016b. Slides, Slumps, Debris Flows, Turbidity Currents, and Bottom Currents. Reference Module in Earth Systems and Environmental Sciences, Elsevier online; https://doi.org/10.1016/B978-0-12-409548-9.04380-3 87 pp.

Shanmugam, G. & Moiola, R. J., 1988. Submarine fans: characteristic, models, classification and reservoir potential. *Earth-Science Reviews*, 24: 383–428.

Shanmugam, G. & Moiola, R. J., 1991. Types of submarine fan lobes: models and implications. *American Association of Petroleum Geologists Bulletin*, 75: 156–179.

Siemińska, A., Starzec, K., Godlewski, P. & Wendorff, M., 2018. Sedimentary response to tectonic uplift of the Dukla basin margin recorded at Skrzydlna – the Menilite Beds (Oligocene), Outer Carpathians, S Poland. *Geology, Geophysics & Environment*, 44: 231–244.

Skulich, J., 1986. Badania magmowych skał egzotycznych we wschodnich Karpatach Fliszowych na obszarze Polski. *Kwartalnik Geologiczny*, 30: 135–136. [In Polish.]

Słomka, T., 1986. Analiza sedymentacji warstw cieszyńskich metodami statystyki matematycznej. *Annales Societatis Geologorum Poloniae*, 56: 227–336.

Słomka, T., 1995. Deep-marine siliciclastic sedimentation of the Godula Beds, Carpathians. *Prace Geologiczne PAN*, 139: 132 pp. [In Polish, with English summary].

Słomka, T. & Słomka, E., 2001. Sequences of the lithofacies and depositional intervals in the Godula Beds of the Polish Outer Carpathians. *Annales Societatis Geologorum Poloniae*, 71: 35–42.

Snedden, J. W. & Liu, C., 2010. A compilation of Phanerozoic sea-level change, costal onlaps and recommended sequence designations. *American Association of Petroleum Geologists Search and Discovery*, Article 40594, 3 pp.

Sprague, A. R., Garfield, T. R., Goulding, F. J., Beaubouef, R. T., Sullivan, M. D., Rossen, C., Campion K. M., Sickafoose, D. K., Abreu, V., Schellpeper, M. E., Jensen, G. N., Jennette, D. C., Pirmez, C., Dixon, B. T., Ying, D., Ardill, J., Mohrig, D. C., Porter, M. L., Farrell, M. E. & Mellere, D., 2005. *Integrated slope channel depositional models: the key to successful prediction of reservoir presence and quality in offshore West Africa*. CIPM, cuarto E-Exitep 2005, February 20–23, 2005, Veracruz, Mexico, pp. 1–13.

Stadnik, R., 2007. Facial development of the Krosno Beds in the Mszana Dolna tectonic window (Polish Western Carpathians). *Geologia*, 33: 375–393.

Stadnik, R., 2009a. Sedimentary development of the Cergowa Beds of the Grybów Unit (Klęczany quarry, Polish Western Carpathians). *Geologia*, 35: 23–29.

Stadnik, R., 2009b. *Studium sedymentologiczne warstw uznanych za cergowskie i warstw krośnieńskich wybranych jednostek przedmagurskich Karpat fliszowych na zachód od Dunajca*. Unpublished PhD. Thesis, AGH University of Science and Technology, 149 pp. [In Polish.]

Staňová, S., Soták, J. & Hudec, N., 2009. Markov Chain analysis of turbiditic facies and flow dynamics (Magura Zone, Outer Western Carpathians, NW Slovakia). *Geologica Carpathica*, 60: 295–305.

Stow, D. A. V. & Mayall, M., 2000. Deep-water sedimentary systems: new models for the 21st century. *Marine and Petroleum Geology*, 17: 125–135.

Stow, D. A. V. & Shanmugam, G., 1980. Sequences of fine grained turbidites – comparison of recent deep-sea and ancient flysch sequences. *Sedimentary Geology*, 25: 23–42.

Strzeboński, P., 2015. Late Cretaceous–Early Paleogene sandy-to-gravelly debris flow sand their sediments in the Silesian Basin of the Alpine Tethys (Western Outer Carpathians, Istebna Formation). *Geological Quarterly*, 59: 195–214.

Talling, P. J., Masson, D. G., Sumner, E. J. & Malgesini, G., 2012. Subaqueous sediment density flows: Depositional processes and deposit types. *Sedimentology*, 59: 1937–2003.

Teťák, F., 2008. Paleogene depositional systems and paleogeography of the submarine fans in western part of the Magura Basin (Javorníky Mountains, Slovakia). *Geologica Carpathica*, 59: 333–344.

Teťák, F., 2010. The gravity flow dynamics of submarine fan sedimentation in the Magura Basin of the Western Carpathians (Magura Nappe, Slovakia). *Geologica Carpathica*, 61: 201–209.

Tietze, E., 1883. Beiträge zur Geologie von Galizien. *Jahrbuch Kaiserlich-Königlichen Geologischen Reichsanstalt*, 33: 443–560.

Unrug, R., 1963. Istebna Beds – a fluxoturbiditic formation in the Carpathian Flysch. *Rocznik Polskiego Towarzystwa Geologicznego*, 33: 49–92.

Walker, R. G., 1978. Deep-water sandstone facies and ancient submarine fans – models for exploration and for stratigraphic traps. *American Association of Petroleum Geologists Bulletin*, 62: 932–966.

Warchoł, M., 2007. Depositional architecture of the Magura Beds from the Siary zone, south of Gorlice (Magura Nappe, Polish Outer Carpathians). *Przegląd Geologiczny*, 55: 601–610. [In Polish, with English summary.]

Wdowiarz, S., 1949. Structure géologique des Karpates marginales au sud-est de Rzeszów. *Biuletyn Państwowego Instytutu Geologicznego*, 11: 1–39. [in Polish, with French summary.]

Żytko, K., 1989: The profile of the bore hole Kuźmina 1 (Eastern Carpathians in Poland). *Kwartalnik Geologiczny*, 33, 2, 360–365. [in Polish only.]

Annales Societatis Geologorum Poloniae (2017), vol. 87: 301–324 doi: https://doi.org/10.14241/asgp.2017.017

FACIES HETEROGENEITY OF A DEEP-SEA DEPOSITIONAL LOBE COMPLEX: CASE STUDY FROM THE SŁONNE SECTION OF SKOLE NAPPE, POLISH OUTER CARPATHIANS

Piotr ŁAPCIK

Institute of Geological Sciences, Jagiellonian University, ul. Gronostajowa 3a, 30-063 Kraków, Poland; e-mail: piotr.lapcik@doctoral.uj.edu.pl

Łapcik, P., 2017. Facies heterogeneity of a deep-sea depositional lobe complex: case study from the Słonne section of Skole Nappe, Polish Outer Carpathians. *Annales Societatis Geologorum Poloniae,* 87: 301–324.

Abstract: This article reports on the first detailed study of the Skole Nappe's Ropianka Formation in the Słonne outcrop section along river San. Lithological and micropalaeontological similarities indicate that the sedimentary succession correlates with the formation's Wiar Member of Campanian–late Maastrichtian age. The sedimentary succession, more than 140 m thick, is interpreted as a deep-marine complex of turbiditic depositional lobes and the study reveals its sedimentary anatomy. Six component facies of sediment gravity-flow deposits and their stratigraphic grouping into four facies associations are recognized, with these latter considered to represent deposits of the lobe axial zone, lateral flank zone and featheredge fringe zone, as well as an interlobe outer-fringe zone. Semi-quantitative characterization and comparison of facies associations gives insight into the succession's sedimentary heterogeneity. Six depositional lobes superimposed upon one another are recognized in the stratigraphic succession, and their pattern of vertical stacking is interpreted in terms of dynamic stratigraphy on the basis of the upward succession of facies associations. The stratigraphic arrangement of facies associations is attributed to autogenic morphodynamic changes within the evolving depositional system, although it cannot be precluded that also eustatic and local tectonic forcing came into play. The case study sheds more light on the sedimentary environment, sediment sourcing system and spatial depositional pattern in the Late Cretaceous Skole Basin, where the aggrading seafloor apparently oscillated around the lysocline depth that could be mid-bathyal at that time.

Key words: Deep-marine turbidites, depositional lobes, dynamic stratigraphy, facies analysis, mass-flow deposits, Upper Cretaceous.

Manuscript received 9th May 2017, accepted 20th December 2017

INTRODUCTION

Modern methodology for the analysis of deep-water turbiditic systems relies on the recognition of architectural elements (Pickering *et al*., 1995; Clark and Pickering, 1996; Stow and Mayall, 2000; Johnson *et al*., 2001; Posamentier and Kolla, 2003; McHargue *et al*., 2011), alluding to the methodology postulated originally for fluvial systems (Miall, 1985, 1989). One of the common architectural elements are packages of thick-bedded sandy turbiditic facies, reported from deep-sea fan feeder canyons/valleys, channel-fills, lateral or terminal splays and depositional lobes (Normark, 1970, 1978; Mutti and Ricci Lucchi, 1975; Walker, 1978; Mutti, 1979, 1985; Pickering *et al*., 1986, 1989, 1995; Shanmugam and Moiola, 1991; Mulder, 2011). Such packages may then occur in various parts of a sand-prone submarine system and their diagnostic significance depends strongly upon the scale of exposure and lateral facies context.

Thick-bedded successions of mainly massive sandstone turbidites are common in the Polish Carpathian Flysch (Dżułyński *et al*., 1959; Unrug, 1963; Leszczyński, 1981; Ślączka. and Thompson, 1981; Warchoł, 2007 and references therein), but the poor exposure with widely isolated outcrops has hindered their interpretation as specific parts of a depositional system. In regional studies, the thicker and laterally most extensive packages with little or no evidence of flow channelization are generally considered to represent depositional lobes.

One of such lithostratigraphic units in the Polish Outer Carpathians is the Ropianka Formation (Turonian––Palaeocene) of the Skole Nappe (Fig. 1A). The present field study is from the Słonne section, a 143-m long outcrop of the Ropianka Formation in the eastern bank of river San (Fig. 1B), interpreted herein as representing a stratigraphic complex of laterally shifting depositional lobes. The study has two aims: (1) to distinguish and characterize differing assemblages of turbiditic facies and assign them interpretively to specific zones of depositional lobe (i.e., the axial,

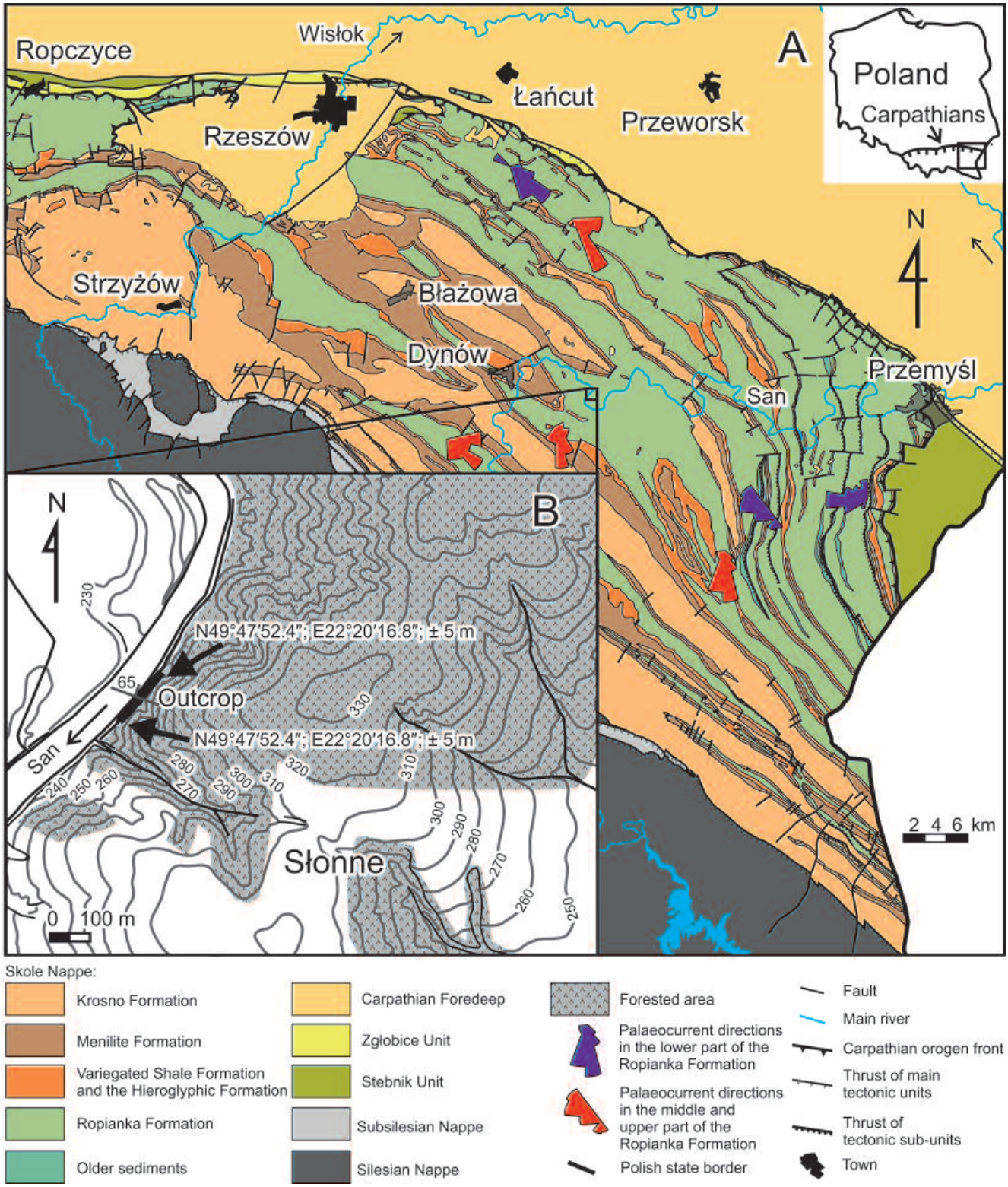

Fig. 1. Location of the study area. **A.** Geological map of the Skole Nappe; compiled from Gucik *et al*. (1980), Jurkiewicz and Woiński (1981), Woiński (1994) and Niescieruk *et al*. (1995), with palaeocurrent directions after Bromowicz (1974). **B**. Location of the Słonne outcrop section at the bank of river San.

flank, fringe and interlobe zones); and (2) to analyse further the vertical changes of facies assemblages in the stratigraphic section as a hypothetical record of the lateral shifting of depositional lobes. This case study contributes to the general knowledge on the facies heterogeneity of turbiditic depositional lobes and their complexes.

THE ROPIANKA FORMATION

The Skole (or Skyba) Nappe is the northernmost major tectono-stratigraphic unit of the Polish Outer Carpathians, known also as the Polish Flysch Carpathians. The term "flysch", as defined by Dżułyński and Smith (1964), denotes a group of deep-marine facies dominated by deposits of sediment gravity flows. The flysch of the Skole Nappe represents a deep-water basin that formed in the Early Cretaceous as the northern branch of the Tethys and existed until the Miocene (Fig. 1), when the northward movement of the Apulian Plate closed the remnant Outer Carpathian basin (Golonka *et al*., 2006). The Skole Nappe, thrust northwards over the Carpathian Foredeep, was internally folded and cut by internal thrusts (Książkiewicz, 1972; Kotlarczyk, 1978, 1988).

In the Turonian, tectonic activity in the Skole Basin and its hinterland initiated deposition of the flysch of the Ropianka Formation upon an extensive unit of late Cenomanian radiolarian shales (Fig. 2; Kotlarczyk, 1978, 1988; Malata and Poprawa, 2006). The sedimentation of the Ropianka Formation, known also as the Inoceramian Beds, proceeded until the early Palaeogene (Fig. 2). The sedimentation history of the Ropianka Formation comprised three phases, each starting with the deposition of calcareous flysch facies and ending with the deposition of siliciclastic flysch facies (Kotlarczyk, 1978, 1988).

The Ropianka Formation is up to 1.6 km thick and shows a marked facies change across the basin. With respect to the orogen interior, some authors have distinguished an "internal zone" dominated by sandstones with sparse marlstone intercalations, and an "external zone" with widespread marlstones and with evidence of slumping and debris flows (e.g., Burzewski, 1966; Kotlarczyk, 1978). The present study is from the internal zone. The sediment was generally derived from the NW, N and NE (see palaeocurrents in Fig. 1A; Książkiewicz, 1962; Bromowicz, 1974; Kotlarczyk, 1978, 1988), and the compositional diversity of source terrane is reflected in the wide range of exotic debris in the turbidites, debrites and slump deposits (Kropaczek, 1917; Bukowy, 1957a, b; Bukowy and Geroch, 1957; Kotlarczyk and Śliwowa, 1963; Nowak, 1963; Bromowicz, 1974; Dżułyński *et al*., 1979; Skulich, 1986; Malata, 2001; Łapcik *et al*., 2016) as well as in the variation of detrital heavy-mineral suites (Salata and Uchman, 2013; Salata, 2014).

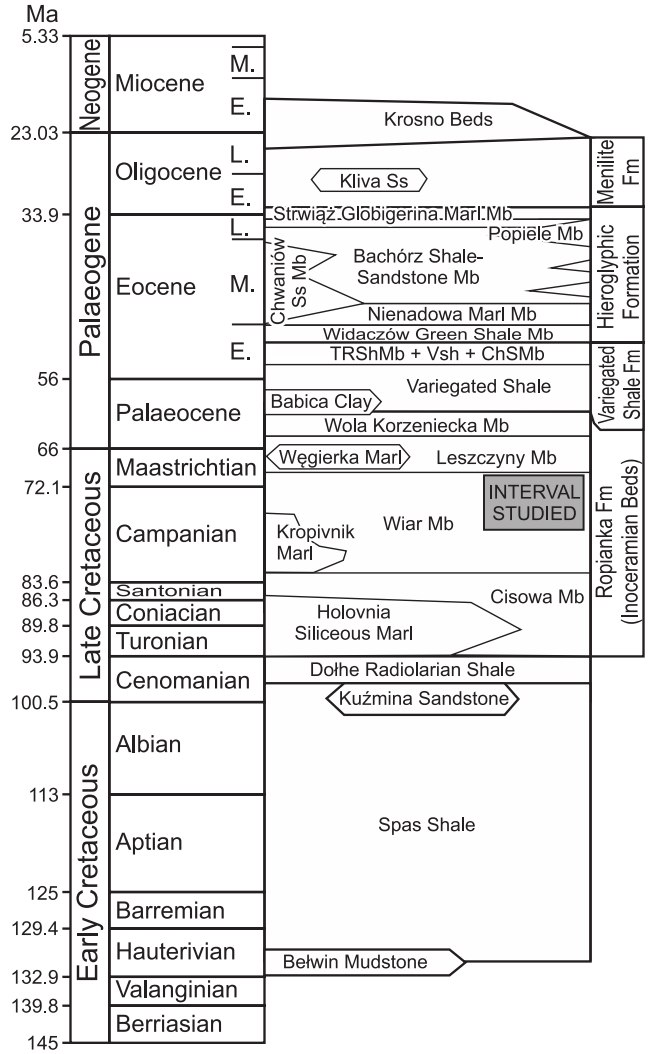

Fig. 2. Stratigraphy of the Skole Nappe, based on Kotlarczyk (1988), Rajchel (1990), Rajchel and Uchman (1998) and Ślączka and Kaminski (1998), with modifications by Gedl (1999) and Kotlarczyk *et al*. (2006). The time scale is according to Gradstein *et al*. (2012). Abbreviations: TRSh Mb – Trójca Red Shale Member; VSh – Variegated Shale; and ChS Mb – Chmielnik Stripy Sandstone Member.

THE SŁONNE SECTION

The Słonne outcrop section studied is in the right-hand bank of river San, about 7 km to the east of the town of Dynów (Fig. 1). The river-escarpment outcrop is more than 150 m long and up to 12 m high, showing flysch beds tectonically tilted to the NNE (general dip 020/65°). The outcrop section exposes the northern limb of the Słonne Anticline (Rajchel, 1989). Since the Skole Nappe is strongly folded and disrupted by internal thrusts (Wdowiarz, 1939; Jednorowska, 1957; Rajchel, 1989), spatial stratigraphic correlations are a formidable task. Biostratigraphic dating is sparse and its age-resolution insufficient. Local drilling cores (see boreholes Słonne 1, 4 and 9–12 in Jednorowska, 1957) and surface mapping (Rajchel, 1989) in the close surroundings of the study area suggest that the investigated stratigraphic section corresponds to the Wiar Member (Campanian–early Maastrichtian) and possibly the lower part of the overlying Leszczyny Member (late Maastrichtian–earliest Palaeocene) of the Ropianka Formation (Fig. 2). Lithological similarity to Rajchel's (1989) stratigraphic "Complex I" favours correspondence to the middle to upper Wiar Member (Fig. 2).

The outcrop section shows alternating intervals, from a couple of metres to more than 10 m thick, that range from thick-bedded amalgamated sandstones to thin-bedded heterolithic deposits with mudstone and marlstone interlayers (Fig. 3). Local gaps in the outcrop are due to the riverbank collapse, modern fluvial cover or low relief, which suggests mainly mud-rich intervals of the section (Fig. 3).

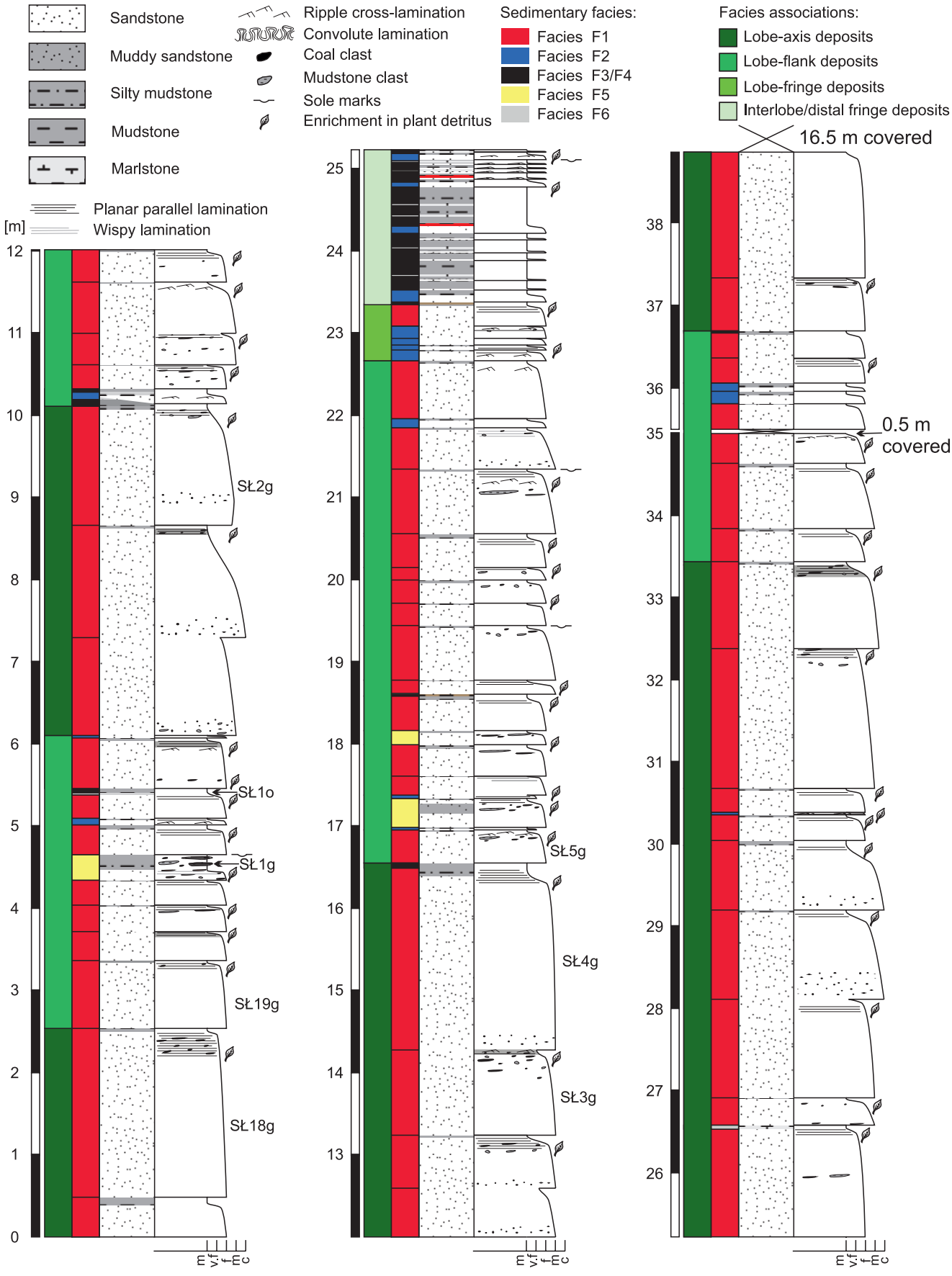

Fig. 3. Detailed sedimentological log of the Ropianka Formation in the Słonne outcrop section, with the distinction of sedimentary facies and their associations (see legend). Symbols SŁo along the log indicate samples taken for micropalaeontological analysis and symbols SŁg indicate samples taken for grain-size analysis. Continuation in the next pages.

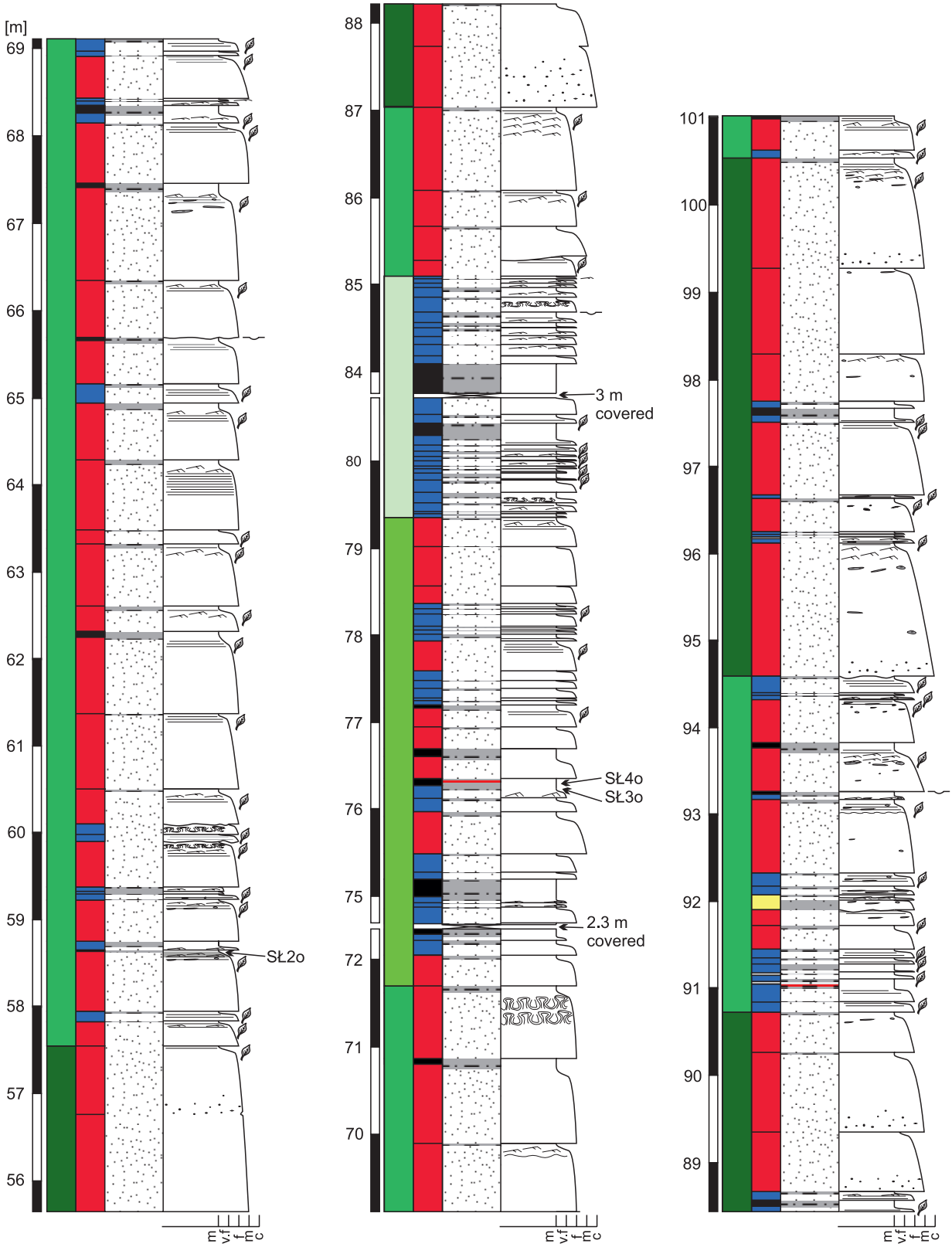

Fig. 3. Continuation from the previous page.

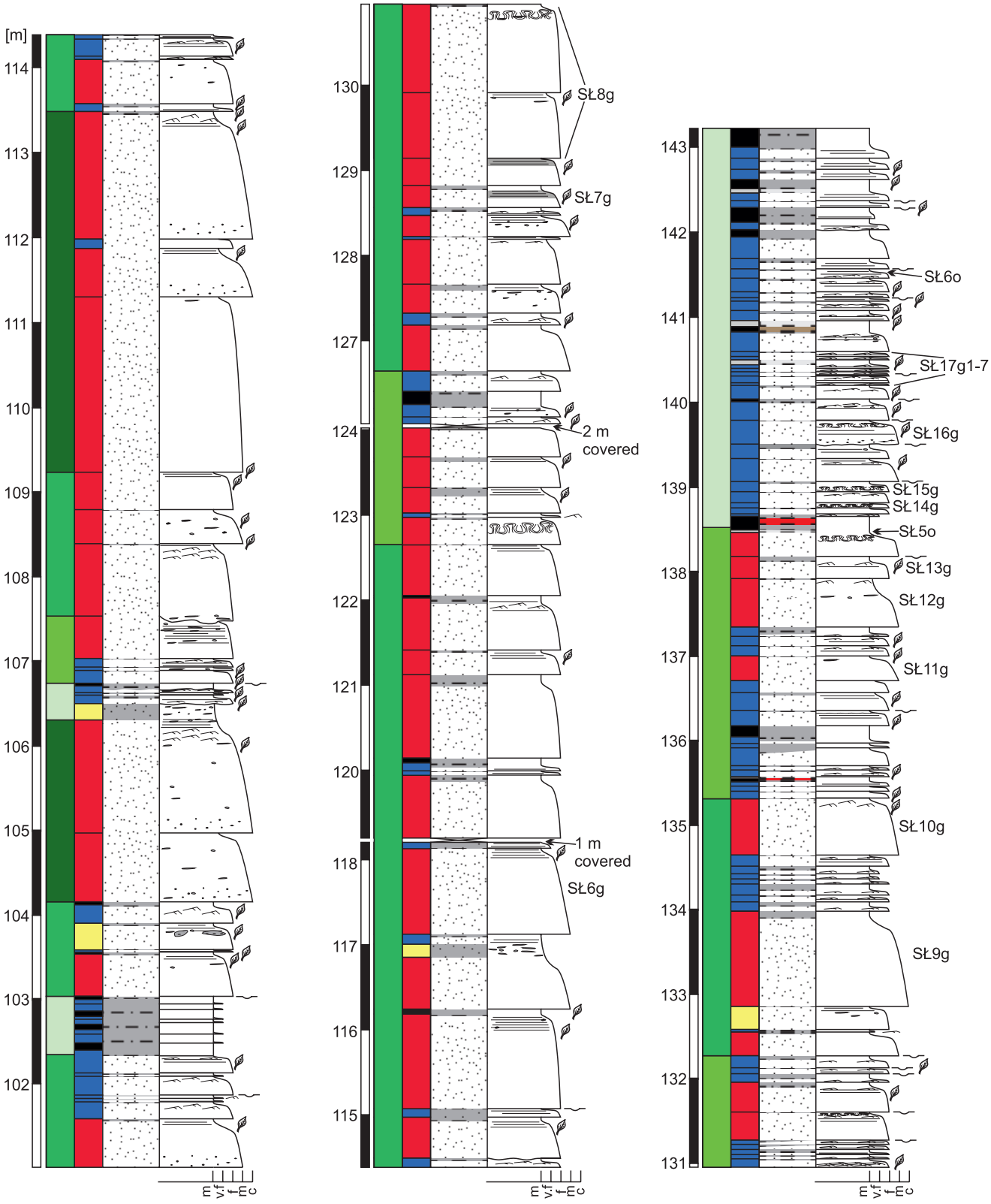

Fig. 3. Continuation from the previous page.

Sandstones are yellowish-white to rusty orange, calcareous quartz arenites. Most of them are poorly cemented, as is typical of the Ropianka Formation (Bromowicz, 1974). In addition to quartz, the sandstones contain grains of muscovite, glauconite, biotite, feldspar, pyrite, coal debris and plant detritus, as well as fragments of siliceous rocks, metamorphic green schists, grey mudstone and tests of agglutinated foraminifers. Petrographic studies (Bromowicz, 1974, 1986) show little regional variation in the mineral composition of sandstones in the Ropianka Formation. Current-ripple cross-lamination in sandstone beds indicates sediment transport direction generally from the north.

METHODS AND TERMINOLOGY

The fieldwork focused on a detailed logging of the stratigraphic succession, with special attention given to the texture and primary structure of deposits, which allowed distinguishing a range of sedimentary facies. The descriptive sedimentological terminology is after Harms *et al.* (1975) and Collinson and Thompson (1982). Bed thickness categories are after Nichols (2009), with very thin (<1 cm), thin (1–10 cm), medium (10–30 cm), thick (30–100 cm) and very thick (>100 cm) classes. Statistical terminology is after Davis (2002).

Sedimentary facies are basic types of deposits distinguished on the descriptive basis of their bulk macroscopic characteristics (Walker, 1984). When dealing with episodic "event sedimentation" (*sensu* Dott, 1983), as in the present case of a flysch succession, the distinction of facies pertains to the products of individual sedimentary gravity-flow events and inter-flow episodes of background sedimentation (e.g., see Janbu *et al.*, 2007). Differing assemblages of spatially and temporarily related facies are regarded as facies associations and considered to represent specific zones (subenvironments) of the sedimentary system. For simplicity, they are given interpretive genetic labels, but their descriptions are separated from interpretations in the text.

In order to determine vertical grain-size trends, particularly in massive sandstone beds, 80 sandstone samples were collected, disintegrated and processed by sieve analysis**.** Clay fraction was removed by washing on 0.05-mm sieve. After drying, the clay-free sediment was passed through a column of standard sieves with apertures of 2, 1, 0.5, 0.25, 0.1 and 0.063 mm. In addition, eleven thin sections of fine-grained sandstones, marlstones and mudstones were analysed for mineral composition and grain-size characteristics. Thin sections perpendicular to bedding were used to measure the grain size by the conventional grid technique with an optical microscope. The longest dimension of 300 grains was measured in each thin section. This technique gives reasonably good estimates, but has its limitations (Johnson, 1994). For details of sedimentary and bioturbation structures, 24 rock slabs were collected, cut smooth and analysed macroscopically.

As many as 377 measurements of magnetic susceptibility were made, mainly on massive sandstone beds and in a 20-cm interval, in order to recognize possible sub-macroscopic sediment grading. The measurements were taken with a ZM Instrument's SM30 magnetic susceptibility meter, using a resolution interpolation mode of 10^{-7} and a correction for the estimated air gap between the measuring device and the rock. However, the analytical procedure involves some assumptions and the dataset thus cannot be claimed to be free of systematic error.

Six mudstone samples were collected for micropalaeontological analysis of foraminifers in attempt to determine the biostratigraphic age of deposits. These samples were disintegrated with the Glauber salt and their foraminifer assemblages were analysed on quantitative basis.

SEDIMENTARY FACIES

Sedimentological analysis of the detailed outcrop log allowed distinguishing six sedimentary facies, F1–F6 (Fig. 4), on the basis of the deposit texture, structures, bed thickness, bed upward grain-size trend and mud-content change

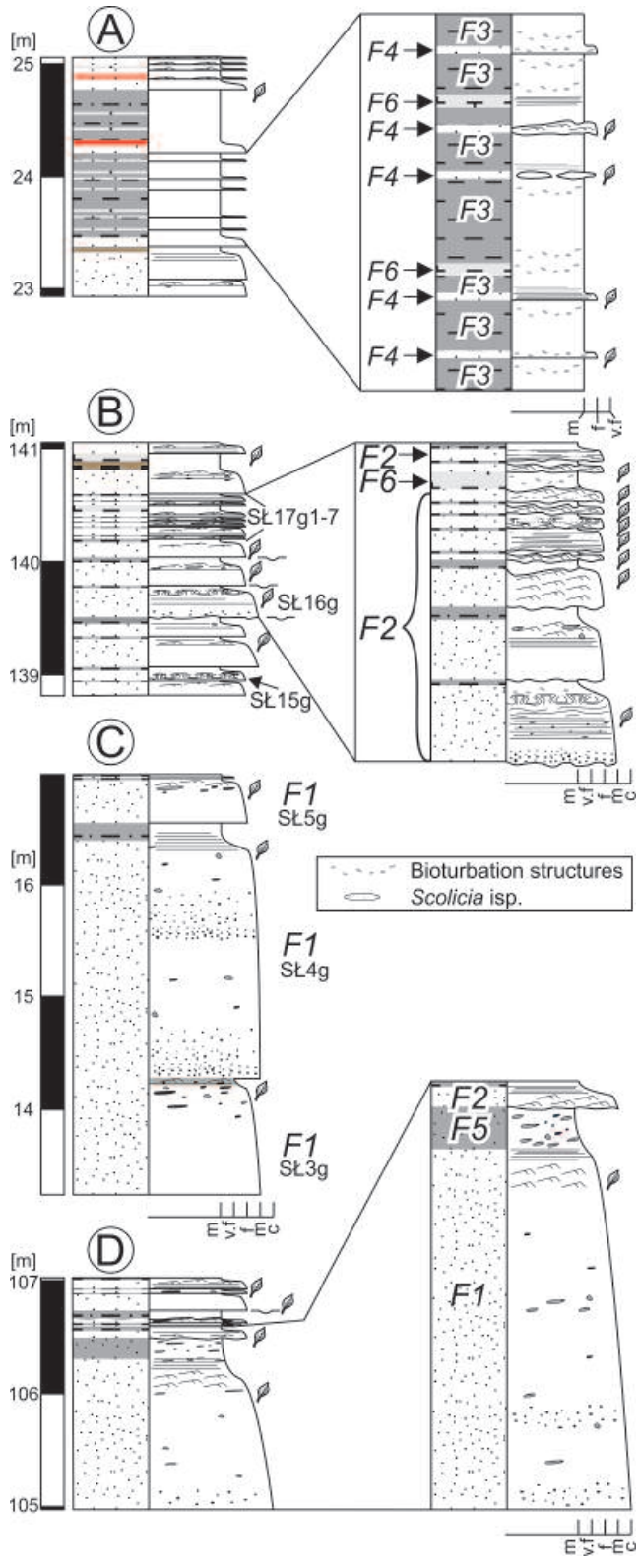

Fig. 4. Selected portions **A**–**D** of the outcrop log (log heights as in Fig. 3) showing examples of the sedimentary facies F1–F6.

(Fig. 5), with an additional attempt to use also magnetic susceptibility signature. The distribution of facies in the stratigraphic log is shown in Figure 3. In this section of the article, the sedimentary facies are described and interpreted in terms of their mode of deposition.

Facies F1

Description: This facies consists of coarse- to very fine-grained, medium- to very thick-bedded sandstones (Figs 4, 6A). Sandstone beds are tabular on the outcrop scale, with sharp and visibly erosional lower boundaries. Sole marks occur, but the bed soles in most cases are poorly exposed. The majority of beds show normal grading with chaotically distributed pebble-sized coal and mudstone clasts, although some beds are non-graded or slightly inverse-graded (Fig. 5). Bed amalgamation is indicated by an abrupt grain-size increase or by the occurrence of lamination between consecutive massive bed divisions. The mud content of massive divisions ranges from 15 to 30 wt.% and reaches 40 wt.% in some cases (Fig. 5).

Mudstone and coal clasts are largest and most abundant towards the top of massive bed divisions. They are oriented mainly parallel to bedding and tend to be concentrated in discrete horizons (Fig. 6B). Mudclasts are recognizably intraformational, reaching up to 20 cm in length. Some of the largest mudstone clasts include laminated siltstone

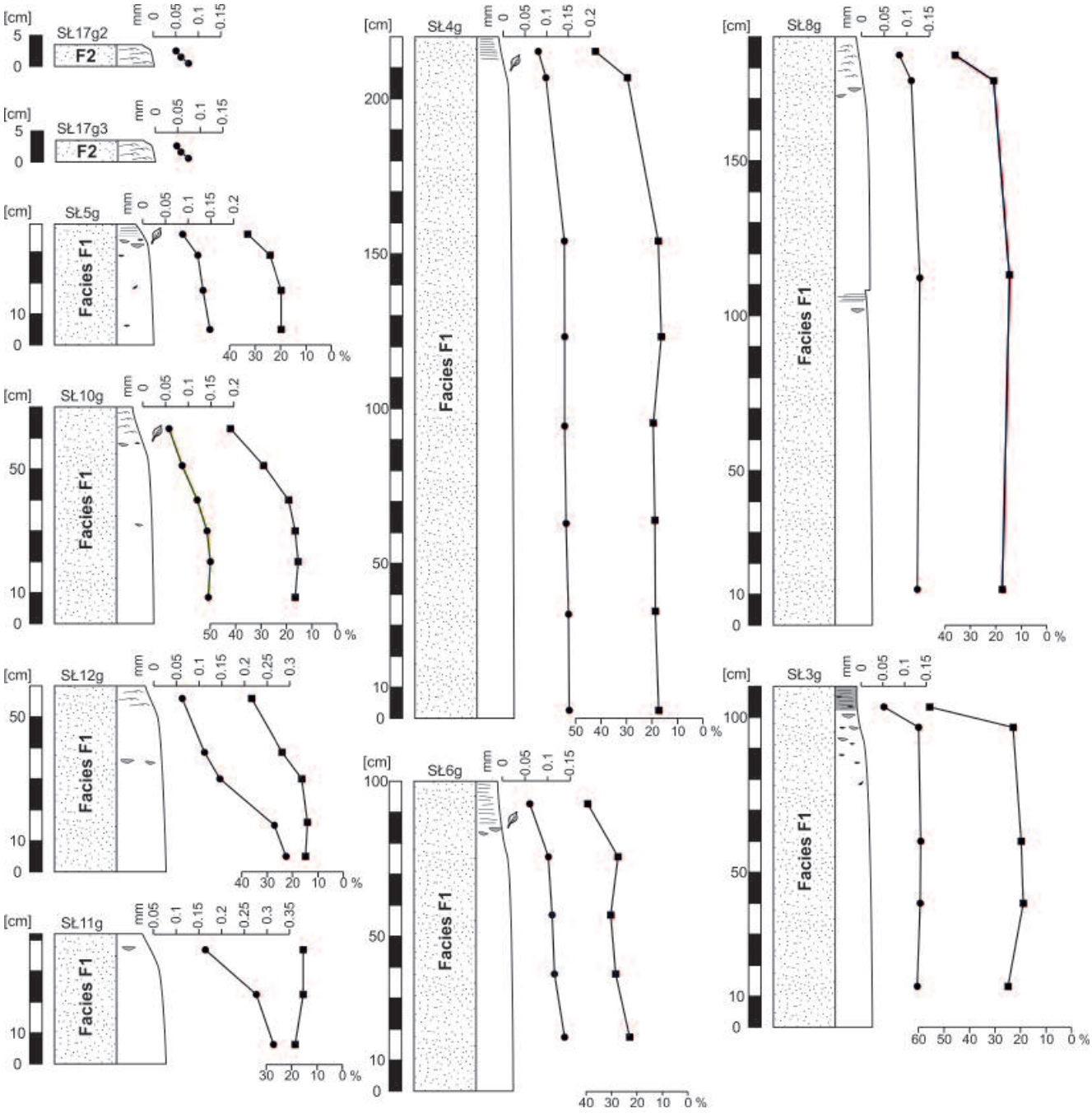

Fig. 5. Sediment grain-size and mud-content trends in the sandstone beds of facies F1, F2 and F5. The plot with circular dots indicates the sediment mean grain size (mm) and the plot with square dotes indicates mud content (wt.%). Continuation in the next pages.

layers and seem to have been derived by erosion of the thin-bedded deposits of alternating facies F3 and F4 (described farther in the text). Bed top divisions show planar parallel lamination and/or ripple cross-lamination (Fig. 6C) and as such resemble beds of facies F4, but differ from the latter by capping gradationally a massive and generally much thicker bed division. The laminated top division often passes upwards into a siltstone/mudstone cap, although the latter is lacking in all cases of sandstone bed amalgamation. The upward increase of the amount of coalified plant detritus in many beds makes their top division an alternation of the brownish-black sandy bands with concentrated mudstone and coal clasts, 0.5 to 3 cm thick, and similar bands of laminated fine-grained 'clean' sand, often with some hydroplastic deformation (Fig. 6D).

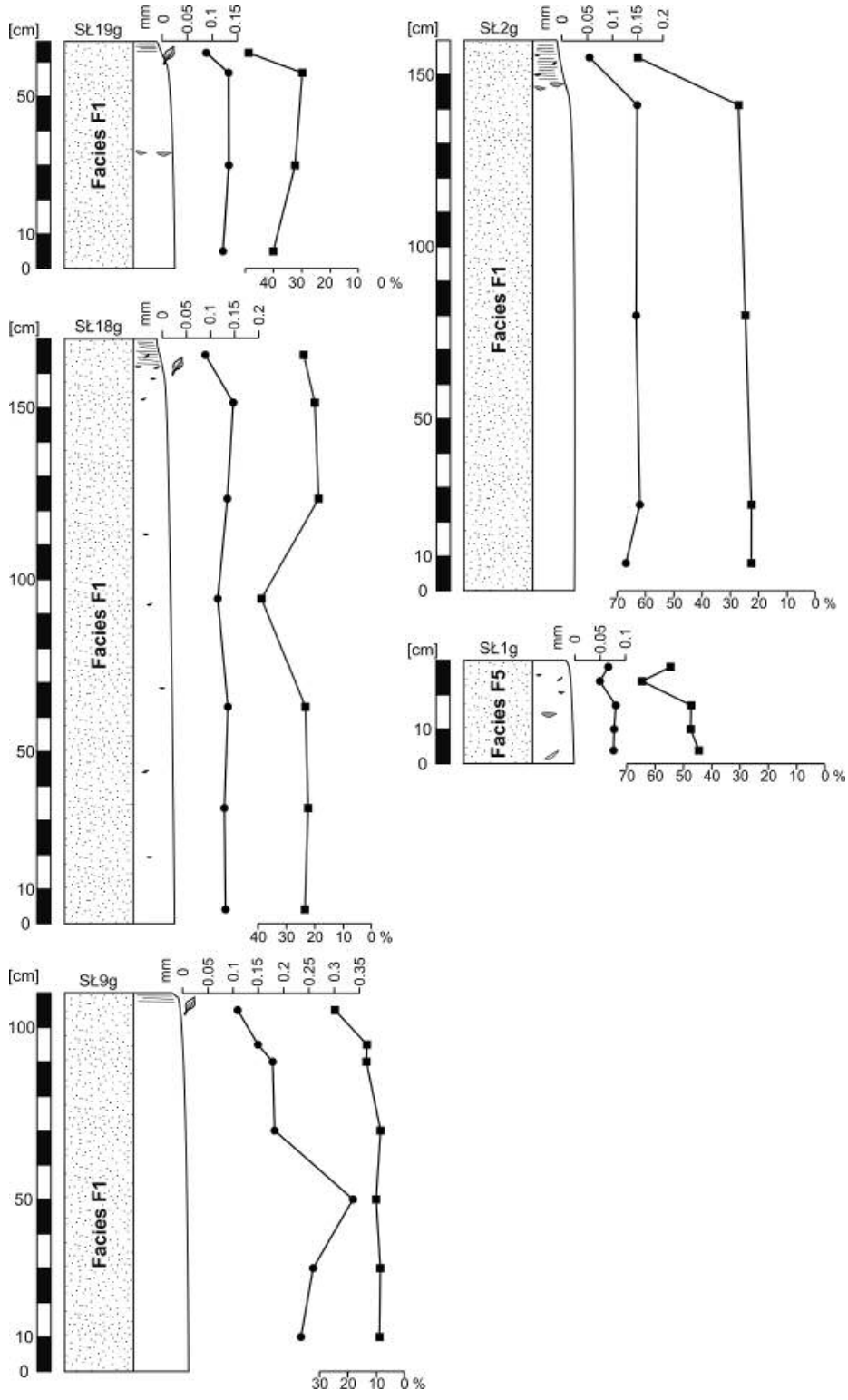

Fig. 5. Continuation from the previous page.

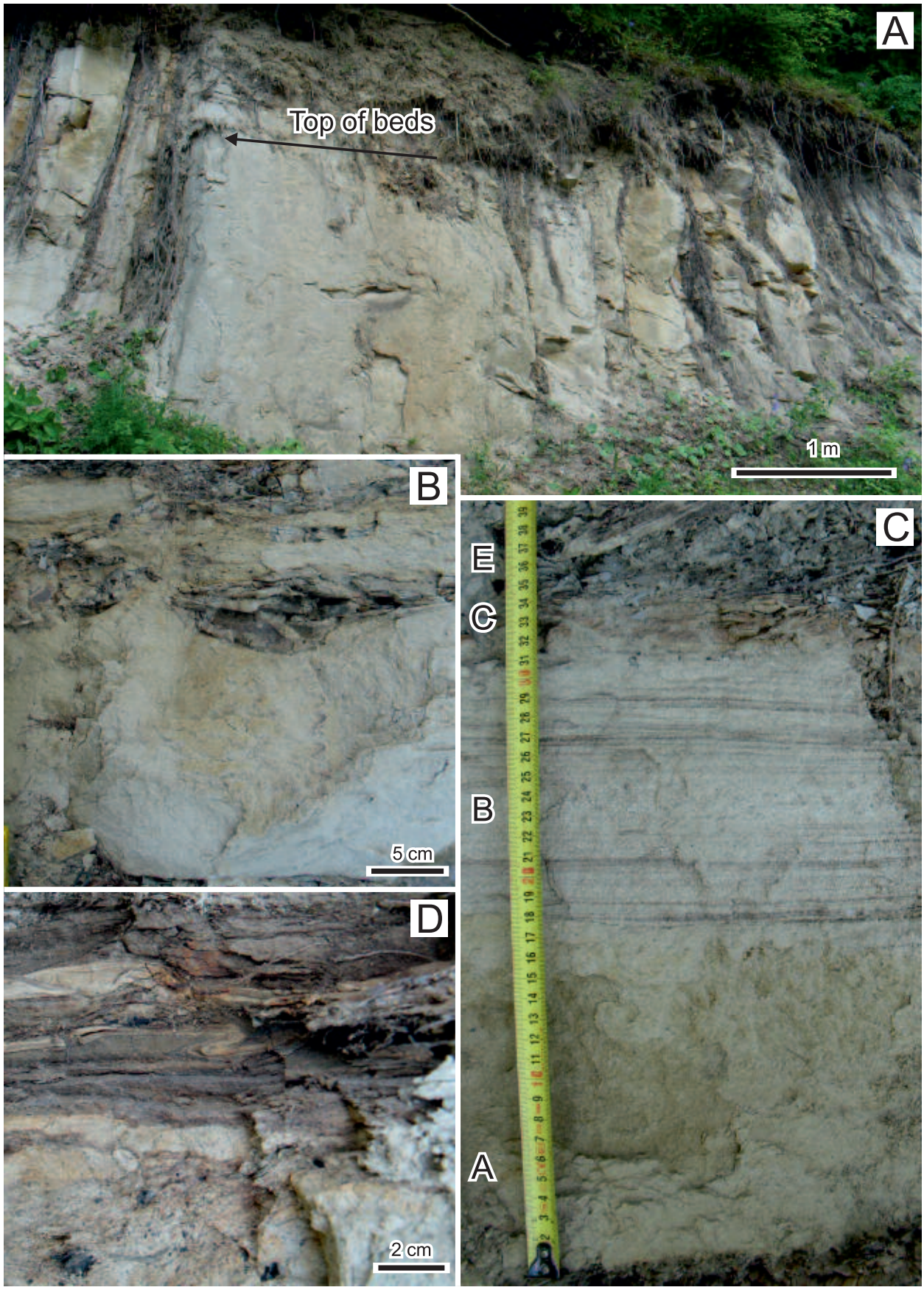

Fig. 6. Examples of the deposits of facies F1. **A**. Typical thick massive sandstone bed. **B**. Massive sandstone bed rich in bedding-parallel mudclasts at its top. **C**. Massive sandstone bed (A) with planar-laminated (B) to ripple cross-laminated (C) upper part capped with grey mudstone (E). **D**. The top part of a massive sandstone bed showing an alteration of dark brownish bands of massive sand rich in plant detritus and lighter-colour bands of parallel-laminated sand, with some hydroplastic deformation.

Interpretation: The deposits of facies F1 are interpreted as products of high-density turbidity currents (*sensu* Lowe, 1982), inevitably capped with a laminated deposit of the final phase of low-density flow (cf. Talling *et al*., 2012). The thick massive lower division of the sandstone beds of facies F1 is comparable to Bouma's (1962) turbidite division A and corresponds to the S_3 division of Lowe (1982). This massive division was formed by a rapid, non-tractional dumping of sand from a highly concentrated turbulent flow (see also Lowe, 1988; Allen, 1991). The occasional non-graded or weakly inverse-graded massive divisions may represent the high-density "moving-bed" part of a relatively thin flow (Vrolijk and Southard, 1997). Inverse grading may as well indicate a waxing flow (Kneller and Branney, 1995; Mulder *et al*., 2001).

As the rapid dumping hugely depleted the flow sediment load, a subsequent low-density phase of substrate reworking and tractional deposition occurred (Lowe, 1982), demarcated by grain-size fining and flow dissipation (see also Sumner *et al*., 2008). The planar parallel-laminated and/or ripple cross-laminated top division of sandstone beds corresponds to the Bouma turbidite divisions B and C, respectively, and represents deposition from low-density tractional flow (Harms *et al.*, 1975; see tractional division T_t of Lowe, 1982; also Best and Bridge, 1992; Leclair and Arnot, 2005). The fine-grained sandy to muddy capping, only occasionally preserved, comprises Bouma divisions CD(E) and resembles the independent thin beds of facies F2 (described farther in the text).

The emplacement of large intraformational mudclasts and plant debris, concentrated in the top part of massive bed divisions, occurred apparently along the rheological interface between the high-density lower part and low-density upper part of the flow (see Postma *et al.,* 1988). The interface was probably fluctuating and generally rising, as suggested for the origin of dark/light turbidite banding by Lowe and Guy (2000). Such an upward concentration of mudclasts in discrete bands (Fig. 6D) is considered typical of high-density turbidity currents (Talling *et al*., 2012). Clasts dispersed randomly within the bed lower massive division were probably arrested therein by high sediment concentration and unable to float upwards to the flow rheological interface.

The bed-top banding indicates fluctuating sustained (long-duration) turbidity currents (Lowe and Guy, 2000), which – together with the abundance of plant detritus – may suggest delta-derived hyperpycnal flows (Mulder *et al*., 2001, 2002, 2003; Porębski and Warchoł, 2006; Zavala *et al*., 2012). No shallow-marine equivalents of the Ropianka Formation have thus far been documented and are rather unlikely to be preserved, but an occurrence of shelf-margin deltas in the high-relief narrow Skole Basin cannot be precluded.

Facies F2

Description: This facies consists of thin- to medium-bedded, medium- to very fine-grained sandstones (Fig. 4). Bed thicknesses are lower than in facies F1 and highly uneven on the outcrop scale, with occasional lateral pinch-outs. Bed lower boundaries are invariably sharp and erosional, with abundant sole marks (where exposed). These sandstone beds show normal grading with plane-parallel lamination, often wavy, and with ripple cross-lamination (often climbing ripples) and frequent convolutions (Fig. 7A, B). Only some beds are massive in their basal part. Sand laminae commonly alternate between 'dark', rich in coalified plant detritus, and 'light' dominated by clean quartz sand. The dark laminae have a less steep dip than the light ones (Fig. 7C). Bed tops sporadically include small flaky mudstone chips, oriented parallel to the planar or cross-lamination. The sandstone beds are capped with a calcareous siltstone and mudstone, occasionally containing scattered coaly detritus and showing wispy planar lamination. Bioturbation abounds at the lower bed boundaries, represented mainly by *Ophiomorpha* isp. and *Thalassinoides* isp. The endichnial trace fossils often disturb or virtually destroy primary sedimentary structure, particularly in thin beds (Fig. 7A, B) where bedding-parallel *Scolicia* isp. dominates. Other recognizable trace fossils are *Chondrites* isp. and *Planolites* isp. Convolute lamination is common, involving deformation of trace fossils (Fig. 7A) and indicating an early post-depositional sediment disturbance by dewatering and some loading (cf. Dżułyński and Walton, 1965).

Interpretation: Facies F2 is interpreted as deposits of smaller-volume, high- to mainly low-density turbidity currents (*sensu* Lowe, 1982; see also Talling *et al.*, 2012). Deposits of high-density flows, with a graded basal massive division, are subordinate. Most common are sandstone beds with the Bouma division B and/or C at the base, passing upwards into a muddy divisions D(E). Turbidites $T_{CD(E)}$ dominate, which indicates fully turbulent, tractional flows with a moderate to high (climbing ripples) rate of sediment suspension fallout (Ashley *et al*., 1982; Lowe, 1982; Talling *et al.,* 2012).

Facies F3

Description: This facies consists of light- to dark-grey (locally greenish, yellowish or reddish brown) mudstones forming beds a few centimetres thick, rarely thicker than 5 cm (Figs 6C, 7C). Their lower boundary is mainly gradational, but their sand-covered top is sharp. These siliciclastic mudstone beds are slightly calcareous to non-calcareous and typically massive (non-laminated), bearing an admixture of muscovite, plant detritus, foraminifers, pyrite and small siderite concretions or diffuse sidertic impregnations. Trace fossils abound, but the only identifiable are *Chondrites* isp., *Ophiomorpha* isp., *Thalassinoides* isp. and *Planolites* isp. This sedimentary facies occurs at the top of sandstone-dominated bed packages, where it alternates with facies F2, F4 or F6 (Fig. 3) and sporadically also overlies beds of facies F1 and F5.

Interpretation: Similar muddy deposits in deep-sea facies models are commonly ascribed to a post-turbiditic hemipelagic to pelagic sedimentation (e.g., Bouma, 1962; Mutti and Ricci Lucchi, 1975; Stow and Shanmugam, 1980; Pickering *et al*., 1986). Beds with an upward decrease of

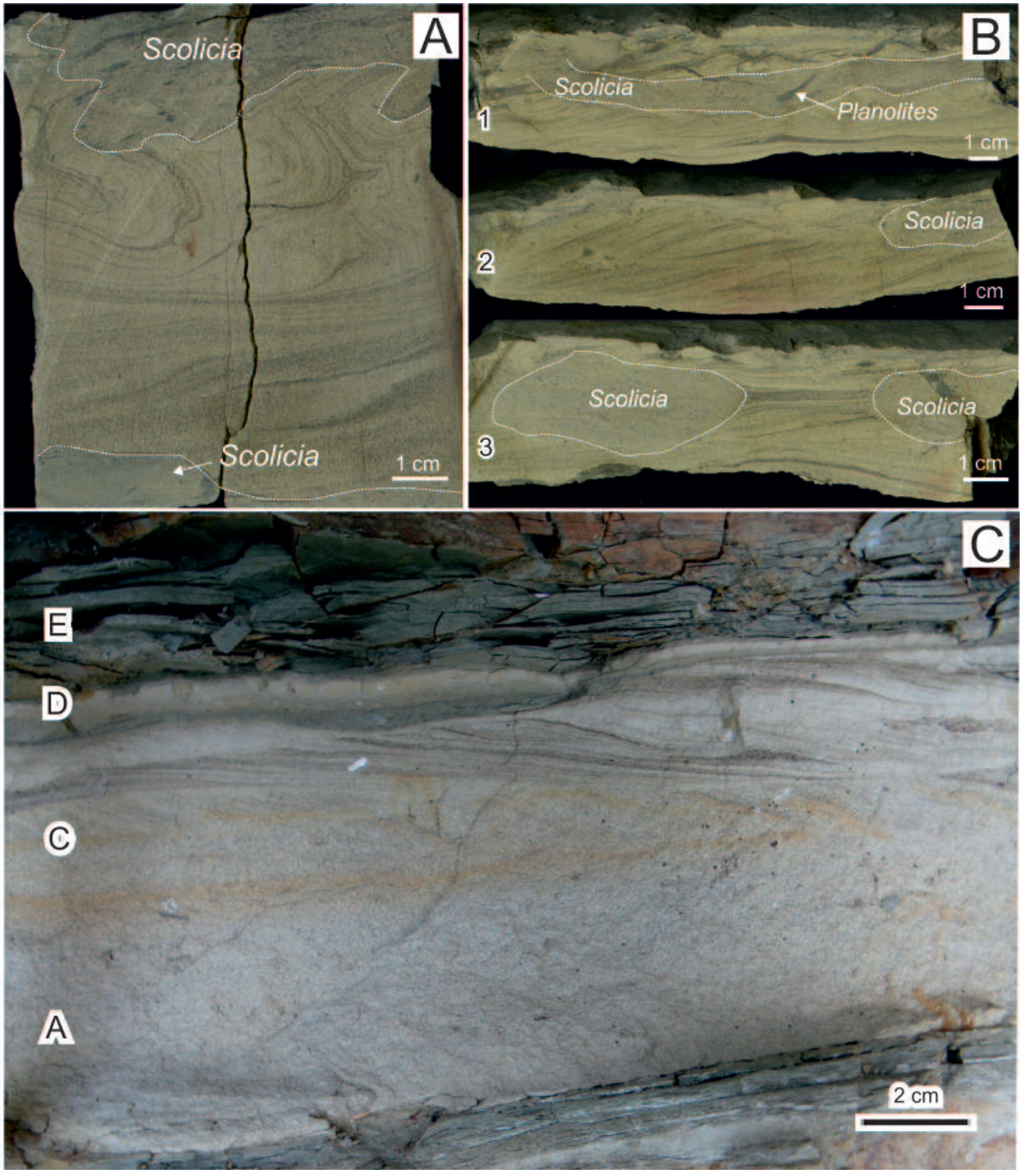

Fig. 7. Examples of the thin-bedded deposits of facies F2. **A.** Fully laminated and hydroplastically deformed bed with *Scolicia* traces. **B.** Three laminated beds (1–3) with trace fossils *Scolicia* and *Planolites*. **C.** Somewhat atypical turbidite bed T_{ACDE}.

calcium carbonate content suggest deposition around the lysocline. The calcareous lower part of these mudstone beds would be derived as turbidity-current suspension, whereas their non-calcareous upper part would represent basin background sedimentation. The abundance of trace fossils indicates well-oxygenated seafloor conditions.

Facies F4

Description: This facies is represented by beds of fine- to very fine-grained calcareous sandstone and siltstone, with thicknesses not exceeding 2 cm (Fig. 4). These beds only rarely pinch out laterally on the outcrop scale. Beds have

sharp lower boundary and show normal grading (Fig. 8A) with mainly planar parallel and/or ripple cross-lamination. They are gradationally capped by a wispy-laminated mudstone rich in plant detritus (Fig. 8B). Many beds are cut across by the trace fossils *Chondrites* isp., *Ophiomorpha* isp., *Thalassinoides* isp. and *Planolites* isp., and some beds are totally bioturbated. Facies F4 occurs mainly as solitary beds in the upper part of sandstone-dominated bed packages, where it alternates with facies F2, F3, F6 and rarely F1.

Interpretation: This facies is interpreted as thin classical turbidites $T_{(B)CDE}$ deposited by low-density turbidity currents (*sensu* Lowe, 1982). Their mode of deposition, with a gradual change from traction to suspension fallout, indicates waning surge-type flows. Such turbidites may represent: (1) the dilute tail of a bypassing larger and denser turbidity current; (2) the overbank spill-out of channelized flow; (3) the lateral pinch-out of a thinly spread turbidity current; or possibly (4) deep-water tidal or contour currents (Talling *et al*., 2012; Shanmugam, 2016). The first two possibilities are unlikely in the present case, because facies F4 is not associated with erosional bypass surfaces and there are no recognizable palaeochannels in the Słonne section. However, an evidence of palaeochannels is found in the advancing younger part of the Ropianka Formation (Łapcik, 2018), which renders the third possibility of unconfined flow spreading most probable, albeit also the last possibility cannot be precluded.

Facies F5

Description: This subordinate facies forms medium to thick beds of fine- to very fine-grained sandstone with chaotically dispersed plant detritus and randomly oriented clasts of mudstone and coal, up to large pebble size. Relatively high content of mud (Fig. 5) contributes to the dark grey colour of the deposit. Bed bases are flat to wavy and not recognizably erosional, and also their tops are flat to wavy (Fig. 9A). The beds are massive and lack grading, but tend to be capped by the Bouma turbidite divisions CDE (Fig. 9B) or are sporadically overlain sharply by facies F1 with sole marks.

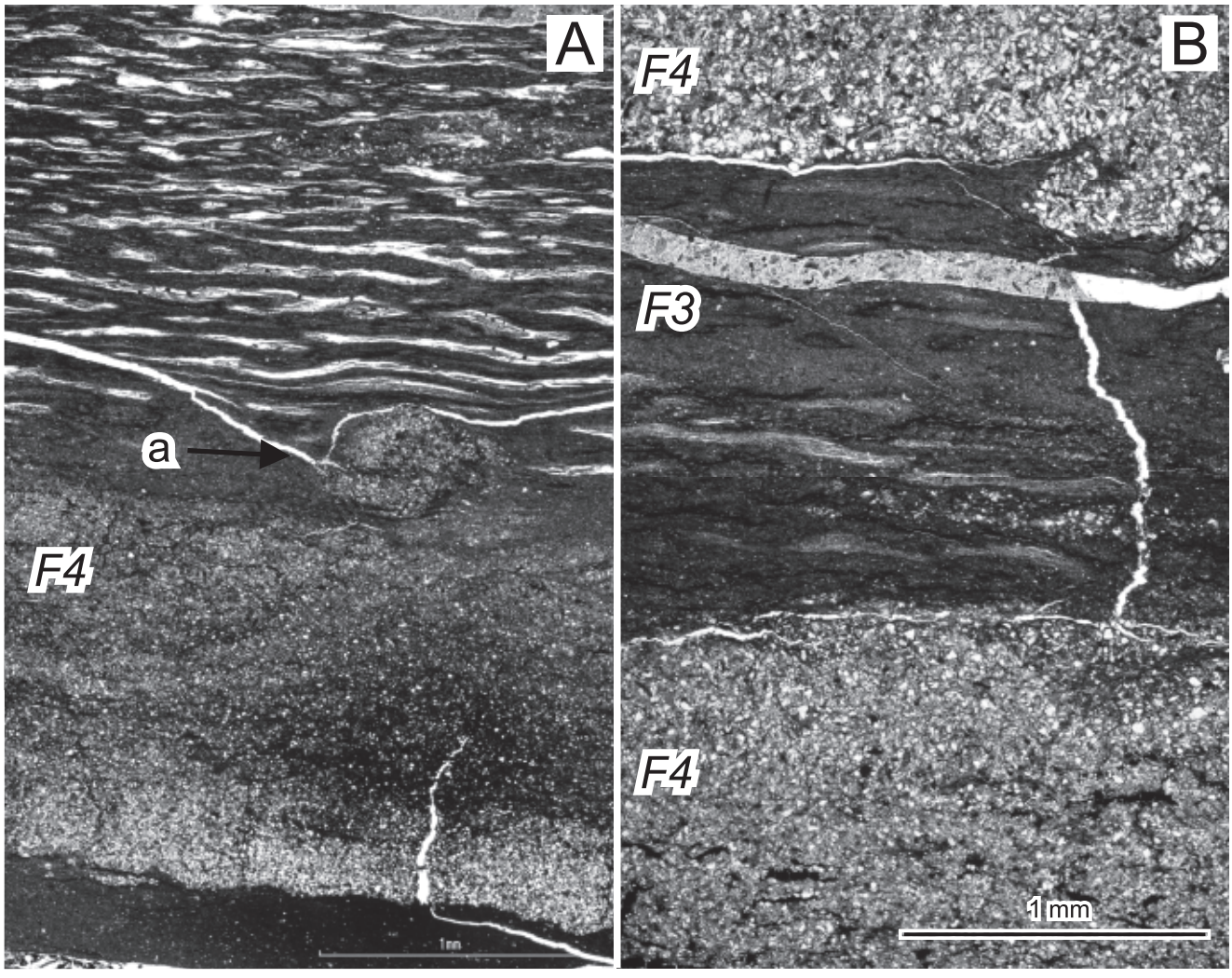

Fig. 8. Microstructure images of facies F3 and F4. **A**. Normal-graded very fine-grained sandstone with a high content of plant detritus passing upwards into a wispy-laminated mudstone with animal burrow (a) at their transition. **B.** Graded sandstone beds of facies F4, separated by a wispy-laminated mudstone of facies F3 with an upward-decreasing content of plant detritus.

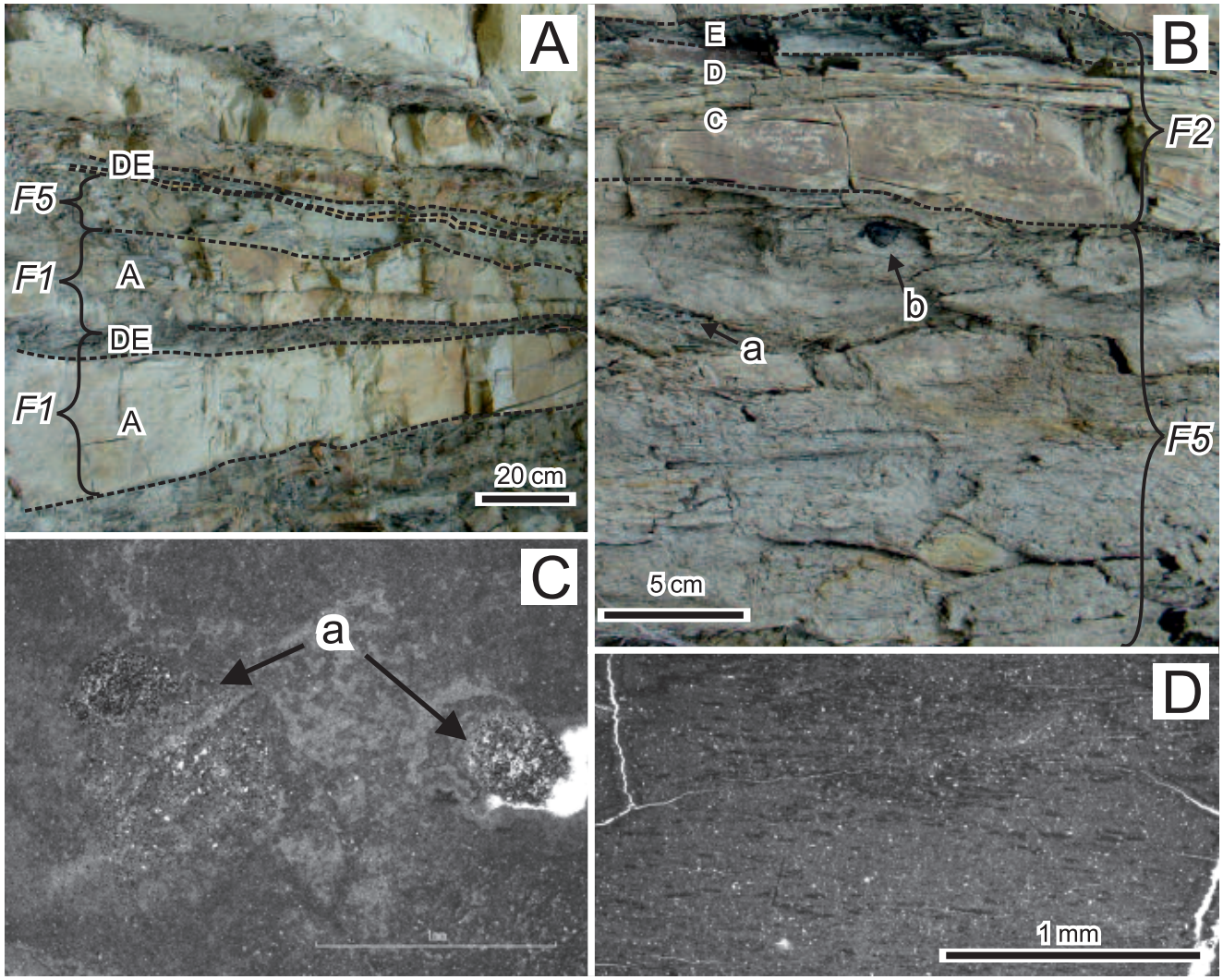

Fig. 9. Example beds of facies F5 and microstructures in facies F6. **A.** Massive sandstone bed of facies F1 with turbidite division A capped by laminated division D and grey mudstone division E, overlain by another massive bed of same facies, showing a wavy boundary with clast-rich massive debrite of facies F5 capped by laminated sandstone division D and grey mudstone division E. **B.** Sandy debrite of facies F5, with mudstone clasts (a) and coal debris (b), capped by turbidite divisions C, D and mudstone E. **C.** Massive marlstone of facies F6, with burrows filled with coarser sediment and faecal pellets (a). **D.** Patchy distribution of coalified plant detritus in facies F6 bed.

Interpretation: The deposits of facies F5 are interpreted as debrites emplaced by the *en masse* freezing of non-turbulent dense flow (cf. Breien *et al*., 2010; Strzeboński, 2015). From the bed characteristics, it is unclear as to whether the debris flow was a parental mass movement, diluted at the top (turbidite cap T_{CDE}), or whether it was spawned by a large turbidity current excessively charged with mud and plant detritus (with the T_{CDE} cap as low-density flow relic). Either of these possibilities seems viable (cf. Lowe, 1982; Fisher, 1983; Postma *et al*., 1988; Marr *et al.,* 2001). Similar, albeit much thinner, massive basal divisions in some of the turbidite beds of facies F1 and F5 suggest basal densification of flow with suppression of turbulence by an erosional incorporation of mud and plant detritus. On the other hand, it cannot be precluded that the CDE capping is a signature of deep-water tidal or contour currents (cf. Strzeboński, 2015; Shanmugam, 2016).

Facies F6

Description: This facies is rare and represented by thin beds of bluish-grey marlstone (Fig. 4), poor in quartz and bioclasts, dominated by micrite with patchily distributed plant detritus (Fig. 9D). The lower bed boundary is sharp to gradational, whereas the top is a gradual transition into darker-grey mudstone. Some beds show plane-parallel wispy lamination, but the majority are massive. Bioturbation structures abound, with *Chondrites* isp., *Planolites* isp. and *Ophiomorpha* isp. burrows are invariably filled with a darker and coarser sediment (Fig. 9C). Tunnels of *Ophiomorpha* are locally branched and 3–5 mm in diameter. This marlstone facies occurs mainly at the top of sandstone-dominated bed packages, where it alternates with facies F2, F3 and F4.

Interpretation: The occurrence of marlstones in alternation with non-calcareous pelagic to hemipelagic mudstones

(facies F3) is rather unusual and, therefore, facies F6 is interpreted as representing allodapic limestones, or calciturbidites T_{DE} (e.g., Flügel, 2010). The mode of deposition by a highly dilute turbidity current would be similar as for facies F4, with the parallel wispy lamination representing Bouma division D. The apparent scarcity of lamination in facies F4 beds is partly due to sediment bioturbation.

MAGNETIC SUSCEPTIBILITY

The measurements of magnetic susceptibility (MS) were conducted mainly for massive sandstone beds or bed divisions to check if they show any particular upward trend that might help distinguish facies and interpret their origin. The underlying theoretical expectation was that the massive sandstones deposited by turbulent flows, as opposed to those deposited by non-turbulent flows, might show a subtle, macroscopically unrecognizable upward decrease in grain size and increase in mud content.

A comparison of the apparent macroscopic trends in grain size and mud content with the corresponding MS trends of the massive beds of facies F1 (Fig. 10) shows common discrepancies. The inconsistent and highly variable MS values of some beds may be due to a non-uniform compositional mixing of sediment dumped by flow as turbidite division A and possibly to the irregular 'cloudy' development of siderite cement. This interpretive notion is supported by the MS measurements taken laterally along the same bed horizons, which show similarly variable values and confirm lack of any consistent upward trend. The vertical distribution of detrital magnetic minerals correlates poorly with the trend of the host-sediment grain size and mud content, because these heavy mineral grains have specific settling velocities, commonly vary in size and hence may be associated with various grain-size fractions and occur irregularly at various levels within the deposit. For the same reason, perhaps, even the markedly different turbidite divisions A, B and C failed to show any systematic differences in their MS values (Fig. 10).

The MS measurements have thus shed some light on the distribution of magnetic mineral grains in the deposits, but helped little in the recognition of the sediment mode of deposition and in distinguishing between turbidites and debrites. These analytical results are reported herein chiefly as an instructive cautionary note for researchers who may be contemplating the use of this petrophysical technique in flysch studies.

SEDIMENTARY FACIES ASSOCIATIONS

The sedimentary facies in the outcrop stratigraphic successions appear to be grouped into packages, several metres thick, ranging from thick-bedded and sandstone-dominated to thin-bedded and mudstone-dominated (Fig. 3). Four types of such packages have been distinguished as facies associations on the basis of their facies composition, the mean value and variance of bed thicknesses and the net/gross sandstone percentage (see data summary in Table 1).

Table 1.

Quantitative summary of the characteristics of depositional lobe facies associations in the Słonne section (see lobe model in Fig. 11A).

Lobe-axis facies association

Package thickness: 2.3–8.5 m (mean 4.7 m)

Component facies thickness contribution:		Individual facies bed thicknesses:
F1	97.7 %	30–222 cm (mean 102.4 cm)
F2	1.6 %	3–11 cm (mean 6.2 cm)
F3/F4	0.5 %	6–8 cm (mean 7 cm)
F6	0.2 %	2–5 cm (mean 3.5 cm)

Sandstone bed thicknesses:
Median = 79 cm
Mean = 79.1 cm
Variance = 3690 cm^2
Standard deviation = 60.8 cm
Sandstone net/gross = 93.6–100 % (mean 96.8 %)

Lobe-flank facies association

Package thickness: 1.2–14 m (mean 4.3 m)

Component facies thickness contribution:		Individual facies bed thicknesses:
F1	83.8 %	16–115 cm (mean 53.4 cm)
F2	11.1 %	2.5–22.5 cm (mean 9.3 cm)
F5	3.2 %	16–36 cm (mean 25.3 cm)
F3/F4	1.7 %	2.5–9 cm (mean 4.8 cm)
F6	0.2 %	2.5–4 cm (mean 3.3 cm)

Sandstone bed thicknesses:
Median = 24 cm
Mean = 31.9 cm
Variance = 873.2 cm^2
Standard deviation = 29.6 cm
Sandstone net/gross = 62.5–97.6% (mean 86.1 %)

Lobe-fringe facies association

Package thickness: 0.6–7.5 m (mean 2.9 m)

Component facies thickness contribution:		Individual facies bed thicknesses:
F1	53.2 %	20.5–60 cm (mean 34.2 cm)
F2	40.2 %	3–24.5 cm (mean 10.29 cm)
F3/F4	6.2 %	3–16 cm (mean 7.1 cm)
F6	0.4 %	2–3 (mean 2.5 cm)

Sandstone bed thicknesses:
Median = 10 cm
Mean = 14.2 cm
Variance = 138.6 cm^2
Standard deviation = 11.8 cm
Sandstone net/gross = 74.8–94.9 % (mean 77.1 %)

Interlobe facies association

Package thickness: 0.4–5.8 m (mean 2.7 m)

Component facies thickness contribution:		Individual facies bed thicknesses:
F2	66 %	2–28 cm (mean 9.9 cm)
F3/F4	29.1 %	3–34 cm (mean 7.2 cm)
F6	3.1 %	2–7 cm (mean 3.7 cm)
F5	1.8 %	20 cm

Sandstone bed thicknesses:
Median = 6 cm
Mean = 6.8 cm
Variance = 34.5 cm^2
Standard deviation = 5.9 cm
Sandstone net/gross = 5.7–62.2% (mean 47.2 %)

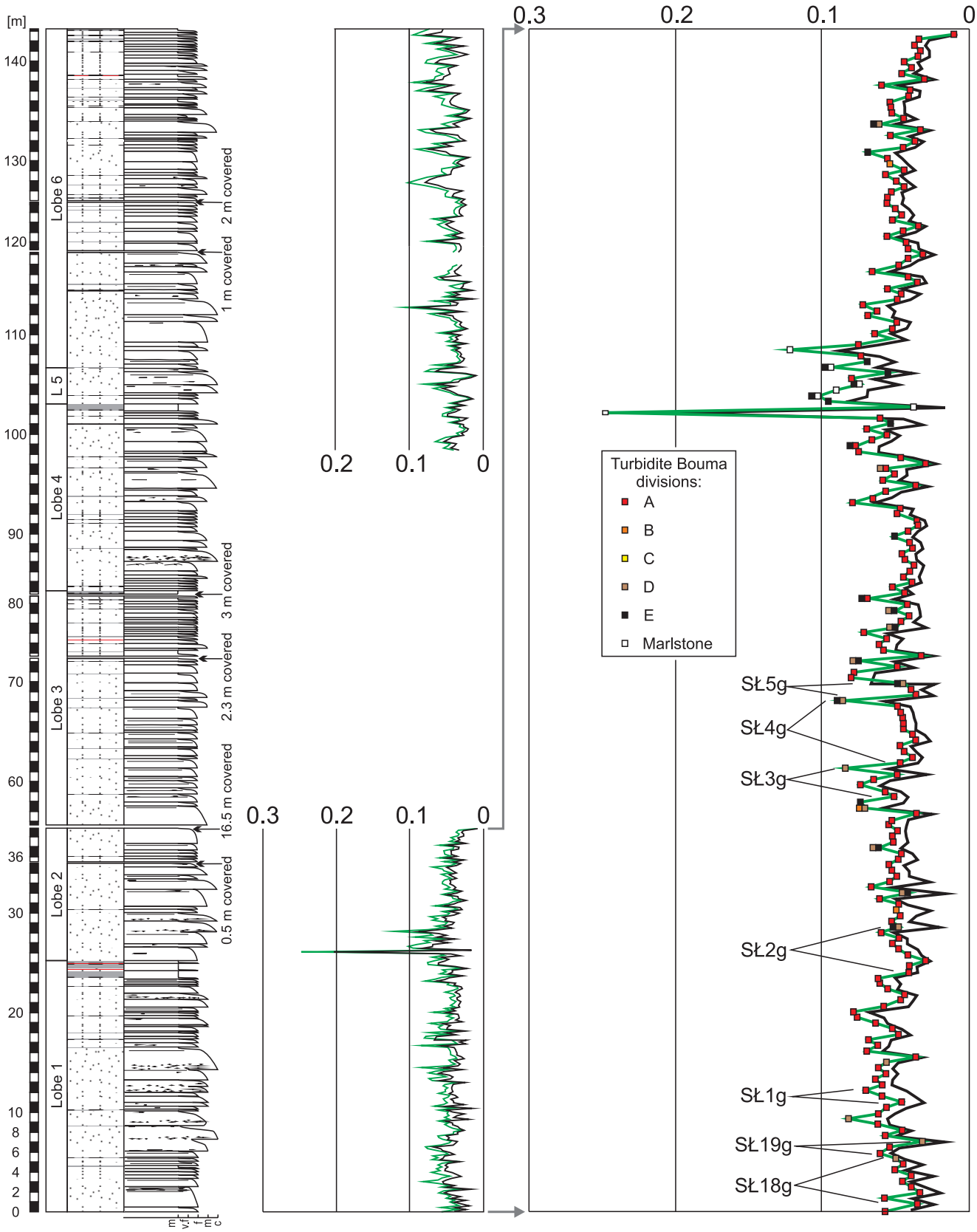

Fig. 10. Simplified sedimentological log with the corresponding magnetic susceptibility log (green curve – uncorrected raw data; black curve – data corrected for an estimated air gap between the measuring device and the rock). Note that the log to the far right is an enlarged detailed version of the MS log from the lower part of the succession.

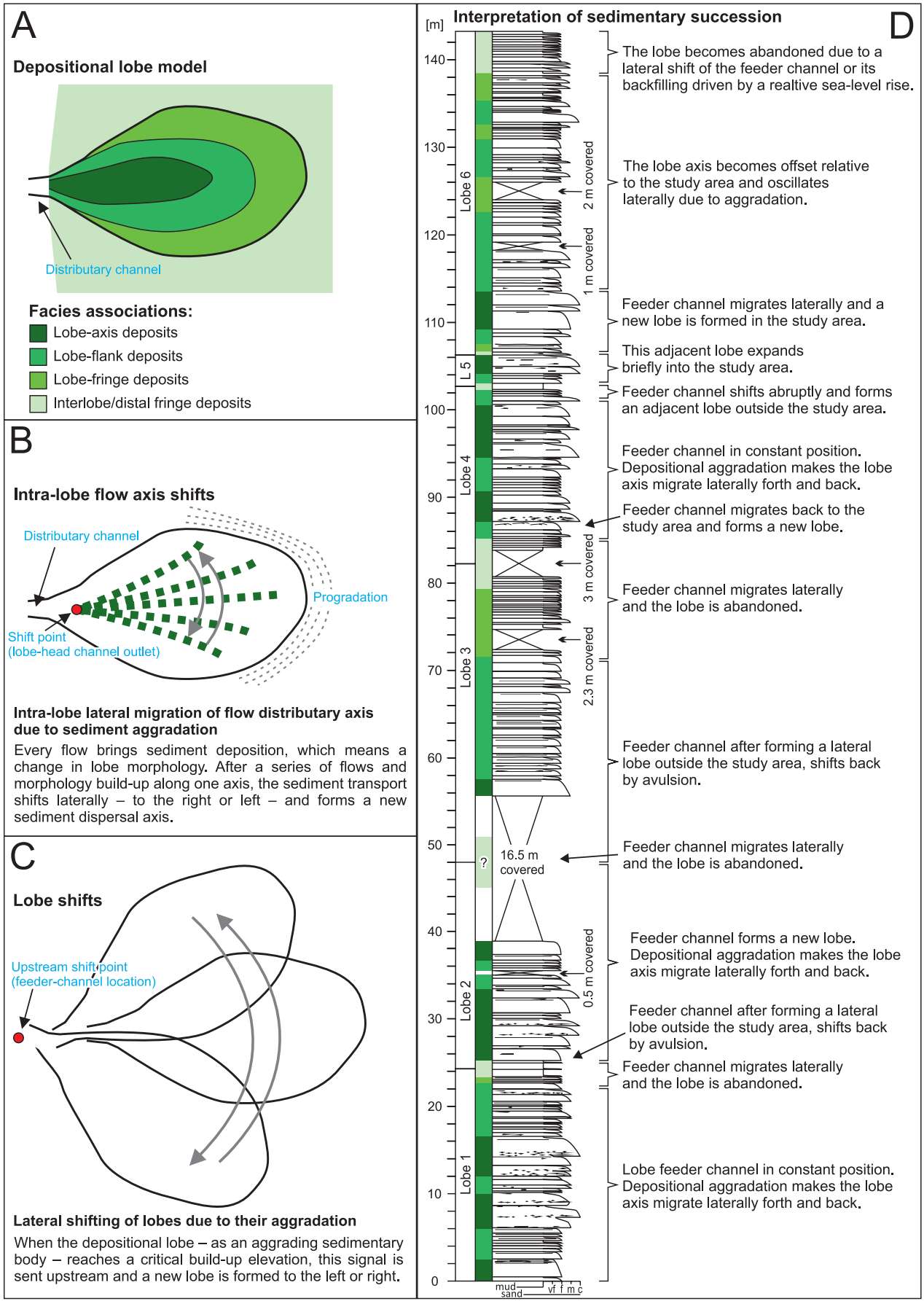

Fig. 11. Interpretive summary of the Słonne section. **A**. Model of depositional lobe with its facies associations. **B.** Depositional lobe growth by lateral migration of its sediment dispersal axis. **C.** Depositional lobe lateral shifts by feeder-channel switching. **D.** Interpretation of the sedimentary succession in terms of dynamic stratigraphy.

The sandstone beds in the whole succession are tabular on the outcrop scale and the facies associations show mainly transitional boundaries, with no evidence of deep scouring and possible palaeochannels. Classical sheet-like turbidites dominate and typical channel-fill facies (e.g., see Pickering *et al*., 1995; Janbu *et al*., 2007) are absent. These characteristics suggest a sedimentary system of channel-fed depositional turbiditic lobes formed by unconfined flows (cf. Mutti and Ricci Lucchi, 1972; Shanmugam, and Moiola, 1988, 1991; Pickering *et al*., 1995; Mulder, 2011; Shanmugam, 2016). These four facies associations distinguished in the outcrop profile are considered to represent different morphodynamic zones of a depositional lobe (Table 1). They are characterized and interpretively compared in this section of the article.

Lobe-axis facies association

Description: These bed assemblages are 2.3–8.5 m thick, have a sandstone net/gross of ~94% to 100% and are dominated (~98% thickness) by the sandstone facies F1 with only minor contribution of facies F2, F3/F4 and F6 (Table 1). Facies F1 reaches here its greatest bed thicknesses, in the range of 30–222 cm and averaging 102 cm. The overall variance of bed thicknesses in this facies assemblage is the highest, with a standard deviation (*SD*) of ~61 cm, whereas the median (*Md*) and mean (*M*) are equal. The latter relationship indicates a perfectly normal, symmetrical bed-thickness frequency distribution and implies that ~70% of the component beds are in the thickness range of *M*±1*SD*, ~95% of beds are in the range of *M*±2*SD* and ~100% of beds are in the range of *M*±3*SD*.
Interpretation: This facies assemblage, as the most sandstone-rich and thickest-bedded, is interpreted to represent the axial sediment-dispersal zone of a turbiditic depositional lobe (cf. Mutti and Normark, 1987; Pickering *et al*., 1995; Stow and Mayall, 2000; Deptuck *et al*., 2008; Prélat *et al*., 2009; Mulder, 2011; Grundvåg *et al*., 2014; Marini *et al*., 2015).

Lobe-flank facies association

Description: These bed assemblages are 1.2–14 m thick, have a sandstone net/gross of ~63% to 98% and are similarly dominated (~84% thickness) by the sandstone facies F1, but with a contribution of facies F5 and also greater contribution of facies F2 and F3/F4 (Table 1). The beds of facies F1 are thinner, in the range of 16–115 cm and averaging 53 cm. The bulk variance of bed thicknesses in this facies assemblage is much lower, with a standard deviation of ~30 cm. The mean (32 cm) is higher than median (24 cm), which indicates a positively skewed bed-thickness frequency distribution (i.e., some excess of thicker beds).
Interpretation: This type of facies assemblage is the second richest in sandstones and resembles the previous one in being dominated by facies F1, but is distinctly thinner bedded and shows a nearly 20% contribution of finer-grained facies, notably including F5. These characteristics suggest that this facies association is probably a lateral, off-axis equivalent of the previous one and represents depositional lobe flank (cf. Shanmugam and Moiola, 1991; Pickering *et al*., 1995; Deptuck *et al*., 2008; Grundvåg *et al*., 2014).

Lobe-fringe facies association

Description: The facies assemblages of this third type are only 0.6–7.5 m thick (mean ~3 m), have a sandstone net/gross of 75% to 95% and consist in nearly equal proportion of facies F1 and of the finer-grained facies F2, F3/F4 and F6 (Table 1). The beds of facies F1 are here even thinner, averaging 34 cm, whereas those of facies F2 and F3/F4 are slightly thicker. Overall, bed thicknesses are more than half-thinner than in the previous facies association, with a mean of 14 cm and median of 10 cm. The bulk variance of bed thicknesses is also much lower, with a standard deviation of only 12 cm. The mean slightly higher than median indicates likewise a slight positive skewness of bed-thickness frequency distribution.
Interpretation: The markedly lower bed thicknesses, lower sandstone net/gross and strikingly lower proportion of facies F1 suggest that this third type of facies association probably represents the thin featheredge fringe zone of depositional lobes (cf. Pickering *et al*., 1995; Deptuck *et al*., 2008; Prélat *et al*., 2009; Grundvåg *et al*., 2014).

Interlobe facies association

Description: This fourth type of facies assemblages is only 0.4–5.8 m thick (mean 2.7 m), has a low sandstone net/gross of ~6% to 62% (mean 47%) and strikingly lacks component facies F1 (Table 1). Dominant are facies F2 (66%) and F3/F4 (29%). The beds here are thinnest, with their mean thickness (~7 cm) nearly equal to median (6 cm) and with a low standard deviation of 6 cm.
Interpretation: This thinly bedded association of fine-grained facies lacks the lobe signature facies F1 and is thought to represent the interlobe zone, or most distal lobe fringe, of the turbiditic depositional system (cf. Pickering *et al*., 1995; Deptuck *et al*., 2008; Prélat *et al*., 2009; Grundvåg *et al*., 2014).

PALAEONTOLOGICAL EVIDENCE

The deposits in the Słonne outcrop section show sporadic to abundant animal burrows and contain small benthic foraminifers. The identified trace fossils include *Planolites* isp., *Ophiomorpha* isp., *Chondrites* isp., *Scolicia* isp. and *Thalassinoides* isp. Deep-water turbiditic depositional lobes, with the frequent incursions of large and small sediment-gravity flows and a relatively high sedimentation rate, provide a generally stressful habitat for benthic organisms (MacEachern *et al.*, 2010; Uchman and Wetzel, 2012). The evidence of benthic life in the present case is limited mainly to the thin-bedded and finer-grained facies F2–F6. However, the amount of plant detritus (potential nutrient) delivered

by sediment gravity flows was apparently much higher than the nutrient supplied by hemipelagic and pelagic suspension fallout, and thereby the optimal time for seafloor colonization was when the local rate of sedimentation declined with the lateral switching of depositional lobe (Fig. 11C).

Samples collected for micropalaeontological analysis (Fig. 3) showed low-diversity assemblages of agglutinated foraminifers. As representative and relatively rich, sample SŁ3o (log height 76.2 m, Fig. 3) contained: *Nothia excelsa* (Grzybowski), *Psammosiphonella discreta* (Brady), *Rhizammina* sp., *Saccammina grzybowskii* (Schubert), *Placentammina placenta* (Grzybowski), *Hyperammina dilatata* Grzybowski, *Ammodiscus* cf. *cretaceus* (Reuss), *Ammodiscus peruvianus* Berry, *Ammodiscus tenuissimus* Grzybowski, *Glomospira irregularis* (Grzybowski), *Caudammina excelsa* (Dylążanka), *Caudammina gigantea (*Geroch), *Caudammina ovula* (Grzybowski) emend Geroch, 1960, *Caudammina ovuloides* (Grzybowski), *Hormosinelloides guttifer* (Brady), *Hormosina velascoensis* (Cushman), *Kalamopsis grzybowskii* (Dylążanka), *Subreophax scalaris* (Grzybowski), *Paratrochamminoides* div.sp., *Haplophragmoides* cf. *suborbicularis* (Grzybowski), *Recurvoides* indet., *Gerochammina obesa* Neagu and *Dorothia crassa* (Marsson). These foraminifers indicate water depth below the local lysocline, which is consistent with the deposition of mainly non-calcareous pelagic to hemipelagic mudstones. The occurrence of agglutinated foraminifera with carbonate cement, such as *Dorothia crassa*, suggests a temporal depth slightly above lysocline. Seafloor aggradation probably combined with lysocline fluctuations, and the lysocline in the Late Cretaceous could be up to ~50% shallower than today (Lyle, 2003; Rea and Lyle, 2005), perhaps at a mid-bathyal sea depth.

Analysis of foraminifer assemblages indicates a late Cretaceous age (Campanian–Maastrichtian) of the deposits, with a similarity to the Wiar Member of the Ropianka Formation (Fig. 2). This evidence compares well with the lithological similarity of the deposits to Rajchel's (1989) stratigraphic Complex I.

DYNAMIC STRATIGRAPHY

The four facies associations described in the previous section (Table 1) are thus considered to represent different morphodynamic zones of a turbiditic depositional lobe (Fig. 11A). They alternate with one another in the stratigraphic succession (Fig. 3), and these vertical changes at the Słonne intra-basinal locality are attributed to the lateral migration (Fig. 11B) and wholesale shifting (Fig. 11C) of successive depositional lobes. The Late Cretaceous Skole Basin in its Polish segment had a WNW–ESE trend (Kováč *et al.*, 2016), and the southward directions of sediment transport – roughly perpendicular to the basin axis – suggests transversely-built depositional lobes unconfined by the basin topography, although often skewed towards the east or west by their expansion in the basin. The stepwise 'in-sequence' upward changes of lobe directly adjacent zones (Fig. 11A) are attributed to the lobe lateral migration by the shifting of its sediment dispersal axis (Fig. 11B). The abrupt 'out-of-sequence' changes, with the appearance of interlobe facies association, are ascribed to a wholesale shift of the depositional lobe due to an upstream change of its feeder-channel position (Fig. 11C).

The logic behind this morphodynamic interpretation (see Mutti and Ricci Lucchi, 1972; Mutti and Sonnino, 1981; Shanmugam, and Moiola, 1988, 1991; Pickering *et al*., 1995; Deptuck *et al*., 2008; Prélat *et al*., 2009; Shanmugam, 2016) is that – as the depositional lobe aggrades along its axis of sediment dispersal – the dispersal axis inevitably shifts sideways and hence the lobe migrates laterally (Fig. 11B). As the whole lobe gradually builds up in this way, its feeder channel eventually shifts laterally by avulsion and a new lobe forms (Fig. 11C), onlapping sideways the previous one while growing.

The Słonne stratigraphic section (Fig. 3) is then interpreted to represent the turbiditic system's local morphodynamic changes on both intra-lobe and interlobe depositional scale (Fig. 11B, C). Based on the in-sequence and out-of-sequence upward changes of facies associations, six successive vertically stacked depositional lobes are distinguished in the stratigraphic succession with a tentative reconstruction of their depositional morphodynamics (see Fig. 11D and interpretation therein). The thicknesses of the inferred lobes and their inter-lapping flanks are comparable to those reported from elsewhere by other authors (e.g., Deptuck *et al*., 2008; Prélat *et al*., 2009; Bernhardt *et al*., 2011; Grundvåg *et al*., 2014; Marini *et al*., 2015). The depositional lobes were likely elongate (Fig. 11A), but their dimensions probably varied, depending on the lobe growth time, and are difficult to estimate from a single outcrop section. For a radial lobe with surface inclination of ~0.3° (i.e., topographic gradient ~0.005, typical for small radial turbiditic fans; Bouma *et al.*, 1985) and a mid-lobe axial thickness of ~10 m (Table 1), the lobe estimated width would be ~2 km and length perhaps ~3.5 km. The lateral shingling of lobes (Fig. 11C) would render their complex at least 3 times wider, without necessarily extending significantly its length, while possibly skewing the lobes and merging their adjacent complexes.

The facies associations differ markedly from one another (Table 1), but individually show consistent facies composition and bed thicknesses, which suggests that the growth rate of the successive depositional lobes composed of these associations was similar. However, the actual time span of lobe growth and the rate of its lateral migration may have varied, as the 'compensational' offset stacking of lobes would depend upon the turbiditic system's net equilibrium profile and the seafloor topographic accommodation (cf. Mutti and Sonnino, 1981; Deptuck *et al*., 2008; Picot *et al*., 2016; Shanmugam, 2016). Therefore, some of the lobes grew at the study locality longer than other lobes, and yet some other lobes extended laterally into this area only briefly (Fig. 11D).

Deposits interpreted as interlobe facies association demarcate the successive depositional lobes stacked upon one another in the outcrop section. In the hypothetical interpretation of the succession (Fig. 11D), lobe 1 formed with a stable position of its feeder channel and with the sediment aggradation making the lobe axis migrate laterally forth and back (log interval 0–24 m, lobe base unexposed).

The build-up of lobe 1 eventually caused its feeder channel to shift laterally by avulsion and the lobe was abandoned. After forming a new lobe outside the study area, the feeder channel had shifted back and formed lobe 2 (log interval 24–48 m). Similar shifts of feeder channel resulted in lobes 3 and 4 (log intervals 48–82 m and 82–102 m, respectively). Lobe 5 formed outside the study area, but expanded briefly into it by the lobe axis lateral migration (log interval 102––106 m). The feeder channel then switched back and formed the thick lobe 6 (log interval 106–144 m), with the lobe axis oscillating laterally while migrating sideways until the lobe abandonment.

This stratigraphic interpretation refers to an autogenic morphodynamics of the depositional system, with the intra-lobe migration of dispersal axis and lobe aggradation (Fig. 11B) leading to the lateral switching of distributary channel (Fig. 11C). However, it cannot be precluded that at least some of the lobe abandonment phases were caused by a relative sea-level rise, with a decline of sediment supply and the system bulk retreat. The Campanian–Maastrichtian period had witnessed 4 major (>75 m), 4 moderate (25––75 m) and 5 minor (<25 m) eustatic changes (Snedden and Liu, 2010). It is possible that at least these larger changes had an impact in the Skole Basin and that the thicker interlobe packages (Fig. 11D) are transgressive outer lobe-fringe deposits. The biostratigraphic dating is insufficient to allow time correlations. On the other hand, the basin was tectonically active and a similar impact of tectonic forcing could possibly come into play.

IMPLICATIONS FOR THE SKOLE BASIN

The sediment to the deep-water Skole Basin was derived from its northern passive margin (Bromowicz, 1974), with the mud-rich deposits of the basin "external" (northern) zone representing the basin slope and the sand-rich deposits in the "internal" (southern) zone, such as the Wiar Member of the Ropianka Formation, probably representing some base-of-slope or basin-floor turbiditic fans (cf. Kotlarczyk, 1978, 1988; Kotlarczyk and Leśniak, 1990). The northern passive margin evolved from immature to mature in the Cretaceous to Oligocene (Salata and Uchman, 2013). Kotlarczyk and Leśniak (1990) have recognized three main fairways of sand transport from the north in the Oligocene Menilite Formation (Fig. 2). The spatial distribution of thick-bedded sandstones in the Ropianka Formation shows a similar pattern (e.g., Gucik *et al.,* 1980; Salata and Uchman, 2013). The occurrence of Lower Cretaceous black mudstone clasts in the Ropianka Formation (Kotlarczyk, 1988) indicates canyons or valleys deeply incised in the basin older deposits already in the Campanian time, when the main fairways were probably established.

According to Bromowicz (1974), the transport direction during the deposition of Ropianka Formation was mainly from the north and northwest (Fig. 1), and only the oldest deposits of this formation, in the SE part of the Skole Nappe, show palaeocurrent directions from the east and southeast. This evidence, supported by the present study, puts in question the earlier notions of sand dispersal along the basin axis, based on the spatial distribution of sandstones (Gucik *et al*., 1980; Burtan *et al*., 1981; Jurkiewicz and Woiński, 1981; Kotlarczyk, 1988; Woiński, 1994; Nescieruk *et al*., 1995). The Campanian–Early Maastrichtian base-of-slope depositional lobe complexes may have merged laterally at the stages of their maximum expansion in the narrow basin, giving the false impression of a narrow sand depocentre parallel to the basin axis. The south-built lobe complexes would likely become skewed eastwards or westwards in the narrow basin according to its floor local accommodation (cf. Rajchel, 1989), but this would not mean that the main sediment dispersal was longitudinal, parallel to the basin axis.

The high amount of plant detritus in the Słonne section (Fig. 3) suggests a deltaic or paralic source of sediment supply. The deeply incised fluvial feeder canyons or valleys would inevitably host bayhead deltas, from which also hyperpycnal flows may have been issued (as suggested by some of the beds of facies F1). The fluctuating supply of siliciclastic and carbonate sediment indicates an involvement of both fluvio-deltaic and carbonate sources. Their interplay is highlighted by the occurrence of marlstone beds containing plant detritus (Fig. 9D). The relatively small and sporadic contribution of facies F6 suggests that the sediment sourcing system only occasionally involved a calcareous source, which may indicate episodic carbonate production on basin-margin narrow shelf, perhaps driven by the Campanian eustatic sea-level rises (cf. Snedden and Liu, 2010).

CONCLUSIONS

This first detailed study of the Ropianka Formation in the Słonne outcrop section along river San has indicated from lithological and micropalaeontological similarities that the sedimentary succession exposed there corresponds regionally to the formation's Wiar Member of Campanian–Maastrichtian age.

The sedimentary succession, more than 140 m thick, exposed in the Słonne section is interpreted as a deep-marine complex of turbiditic depositional lobes. The study has revealed its sedimentary anatomy by recognizing six component facies of sediment gravity-flow deposits and their stratigraphic grouping into four facies associations – interpreted as deposits of the lobe dispersal-axis zone, lateral flank zone and featheredge fringe zone, as well as an interlobe outer-fringe zone.

The component facies associations of the succession have been individually characterized and compared on a semi-quantitative basis, which gave a detailed insight into the succession's sedimentary heterogeneity.

Six depositional lobes stacked upon one another have been recognized in the succession, and their vertical stacking pattern has been hypothetically interpreted in terms of dynamic stratigraphy based on the upward succession of facies associations.

The stratigraphic arrangement of facies associations is attributed to autogenic morphodynamic changes in the depositional system, but it cannot be precluded that also eustatic and local tectonic forcing came into play.

This case study sheds more light on the sedimentary environment, sediment sourcing system and spatial depositional pattern in the Late Cretaceous Skole Basin, where the aggrading seafloor apparently oscillated around the lysocline depth, which at that time could be mid-bathyal.

ACKNOWLEDGEMENTS

The study was funded by the Jagiellonian University. Ewa Malata (Jagiellonian University) helped in the identification of foraminifers. Alfred Uchman (Jagiellonian University) and Wojciech Nemec (Bergen University) offered discussions and improved the manuscript, which was formally reviewed with helpful comments by Juraj Janočko (Technical University of Košice) and Michał Warchoł (Statoil Research Centre in Bergen).

REFERENCES

Allen, J. R. L., 1991. The Bouma division A and the possible duration of turbidity currents. *Journal of Sedimentary Research*, 61: 291–295.

Ashley, G. M., Southard, J. B. & Boothroyd, J. C., 1982. Deposition of climbing-ripple beds: a flume simulation. *Sedimentology*, 29: 67–79.

Bernhardt, A., Jobe, Z. R. & Lowe, D. R., 2011. Stratigraphic evolution of a submarine channel-lobe complex system in a narrow fairway within the Magallanes foreland basin, Cerro Toro Formation, southern Chile. *Marine and Petroleum Geology*, 28: 785–806.

Best, J. & Bridge, J., 1992. The morphology and dynamics of low amplitude bedwaves upon upper stage plane beds and the preservation of planar laminae. *Sedimentology*, 39: 737–752.

Bouma, A. H., 1962. *Sedimentology of Some Flysch Deposits: A Graphic Approach to Facies Interpretation.* Elsevier, Amsterdam, 168 pp.

Bouma, A. H., Normark, W. R. & Barnes, N. E., 1985. *Submarine Fans and Related Turbidite Systems.* Springer Verlag, New York, 351 pp.

Breien, H., De Blasio, F. V., Elverhøi, A., Nystruen, J. P. & Harbitz, C. B., 2010. Transport mechanisms of sand in deep-marine environments – insights based on laboratory experiments. *Journal of Sedimentary Research*, 80: 975–990.

Bromowicz, J., 1974. Facial variability and lithological character of Inoceramian Beds of the Skole-Nappe between Rzeszów and Przemyśl. *Prace Geologiczne*, 84: 1–83. [In Polish, with English summary.]

Bromowicz, J., 1986. Petrographic differentiation of source areas of Ropianka Beds east of Dunajec River (Outer Carpathians, Poland). *Annales Societatis Geologorum Poloniae*, 56: 253–276. [In Polish, with English summary.]

Bukowy, S., 1957a. Remarks on the sedimentation of the Babica Clays. *Rocznik Polskiego Towarzystwa Geologicznego*, 26: 147–155. [In Polish, with English summary.]

Bukowy, S., 1957b. Węgiel kamienny w Karpatach brzeżnych. *Przegląd Geologiczny*, 5: 577–578. [In Polish.]

Bukowy, S. & Geroch, S., 1957. On the age of exotic conglomerates at Kruhel Wielki near Przemyśl (Carpathians). *Rocznik Polskiego Towarzystwa Geologicznego*, 26: 297–329. [In Polish, with English summary.]

Burtan, J., Golonka, J., Oszczypko, N., Paul, Z. & Ślączka, A., 1981. *Mapa geologiczna Polski, 1:200 000, arkusz Nowy Sącz*. Wydawnictwa Geologiczne, Warszawa. [In Polish.]

Burzewski, J., 1966. Les marnes à Baculithes sur le fond de la lithostratigraphie des à Inocérames dans les Carpathes de skibas". *Zeszyty Naukowe AGH, Geologia*, 7: 89–115. [In Polish, with French summary.]

Clark, J. D. & Pickering, K. T., 1996. Architectural elements and growth patterns of submarine channels: application to hydrocarbon exploration. *American Association of Petroleum Geologists Bulletin*, 80: 194–220.

Collinson, J. D. & Thompson, D. B., 1982. *Sedimentary Structures*. Allen and Unwin, London, 207 pp.

Davis, J. C., 2002. *Statistics and Data Analysis in Geology.* 3rd ed., John Wiley & Sons, New York, 638 pp.

Deptuck, M. E., Piper, D. J. W., Savoye, B. & Gervais, A., 2008. Dimensions and architecture of Late Pleistocene submarine lobes off the northern margin of East Corsica. *Sedimentology*, 55: 869–898.

Dott, R. H., Jr., 1983. Presidential address: Episodic sedimentation – How normal is average? How rare is rare? Does it matter? *Journal of Sedimentary Petrology*, 53: 5–23.

Dżułyński, S., Kotlarczyk, J. & Ney, R., 1979. Podmorskie ruchy masowe w basenie skolskim. In: Kotlarczyk, J. (ed.), *Poziomy z olistostromami w Karpatach przemyskich. Materiały Terenowej Naukowej Konferencji w Przemyślu: Stratygrafia formacji z Ropianki (fm)*. Powielarnia AGH, Przemyśl, pp. 17–27. [In Polish.]

Dżułyński, S., Książkiewicz, M. & Kuenen, P. H., 1959. Turbidites in flysch of the Polish Carpathian Mountains. *Geological Society of America Bulletin*, 70: 1089–1118.

Dżułyński, S. & Smith, A. J., 1964. Flysch facies. *Rocznik Polskiego Towarzystwa Geologicznego*, 34: 245–266.

Dżułyński, S. & Walton, E. K., 1965. *Sedimentary Features of Flysch and Greywackes. Developments in Sedimentology,* 7: 1–272.

Fisher, R. V., 1983. Flow transformations in sediment gravity flows. *Geology*, 11: 273–274.

Flügel, E., 2010. *Microfacies of Carbonate Rocks. Analysis, Interpretation and Application*. Springer-Verlag, Berlin, 984 pp.

Gedl, E., 1999. Lower Cretaceous palynomorphs from the Skole Nappe (Outer Carpathians, Poland). *Geologica Carpathica*, 50: 75–90.

Golonka, J., Gahagan, L., Krobicki, M., Marko, F., Oszczypko, N. & Ślączka, A., 2006. Plate-tectonic evolution and paleogeography of the Circum-Carpathian region. In: Golonka, J. & Picha, F. J. (eds), *The Carpathians and their foreland: Geology and hydrocarbon resources*. *American Association of Petroleum Geologists, Memoir*, 84: 11–46.

Gradstein, F., Ogg, J., Schmitz, M. & Ogg, G., 2012. *The Geological Time Scale 2012*. Elsevier, Oxford, 1176 pp.

Grundvåg, S. A., Johannessen, E. P., Hansen, W. H. & Plink-Björklund, P., 2014. Depositional architecture and evolution of progradationally stacked lobe complexes in the Eocene Central Basin of Spitsbergen. *Sedimentology*, 61: 535–569.

Gucik, S., Paul, Z., Ślączka, A. & Żytko, K., 1980. *Mapa geologiczna Polski 1:200 000, arkusz Przemyśl, Kalników*. Wydawnictwa Geologiczne, Warszawa. [In Polish.]

Harms, J. C., Southard, J. B., Spearing, D. R. & Walker, R. G., 1975. *Depositional Environments as Interpreted from Primary Sedimentary Structures and Stratifcation Sequences*. *Lecture Notes, SEPM Short Course No. 2*. Society of Economic Paleontologists and Mineralogists, Dallas, 161 pp.

Janbu, N. E., Nemec, W., Kırman, E. & Özaksoy, V., 2007. Facies anatomy of a channelized sand-rich turbiditic system: the Eocene Kusuri Formation in the Sinop Basin, north-central Turkey. In: Nichols, G., Paola, C. & Williams, E. A. (eds), *Sedimentary Environments, Processes and Basins – A Tribute to Peter Friend*. *International Association of Sedimentologists Special Publication*, 38, 457–517.

Jednorowska, A., 1957. On the microfauna of the Inoceramus Beds within the "Skiba" region in the vicinity of Słonne and Wara. *Acta Geologica Polonica*, 7: 303–320. [In Polish, with English summary.]

Johnson, M. R., 1994. Thin section grain size analysis revisited. *Sedimentology*, 41: 985–999.

Johnson, S. D., Flint, S., Hinds, D. & De Ville Wickens, H., 2001. Anatomy, geometry and sequence stratigraphy of basin floor to slope turbidite systems, Tanqua Karoo, South Africa. *Sedimentology*, 48: 987–1023.

Jurkiewicz, H. & Woiński, J., 1981. *Mapa geologiczna Polski, 1:200 000, arkusz Mielec*. Wydawnictwa Geologiczne, Warszawa. [In Polish.]

Kneller, B. C. & Branney, M. J., 1995. Sustained high-density turbidity currents and the deposition of thick massive sands. *Sedimentology*, 42: 607–616.

Kotlarczyk, J., 1978. Stratigraphy of the Ropianka Formation or of Inoceramian beds in the Skole Unit of the Flysch Carpathians. *Prace Geologiczne*, 108: 1–75. [In Polish, with English summary.]

Kotlarczyk, J., 1988. *Przewodnik LIX Zjazdu PTG w Przemyślu*. Wydawnictwa AGH, Kraków, 298 pp. [In Polish.]

Kotlarczyk, J., Jerzmańska, A., Świdnicka, E. & Wiszniowska, T., 2006. A framework of ichtyofaunal ecostratigraphy of the Oligocene-Early Miocene strata of the Polish Outer Carpathian Basin. *Annales Societatis Geologorum Poloniae*, 76: 1–111.

Kotlarczyk, J. & Leśniak, T., 1990. *Lower Part of the Menilite Formation and Related Futoma Diatomite Member in the Skole Unit of the Polish Carpathians*. Instytut Geologii i Surowców Mineralnych AGH, Wydawnictwo Akademii Górniczo-Hutniczej, Kraków, 74 pp. [In Polish, with English summary.]

Kotlarczyk, J. & Śliwowa, M., 1963. On knowledge of the productive Carboniferous formations in the substratum of the eastern part of the Polish Carpathians. *Przegląd Geologiczny*, 11: 268–272. [In Polish, with English summary.]

Kováč, M., Plašienka, D., Soták, J., Vojtko, R., Oszczypko, N., Less, G., Ćosović, V., Fügenschuh, B. & Králiková, S., 2016. Paleogene palaeogeography and basin evolution of the Western Carpathians, Northern Pannonian domain and adjoining areas. *Global and Planetary Change*, 140: 9–27.

Kropaczek, B., 1917. Kleine Beiträge zur Geologie der nördlichen Karpaten Mittelgaliziens. *Sprawozdania Komisji Fizjograficznej Akademii Umiejętności*, 51: 106–146. [In Polish, with German summary.]

Książkiewicz, M., 1962. *Geological Atlas of Poland. Stratigraphic and Facial Problems. Cretaceous and Early Tertiary in the Polish External Carpathians, 13*. Wydawnictwa Geologiczne, Warszawa. [In Polish, with English summary.]

Książkiewicz, M., 1972. Karpaty. In: *Budowa geologiczna Polski, 4. Tektonika Volume 3*, Wydawnictwa Geologiczne, Warszawa, pp. 121–196. [In Polish.]

Łapcik, P., 2018. Sedimentary processes and architecture of Upper Cretaceous deep-sea channel deposits: a case from the Skole Nappe, Polish Outer Carpathians. *Geologica Carpathica*, 69: 71–88.

Łapcik, P., Kowal-Kasprzyk, J. & Uchman, A., 2016. Deep-sea mass-flow sediments and their exotic blocks from the Ropianka Formation (Campanian–Paleocene) in the Skole Nappe: a case study of the Wola Rafałowska section (SE Poland). *Geological Quarterly*, 60: 301–316.

Leclair, S. F. & Arnott, R. W. C., 2005. Parallel lamination formed by high-density turbidity currents. *Journal of Sedimentary Research*, 75: 1–5.

Leszczyński, S., 1981. Ciężkowice Sandstones of the Silesian Unit in the Polish Carpathians: a study of coarse-clastic sedimentation in deep water. *Annales Societatis Geologorum Poloniae,* 51: 435–502.

Lowe, D. R., 1982. Sediment gravity flows: II. Depositional models with special reference to the deposits of high-density turbidity currents. *Journal of Sedimentary Petrology*, 52: 279–297.

Lowe, D. R., 1988. Suspended-load fallout rate as an independent variable in the analysis of current structures. *Sedimentology*, 35: 765–776.

Lowe, D. R. & Guy, M., 2000. Slurry-flow deposits in the Britannia Formation (Lower Cretaceous), North Sea: a new perspective on the turbidity current and debris flow problem. *Sedimentology*, 47: 31–70.

Lyle, M. W., 2003. Neogene carbonate burial in the Pacific Ocean. *Paleoceanography*, 18: PA1059.

MacEachern, J. A., Pemberton, S. G., Gingras, M. K. & Bann, K. L., 2010. Ichnology and facies models. In: James, N. P. & Dalrymple, R. W. (eds), *Facies Models 4*. Geoscience Canada, St. John's, pp. 19–59.

Malata, T., 2001, Jednostka skolska na E od Rzeszowa. *Posiedzenia Naukowe Państwowego Instytutu Geologii*, 57: 60–63. [In Polish.]

Malata, T. & Poprawa, P., 2006. Evolution of the Skole Subbasin. In: Oszczypko, N., Uchman, A. & Malata, E. (eds), *Rozwój paleotektoniczny basenów Karpat zewnętrznych.* Institute of Geological Sciences, Jagiellonian University, Kraków, pp. 101–110. [In Polish, with English abstract.]

Marini, M., Salvatore, M., Ravnås, R. & Moscatelli, M., 2015. A comparative study of confined vs. semi-confined turbidite lobes from the Lower Messinian Laga Basin (Central Apennines, Italy): Implications for assessment of reservoir architecture. *Marine and Petroleum Geology*, 63: 142–165.

Marr, J. G., Harff, P. A., Shanmugam, G., Parker, G., 2001. Experiments on subaqueous sandy gravity flows: The role of clay and water content in flow dynamics and depositional structures. *Geological Society of America Bulletin*, 113: 1377–1386.

McHargue, T., Prycz M. J., Sullivan, M. D., Clark, J. D., Fildani, A., Romans, B. W., Covault, J. A., Levy, M., Posamentier, H.

W. & Drinkwater, N. J., 2011. Architecture of turbidite channel systems on the continental slope: Patterns and predictions. *Marine Petroleum Geology*, 28: 728–743.

Miall, A. D., 1985. Architectural-element analysis: a new method of facies analysis applied to fluvial deposits. *Earth-Science Reviews*, 22: 261–308.

Miall, A. D., 1989. Architectural elements and bounding surfaces in channelized clastic deposits: notes on comparisons between fluvial and turbidite systems. In: Taira, A. & Masuda, F. (eds), *Sedimentary Facies in the Active Plate Margin*. Terra Scientific Publishing Company (TERRAPUB), Tokyo, pp. 3–15.

Mulder, T., 2011. Gravity processes and deposits on continental slope, rise and abyssal plains. In: Hüeneke, H. & Mulder, T. (eds), *Deep-sea Sediments. Developments in Sedimentology,* 63: 25–148.

Mulder, T., Migeon, S., Savoye, B. & Faugères, J. C., 2001. Inversely-graded turbidite sequences in the deep Mediterranean. A record of deposits by flood-generated turbidity currents. *Geo-Marine Letters*, 21: 86–93.

Mulder, T., Migeon, S., Savoye, B. & Faugères, J. C., 2002. Inversely-graded turbidite sequences in the deep Mediterranean. A record of deposits by flood-generated turbidity currents. Reply. *Geo-Marine Letters*, 22: 112–120.

Mulder, T., Syvitski, J. P. M., Migeon, S., Faugères, J. C. & Savoye, B., 2003. Marine hyperpycnal flows: initiation, behavior and related deposits. A review. *Marine and Petroleum Geology*, 20: 861–882.

Mutti, E., 1979. Turbidites et cones sous-marins profonds. In: Homewood, P. (ed.), *Sedimentation Detrique (Fluviatile, Littorale et Marine)*. Institut de Geologie, Université de Fribourg, Fribourg, pp. 353–415.

Mutti, E., 1985. Turbidite systems and their relations to depositional sequences. In: Zuffa, G. G. (ed.), *Provenance of Arenites*. D. Reidel Publishing Company, Dordrecht, pp. 65–93.

Mutti, E. & Normark, W. R., 1987. Comparing examples of modern and ancient turbidite systems: problems and concepts. In: Leggett, J. K. & Zuffa, G. G. (eds), *Marine Clastic Sedimentology*. Graham and Trotman, London, pp. 1–38.

Mutti, E. & Ricci Lucchi, F., 1972. Turbidites of the Northern Apennines, introduction to facies analysis (English translation by T. H., Nilsen, 1978). *International Geology Review*, 20: 125–166.

Mutti, E. & Ricci Lucchi, F., 1975. Turbidite facies and facies association. In: Mutti, E., Parea, G. C., Ricci Lucchi, F., Sagri, M., Zanzucchi, G., Ghibaudo, G. & Iaccarino, S. (eds), *Example of Turbidite Facies Associations from Selected Formations of Northern Apennines. 9th International Sedimentological Congress.* International Association of Sedimentologists, Nice, France, pp. 21–36.

Mutti, E. & Sonnino, M., 1981. Compensation cycles: a diagnostic feature of sandstone lobes. In: *Abstracts: 2nd European Regional Meeting, 1981*. International Association of Sedimentologists, Bologna, pp. 120–123.

Nescieruk, P., Paul, Z., Ryłko, W., Szymakowska, F., Wójcik, A. & Żytko. K., 1995. *Mapa geologiczna Polski, 1:200 000, arkusz Jasło*. Polska Agencja Ekologiczna, Warszawa. [In Polish.]

Nichols, G., 2009. *Sedimentology and Stratigraphy.* 2nd ed., Wiley-Blackwell, 419 pp.

Normark, W. R., 1970. Growth patterns of deep sea fans. *American Association of Petroleum Geologists Bulletin*, 54: 2170–2195.

Normark, W. R., 1978. Fan valleys, channels, and depositional lobes on modern submarine fans, characters for recognition of sandy turbidite environments. *American Association of Petroleum Geologists Bulletin*, 62: 912–931.

Nowak, W., 1963. Preliminary results of study on exotics from the Inoceramian Beds of the Skole Series, of several sites in the Przemyśl and the Bircza, Carpathians. *Kwartalnik Geologiczny* 7: 421–430. [In Polish, with English summary.]

Pickering, K. T., Stow, D., Watson, M. & Hiscott, R., 1986. Deep-water facies, processes and models: A review and classification scheme for modern and ancient sediments. *Earth-Science Reviews*, 23: 75–174.

Pickering, K. T., Hiscott, R. N. & Hein, F. J., 1989. *Deep Marine Environments: Clastic Sedimentation and Tectonics*. Unwin Hyman, London, 416 pp.

Pickering, K. T., Hiscott, R. N., Kenyon, N. H., Ricci Lucchi, F. & Smith, R. D. A., 1995. *Atlas of Deep Water Environments: Architectural Style in Turbidite Systems*. Chapman and Hall, London, 334 pp.

Picot, M., Droz, L., Marsset, T., Dennielou, B. & Bez, M., 2016. Controls on turbidite sedimentation: Insights from a quantitative approach of submarine channel and lobe architecture (Late Quaternary Congo Fan). *Marine and Petroleum Geology*, 72: 423–446.

Porębski, S. J. & Warchoł, M., 2006. Hyperpycnal flows and deltaic clinoforms – implications for sedimentological interpretations of Late Middle Miocene fill in the Carpathian Foredeep Basin. *Przegląd Geologiczny*, 54: 421–429. [In Polish, with English summary.]

Posamentier, H. W. & Kolla, V., 2003. Seismic geomorphology and stratigraphy of depositional elements in deep-water settings. *Journal of Sedimentary Research*, 73: 367–388.

Postma, G., Nemec, W. & Kleinspehn, K. L., 1988. Large floating clasts in turbidites: a mechanism for their emplacement. *Sedimentary Geology*, 58: 47–61.

Prélat, A., Hodgson, D. M. & Flint, S. S., 2009. Evolution, architecture and hierarchy of distributary deep-water deposits: a high-resolution outcrop investigation from the Permian Karoo Basin, South Africa. *Sedimentology*, 56: 2132–2154.

Rajchel, J., 1989. The geological structure of the San Valley in the Dynów-Dubiecko region. *Biuletyn Państwowego Instytutu Geologii*, 361: 11–53. [In Polish, with English summary.]

Rajchel, J., 1990. Lithostratigraphy of the Upper Palaeocene and Eocene sediments from the Skole Unit. *Zeszyty Naukowe AGH 1369, Geologia,* 48: 1–112. [In Polish, with English summary.]

Rajchel, J. & Uchman, A., 1998. Ichnological record of palaeoenvironment in the transgressive Miocene deposits of the Skole Unit in the Dubiecko region (SE Poland). *Przegląd Geologiczny*, 46: 523–529. [In Polish, with English summary.]

Rea, D. K. & Lyle, M. W., 2005. Paleogene calcite compensation depth in the eastern subtropical Pacific: answers and questions. *Paleoceanography*, 20: PA1012.

Salata, D., 2014. Detrital tourmaline as an indicator of source rock lithology: an example from the Ropianka and Menilite formations (Skole Nappe, Polish Flysch Carpathians). *Geological Quarterly*, 58: 19–30.

Salata, D. & Uchman, A., 2013. Conventional and high-resolution heavy mineral analyses applied to flysch deposits: comparative provenance studies of the Ropianka (Upper Cretaceous–Paleocene) and Menilite (Oligocene) formations (Skole Nappe, Polish Carpathians). *Geological Quarterly*, 57: 649–664.

Shanmugam, G., 2016. Submarine fans: A critical retrospective (1950-2015). *Journal of Palaeogeography,* 5: 2–76.

Shanmugam, G. & Moiola, R. J., 1988. Submarine fans: characteristic, models, classification and reservoir potential. *Earth-Science Reviews,* 24: 383–428.

Shanmugam, G. & Moiola, R. J., 1991. Types of submarine fan lobes: models and implications. *American Association of Petroleum Geologists Bulletin*, 75: 156–179.

Skulich, J., 1986. Badania magmowych skał egzotycznych we wschodnich Karpatach Fliszowych na obszarze Polski. *Kwartalnik Geologiczny*, 30: 135–136. [In Polish.]

Snedden, J. W. & Liu, C., 2010. A compilation of Phanerozoic sea-level change, costal onlaps and recommended sequence designations. *American Association of Petroleum Geologists Search and Discovery*, Article 40594, 3 pp.

Stow, D. A. V. & Shanmugam, G., 1980. Sequences of fine grained turbidites – comparison of recent deep-sea and ancient flysch sequences. *Sedimentary Geology*, 25: 23–42.

Stow, D. A. V. & Mayall, M., 2000. Deep-water sedimentary systems: new models for the 21st century. *Marine and Petroleum Geology*, 17: 125–135.

Strzeboński, P., 2015. Late Cretaceous–Early Paleogene sandy-to-gravelly debris flowsand their sediments in the Silesian Basin of the Alpine Tethys (Western Outer Carpathians, Istebna Formation). *Geological Quarterly*, 59: 195–214.

Sumner, E. J., Amy, L. & Talling, P. J., 2008. Deposit structure and processes of sand deposition from a decelerating sediment suspension. *Journal of Sedimentary Research*, 78: 529–547.

Ślączka, A. & Kaminski, M. A., 1998. A guidebook to excursions in the Polish Flysch Carpathians. *Grzybowski Foundation Special Publication*, 6: 11–71.

Ślączka, A. & Thompson, S., III, 1981. A revision of the fluxoturbidite concept based on type examples in the Polish Carpathian Flysch. *Annales Societatis Geologorum Poloniae*, 51: 3–44.

Talling, P. J., Masson, D. G., Sumner, E. J. & Malgesini, G., 2012. Subaqueous sediment density flows: Depositional processes and deposit types. *Sedimentology*, 59: 1937–2003.

Uchman, A. & Wetzel, A., 2012. Deep-sea fans. In: Knaust, D. & Bromley, R. G. (eds), *Trace Fossils as Indicators of Sedimentary Environments*. *Developments in Sedimentology*, 64: 643–671.

Unrug, R., 1963. Istebna Beds – a fluxoturbiditic formation in the Carpathian Flysch. *Rocznik Polskiego Towarzystwa Geologicznego*, 33: 49–92.

Vrolijk, P. J. & Southard, J. B., 1997. Experiments on rapid deposition of sand from high-velocity flows. *Geoscience Canada*, 24: 45–54.

Walker, R. G., 1978. Deep-water sandstone facies and ancient submarine fans – models for exploration and for stratigraphic traps. *American Association of Petroleum Geologists Bulletin*, 62: 932–966.

Walker, R. G., 1984. General introduction: facies, facies sequences and facies models. In: Walker, R. G. (ed.), *Facies Models*, 2nd ed. *Geoscience Canada Reprint Series*, 1: 1–9.

Warchoł, M., 2007. Depositional architecture of the Magura Beds from the Siary zone, south of Gorlice (Magura Nappe, Polish Outer Carpathians). *Przegląd Geologiczny*, 55: 601–610. [In Polish, with English summary.]

Wdowiarz, J., 1939. Structure géologique des Karpates dans la région de Dynów. *Biuletyn Państwego Instytutu Geologicznego*, 10: 1–22. [In Polish, with French summary.]

Woiński, J., 1994. *Mapa geologiczna Polski, 1:200 000, arkusz Rzeszów*. Polska Agencja Ekologiczna, Warszawa. [In Polish.]

Zavala, C., Arcuri, M. & Blanco Valiente, L., 2012. The importance of plant remains as diagnostic criteria for the recognition of ancient hyperpycnites. *Revue de Paléobiologie (Genève)*, 11: 457–469.

GEOLOGICA CARPATHICA, FEBRUARY 2018, 69, 1, 71–88 doi: 10.1515/geoca-2018-0005

Sedimentary processes and architecture of Upper Cretaceous deep-sea channel deposits: a case from the Skole Nappe, Polish Outer Carpathians

PIOTR ŁAPCIK

Institute of Geological Sciences, Jagiellonian University, Gronostajowa 3a, 30-063 Kraków, Poland; piotr.lapcik@doctoral.uj.edu.pl

(Manuscript received July 4, 2017; accepted in revised form December 12, 2017)

Abstract: Deep-sea channels are one of the architectonic elements, forming the main conduits for sand and gravel material in the turbidite depositional systems. Deep-sea channel facies are mostly represented by stacking of thick-bedded massive sandstones with abundant coarse-grained material, ripped-up clasts, amalgamation and large scale erosional structures. The Manasterz Quarry of the Ropianka Formation (Upper Cretaceous, Skole Nappe, Carpathians) contains a succession of at least 31 m of thick-bedded high-density turbidites alternated with clast-rich sandy debrites, which are interpreted as axial deposits of a deep-sea channel. The section studied includes 5 or 6 storeys with debrite basal lag deposits covered by amalgamated turbidite fills. The thickness of particular storeys varies from 2.5 to 13 m. Vertical stacking of similar facies through the whole thickness of the section suggest a hierarchically higher channel-fill or a channel complex set, with an aggradation rate higher than its lateral migration. Such channel axis facies cannot aggrade without simultaneous aggradation of levee confinement, which was distinguished in an associated section located to the NW from the Manasterz Quarry. Lateral offset of channel axis facies into channel margin or channel levee facies is estimated at less than 800 m. The Manasterz Quarry section represents mostly the filling and amalgamation stage of channel formation. The described channel architectural elements of the Ropianka Formation are located within the so-called Łańcut Channel Zone, which was previously thought to be Oligocene but may have been present already in the Late Cretaceous.

Keywords: Carpathians, sedimentary processes, architectural elements, deep-sea channel, massive sandstone, turbidite, debrite.

Introduction

The architectural elements concept is widely accepted for analysis of deep-sea depositional environments (Mutti & Normark 1987). According to this concept, sedimentary bodies are distinguished as parts of a hierarchically organized deep-sea fan model. A high variety of architectural elements are conditioned by material deposited, size and latitudinal position of depositional system, sea level changes, tectonic regime and sedimentary processes (e.g., Stow & Mayall 2000; Mulder 2011; Cossu et al. 2015; Shanmugam 2016). Architectural elements are usually distinguished in very well exposed depositional systems through analysis of facies associations (e.g., Gardner et al. 2003; Prélat et al. 2009; Hubbard et al. 2014; Bayliss & Pickering 2015a, b; Pickering et al. 2015). However, this concept was so far not applied to numerous formations, including the Ropianka Formation (Turonian–Paleocene) in the Skole Nappe (Polish Carpathians). This formation, up to 1.6 km thick, contains a succession of deep-sea deposits with numerous facies associations suggesting occurrence of different architectural elements (e.g., Bromowicz 1974; Kotlarczyk 1978, 1988; Łapcik in press), which remain almost undetermined. Tectonic deformation and poor exposure of the Ropianka Formation make difficulties in correlations of facies and architectural elements over longer distances. Nonetheless, large outcrops with high contribution of thick-bedded sandstones give a chance to distinguish such bodies in some places, for example, in the Słonne section, where Łapcik (in press) distinguished over 140 m thick lobe complex.

In this paper, deep-sea channel-fill and its internal architecture are presented in structureless and graded thick-bedded sandstones from the Manasterz Quarry, in references to associated sections. Moreover, depositional processes are interpreted on the basis of sedimentary structures and the internal architecture of the channel-fill.

Geological setting

This study is focused on the Ropianka Formation (after Kotlarczyk 1978), also known as the Inoceramian Beds (Uhlig 1888), which is referred to sand-rich deposits in the northern part of the Skole Nappe (also known as the Skyba Nappe). The formation comprises a succession of turbidity current, debris flow, slump, pelagic and hemipelagic deposits of the Turonian–Palaeocene age up to about 1.6 km thick (e.g., Kotlarczyk 1978, 1988). The Skole Nappe is the most external major tectonic unit in the Polish Carpathians (Fig. 1A). Deposits of the Skole Nappe accumulated in a separate

sub-basin (e.g., Kotlarczyk 1988), however, some authors regard part of the Skole Basin as the Carpathian marginal zone which corresponds to the basin slope (e.g., Jankowski et al. 2012). Sedimentation in the Outer Flysch Carpathians started in the Late Jurassic. The Carpathians evolved from a rift basin (since the Late Jurassic) to a remnant foreland basin in the Oligocene (Golonka et al. 2006; Nemčok et al. 2006; Ślączka et al. 2006, 2012; Gągała et al. 2012) and ultimately during the Miocene the basin was folded and thrusted upon the Carpathians Foredeep. During the Turonian–Paleocene times, the sediments of the Skole Basin are thought to have been derived from the southern part of the Upper Silesia and Małopolska blocks to the north (Książkiewicz 1962; Bromowicz 1974; Salata & Uchman 2013) and from the side of the Subsilesian Ridge (Węglówka Ridge) to the south (Książkiewicz 1962). The petrographic variety of the source area was repeatedly mentioned in the literature (e.g., Salata & Uchman 2013; Salata 2014; Łapcik et al. 2016 and references therein).

Four lithostratigraphic members of the Ropianka Formation were distinguished based on repeated carbonate-siliciclastic deposits (Fig. 1B; Kotlarczyk 1978). Each member (excluding the Wola Korzeniecka Member) contains carbonate-rich succession which passes into siliciclastic dominated deposits towards the top. Moreover, a decreasing contribution of carbonate material from the proximal area to the north to the distal area to the south of the Skole Basin is observed (Kotlarczyk

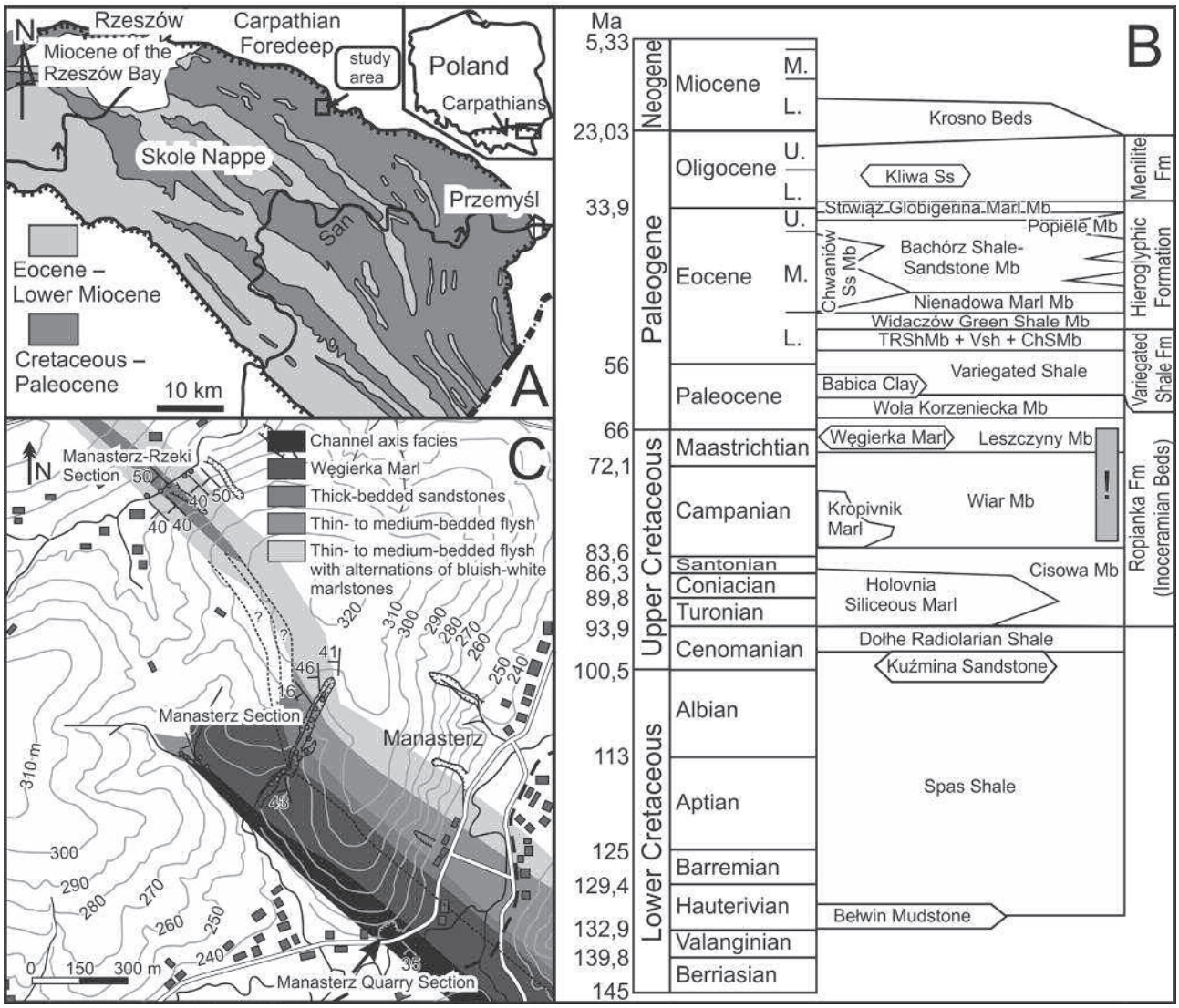

Fig. 1. Geographical and stratigraphic location of studied area. **A** — location map of the studied area in the Skole Nappe. Based on Kotlarczyk (1988) and modifications by Gasiński & Uchman (2009 and references therein); **B** — location of the Manasterz-Rzeki, Manasterz and Manasterz Quarry sections with some indicators of the orientation of beds as measured in the field and prediction of spatial distribution of facies; **C** — stratigraphic column of the Skole Nappe. Based on Kotlarczyk (1988), Rajchel (1990), Rajchel & Uchman (1998), Ślączka & Kaminski (1998), with further corrections based on further data by Gedl (1999) and Kotlarczyk et al. (2007). The investigated interval indicated by „!". The time scale is after Gradstein et al. (2012). TRSh Mb — Trójca Red Shale Member, VSh — Variegated Shale, ChS Mb — Chmielnik Striped Sandstone Member.

1978). Some areas show domination of mass transport deposits typical of slope areas (Burzewski 1966; Bromowicz 1974; Kotlarczyk 1978, 1988; Dżułyński et al. 1979; Geroch et al. 1979; Malata 2001; Jankowski et al. 2012; Łapcik et al. 2016). Foraminiferid assemblages point to deposition of the Ropianka Formation in bathyal depths below and above the calcite compensation depth (Uchman et al. 2006). The lithostratigraphy of the Ropianka Formation is still debated (e.g., Malata 1996; Jankowski et al. 2012).

Methodology

The fieldwork was based on sedimentological and facies analysis of sandy dominated thick-bedded deposits. The texture and primary structure of these deposits were described during detailed profiling. Grain-size analysis was conducted in order to determine the depositional processes of the thick-bedded sandstones and estimate the thickness of amalgamated beds. Fifty samples were taken for grain-size and petrographic analysis which was conducted as described in Łapcik (in press). The samples for grain-size analysis were collected from 4–5 cm thick layers with different distance intervals described further in the text. The orientation of the longer axis of 103 mudstone and marlstone clasts, orientation of grains and pebbles imbrication and orientation of the axis of flute casts from the MQ section were measured by mean of a geological compass in order to determine direction of palaeotransport. The last stage of the sedimentological and facies analysis of the thick-bedded sandstones was distinguishing the channel elements.

The sections studied

The studied deposits belong to the internally deformed Husów Thrust Sheet (Wdowiarz 1949), which is the second thrust sheet from the northern margin of the Carpathians. The majority of research was focused on sandy deposits in the well exposed Manasterz Quarry (MQ). Additional sedimentological study was conducted in two associated sections. Description of the whole Manasterz section is presented below in the stratigraphic order.

The Manasterz-Rzeki section

The oldest part of the section studied is located in a small gorge of an unnamed stream, a tributary of the Husówka Stream at Manasterz-Rzeki (Fig. 1C). The section is represented by five isolated outcrops containing thin- to thick-bedded sandstones, siltstones, mudstones and marlstones (Fig. 2). Beds are dipping to the SW at angles of 40°–50° (Fig. 1C). The contribution of each facies class in particular outcrops is presented in Figure 3. Sandstones are quartz-dominated, very fine- to medium-grained, with abundant parallel, convolute and cross-laminations underlined by carbonized plant detritus. Medium- and thick-bedded sandstones are graded or structureless at the basal part. Sole marks are numerous with a high contribution of the trace fossils *Ophiomorpha* and *Thalassinoides*. Some thin-bedded sandstones rich in plant detritus show chaotic structure, which probably resulted from bioturbation (the trace fossil *Scolicia* is present). Sandstones are alternated with grey mudstones, which often include thin layers of parallel and cross-laminated siltstones. The latest lithology is represented by bluish-white marlstones with sandstone alternations, which are 0.2–1 cm thick. Abundant bioturbation structures within marlstones are dominated by *Planolites* and *Chondrites*.

The Manasterz-Rzeki section begins as thin-bedded flysch with abundant alternation of marlstones (Fig. 2). Contribution of marlstones decreases in the middle part of the section with simultaneous significant increase in medium- and thick-bedded sandstones (Fig. 3). The top of the section is again represented by thin-bedded flysch with abundant alternation of marlstones similar looking to the bottom part of the section. The total thickness of the Manasterz-Rzeki section is 116 m with a 28 m-thick middle part showing numerous medium and thick sandstone beds. The Manasterz-Rzeki section belongs to the Campanian Wiar Member (Fig. 1B; Kotlarczyk 1978).

The Manasterz section

Higher part of the section crops out in gorges of unnamed tributaries of the Mleczka River, south of Manasterz-Rzeki, where beds dip to the W and SW (Fig. 1C). The lower part of the section is represented by thin-bedded flysch with alternation of marlstones showing similar appearance to the top and bottom part of the Manasterz-Rzeki section (Fig. 2). To the top of the section, the contribution of marlstones decreases with simultaneous increasing of mudstones (Fig. 2). The higher part of the section contains a medium- and thick-bedded sandstone interval. These sandstones are dominated by fractionally graded and parallel laminated parts with abundant, clasts of coal. However, some of the medium- and thick-bedded sandstones are structureless at their base. Above the sandy interval, packages of fine-grained, structureless, muddy sandstones with clasts of mudstone and marlstone are alternated with up to tens of centimetres thick, silty and sandy calcareous, structureless mudstones with dispersed quartz pebbles. This type of deposit is abundant in the external (northern) part of the Skole Nappe and they are known as the Węgierka Marl (Baculites Marl). This unit is included in the Leszczyny Member (upper Maastrichtian–lower Palaeocene). The Manasterz section is 375 m thick (Fig. 2). Tectonic deformations leave uncertainty if the thick-bedded sandstone interval in the Manasterz section corresponds to the similar one in the Manasterz-Rzeki section (Fig. 1C).

The Manasterz Quarry section

The highest part of the section studied is exposed in a small quarry at Manasterz where beds are inclined to the south-west

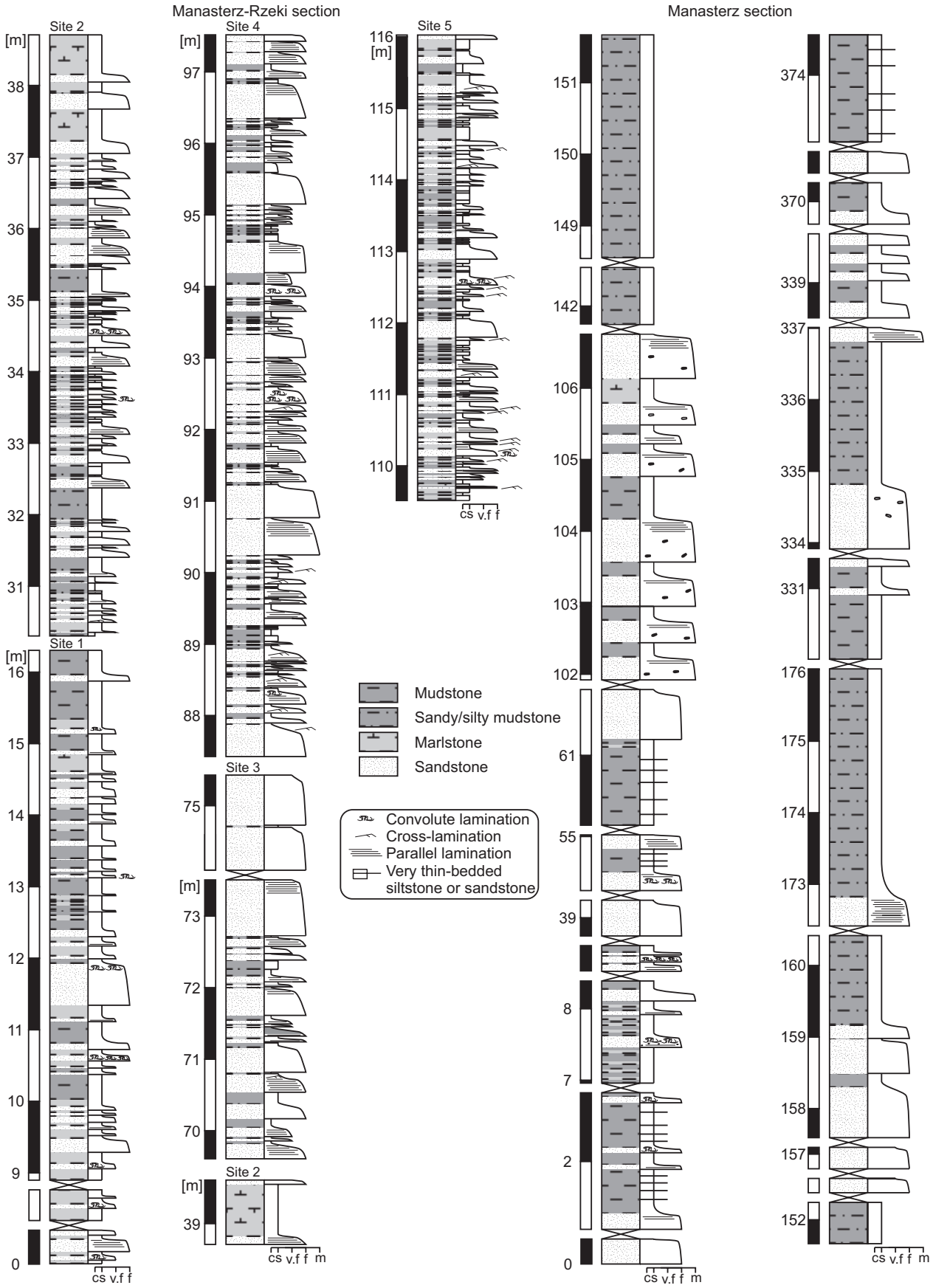

Fig. 2. Lithological columns of the Ropianka Formation at the Manasterz. Logs refer to the Manasterz-Rzeki and the Manasterz sections.

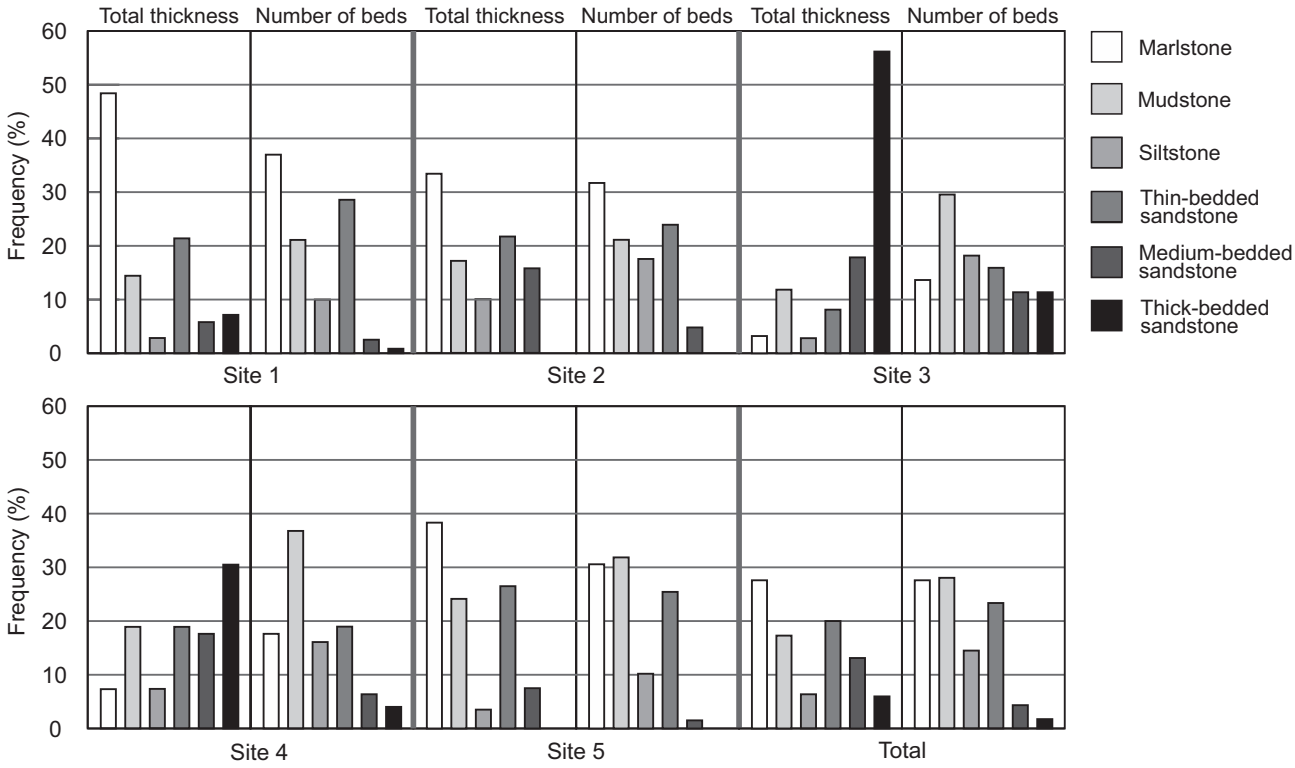

Fig. 3. Facies class abundance in the Manasterz-Rzeki section.

at angles of 30–40°. The quarry is 85 m long and up to 12 m high. The outcrop consists of 31 m of fully sandstone section where yellowish-orange, graded and structureless, amalgamated sandstones are fine- to coarse-grained with locally abundant dispersed quartz gravel, mudstone and marlstone cobbles and boulders (Fig. 4). Mudstone clasts are usually very poor in microfauna, however, some contain abundant bryozoans. The sandstones are quartz arenites, which contain minor admixture of siliceous grains, muscovite, sericite, glauconite, biotite, feldspar, mica schists, pyrite concretions, granite, gneiss and coal. A minor contribution of biogenic material is represented by abraded bivalve shells, siliceous sponge spicules and agglutinated benthic foraminifer tests. The contribution of accessory components never exceeds a few percent in total. Quartz grains are almost always well rounded. Polymineralic grains are limited to the largest fractions of 0.25–2 mm. The sandstone contains variable amounts of carbonate, silica and clay minerals cement and passes from hard lithified to almost loose sand. The MQ sandstone facies significantly differ from the thick-bedded sandstone intervals from the Manasterz-Rzeki and Manasterz sections. A detailed description of the MQ section is presented in "Material studied".

In a similar stratigraphic position, to the NW of the quarry, thin- to medium-bedded sandstones alternated with grey mudstones are present (Figs. 1C, 2). These deposits are very similar to these in the lower part of the Manasterz section and they represent a lateral facies equivalent of the Manasterz section.

Material studied

The Manasterz Quarry facies

The majority of research was focused on the well exposed MQ sandy deposits. Sedimentological and facies analyses of the structureless and graded sandstones allowed to distinguish two or optionally three facies, descriptions and interpretations of which are presented below.

Facies 1

The majority of deposits in the MQ section are represented by fine- to coarse-grained, graded or macroscopically structureless sandstones with quartz gravel and clasts of mudstone and marlstone. Their bedding is poorly expressed because of abundant amalgamation and paucity of sedimentary structures. The amalgamation surfaces are uneven and marked by abrupt grain-size changes (Fig. 5A), which tend to decline laterally in the scale of metres. Some of the sandstones show crude lamination, which is underlined by parallel orientation of coarse grains and pebbles and very rare imbrication. Clasts are similar to mudstones and marlstones from the Manasterz and Manasterz-Rzeki sections and are mostly oriented parallel to the bedding (Fig. 5B). Clasts of mudstone are usually several tens of centimetres long and a few centimetres thick, whereas, clasts of marlstone are mostly rounded to subrounded and do not exceed 20 cm in diameter. Marlstones contain abundant *Chondrites*, *Planolites* and some

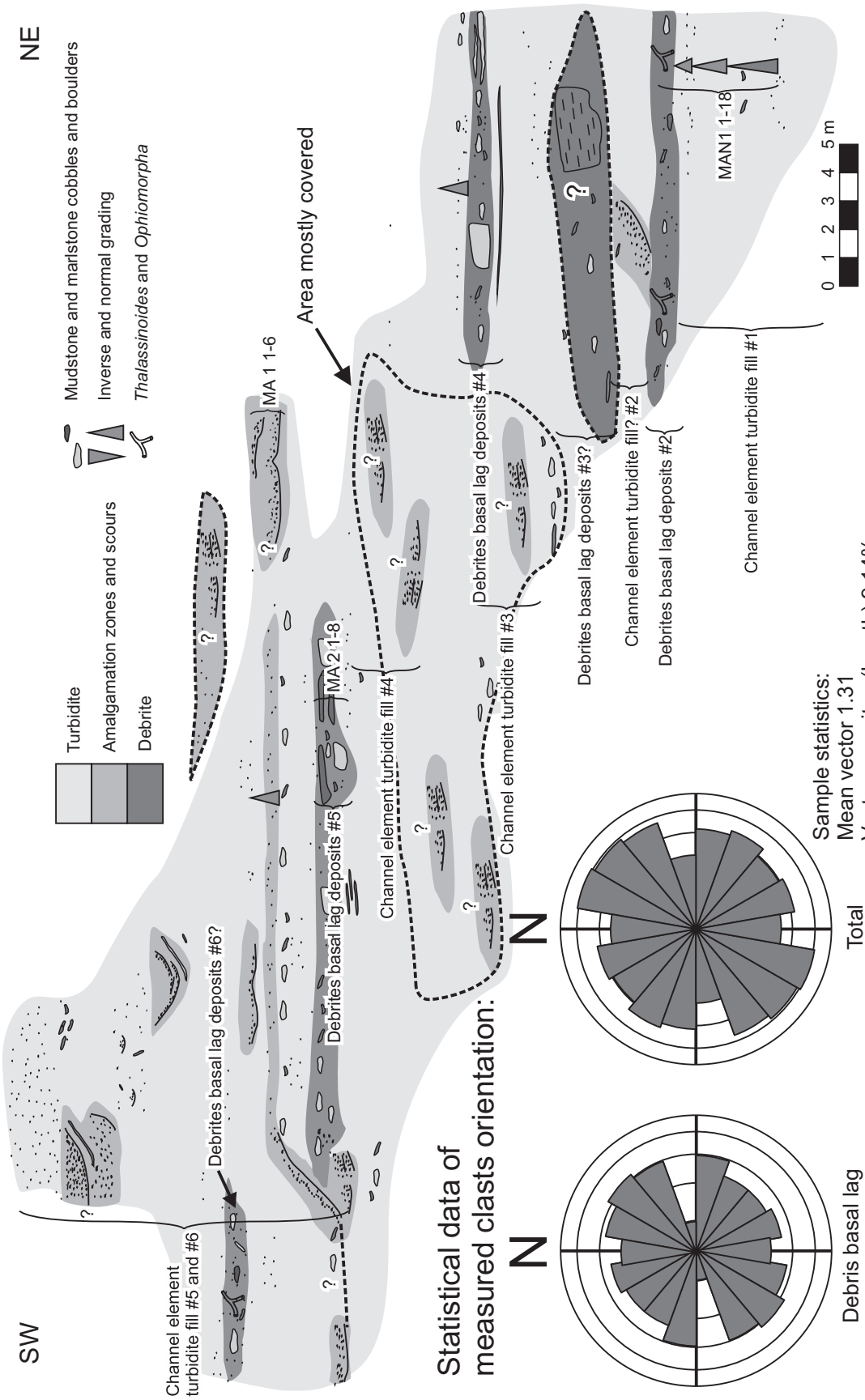

Fig. 4. Interpretation of the Manasterz Quarry section with distinguishing of the channel elements and statistical data of measured clast orientation.

unidentified bioturbation structures. Several erosional incisions up to 1.5 m deep and 2.5–6.5 m wide, with margins inclined at angles from 30° to almost 90° occur within the massive sandstones. They are filled with sandstone with quartz pebbles and shell debris. These structures are considered as mega-flutes. Some of them are filled exclusively with coarse-grained material, whereas others contain coarse-grained deposits in the lower part which is covered by medium- to fine-grained macroscopically structureless sandstone (Fig. 5C). However, coarse-grained layers can occur in multiple levels in one mega-flute. Particular coarse-grained layers may show normal or inverse to normal grading. Most of the mega-flutes are partly covered by recent debris or they are partly truncated by recent erosion. Therefore, their total width was impossible to estimate. Moreover, smaller, several centimetres thick scours are abundant within the macroscopically structureless and graded sandstone (Fig. 5A). The measured mean axis of the scours and grain imbrication indicate N–S and NW–SE orientations.

In order to determine the depositional process of facies 1 sandstones, two series of samples for grain-size analysis were collected (Fig. 6). Series MAN1 1–16 was collected in 20–30 cm intervals from 3.8 m thick bottom part of the section (Fig. 4). This sandstone interval rarely contains small mudstone clasts and amalgamation surfaces, which disappear at the distance of 1–3 m. Clasts are oriented parallel to the bedding in a discrete horizons. Grain-size analysis showed that sampled interval contains three fractionally graded amalgamated beds with mud content never exceeding 15 % by weight (Fig. 6). Estimated beds thickness decreases from 180 cm at the bottom, 80 cm in the middle to 40 cm at the top of the sampled interval (Fig. 6).

The second series of samples MA1 1–6 was collected in 10 cm intervals, from the middle part of the section, which include coarse-grained amalgamated sandstone (Fig. 4). The series starts at the bottom of an abrupt coarsening surface and includes two such surfaces. The analysis shows presence of the normal grading at the bottom amalgamation surface and the inverse to normal grading in the upper one (Fig. 6). The contribution of mud does not exceed 12 % by weight in the whole sample series (Fig. 6).

Interpretation: Facies 1 sandstones are interpreted as deposits of high-density turbidity currents mostly formed by layer-by-layer incremental deposition (e.g., Lowe 1982; Talling et al. 2012). Rapid fallout of grains from turbulent suspension suppressed the formation of sedimentary structures (Lowe 1982), however, grading was preserved. Mathematical modelling studies of Baas (2004) showed that lack of T_{bc} Bouma intervals in the top of structureless sandstones cannot be explained by abrupt deceleration of density flow only. Macroscopically structureless and graded sandstone beds at the MQ have no sign of water escape structures and lamination in the upper part, they are within grain-size limit for ripple lamination (<0.7 mm), show wide grain-size distribution (Fig. 6), and they do not have bioturbation structures. Therefore, the laminated top of structureless beds was eroded or bedforms are too thin to be recognized if duration of flow was too short within plane bed and ripple stability fields (Baas 2004). Occurrence of amalgamation surfaces, clasts of mudstone and marlstone and scours directly indicate strong erosional forces of the flows. Moreover, grain-size analysis showed that amalgamation surfaces are not restricted only to macroscopically abrupt grain-size coarsening but also occur within the structureless part. Therefore, amalgamation surfaces are more abundant than Figure 4 shows.

Isolated and laterally discontinuous mega-flutes reflect complex internal structure of the concentrated density flows (*sensu* Mulder & Alexander 2001) responsible for their origin. Such flows are featured by abrupt lateral transition from erosional through bypass to depositional conditions near the bottom. Fillings of the mega-flutes record a variety of depositional conditions which are expressed by lateral changes in the texture and primary structure of sediments (e.g., Leszczyński 1989 and references therein). Coarse-grained flute filling and coarse-grained amalgamation zones are basal lag deposits, which represent the thickest material carried by traction near the bottom (e.g., Dżułyński & Sanders 1962; Lowe 1982; Postma et al. 1988; Sohn 1997; Strzeboński 2015). Vertical multiple grain-size coarsening surfaces within some mega-flutes indicate deposition from an unsteady fluctuating flow or multiple filling of the flute by different events. Origin from multistage filling from independent flows is more probable because particular events would erode the top of the previous filling and leave lag deposits to underline amalgamation surface. Moreover, particular coarse-grained layers within the mega-flute fills show normal grading and inverse to normal grading from one coarse layer to another (Fig. 5C). Inversely graded coarse-grained amalgamation zones like the one from the M1 1–6 sampled interval imply deposition from high concentrated frictional traction where inversely grading is formed in the basal layer by shearing and kinematic sieving (Sohn 1997; Cartigny et al. 2013). Sediments deposited from traction are also confirmed by rare occurrence of coarse grains and imbrication of pebbles.

One of the features of the high-density turbidites is concentration of clasts in discrete horizons like in some structureless and graded sandstones in the MQ (Talling et al. 2012). Clast transportation within the high-density turbidity current is mostly on the rheological boundary between the turbulent damped bottom part of the flow and the more turbulent top or highly concentrated, turbulent damped, near bottom layer driven by turbulence from a more diluted top (e.g., Postma et al. 1988). Most of the elongated mudstone clasts suggest transportation on top of the highly concentrated bottom part of the high-density turbidity current, which prevented their further erosion and allowed them to keep their longitudinal shape. However, some authors suggest that preservation of mudstone clasts and their planar concentration to the top of bed is rather typical of sandy debrites (e.g., Shanmugam 2006; Strzeboński 2015). The well-rounded marlstone clasts imply relatively long traction transportation. Therefore, two importantly different shapes of clasts of lithologies which are easily

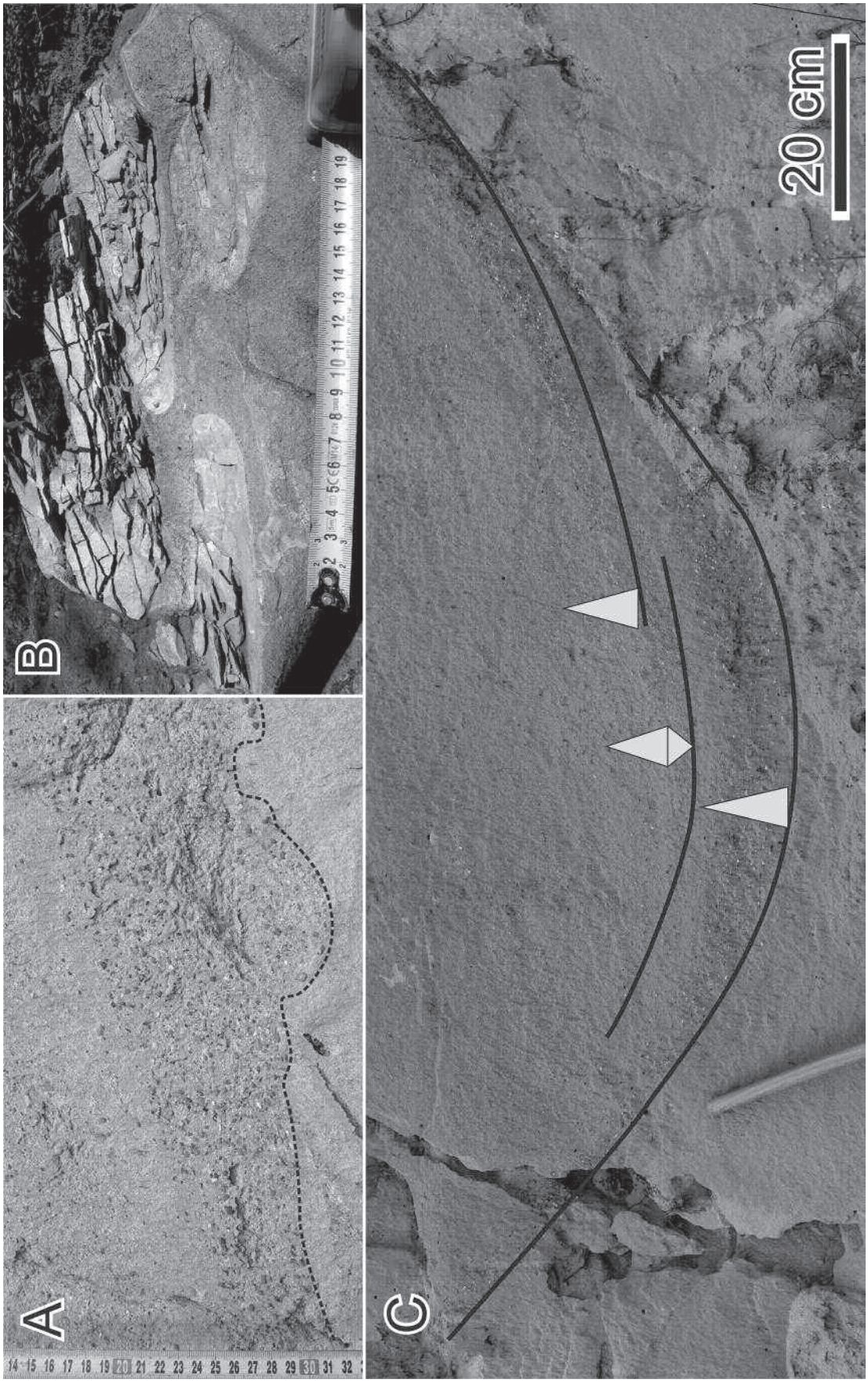

Fig. 5. Sedimentological features of facies 1 from the Manasterz Quarry section. **A** — coarse-grained amalgamation surface with small scale scours within the structureless sandstone of facies 1; **B** — well-rounded clasts of bluish-white marlstone oriented parallel to the bedding in a discrete horizon; **C** — large scour within the massive sandstone of facies 1 filled with multiple levels of coarse-grained layers. Particular coarse-grained layers show normal grading or inverse to normal grading which correspond to multistage filling of the scour.

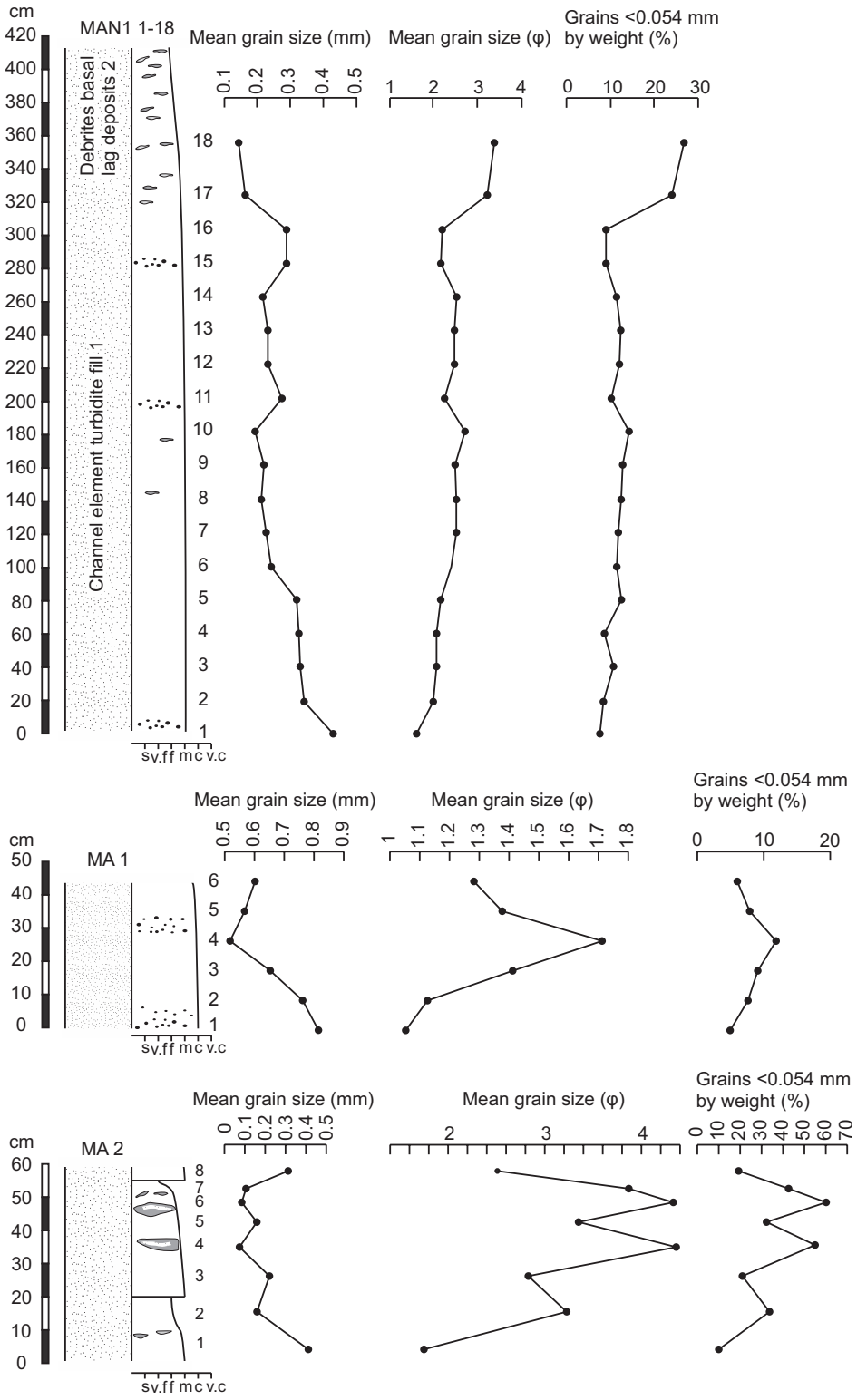

Fig. 6. Grain-size trends and mud content in MAN1 1–18, MA 1 1–6 and MA 2 1–8 sample series from the Manasterz Quarry section.

abraded suggest two different sources of the material and different distance of transportation. The marlstones clasts suggest erosion in a more proximal slope setting and longer transportation, whereas, elongated mudstones probably originated from undercutting of local overbanks.

The relatively small contribution of mud (Fig. 6) probably corresponds to flow stripping, which caused grain segregation in the long run confined flows and bypass of muddy dilute upper part of the stratified density flow (e.g., Piper & Normark 1983; Peakall et al. 2000; Posamentier & Walker 2006;

McHargue et al. 2011). In such a case, sediments of the MQ should be deposited in the relatively distal area to have enough time for grain segregation during transportation.

Facies 2

The MQ section contains a few layers of very fine- to coarse-grained sandstones with abundant large clasts of grey and reddish-brown mudstone and bluish-white marlstones (Fig. 7A). The layers are 1–2 m thick and can be traced over distance up to tens of metres. The boundary between facies 1 and facies 2 is usually reflected by a change in grain-size and mud content. Nevertheless, some beds of facies 1 seem to pass into structureless clast-rich sandstone of facies 2 with no sharp boundary. Angular to sub-rounded clasts represent the same lithology as in the facies 1. However, marlstones in some clasts, which are much thicker and poorly bioturbated, lithologically resemble the Węgierka Marl (e.g., Burzewski 1966; Geroch et al. 1979; Fig. 7B). Clasts are mostly oriented with their longer axis parallel to the bedding with maximum size up to 150x60 cm. However, those with size up to tens of centimetres in diameter dominate. Some clasts contain incised sand- and gravel-size grains chaotically distributed within the clasts or filling clastic veins. Matrix is represented by fine- to coarse-grained sandstone with slightly higher contribution of mud than in facies 1, which laterally may pass into fine- to medium-grained, dark, muddy sandstone with abundant small mudstone clasts and veins and lenses of clean sandstone similar to facies 1. Chaotic distribution of coarse grains within the matrix is reflected by their nest or patchy distribution and lateral changes in their density (Fig. 7C). Fine-grained matrix contains *Thalassinoides* and *Ophiomorpha* preserved as endichnial full reliefs. Moreover, some of the trace fossils cross-cut marlstone clasts and are filled by the matrix (Fig. 7D).

Grain-size analysis of clast-rich layers includes samples MAN1 17–18 from the bottom part and MA2 1–8, which were collected in 5–10 cm intervals from the middle part of the section (Fig. 5). Samples MAN1 17–18 show relatively muddy (>25 % of mud content by weight) fine-grained sandstones. There is an important decrease in mean grain-size and mud content from facies 1 to facies 2 in the sample series MAN1 1–18.

Samples MA2 1–8 show alternations of fine- to medium-grained, graded, clean sandstone and muddy sandstone. Layers of muddy fine-grained sandstone are discontinuous laterally and change their thickness from a few to tens of centimetres. They correspond to matrix with veins and lenses of clean sandstone described above. Amalgamation surfaces are present at the bottom of the lower structureless clean sandstone and above the fine-grained sandstone and stand as boundaries between facies 1 and facies 2. Similarly to MAN1 1–18, muddy layers are much finer-grained than in facies 1 clean sandstones.

Orientation of the longer axes of 103 clasts was measured in different clast-rich layers (Fig. 4). Most of the clasts, which were accessible for measurement, are concentrated within the lowermost clast-rich layer. These data do not correlate with orientation of erosional structures and grain imbrication, which indicate NW-SE and N-S palaeotransport direction. Collected data show that majority of clasts are oriented randomly without any specific trend which may indicate palaeoflow direction (Fig. 4).

Interpretation: Fine- to coarse-grained, clast-rich, muddy structureless sandstones of facies 2 are interpreted as debrites. Numerous, chaotically oriented huge clasts could be transported only by matrix supported debris flows (e.g., Shanmugam 2006; Strzeboński 2015). Moreover, patchy and nest distribution of coarse-grains imply poor conditions for grain segregation, which is the feature typical of laminar flow. Each clast-rich layer represents one or more debrites, which in some cases tend to abruptly pinch out laterally. Abrupt change in thickness and pinch-out of clast layers over a distance of several metres agrees with the spatial shape typical of debrites (e.g., Amy & Talling 2006). In some case laterally discontinuous muddy type of matrix with veins and lenses of clean sandstone may represent large eroded muddy boulders, which were poorly mixed during transportation with sandy matrix of the previous flow. Moreover, the poor roundness of larger clasts confirms weak interactions between components during transportation. Parallel orientation of clasts to the bedding and occurrence of veins filled by sand- and gravel-size grains imply matrix internal shear stress during debris flows movement. The occurrence of huge boulders of marlstone typical of the Węgierka Marl suggests shelf origin of some debrites and therefore, relatively long distance of transportation. However, rare occurrence of thin, tens of centimetres long, unfolded mudstone clasts imply that there were also short-lived slides with internal shear low enough to prevent clast deformation and folding. Similarly to facies 1, they may derived from undercutting of local overbank deposits. The erosional potential of some debris flows is reflected by uneven bottom surfaces and incision of debrites into turbiditic sandstone of facies 1.

Particle-size analysis shows important change in grain-size and mud contribution from deposits of turbidity currents and debris flows in both MAN1 and MA2 samples series (Fig. 6). Some of the debris flows were probably transformed from concentrated to hyperconcentrated density flows by increasing contributions of cohesive mud from disintegration of eroded clasts (Mulder & Alexander 2001), which agrees with the abundance of clasts and poor boundary between some beds of facies 1 and 2.

Occurrence of clasts of marlstone cross-cut by bioturbation structures filled with surrounding matrix implies bioturbation after deposition of debrites (Fig. 7C). This indicates good post-depositional environmental oxic conditions for benthic life. Preferential occurrence of bioturbation structures within the debrites may result from higher contributions of supplied nutrients or from periods of decreased sedimentation rate after deposition of debrites. Nevertheless, lack of bioturbation structures at the top of facies 1 beds may result from erosion.

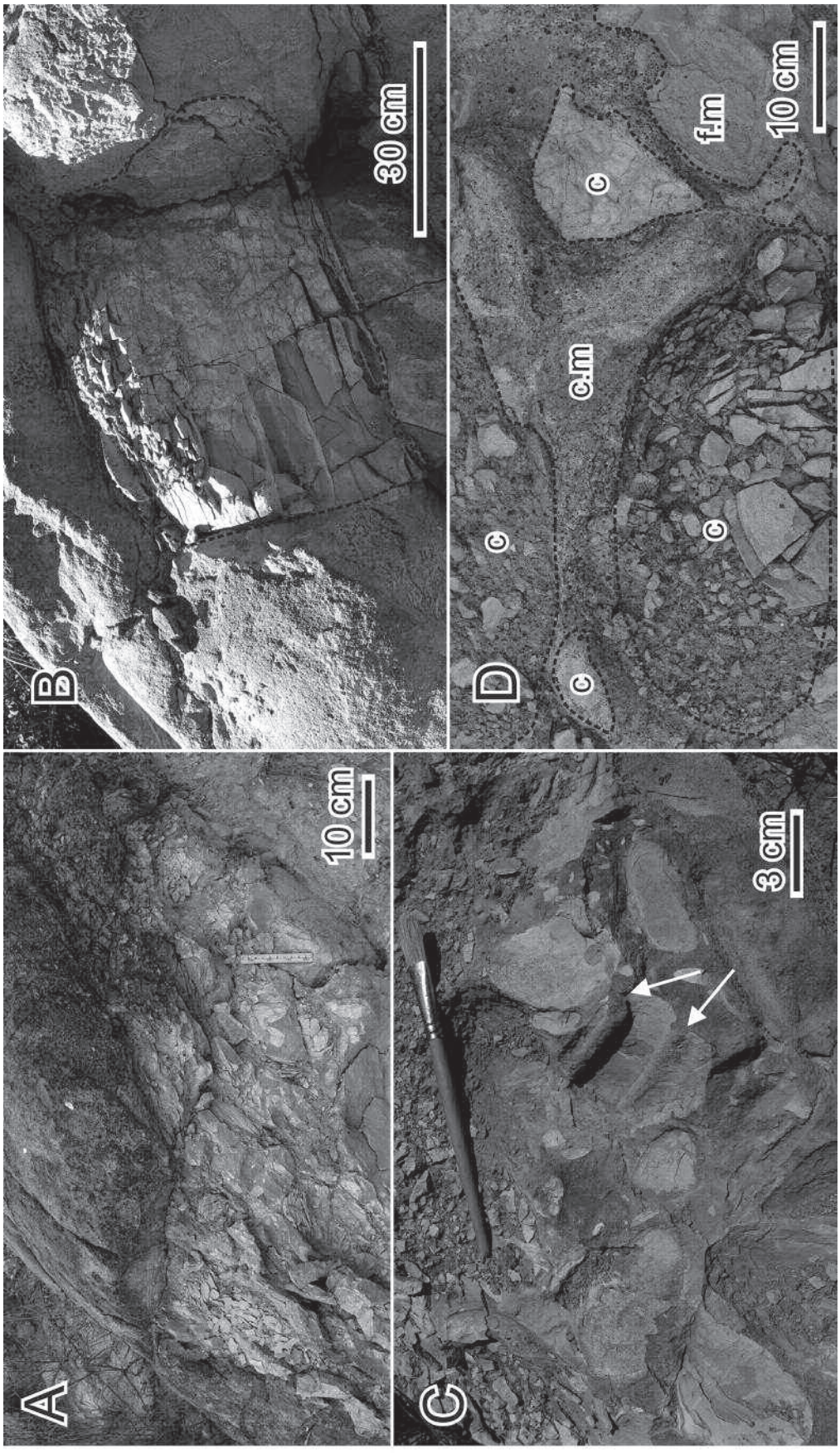

Fig. 7. Sedimentological feature of facies 2 from the Manasterz Quarry section. **A** — clast-rich sandy debrite; **B** — a huge boulder of bluish-white marlstone similar to the Węgierka Marl in the sandy debrite of facies 2; **C** — sandy debrite with clast of marlstone cross-cut by bioturbation structures filled with surrounded matrix. White arrows show bioturbation structures; **D** — clast-rich (c) sandy debrite with sharp boundary between coarse-grained (c.m) and fine-grained matrix (f.m).

Facies 3 or large boulder?

In the lower part of the MQ section, a 1.8 m thick layer of grey to bluish-white, calcareous mudstone with rare alternation of <0.6 cm thick siltstone is present. To the top and bottom, sharp boundary with sandstone of facies 1 is observed. Laterally, mudstone layer is continuous over a distance of at least 3 m. Nevertheless, incomplete exposition does not allow determination of its true lateral size and continuity. The mudstone is structureless and it shows no sign of bioturbation. The siltstone is laminated and rich in plant detritus. It shows sharp bottom boundaries.

Interpretation: Grey, calcareous mudstones are hemipelagic to pelagic facies typical of basin slope. Laminated siltstones are interpreted as deposits of dilute low-density turbidity currents and correspond to the T_d Bouma division, but their origin from bottom currents cannot be totally excluded. Uncertain lateral continuation and exceptional thickness suggest that this mudstone-dominated layer may represent a large boulder within a debris flow rather than a cape of thick sandstones from below. Moreover, some transition from very thick-bedded sandstone to very thick mudstones might be expected, but it is absent in the section studied. Nevertheless, such a mudstone layer may also originate from an abrupt decrease of activity in the source area, which resulted in vanishing of sand deposition in the study area.

Manasterz Quarry section as a channel-fill

Deep-sea channels are often thought as prolongation of deep-sea canyons or gullies, which distribute boulder to clay size material from upper and middle slope to abyssal plain. Deep-sea channels show many different forms with two end members where dominating processes are erosion (incising channels) or aggradation (constructive channels) respectively (e.g., Normark 1970; Flood et al. 1991; Hübsher et al. 1997; Babonneau et al. 2002). Deep-sea channels are distinguished as one of the hierarchical elements within deep-water depositional systems. Stacking of storeys or channel elements form channel complexes, channel complex sets and channel systems (Sprague et al. 2002, 2005; Abreu et al. 2003). Channels are relatively temporary structures, which migrate laterally by avulsion and lateral accretion. In this paper the MQ section facies are interpreted as deep-sea channel deposits with features and characteristics that are discussed below.

Channel characteristics of the Manasterz Quarry section

The MQ section shows the following features typical of deep-sea channel facies: high sand-to-mud ratio, occurrence of thick structureless and graded sandstones with paucity of sedimentary structures, a relatively high contribution of coarse material, numerous amalgamation surfaces, abundant scours and rip-up clasts and basal lag deposits (e.g., Mutti & Normark 1987; Shanmugam & Moiola 1988; Mayall et al. 2006; McHargue et al. 2011; Hubbard et al. 2014). Facies comparison in the same basin is a useful tool for distinguishing between particular facies of deep-sea channels (McHargue et al. 2011). The MQ section shows an extremely high sand-to-mud ratio in comparison to other outcrops of the Ropianka Formation (e.g., Bromowicz 1974; Kotlarczyk 1978). In the close vicinity of the study area, only a few small isolated outcrops with facies similar to the MQ section are available (Salata & Uchman 2013; Łapcik et al. 2016). This may suggest that deposits in the MQ section are related to a channel axis depositional environment.

An important feature of deep-sea channels is the lateral transition from channel axis to channel margin and channel-levee facies (e.g., Campion et al. 2000; Sprague et al. 2002, 2005; Gardner et al. 2003; Mayall et al. 2006; McHargue et al. 2011; Hubbard et al. 2014). Usually, the transition from channel axis to channel margin facies occurs at a distance of a few hundreds of metres (e.g., Shanmugam & Moiola 1988; Bruhn & Walker 1997; Campion et al. 2000; McHargue et al. 2011; Hubbard et al. 2014). The MQ thick-bedded sandstones are estimated to totally pinch-out to the NW at a distance of no more than 800 m (Fig. 1C). The outcrops which occupy similar stratigraphic positions to the MQ sandstones are dominated by thin- and medium-bedded sandstones alternated with mudstones and siltstones (Fig. 2). This facies change suggests a lateral offset of channel facies, which passes into channel margin or channel levee facies. In the close vicinity to the SE, facies similar to the MQ section are unknown (Gucik et al. 1980). Therefore, thick-bedded sandstones probably pinch-out laterally at a distance of tens to hundreds of metres. The total width of the Manasterz Quarry channel should not exceed a few hundreds of metres.

Formation and filling of the Manasterz Quarry channel

Deep-sea channels can be filled by turbidites, debrites, slumps and hemipelagic deposits with different contributions of these components but with a generally decreasing quantity of mass transport deposits downcurrent (e.g., Shanmugam & Moiola 1988; Dakin et al. 2013; Bayliss & Pickering 2015a). Channel incision is mostly attributed to erosion by previous high-density turbidity currents or the current responsible for channel filling. However, some of them can be created during bypass of debris flows when erosion can reach tens of metres (e.g., Dakin et al. 2013). The MQ channel is filled with mixed deposits of high-density turbidity currents and debris flows. Numerous amalgamation surfaces and alternations of turbidites and debrites imply a multistage process of filling characterized by repetitive transitions from deposition with a basal lag through erosion of the lag and to channel filling with domination of structureless and graded sandstones (e.g., Clark & Pickering 1996; Gardner et al. 2003). Thickness of the MQ channel reaches at least 31 m and is in range of channel-fill thickness (e.g., Sprague et al. 2005; Mayall et al. 2006; McHargue et al. 2011; Hubbard et al. 2014). The lowest hierarchical architectural element in channel settings are storeys or channel elements with thicknesses usually does not

exceeding 5 m (Sprague et al. 2002). The internal architecture of the MQ section allowed to distinguish storeys with two basic elements, which repeatedly occur within the section. The first basic element includes debrites of facies 2, which correspond to basal lag deposits at the bottom of a particular storey (e.g., Mayall et al. 2006). Occurrence of these deposits determines the boundary between different storeys located at their base. Facies 1 represents storey-fill, deposited after sedimentation of debrite basal lag deposits. The MQ section consists of five storey-fills alternating with three debrite basal lag deposits (Figs. 4, 8). It is uncertain if the channel element turbidite fill 5 represents two different elements separated by poorly exposed debrite or one very thick storey-fill (Figs. 4, 8). Thickness of particular storey varies from 2.5 m to 8 m or up to 13 m if the channel element 5 represents one channel element (Fig. 4). The thickness of particular debrite basal lag deposits is much thinner and reaches 1–2 m. The cover of the bottom part of the section does not allow us to distinguish the basal lag deposits of the first storey. Alternatively, debrites may represent event deposits, which randomly interrupted turbidite sedimentation during formation of the channel-fill. However, multiple repetition of 1) deposition of debrite lag deposits, 2) erosion of debrite lag deposits and 3) deposition of high-density turbidites supports the first alternative.

Thick-bedded structureless and graded sandstone facies and their vertical stacking suggest that the MQ section may represent an area near the thickest part of the channel where the coarsest material is stacked. Moreover, vertical stacking of couplets of facies 1 and facies 2 suggests affiliation to a larger channel-fill or a channel complex set with an aggradation rate higher than its lateral migration. Such channel facies cannot aggrade without simultaneous aggradation of levee confinement (McHargue et al. 2011). Hence, interpretation of the outcrops in the similar stratigraphic position to the NW as channel margin or channel levee is most probable (Figs. 1C, 2).

Channel formation can be subdivided into three stages: 1) erosion and bypass when large scale erosional surfaces up to tens of metres are formed and capped by lag deposits, 2) channel fill when the coarsest material is repeatedly deposited and eroded with simultaneous sediment spill outside the channel, and 3) abandonment when the finest material caps and separates two channel elements (e.g., Clark & Pickering 1996; Gardner et al. 2003; Mayall et al. 2006; Labourdette et al. 2008; Dakin et al. 2013; Bayliss & Pickering 2015a,b). Abundant amalgamation and small scale erosion, relatively low contribution of lag deposits and domination of deposits of collapsing flows imply that the MQ deposits represent the channel fill stage. According to McHargue et al. (2011), early filling and amalgamation of a channel begins after stabilization of the equilibrium profile by the previous erosional stage. Despite lower energy of the flows during the filling stage, erosion is still prominent, especially near the channel axis. Moreover, occurrence of clast-rich debrites is common during the early amalgamation stage (McHargue et al. 2011). Most of the models assume that the last stage of the channel formation is abandonment recorded by sedimentation of thin-bedded deposits. Lack of fining and thinning upward trend in the MQ section may derive from poor exposure where all deposits represent only a small part of a larger channel complex set. Alternatively, the presence of a nearby strongly developed levee, may also preclude development of fining and thinning upward trends (Shanmugam & Moiola 1988). Such a levee may be represented by previously mentioned facies in the similar stratigraphic position to the NW of the MQ. It is possible to speculate that highly amalgamated deposits forming architecture of the MQ channel correspond probably to abundant avulsion and low aggradation of secondary (inner) overbank on the scale of channel elements (Deptuck et al. 2003; Posamentier & Kolla 2003; McHargue et al. 2011).

Location of the Manasterz channel in the Skole Basin

Abundance of mass movement and sediment gravity flow deposits with extrabasinal material and distribution of marlstone facies suggest that sedimentation of the most external part of the Ropianka Formation took place on the middle or lower basin slope or close to the base of the slope (e.g., Burzewski 1966; Bromowicz 1974; Kotlarczyk 1978, 1988; Jankowski et al. 2012; Łapcik et al. 2016). Analysis of heavy minerals from the Ropianka Formation showed that its deposits derive from an immature passive margin setting (Salata & Uchman 2013). The MQ section represents an area of abundant erosion and abrupt waning flows, which correspond to hydraulic jump of the flow. The channel-lobe transitional zone is considered as a site of abundant hydraulic jump with common scouring and erosional structures (e.g., Mutti & Normark 1987; Wynn et al. 2002, Gardner et al. 2003). However, the channel-lobe transitional zone usually includes traction structures (often large scale), which are absent at the MQ (e.g., Mutti & Normark 1987; Wynn et al. 2002). High contribution of large intrabasinal rip-up clasts in the MQ section suggests strong erosional forces in the previous flow stage. Hence, the MQ channel is probably incised into mudstone- and marlstone-rich deposits of the Skole Basin slope or such clasts derived from undercutting of the channel levees. The occurrence of extrabasinal, shallow water material in the MQ deposits suggests a strong relationship with the Skole Basin shelf. Carbonate mud and shell debris were redeposited into offshore and afterwards slope areas probably by lowering of the storm wave base. Such material suggests a relationship with canyons or gullies which captured it after redeposition by storm events from more proximal areas.

Previously postulated simultaneous aggradation of overbank deposits and channel-fill is strongly related to contribution of overspilled mud from turbidity currents and with proximal-to-distal position of the channel. The height of levees can reach hundreds of metres and decreases downcurrent with decreasing amounts of the fine-grained cohesive material which stabilize levee banks (Damuth & Flood 1985). The low contribution of mud within deposits of high-density turbidity current in the MQ section suggests spillover and bypass of more muddy parts of the flow. Further evidence for

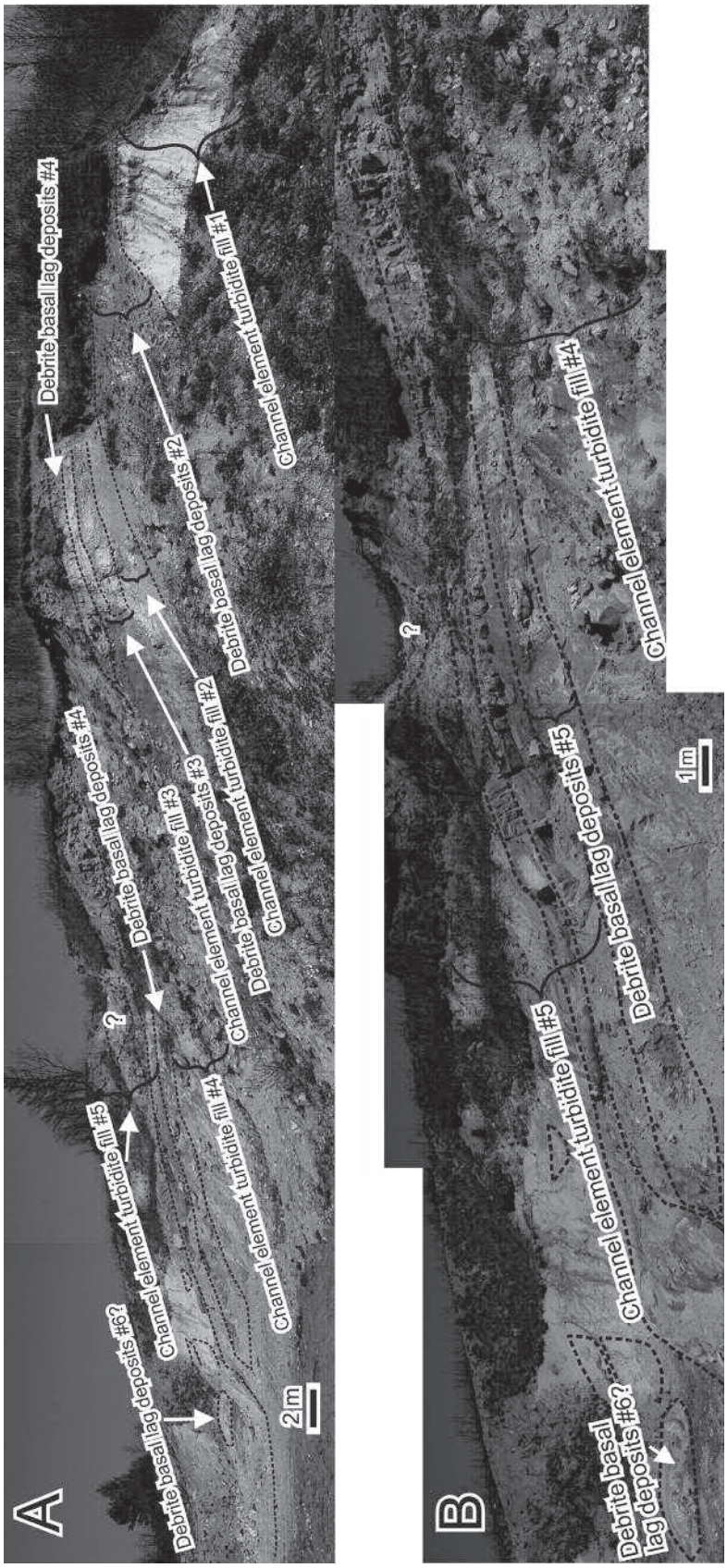

Fig. 8. The Manasterz Quarry section with distinguished channel elements. **A** — the Manasterz Quarry with distinguished channel elements. **B** — top of the Manasterz Quarry with distinguished channel elements.

strong bypass is the almost complete lack of organic detritus and coal debris in the MQ section. Such material is often an important component of thick-bedded sandstones in the Ropianka Formation (e.g., Kotlarczyk & Śliwowa 1963; Łapcik et al. 2016; Łapcik in press). It is unlikely that these deposits are related to another source area than sandstones from the lower part of the section (Manasterz-Rzeki) because such material is known from even younger deposits (e.g., Kotlarczyk & Śliwowa 1963). Therefore, the most probable scenario is bypass of organic detritus and coal, which was deposited in a more distal area, for example, in the lobe-like deposition of the Słonne section (Łapcik in press). Hence, the MQ channel should be situated in relatively proximal area on the lower slope or near base of the slope. According to Gardner et al. (2003), the MQ section shows features of the fill stage of a channel situated in the lower slope or base of the slope. This also stands in agreement with the proximal location of the MQ section within the second thrust sheet from the northern Carpathian margin.

Palaeotransport directions and sinuosity of the Manasterz Channel

Deposits of the Ropianka Formation show directions of the palaeotransport from NW, N and NE with dominance of the NW direction in the vicinity of the study area (Książkiewicz 1962; Bromowicz 1974). The palaeotransport data from the MQ include only measurements of scour orientation and grain imbrication within the structureless and graded sandstones, which indicate transportation from the NW. Nevertheless, directions of transport in a deep-sea channel may be variable and are rarely unidirectional. Spatial distribution and orientation of long belts of thick-bedded sandstone facies in the external part of the Ropianka Formation is consistent with the presented data and also point to the NW–SE axis (Gucik et al. 1980). All these data are premises for deposition of thick-bedded sandstone facies in the vicinity of

the study area longitudinal to the slope of the Skole Basin. Most of these facies suggest a strong relationship with the Łańcut Channel Zone proposed by Kotlarczyk & Leśniak (1990) for the Oligocene deposits (see also Salata & Uchman 2012, 2013). It seems that this channel zone was already active during the Late Cretaceous.

The previously mentioned lateral offset of the facies from the channel axis to the channel margin or channel levee from the MQ section to the Manasterz section allows speculation about sinuosity of the studied channel. Otherwise, axial or off-axial channel facies would be continued to the NW in the Manasterz section. Hence, the channel facies outcropping in the MQ should change their orientation to the N or the W to evade the Manasterz channel levee facies. Nevertheless, the MQ section does not appear to have lateral accretion packages that have been described in other meandering channel-fill deposits (e.g., Bouma & Coleman 1985; Mutti & Normark 1991; Abreu et al. 2003; Janocko et al. 2013). Unfortunately, covering of the area, tectonic deformations and inclination of beds does not allow tracking of the channel facies.

Interpetation of the Manasterz-Rzeki and Manasterz facies

Bottom and top parts of the Manasterz-Rzeki and the Manasterz section

The bottom and top parts of the Manasterz-Rzeki section show many similarities to the bottom part of the Manasterz section (Fig. 2). Thin- to medium-bedded sandstones and marlstones with abundant parallel, cross and convolute laminations probably correspond to channel levee or inter-channel deposits. The decreasing contribution of marlstones in the bottom part of the Manasterz section suggests that this interval is situated above the second marlstone-rich interval of the Manasterz-Rzeki section (Figs. 1C, 2). Such marlstones are widely distributed in the Ropianka Formation in the whole marginal part of the Skole Nappe (e.g., Kotlarczyk 1978, 1988; Leszczyński et al. 1995). The marlstones are considered as calciturbidites with their source area situated in the shelf surrounding the Skole Basin. They were deposited by low-density turbidity currents in the marginal part of the Skole Basin, which probably corresponds to the basin slope and base of the slope. However, marlstone clasts from the MQ derive from erosion of marlstones form the older part of the Ropianka Formation. After partly lithification they, were ripped up by high-density turbidity currents and redeposited into a more distal area.

Thick-bedded sandstones occur in the Manasterz-Rzeki and Manasterz sections. Stacking of thick-bedded, structureless and graded sandstones often with parallel laminated top alternating with thin- and medium-bedded laminated sandstones suggest channel or depositional lobe facies. However, the thickness and sand-to-mud ratio of these intervals together with sparse amalgamation and scours suggest some distance from the axis of such bodies in comparison to the MQ section. Both sections represent progradation and aggradation of some sand-rich body. Decreasing contribution of marlstones with simultaneous increase in thick-bedded sandstones (Fig. 3) may imply: 1) decreasing activity in the carbonate source area, 2) progradation of a sand body which temporarily became an obstacle for calciturbidites, or 3) increasing activity in the siliciclastic source area, sediments from which diluted the carbonate sedimentation. The relative proximity of these deposits can be referred to the marginal position of the study area in the Skole Nappe (second thrust sheet from the Carpathians margin). Tectonic deformations of the study area do not allow certain correlation between the sections studied. It is not clear whether the two thick-bedded intervals of the Manasterz-Rzeki and Manasterz sections represent the same sand body or two different sand bodies. The main difference between these thick-bedded sandstones is abundance of coal debris in the Manasterz section. However, this is too weak a premise to exclude any alternative. If the two intervals represent different bodies, the interval with decreasing contribution of marlstones at the bottom of the Manasterz section may correspond to the lateral offset of channel or lobe facies of the Manasterz-Rzeki section, and the upper part of the Manasterz-Rzeki section may correspond to channel abandonment facies or channel levee facies. These speculations also imply on lateral migration of sandy bodies at the distance of hundreds of metres derived probably from avulsion (Fig. 1C).

The Węgierka Marl

The Węgierka Marl is widely known from the Ropianka Formation in the external part of the Skole Nappe and is mostly represented by packages of fine-grained, muddy sandstones with mudstone and marlstone clasts, up to tens of centimetres thick, and sandy calcareous mudstones with dispersed quartz pebbles and clasts of marlstone. Moreover, huge marlstone olistoliths are also known (Burzewski 1966; Kotlarczyk 1978, 1988; Geroch et al. 1979). Such deposits mostly represent slumps and debris flows originating in the middle to lower slope setting. Their abundance and spatial distribution suggest their classification as mass transport deposits complex, which influenced the basin floor morphology. Mass transport deposits often occur at the bottom of channels and channel complexes (Clark & Pickering 1996; Mayall et al. 2006; Bayliss & Pickering 2015a). In the study area, the Węgierka Marl facies are located at the bottom of the MQ channel facies. Hence, the Manasterz Quarry channel complex was formed on its floor with abundant debrites which could stand as confinement of the initial channel zone. In the Leszczyny Member, the Węgierka Marl and thick-bedded sandstones often alternate (e.g., Burzewski 1966; Bromowicz 1974; Kotlarczyk 1978, 1988; Geroch et al. 1979) but it is not clear if massive sandstones of the MQ section are situated only at the top of the Węgierka Marl, or if they also border with them laterally and/or are capped by them. Some of the debrites in the MQ section contain huge boulders of marlstone very similar to the Węgierka Marl. This suggests that mass transport of the Węgierka Marl deposits also filled some channels

and that the channel filling is influenced by sea-level changes or short tectonic activities, which may trigger deposition of the Węgierka Marl mass transport deposits complex (Burzewski 1966; Geroch et al. 1979). Incision of the channels reflects direct changes in the slope equilibrium profile and may additionally suggest sea-level changes (e.g., Kneller 2003). The whole composite Manasterz section represents transition from lobe or channel off-axis facies alternating with inter-channel or overbank deposits of the Wiar Member to the MQ channel axis facies incised into the Węgierka Marl mass transport deposits complex of the Leszczyny Member.

Conclusions

1. Sandstones of the Manasterz Quarry represent channel axial or near axial facies with abundant amalgamation, coarse lag deposits, intra- and extrabasinal material. The studied section is dominated by deposits of high density turbidity currents (facies 1) with a smaller contribution of debrites (facies 2).
2. The Manasterz Quarry section represents channel-fill with total thickness of 31 m and width up to several hundreds of metres. The channel includes 5–6 storeys with debrite basal lag deposits at the bottom of storeys capped by channel turbidite fill. The basal lag deposits are 1–2 m thick, whereas the turbidite channel are 1.5–11.5 m thick. The channel-fill was formed by repeated deposition and amalgamation of turbidites and debrites.
3. Strong bypass, occurrence of lag deposits with material deriving from shallower zones and location relatively close to the northern margin of the Skole Basin suggest slope or base of slope setting of the Manasterz Quarry channel. The Manasterz Quarry deposits correspond to channel fill and amalgamation stage (Gardner et al. 2003; McHargue et al. 2011).
4. The section to the NE of the Manasterz Quarry represents levee or inter-channel deposits related to the Manasterz Quarry channel-fill. Its similar stratigraphic position and occurrence on the path of the palaeoflow direction of the Manasterz Quarry section are premises for sinuosity of the Manasterz Quarry channel.
5. The whole composite Manasterz section represents a transition from lobe off-axis or channel off-axis facies alternated with inter-channel or overbank deposits of the Wiar Member (lower Campanian–lower Maastrichtian) to the Manasterz Quarry channel axis facies incised into the Węgierka Marl mass transport deposits complex of the Leszczyny Member (lower Maastrichtian–lower Palaeocene).
6. The described channel architectural elements of the Ropianka Formation are located within the so-called Łańcut Channel Zone, which was previously proposed for the Oligocene sediments but may already be present in the Late Cretaceous.

Acknowledgements: This study was supported by the Jagiellonian University DS funds. Thanks to W. Nemec (Bergen) for discussion. Special thanks to A. Uchman (Kraków) for discussion and improvements of the paper and for sharing of photographs of the Manasterz Quarry section from the period before this study began. The author is greatful to reviewers Piotr Strzeboński and unknown reviewer for their constructive comments.

References

Abreu V., Sullivan M., Pirmez C. & Mohrig D. 2003: Lateral accretion packages (LAPs): an important reservoir element in deep water sinuous channels. *Mar. Petrol. Geol.* 20, 631–648.

Amy L.A. & Talling P.J. 2006: Anatomy of turbidites and linked debrites based on long distance (120 x 30 km) bed correlation, Marnoso Arenacea Formation, Northern Apennines, Italy. *Sedimentology* 53, 161–212.

Baas J.H. 2004: Conditions for formation of massive turbiditic sandstones by primary depositional processes. *Sediment. Geol.* 166, 293–310.

Babonneau N., Savoye B., Cremer M. & Klein B. 2002: Morphology and architecture of the present canyon and channel system of the Zaire deep-sea fan. *Mar. Petrol. Geol.* 19, 445–467.

Bayliss N.J. & Pickering K.T. 2015a: Transition from deep-marine lower-slope erosional channels to proximal basin-floor stacked channel-levée-overbank deposits, and syn-sedimentary growth structures, Middle Eocene Banastón System, Ainsa Basin, Spanish Pyrenees. *Earth-Sci. Rev.* 144, 23–46.

Bayliss N.J. & Pickering K.T. 2015b: Deep-marine structurally confined channelized sandy fans: Middle Eocene Morillo System, Ainsa Basin, Spanish Pyrenees. *Earth-Sci. Rev.* 144, 82–106.

Bouma A.H. & Coleman J.M. 1985: Mississippi fan, Leg 96 program and principal results. In: Bouma A.H., Normark W.R. & Barnes N.E. (Eds.): Submarine Fans and Related Turbidite Systems. *Springer Verlag*, New York, 247–252.

Bromowicz J. 1974: Facial variability and lithological character of Inoceramian Beds of the Skole-Nappe between Rzeszów and Przemyśl. *Prace Geologiczne, Polska Akademia Nauk, Oddział w Krakowie, Komisja Nauk Geologicznych* 84, 1–83 (in Polish with English summary).

Bruhn C.H.L. & Walker R.G. 1997: Internal architecture and sedimentary evolution of coarse-grained, turbidite channel-levee complexes, Early Eocene Regência Canyon, Espírito Santo Basin, Brazil. *Sedimentology* 44, 17–46.

Burzewski J. 1966: Baculites marls on the lithostratigraphy background of the upper Inoceramian Beds of the Skiba Carpathians. *Zeszyty Naukowe AGH, Geol.* 7, 89–115 (in Polish with French summary).

Campion K.M., Sprague A.R.G., Mohrig D.C., Sullivan M.D., Ardill J., Jensen G.N., Drzewiecki P.A., Lovell R.W. & Sickafoose D.K. 2000: Outcrop Expression of Confined Channel Complexes. In: Weimer P., Slatt R.M., Bouma A.H., & Lawrence D.T. (Eds.): Gulf Coast Section, SEPM, 20th Annual Research Conference. Deep Water Reservoirs of the World, December 3–6, 2000. Houston, 127–151.

Cartigny M.J.B., Eggenhuisen J.T., Hansen E.W.M. & Postma G. 2013: Concentration-dependent flow stratification in experimental high-density turbidity currents and their relevance to turbidite facies models. *J. Sediment. Res.* 83, 1046–1064.

Clark J.D. & Pickering K.T. 1996: Architectural elements and growth patterns of submarine channels: application to hydrocarbon exploration. *AAPG Bull.* 80, 194–220.

Cossu R., Wells M.G. & Peakall J. 2015: Latitudinal variations in submarine channel sedimentation patterns: the role of Coriolis forces. *J. Geol. Soc.* 172, 2, 161–174.

Dakin N., Pickering K.T., Mohrig D. & Bayliss N.J. 2013: Channel-like features created by erosive submarine debris flows: Field evidence from the Middle Eocene Ainsa Basin, Spanish Pyrenees. *Mar. Petrol. Geol.* 41, 62–71.

Damuth J.E. & Flood R.D. 1985: Amazon Fan, Atlantic Ocean. In: Bouma A., Normark W. & Barnes N. (Eds.): Submarine Fans and Related Turbidite Systems. *Springer-Verlag*, New York, 97–106.

Deptuck M.E., Steffens G.S., Barton M. & Pirmez C. 2003: Architecture and evolution of upper fan channel-belts on the Niger Delta slope and in the Arabian Sea. *Mar. Petrol. Geol.* 20, 6–8, 649–676.

Dżułyński S. & Sanders J.E. 1962: On some current markings in Flysch. *Ann. Soc. Geol. Pol.* 32, 143–146.

Dżułyński S., Kotlarczyk J. & Ney R. 1979: Submarine mass movements in the Skole Basin. In: Kotlarczyk J. (Ed.): Poziomy z olistostromami w Karpatach przemyskich. Materiały Terenowej Naukowej Konferencji w Przemyślu: Stratygrafia formacji z Ropianki (fm). *Powielarnia AGH*, Przemyśl, 17–27 (in Polish).

Flood R.D., Manley P.L., Kowsmann R.O., Appi C.J. & Pirmez C. 1991: Seismic facies and late Quaternary growth of Amazon submarine fan. In Weimer P. & Link M.H. (Eds.): Seismic Facies and Sedimentary Processes of Modern and Ancient Submarine Fans. Frontiers in sedimentary geology. *Springer-Verlag*, New York, 415–433.

Gardner M.H., Borer J.M., Melick J.J., Mavilla N., Dechesne M. & Wagerle R.N. 2003: Stratigraphic process-response model for submarine channels and related features from studies of Permian Brushy Canyon outcrops, West Texas. *Mar. Petrol. Geol.* 20, 757–787.

Gasiński M.A. & Uchman A. 2009: Latest Maastrichtian foraminiferal assemblages from the Husów region (Skole Nappe, Outer Carpathians, Poland). *Geol. Carpath.* 60, 283–294.

Gągała Ł., Vergés J., Saura E., Malata T., Ringenbach J., Werner P. & Krzywiec P. 2012: Architecture and orogenic evolution of the northeastern Outer Carpathians from cross-section balancing and forward modelling. *Tectonophysics* 532–535, 223–241.

Gedl E. 1999: Lower Cretaceous palynomorphs from the Skole Nappe (Outer Carpathians, Poland). *Geol. Carpath.* 50, 75–90.

Geroch S., Krysowska-Iwaszkiewicz M., Michalik M., Prochazka K., Radomski A., Radwański Z., Unrug Z., Unrug R. & Wieczorek J. 1979: Sedimentation of Węgierka Marls (Late Senonian, Polish Flysch Carpathians). *Ann. Soc. Geol. Pol.* 49, 105–134 (in Polish with English summary).

Golonka J., Gahagan L., Krobicki M., Marko F., Oszczypko N. & Ślączka A. 2006: Plate-tectonic evolution and paleogeography of the Circum-Carpathian region. In: Golonka J. & Picha F.J. (Eds.): The Carpathians and their foreland: Geology and hydrocarbon resources. *AAPG Memoir*, 84, 11–46.

Gradstein F., Ogg J., Schmitz M. & Ogg G. 2012: The Geological Time Scale 2012. Elsevier, Oxford, 1–1176.

Gucik S., Paul Z., Ślączka A. & Żytko K. 1980: Geological Map of Poland 1:200 000*,* arkusz Przemyśl, Kalników. *Wydawnictwa Geologiczne* Warszawa (in Polish).

Hubbard S.T., Covault J.A., Fildani A. & Romans B.R. 2014: Sediment transfer and deposition in slope channels: Deciphering the record of enigmatic deep-sea processes from outcrop. *GSA Bull.* 126, 857–871.

Hübsher C., Spiess V., Breitzke M. & Weber M.E. 1997: The youngest channel-levee system of the Bengal Fan: results from digital sediment echosounder data. *Mar. Geol.* 141, 125–145.

Jankowski L., Kopciowski R. & Ryłko W. 2012: The state of knowledge of geological structures of the Outer Carpathians between Biała and Risca rivers – discussion. *Biul. Państw. Inst. Geol.* 446, 203–216.

Janocko M., Nemec W., Henriksen S. & Warchoł M. 2013: The diversity of deep-water sinous channel belts and slope valley-fill complexes. *Mar. Petrol. Geol.* 41, 7–34.

Kneller B. 2003: The influence of flow parameters on turbidite slope channel architecture. *Mar. Petrol. Geol.* 20, 901–910.

Kotlarczyk J. 1978: Stratigraphy of the Ropianka Formation or of Inoceramian beds in the Skole Unit of the Flysch Carpathians. *Prace Geol. Polska Akad. Nauk, Oddział w Krakowie, Komisja Nauk Geologicznych* 108, 1–75. (in Polish with English summary).

Kotlarczyk J. 1988: A Guidebook of LIX PTG Congress in Przemyśl. *Wydawnictwa AGH*, Kraków, 1–298 (in Polish).

Kotlarczyk J. & Leśniak T. 1990: Lower Part of the Menilite Formation and Related Futoma Diatomite Member in the Skole Unit of the Polish Carpathians. *Instytut Geologii i Surowców Mineralnych AGH, Wydawnictwo Akademii Górniczo-Hutniczej*, Kraków, 1–74 (in Polish with English summary).

Kotlarczyk J. & Śliwowa M. 1963: On knowledge of the productive Carboniferous formations in the substratum of the eastern part of the Polish Carpathians. *Przegl. Geol.* 11, 268–272 (in Polish with English summary).

Kotlarczyk J., Jerzmańska A., Świdnicka E. & Wiszniowska T. 2007: A frame work of ichtyofaunal ecostratigraphy of the Oligocene–Early Miocene strata of the Polish Outer Carpathian Basin. *Ann. Soc. Geol. Pol.* 76, 1–111.

Książkiewicz M. 1962: Geological Atlas of Poland. Stratigraphic and Facial Problems. Cretaceous and Early Tertiary in the Polish External Carpathians, 13. *Wydawnictwa Geologiczne*, Warszawa (in Polish with English summary).

Labourdette R., Crumeyrolle P. & Remacha E. 2008: Characterisation of dynamic flow patterns in turbidite reservoirs using 3D outcrop analogues: Example of the Eocene Morillo turbidite system (south-central Pyrenees, Spain). *Mar. Petrol. Geol.* 25, 225–270.

Leszczyński S. 1989: Characteristics and origin of fluxoturbidites from the Carpathian flysch (Cretaceous–Palaeogene), South Poland. *Ann. Soc. Geol. Pol.* 59, 351–390.

Leszczyński S., Malik K. & Kędzierski M. 1995: New data on lithofacies and stratigraphy of the siliceous and fucoid marl of the Skole nappe (Cretaceous, Polish Carpathians). *Ann. Soc. Geol. Pol.* 65, 1–4, 43–62 (in Polish with English summary).

Lowe D.R. 1982: Sediment gravity flows, II. Depositional models with special reference to the deposits of high-density turbidity currents. *J. Sediment. Petrol.* 52, 279–297.

Łapcik P. in press: Facies heterogeneity of a deep-sea depositional lobe complex: case study from the Słonne Section of Skole Nappe, Polish Outer Carpathians. *Ann. Soc. Geol. Pol.*

Łapcik P., Kowal-Kasprzyk J. & Uchman A. 2016: Deep-sea mass-flow sediments and their exotic blocks from the Ropianka Formation (Campanian–Paleocene) in the Skole Nappe: a case study of the Wola Rafałowska section (SE Poland). *Geol. Quarterly* 60, 301–316.

Malata T. 1996: Analysis of standard lithostratigraphic nomenclature and proposal of division for Skole unit in the Polish Flysch Carpathians. *Geol. Quarterly* 40, 4, 543–554.

Malata T. 2001: Jednostka skolska na E od Rzeszowa. *Posiedzenia Naukowe Państwowego Instytutu Geologii* 57, 60–63 (in Polish).

Mayall M., Jones E. & Casey M. 2006: Turbidite channel reservoirs – Key elements in facies prediction and effective development. *Mar. Petrol. Geol.* 23, 821–841.

McHargue T., Prycz M.J., Sullivan M.D., Clark J.D., Fildani A., Romans B.W., Covault J.A., Levy M., Posamentier H.W. & Drinkwater N.J. 2011: Architecture of turbidite channel systems on the continental slope: Patterns and predictions. *Mar. Petrol. Geol.* 28, 728–743.

Mulder T. 2011: Gravity processes and deposits on continental slope, rise and abyssal plains. In: Hüeneke H. & Mulder T. (Eds.): Deep-sea Sediments. Developments in Sedimentology, Vol. 63. *Elsevier*, Amsterdam, 25–148.

Mulder T. & Alexander J. 2001: The physical character of subaqueous sedimentary density flows and their deposits. *Sedimentology* 48, 269–299.

Mutti E. & Normark W.R. 1987: Comparing examples of modern and ancient turbidite systems: problems and concepts. In: Leggett J.K. & Zuffa G.G. (Eds.): Marine Clastic Sedimentology. *Graham and Trotman*, London, 1–38.

Mutti E. & Normark W.R. 1991: An Integrated Approach to the Study of Turbidite Systems. In: Weimer P. & Link M.H (Eds.): Seismic Faciesand Sedimentary Processes of Submarine Fans and Turbidite Systems. *Springer*, New York, 75-106.

Nemčok M., Krzywiec P., Wojtaszek M., Ludhová L., Klecker R.A., Sercombe W.J. & Coward M.P. 2006: Tertiary development of the Polish and Eastern Slovak parts of the Carpathian accretionary wedge: insights from balanced cross-sections. *Geol. Carpath.* 57, 5, 355–370.

Normark W.R. 1970: Growth patterns of deep sea fans. *AAPG Bull.* 54, 2170–2195.

Peakall J., McCaffrey B. & Kneller B. 2000: A process model for the evolution, morphology and architecture of sinuous submarine channels. *J. Sediment. Res.* 70, 3, 434–448.

Pickering K.T., Corregidor J. & Clark J.D. 2015: Architecture and stacking patterns of lower-slope and proximal basin-floor channelised submarine fans, Middle Eocene Ainsa System, Spanish Pyrenees: An integrated outcrop–subsurface study. *Earth-Sci. Rev.* 144, 47–81.

Piper D.J.W. & Normark W.R. 1983: Turbidite depositional patterns and flow characteristics, Navy Submarine Fan, California Borderland. *Sedimentology* 30, 681–694.

Posamentier H.W. & Kolla V. 2003: Seismic Geomorphology and Stratigraphy of Depositional Elements in Deep-Water Settings. *J. Sediment. Res.* 73, 3, 367–388.

Posamentier H.W. & Walker R. 2006: Deep-water turbidites and submarine fans. *SEPM Spec. Publ.* 84, 397–520.

Postma G., Nemec W. & Kleinspehn K.L. 1988: Large floating clasts in turbidites, a mechanism for their emplacement. *Sediment. Geol.* 58, 47–61.

Prélat A., Hodgson D.M. & Flint S.S. 2009: Evolution, architecture and hierarchy of distributary deep-water deposits: a high-resolution outcrop investigation from the Permian Karoo Basin, South Africa. *Sedimentology* 56, 2132–2154.

Rajchel J. 1990: Lithostratigraphy of the Upper Palaeocene and Eocene sediments from the Skole Units. *Zeszyty Naukowe AGH, Geol.* 48, 1–112 (in Polish with English summary).

Rajchel J. & Uchman A. 1998: Ichnological analysis of an Eocene mixed marly-siliciclastic flysch deposits in the Nienadowa Marls Member, Skole Unit, Polish Flysch Carpathian. *Ann. Soc. Geol. Pol.* 68, 61–74.

Salata D. 2014: Detrital tourmaline as an indicator of source rock lithology: an example from the Ropianka and Menilite formations (Skole Nappe, Polish Flysch Carpathians). *Geol. Quarterly* 58, 1, 19–30.

Salata D. & Uchman A. 2012: Heavy minerals from Oligocene sandstones of the Menilite Formation of the Skole Nappe, SE Poland: a tool for the provenance specification. *Geol. Quarterly* 56, 4, 803–820.

Salata D. & Uchman A. 2013: Conventional and high-resolution heavy mineral analyses applied to flysch deposits: comparative provenance studies of the Ropianka (Upper Cretaceous–Paleocene) and Menilite (Oligocene) formations (Skole Nappe, Polish Carpathians). *Geol. Quarterly* 57, 4, 649–664.

Shanmugam G. 2006: Deep-water processes and facies models: Implications for sandstone petroleum reservoirs. Handbook of Petroleum Exploration and Production, 5. *Elsevier*, Amsterdam.

Shanmugam G. 2016: Submarine fans: A critical retrospective (1950–2015). *J. Palaeogeography* 5, 2–76.

Shanmugam G. & Moiola R.J. 1988: Submarine fans: characteristic, models, classification and reservoir potential. *Earth-Sci. Rev.* 24, 383–428.

Sprague A.R., Sullivan M.D., Campion K.M., Jensen G.N., Goulding D.K., Sickafoose D.K. & Jennette D.C. 2002: The physical stratigraphy of deep-water strata: a hierarchical approach to the analysis of genetically related elements for improved reservoir prediction. AAPG Annual Meeting abstracts, Houston, Texas, 10–13.

Sprague A.R. Garfield T.R., Goulding F.J., Beaubouef R.T., Sullivan M.D., Rossen C., Campion K.M., Sickafoose D.K., Abreu V., Schellpeper M.E., Jensen G.N., Jennette D.C., Pirmez C., Dixon B.T., Ying D., Ardill J., Mohrig D.C., Porter M.L., Farrell M.E. & Mellere D. 2005: Integrated slope channel depositional models: the key to successful prediction of reservoir presence and quality in offshore West Africa. CIPM, cuarto E-Exitep 2005, February 20–23, 2005, Veracruz, Mexico, 1–13.

Sohn Y.K. 1997: On traction-carpet sedimentation. *J. Sediment. Res.* 67, 502–509.

Stow D.A.V. & Mayall M. 2000: Deep-water sedimentary systems: new models for the 21st century. *Mar. Petrol. Geol.* 17, 125–135.

Strzeboński P. 2015: Late Cretaceous–Early Paleogene sandy-to-gravelly debris flows and their sediments in the Silesian Basin of the Alpine Tethys (Western Outer Carpathians, Istebna Formation). *Geol. Quarterly* 59, 195–214.

Ślączka A. & Kaminski M.A. 1998: A guide book to excursions in the Polish Flysch Carpathians. *Grzybowski Found. Spec. Publ.* 6, 11–71.

Ślączka A., Kruglov S., Golonka J., Oszczypko N. & Popadyuk I. 2006: Geology and hydrocarbon resources of the Outer Carpathians, Poland, Slovakia, and Ukraine. General Geology. In: Golonka J.& Picha F.J. (Eds.): The Carpathians and their fore-land: geology and hydrocarbon resources. *AAPG Memoir* 84, 221–258.

Ślączka A., Renda P., Cieszkowski M., Golonka J. & Nigro F. 2012: Sedimentary basin evolution and olistolith formation: The case of Carpathian and Sicilian region. *Tectonophysics* 568–569, 306–319.

Talling P.J., Masson D.G., Sumner E.J. & Malgesini G. 2012: Subaqueous sediment density flows: Depositional processes and deposit types. *Sedimentology* 59, 1937–2003.

Uchman A., Malata E., Olszewska B. & Oszczypko N. 2006: Palaeobathymetry of the Outer Carpathians Basins. In: Oszczypko N., Uchman A. & Malata E. (Eds.): Rozwój paleotektoniczny basenów Karpat zewnętrznych. *Institute of Geological Sciences, Jagiellonian University*, Kraków, 83–102 (in Polish with English abstract).

Uhlig V. 1888: Ergebnisse geologischer Aufnahmen in den westgalizischen Karpathen. I. Theil. Die Sandsteizone zwischen dem penninischen Klippenzuge und dem Nordrande. *Jb. k.-kön. Geol. Reichsanst.* 38, 83–264.

Wdowiarz S. 1949: Structure géologique des Karpates marginales au sud-est de Rzeszów. *Biul. Państw. Inst. Geol.* 11, 1–39 (in Polish with French summary).

Wynn R.B., Kenyon N.H., Masson D.G., Stow D.A.V. & Weaver P.P.E. 2002: Characterization and recognition of deep-water channel-lobe transition zones. *AAPG Bull.* 86, 8, 1441–1462.

Supplementum

Table S1: Localization of studied samples

The Manasterz-Rzeki section:	49°56'7" N, 22°19'17" E
	49°56'8" N, 22°19'20" E
	49°56'8" N, 22°19'20" E
	49°56'9" N, 22°19'23" E
	49°56'10" N, 22°19'24" E
The Manasterz section:	49°55'36" N, 22°19'35" E
	49°55'37" N, 22°19'36" E
	49°55'38" N, 22°19'36" E
	49°55'38" N, 22°19'37" E
	49°55'38" N, 22°19'38" E
	49°55'40" N, 22°19'39" E
	49°55'40" N, 22°19'39" E
	49°55'41" N, 22°19'42" E
	49°55'42" N, 22°19'41" E
	49°55'43" N, 22°19'42" E
	49°55'45" N, 22°19'43" E
	49°55'45" N, 22°19'44" E
	49°55'46" N, 22°19'44" E
	49°55'40" N, 22°19'40" E
	49°55'39" N, 22°19'40" E
	49°55'39" N, 22°19'25" E
	49°55'40" N, 22°19'22" E
	49°55'40" N, 22°19'21" E
	49°55'40" N, 22°19'21" E
	49°55'40" N, 22°19'20" E
	49°55'40" N, 22°19'24" E
The Manasterz Quarry section:	49°55'21" N, 22°19'53" E

Acta Geologica Polonica, Vol. 69 (2019), No. X, pp. xxx–xxx
DOI: 10.1515/agp-2018-0026

Facies anatomy of a progradational submarine channelized lobe complex: semi-quantitative analysis of the Ropianka Formation (Campanian–Paleocene) in Hucisko Jawornickie section, Skole Nappe, Polish Carpathians

PIOTR ŁAPCIK

Jagiellonian University, Institute of Geological Sciences, ul. Gronostajowa 3a, PL-30-387 Kraków, Poland.
E-mail: piotr.lapcik@doctoral.uj.edu.pl

ABSTRACT:

Łapcik, P. 2019. Facies anatomy of a progradational submarine channelized lobe complex: semi-quantitative analysis of the Ropianka Formation (Campanian–Paleocene) in Hucisko Jawornickie section, Skole Nappe, Polish Carpathians. *Acta Geologica Polonica*, **69** (X), xxx–xxx. Warszawa.

This study is a detailed lithofacies analysis of the Wiar and Leszczyny members of the deep-marine Ropianka Formation (Campanian–Paleocene) exposed in the Hucisko Jawornickie section of the Skole Nappe, Polish Carpathian Flysch. The sedimentary succession (>400 m thick) represents a channelized lobe complex that prograded at the base of submarine slope. Seven sedimentary facies are recognized as a record of the principal modes of sediment deposition. Based on their stratigraphic grouping and grain-size trends, six facies associations are distinguished as representing specific sub-environments of the depositional system: distributary channels, channel-mouth lobes, channel levees, crevasses and interlobe basin plain with crevasse splays. The individual facies associations are characterized statistically and their internal facies organization is analysed by the method of embedded Markov chains to reveal the time pattern of depositional processes. The environmental changes indicated by the vertical succession of facies associations are attributed to the autogenic processes of the distributary channel shifting within an aggrading lobe area and the lateral switching of depositional lobes. Eustatic influences are likely, but difficult to ascertain with poor biostratigraphic data. The bulk basinward advance of the base-of-slope system was probably due to a pulse of the tectonic narrowing of the synclinal Skole Basin.

Key words: Deep-marine turbidites; Depositional lobes; Submarine channels; Dynamic stratigraphy; Facies analysis; Markov-chain analysis.

INTRODUCTION

Worldwide studies of submarine channel–lobe complexes in base-of-slope settings have shown that these sedimentary systems vary enormously in their dimensions, lithofacies assemblages and stratigraphic architecture (e.g., Heller and Dickinson 1985; Nelson *et al.* 1991; Shanmugam and Moiola 1991; Pickering *et al*. 1995; Galloway 1998; Bouma 2000; Wynn *et al.* 2002; Gardner *et al.* 2003; Prélat *et al*. 2009, 2010; Brunt *et al*. 2013; Bayliss and Pickering 2015a, b; Łapcik 2017; Nemec *et al.* 2018). Inconsistent methods of sedimentological description render case studies difficult to compare, and the classification of these systems into some distinctive categories with predictive facies models remains a formidable task. Generalized non-specific models are superficial, short of informative detail (e.g., Stow and Mayall

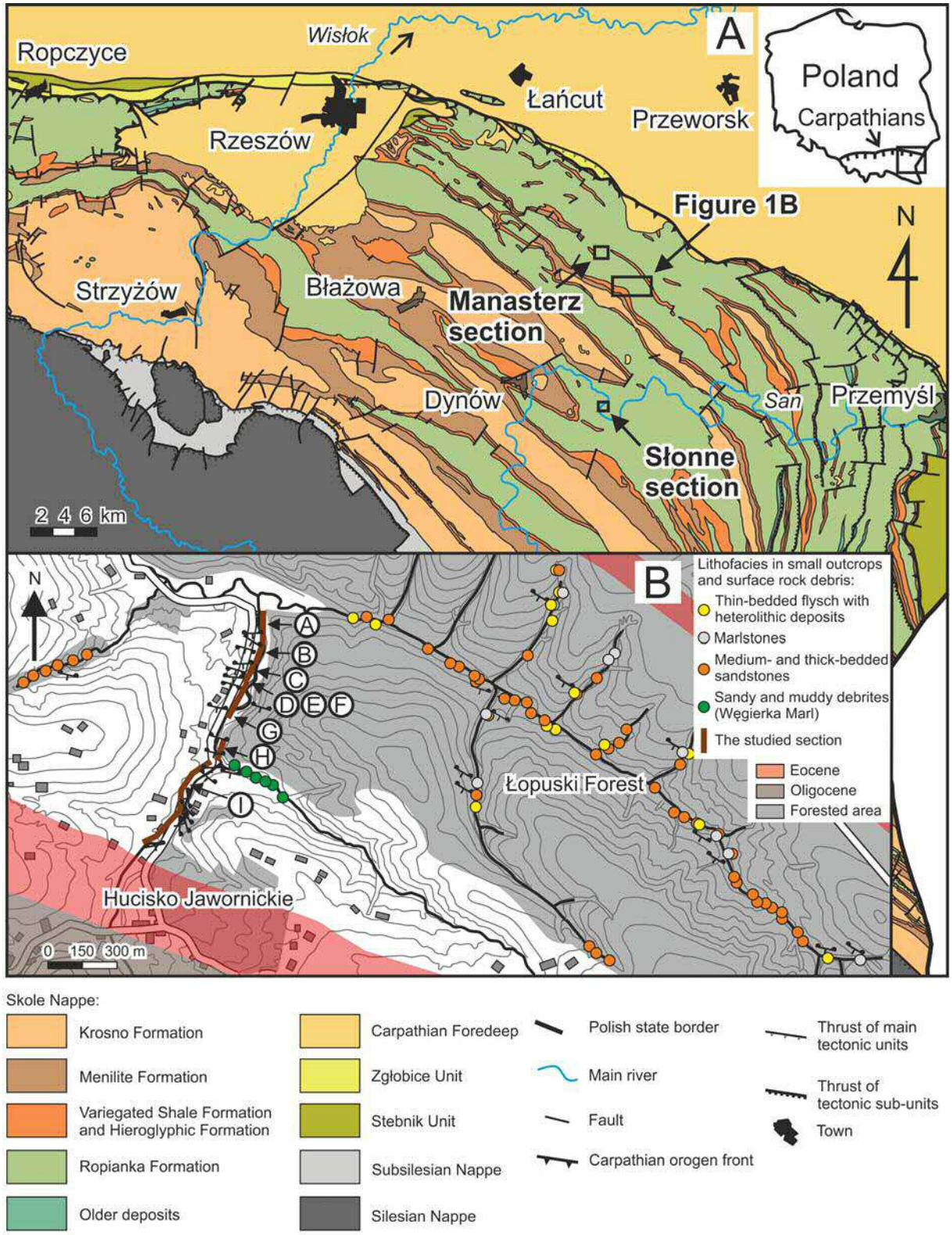

Text-fig. 1. Location of the study area; A – Geological map of the Skole Nappe (compiled from Gucik *et al*. 1980; Jurkiewicz and Woiński 1981; Woiński 1994; and Nescieruk *et al*. 1995). Note the location of present study area and outcrop sections studied by Łapcik (2017, 2018); B – Location of the Hucisko Jawornickie section and small other outcrops of the Ropianka Formation in the study area

2000; Posamentier and Walker 2006), and are of little use as a guide for exploration and reservoir characterization. What is needed is a more consistent and preferably quantitative methodology for the description and synthetic comparison of field cases.

The present case study from the Polish Carpathian Flysch follows the descriptive approach of Łapcik (2017) and uses a semi-quantitative methodology of facies analysis and sedimentological characterization of submarine system, similar as originally postulated by Miall (1973, 1978) for alluvial systems. The subject of this study is the Ropianka Formation (Turonian–Paleocene) of the Skole Nappe, a poorly investigated lithostratigraphic unit up to 1.6 km thick composed of deep-marine sediment gravity-flow deposits. The formation is poorly exposed, with good outcrops limited to river cut-bank sections and rare isolated quarries. Previous sedimentological studies have documented a non-channelized depositional lobe complex in the river San cut-bank section near Słonne (Łapcik 2017) and a large feeder paleochannel in the Manasterz Quarry section (Łapcik 2018) (Text-fig. 1A). The present study from the Hucisko Jawornickie outcrop section (Text-fig. 1A) contributes to an understanding of this formation's palaeoenvironmental jigsaw puzzle by documenting a channelized lobe complex that apparently prograded over the non-channelized distal part of an earlier one at the base of the Skole Basin's northern slope. The sedimentary succession exposed in the Hucisko Jawornickie section is more than 400 m thick and its sedimentological study proceeded in the following main methodological steps:

(i) A detailed bed-by-bed logging of the stratigraphic succession and distinction of its component sedimentary facies as the record of particular depositional processes.

(ii) Analysis of the stratigraphic grouping of sedimentary facies and recognition of their associations as the record of specific sub-environments of the submarine depositional system.

(iii) Quantitative statistical characterization of the individual facies associations in terms of their main descriptive features.

(iv) Analysis of the vertical organization of sedimentary facies (depositional processes) within their individual associations by the stochastic method of Markov chains.

(v) Analysis of the vertical succession of facies associations (sub-environments) as the record of the depositional system's bulk behaviour.

This case study contributes to a better understanding of the Ropianka Formation, while giving a detailed insight into the facies anatomy and sedimentation dynamics of a submarine base-of-slope system. The logging and distinction of facies are based on objective sedimentological criteria, and similarly objective and verifiable are the analytical results of quantitative methods, which jointly provides a reliable and highly informative methodological basis for comparative characterization of such ancient depositional systems. Last, but not least, the study demonstrates that – with appropriate methods – a wealth of valuable sedimentological information can be derived even from poor and isolated outcrops.

GEOLOGICAL SETTING

The Ropianka Formation of Turonian–Paleocene age is one of the major lithostratigraphic units of the Skole Nappe (Text-fig. 1A), subdivided into four members (Text-fig. 2; Kotlarczyk 1978). The deep-marine Skole Basin formed in the Early Cretaceous as the most external of the Carpathian flysch basins (Gucik 1963; Kotlarczyk 1988). After more than 100 Ma of variable deep-water sediment accumulation (Text-fig. 2), the basin was inverted by tectonic contraction and thrust – as the Skole Nappe – onto the Carpathian Foredeep in the early Miocene (Kotlarczyk 1988; Gągała *et al.* 2012; Ślączka *et al.* 2012; Kováč *et al.* 2016). The deposition of the Ropianka Formation was preceded by deposition of black and variegated shales (Cenomanian–Turonian), which accumulated below the local CCD in conditions changing from dysoxic with periodic anoxia to well-oxygenated (Gucik 1963; Bąk 2007; Bąk *et al.* 2014 and references therein). Similar correlative deposits are known from all the basins of the Polish Outer Carpathians. Tectonic activity and increased sand supply in the Skole Basin then caused depositions of the flysch of Ropianka Formation (Malata and Poprawa 2006; flysch definition *sensu* Dżułyński and Smith 1964). This flysch succession, up to 1.6 km thick, was deposited at a bathyal depth range around the local CCD (Uchman *et al.* 2006). The corresponding transport directions, measured in the present-day Skole Nappe, are mainly form the NE, N and NW (Książkiewicz 1962; Bromowicz 1974; Kotlarczyk 1978, 1988).

The Ropianka Formation represents a mixed sand-mud system dominated by siliciclastic sediment, but shows an abundance of marls towards the northerly source area, particularly in the eastern part of the Skole Nappe (Burzewski 1966; Kotlarczyk 1978, 1988; Geroch *et al.* 1979; Leszczyński *et al.* 1995; Leszczyński 2003, 2004; Kędzierski and Leszczyński

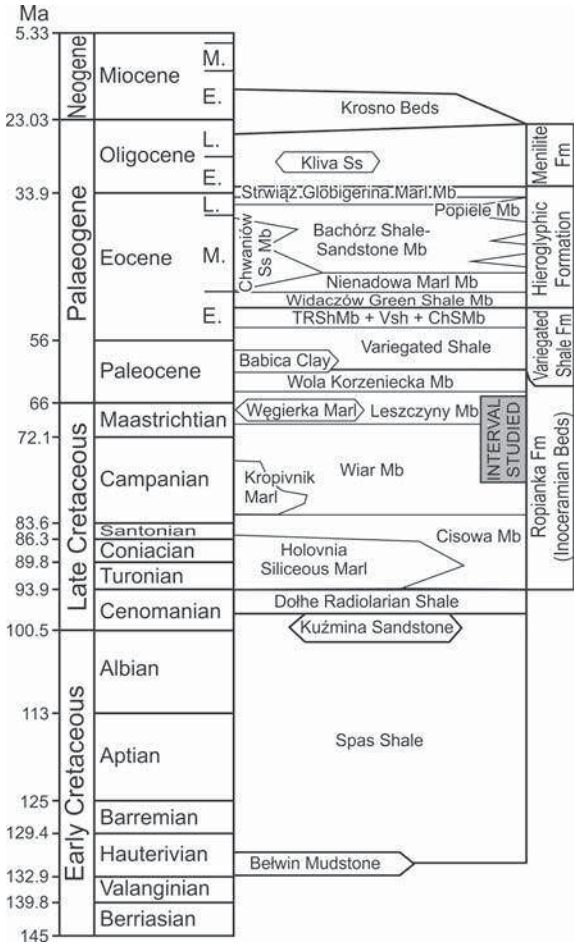

Text-fig. 2. Stratigraphic scheme of the Skole Nappe, based on Kotlarczyk (1988), Rajchel (1990), Rajchel and Uchman (1998) and Ślączka and Kaminski (1998), with modifications by Gedl (1999) and Kotlarczyk *et al*. (2006). The time scale is according to Gradstein *et al*. (2012). Abbreviations: TRSh Mb – Trójca Red Shale Member; VSh – Variegated Shale; and ChS Mb – Chmielnik Stripy Sandstone Member

2013). Exotic components and heavy-mineral assemblages in sandstones indicate a varied crystalline rock suite of the northern hinterland (Salata and Uchman 2013; Salata 2014a, b; Łapcik *et al.* 2016 and references therein). The zone of marl sedimentation between the siliciclastic source and similarly siliciclastic mass-flow system of the Ropianka Formation suggests a slope zone of the Skole Basin and an intra-basinal origin of carbonate mud. In the outcrop of thrust-folded Skole Nappe (Text-fig. 1A), the marlstones occur mainly as wedges in the lower parts of the Cisowa, Wiar and Leszczyny members of the Ropianka Formation (Text-fig. 2), which may indicate basinward slope advances accompanied by base-of-slope sandy sedimentation. At its top, the Ropianka Formation passes into the Paleocene–Eocene Variegated Shale Formation (Text-fig. 2) deposited below the local CCD in variable oxygenation conditions (Rajchel 1990; Leszczyński and Uchman 1991; Barwicz-Piskorz and Rajchel 2012; Olszewska and Szydło 2017), which suggests bulk deepening of the basin and drowning of its sediment-supplying hinterland.

The study area near the village of Hucisko Jawornickie (Text-fig. 1A) is located about 3 km to the SE from the Manasterz Quarry section studied by Łapcik (2018), but the two localities are in different adjacent thrust sheets (cf. Wdowiarz 1949) and their stratigraphic correlation is uncertain. The outcrops studied are in the stream banks to the north of Hucisko Jawornickie and in the Łopuski Forest to the northeast (Text-fig. 1B). The best exposed and longest section north of Hucisko Jawornickie shows the Wiar and Leszczyny members of the Ropianka Formation and the overlying Variegated Shale Formation (Text-fig. 2), although their exact boundary there is unexposed. According to regional literature, the topmost part of the Ropianka Formation in the Hucisko Jawornickie section (its segment I, Text-fig. 1B) represents the Węgierka Marl (Text-fig. 2), known also as the Baculites Marl (Burzewski 1966; Bromowicz 1974; Kotlarczyk 1978).

MATERIAL, METHODS AND TERMINOLOGY

The main part of data for the present study are from a detailed logging of the Hucisko Jawornickie outcrop section, showing a stratigraphic thickness of more than 400 m. The rocks are tectonically deformed and steeply inclined towards the SW, which means that the section is stratigraphically oblique, drifting away from the basin margin in the upward direction. The outcrop section is discontinuous, with some of its parts covered by vegetation and modern fluvial sediments. The section has been subdivided in a stratigraphic order into segments A to I (Text-fig. 1B), with segment B as a stratigraphic equivalent of segment A, measured on the opposite limb of the same syncline. Supplementary observations are from the small isolated outcrops and loose rock debris in the areas to the west and east of the Hucisko Jawronickie section (Text-fig. 1B), although these data on lithofacies variability along the depositional strike are difficult to correlate with the logged outcrop section.

The descriptive sedimentological terminology is after Harms *et al.* (1975) and Collinson *et al.* (2006).

Bed thickness categories are after Nichols (2009), with very thin (<1 cm), thin (1–10 cm), medium (10–30 cm), thick (30–100 cm) and very thick (>100 cm) classes. Statistical terminology and methods are after Davis (2002).

Sedimentary facies are basic types of deposits distinguished on the descriptive basis of their bulk macroscopic characteristics (Walker 1984). In the case of episodic 'event sedimentation' (*sensu* Dott 1983), as in a flysch succession, the distinction of facies pertains to the products of individual sedimentary-gravity flows and inter-flow episodes of background sedimentation (e.g., Janbu *et al.* 2007). Differing assemblages of spatially and temporarily related sedimentary facies are distinguished as facies associations and considered to represent specific parts (sub-environments) of the sedimentary system (e.g., Stow and Mayall 2000; Mulder *et al.* 2011; Shanmugam 2016a). They are given interpretive genetic labels, but their descriptions are separated from interpretations in the text.

SEDIMENTARY FACIES

Seven sedimentary facies are distinguished in the studied succession, ranging from granule conglomerates and sandstones to mudstones and marlstones, and are labelled F1 to F7 in the sedimentological log (Text-fig. 3). Sedimentary facies are distinguished based on the texture, grain size trend, mud content, bed thickness, sedimentary structures and petrographic composition of deposits. Sandstones are quartzose arenites, variably calcareous and mainly whitish grey or yellowish to rusty orange in colour. Some sandstone beds are greenish due to a high content of glauconite. Most sandstone beds are poorly cemented, as is typical of the Ropianka Formation (Bromowicz 1974). In addition to quartz, the sandstones contain grains of muscovite, biotite, feldspar, pyrite, glauconite, coal and plant detritus, as well as fragments of siliceous rocks, greenschist, grey mudstone and agglutinated foraminifer tests. Conglomerates are subordinate, fine-grained and dominated by quartz.

Facies F1: Graded massive conglomerate and sandstone with stratified or banded top

Description: This facies occurs as beds of graded coarse- to fine-grained sandstone or granule conglomerate graded to sandstone. Beds are 4 to 195 cm in thickness and mainly tabular on the outcrop scale, with sharp erosional bases, load features and rarely exposed sole marks. These graded beds are mainly or entirely massive, macroscopically non-stratified (Text-fig. 4A–C). Some beds contain flat-lying intraformational clasts of mudstone, siltstone, marlstone and coal, most often in the basal and/or top part of massive bed. Intraclasts are up to 17 x 6 cm in size and are lithologically similar to facies F4, F5 and F6 (described farther in the text). Exotic pebble-sized clasts of schist, igneous and volcanic rocks, limestone, sandstone and siliceous rocks occur in the basal part of beds. Some beds are multiple, amalgamated, as indicated by erosional surfaces with an abrupt increase is grain size.

The top part of the graded massive beds often shows planar parallel stratification and ripple cross-lamination, occasionally convoluted, and a siltstone to mudstone capping with 'wispy' discontinuous lamination (Text-fig. 4B). Many beds show a significant grain-size decrease and mud content increase at the transition from their graded massive division to laminated top division. The laminated division is typically much thinner than the massive division (Text-fig. 4A), but is occasionally of similar or greater relative thickness (Text-fig. 4B). The top of the laminated division is only rarely disturbed by bioturbation.

Some beds of facies F1 show dark isolated bands, 0.5–5 cm thick and rich in mud and coalified plant detritus, which occur at various heights within the massive graded division or form its capping instead of a laminated division. In the latter case, the banded division (*sensu* Lowe and Guy 2000) consists of thin dark bands of massive sand alternating with 'clean' bands of laminated sand, often loaded (Text-fig. 4C). These bands have comparable thicknesses or either type may dominate, even in portions of one banded division. The sandstone below banded division or beneath an isolated band in massive division commonly shows dewatering structures, and the bands in such cases are hydroplastically deformed. Similar banded divisions were observed by Łapcik (2017) in the turbidites of the Ropianka Formation in the Słonne section.

Interpretation: Facies F1 is interpreted as deposits of high-density turbiditic currents (*sensu* Lowe 1982). The graded massive division represents a phase of rapid, non-tractional dumping of coarse sediment suspension from a highly concentrated turbulent flow (turbidite division A of Bouma 1962; division S_3 of Lowe 1982). The overlying laminated division represents tractional deposition from the remaining, lower-density phase of the current (divisions B–D of Bouma 1962; division T_t of Lowe 1982), with possible brief episodes of bypass and substrate reworking (e.g., Sumner *et al.* 2008; Talling *et al.* 2012). Such a pattern of deposition is generally attributed

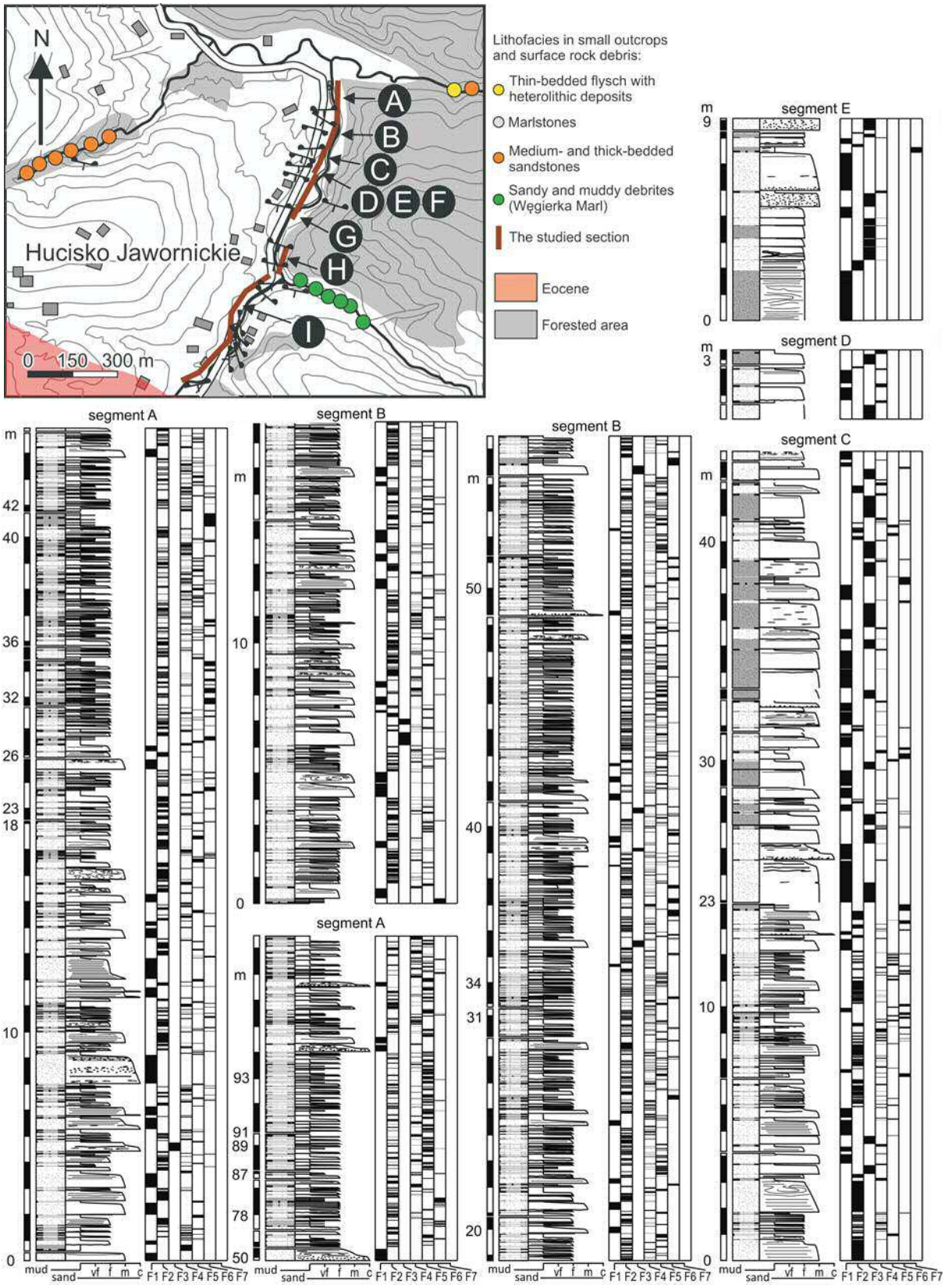

Text-fig. 3 (continued on p. 7)

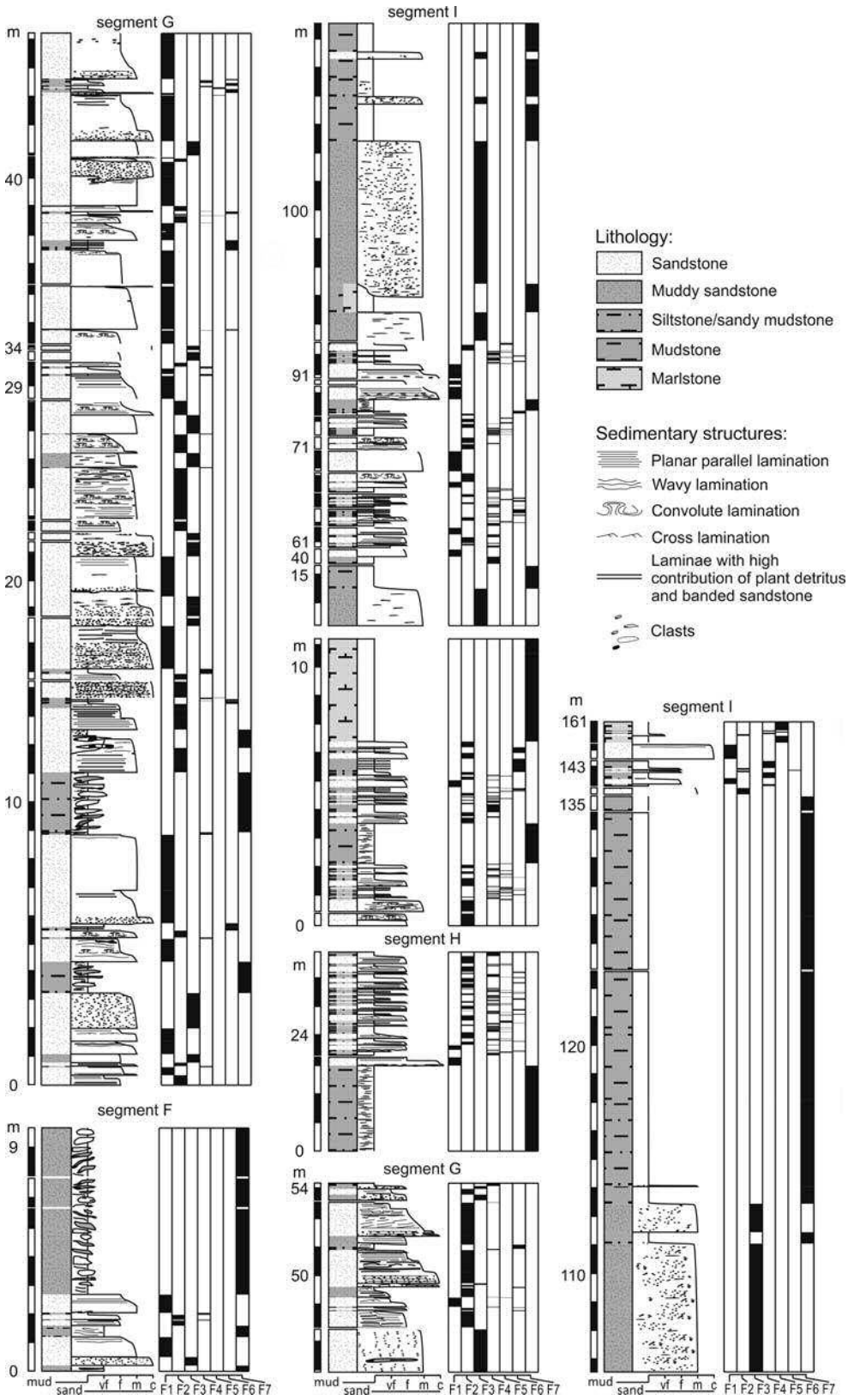

Text-fig. 3. Sedimentological log of the Ropianka Formation in the Hucisko Jawornickie section, with the distinction of sedimentary facies (see F1–F7 in the chequer plot at the log right-hand margin). The inset map shows the location of individual log segments A–I

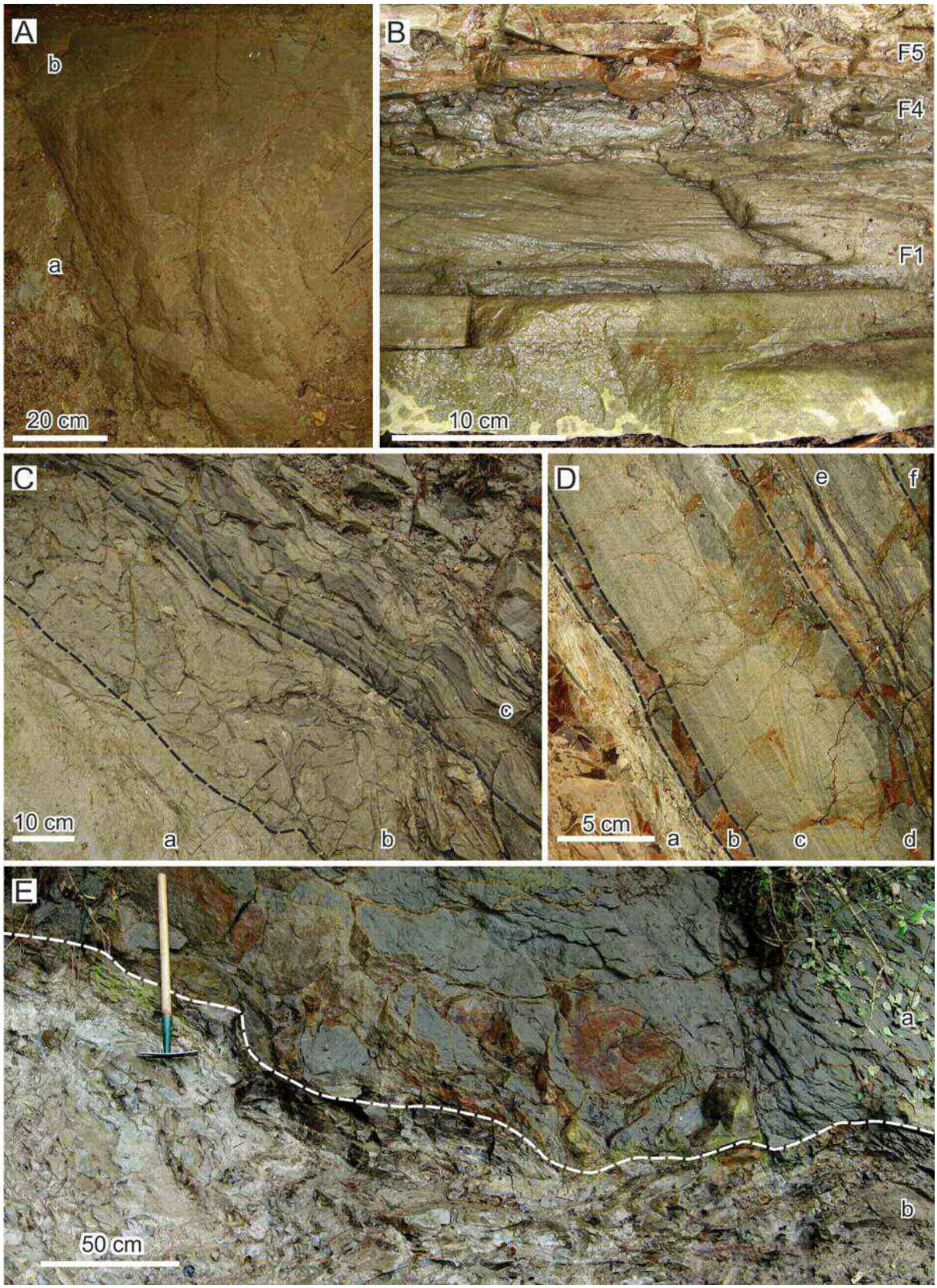
A
b
a
20 cm
B
F5
F4
F1
10 cm
C
c
10 cm
a
b
D
e
f
5 cm
a
b
c
d
E
a
b
50 cm

to the waning of a 'classical', surge-type turbidity current (Bouma 1962; Piper 1978; Stow and Bowen 1978, 1980; Lowe 1982, 1988; McCave and Jones 1988; Best and Bridge 1992; Leclair and Arnot 2005; Sumner *et al.* 2008; Talling *et al.* 2012). However, it cannot be precluded that at least some of the thicker beds of facies F1 were deposited by quasi-steady, 'sustained' (long duration) turbidity currents (see Kneller and Branney 1995; Baas 2004; Leclair and Arnot, 2005). The isolated dark sand bands enriched in mud and coaly detritus within the massive division indicate, indeed, some internal flow pulses, with the mode of deposition perhaps intermediate between turbidity current and debris flow (cf. Lowe *et al.* 2003; Haughton *et al.* 2009). Likewise, the overlying banded division observed in beds indicates rhythmic pulses of deposition from a sustained quasi-steady flow, similar to the flow mode referred to as 'slurry flow' by Lowe and Guy (2000). This flow mode would involve repetitive auto-cyclic formation and *en masse* freezing of cohesive traction carpets (in contrast to the non-cohesive traction carpets of Lowe 1982) due to the settling of flocculated mud and entrapped coaly detritus, with the intervening episodes of tractional sand deposition. The bands in facies F1 are in the thickness range of the meso- (M_{2C}) and micro-banding (M_5) of Lowe and Guy (2000), whereas the massive, dish-structured and wispy-laminated deposits underlying the banded divisions might correspond, respectively, to the divisions M_1, M_4 and M_3 of Lowe and Guy (2000).

Last, but not least, the massive lower division in some of the beds of facies F1 shows little or no macroscopically recognizable grading. It may thus be interpreted as a co-genetic sandy debrite (cf. Strzeboński 2015; Shanmugam 2016b) – representing either a relic of the turbidity current's parental debris flow or an inertial debris flow spawned en route by the current as a 'moving bed' due to excessive bedload concentration (cf. Postma et al. 1988; Talling 2013).

Facies F2: Stratified sandstone and conglomerate

Description: Facies F2 occurs as beds of coarse- to very fine-grained sandstone and granule to pebble conglomerate, 1 to 160 cm in thickness. Beds are mainly tabular on the limited outcrop scale, but the thinner ones, up to a few centimetres, tend to have uneven thicknesses with occasional lateral pinch-outs. Bed bases are invariably sharp, with sole marks including trace fossils as well as flute and groove marks. Bioglyphs and mechanoglyphs co-occur, but one type of sole marks seems to dominate in particular parts of the sedimentary succession. Sedimentary structures include planar parallel stratification, ripple cross-lamination (occasionally with climbing ripples), convolute lamination, water-escape features and mud-draped wavy lamination (Text-fig. 4D). The beds of facies F2 thus resemble the laminated and banded top divisions of facies F1 beds, but lack any related lower massive division. Most beds show macroscopic normal grading and the thicker ones are sparsely capped with a laminated siltstone and mudstone. Rare intraformational and exotic clasts, similar as in facies F1, occur scattered in the basal part of some beds. Trace fossils include *Scolicia* isp., *Thalassinoides* isp. and *Ophiomorpha* isp., which occur as hypichnia and endichnia in thin beds.

Interpretation: Facies F2 represents deposits of low-density turbiditic currents (*sensu* Lowe 1982), with a fully tractional deposition and muddy capping as in the Bouma (1962) turbidites T_{BCDE} and T_{CDE} (see also Best and Bridge 1992; Leclair and Arnot 2005; Talling *et al.* 2012). However, the rate of bed aggradation varied and was highly unsteady. Mud-draped wavy lamination indicates discrete pulses of weak tractional transport (Reineck and Singh 1980). Climbing-ripple cross-lamination implies flow phases with a high rate of suspension fallout (Ashley *et al.* 1982). Water-escape structures indicate rapid sediment deposition (Collinson *et al*. 2006), whereas banded divisions suggest transient phases of 'slurry flow' (*sensu* Lowe and Guy 2000).

Within the general concept of turbidity-current evolution (Mulder and Alexander 2001), facies F2 may be considered a downstream equivalent of facies F1 for their parental flows in the depositional system, while it should also be kept in mind that the variation of bed thicknesses and grain size indicates flows with variable volumes and runout distances.

← Text-fig. 4. Outcrop examples of facies F1, F2, F3 and F4; A – Sandstone bed of facies F1 with thick massive division (a) capped by much thinner planar parallel-stratified division (b); B – Sandstone bed of facies F1 with Bouma-type pattern of divisions T_{ABCDE}, capped with a thin mudstone of facies F4 overlain by marlstone of facies F5; C – Massive sandstone bed of facies F1 (a) with mud-richer, darker middle part containing clasts of mudstone, marlstone and laminated siltstone (b); its cap is a banded sandstone division with bands of 'clean' parallel-stratified sand, partly loaded, and dark bands rich in mud and coalified plant detritus (c); D – Marlstone bed of facies F5 (a) overlain by mudstone facies F4 (b), slightly erosional sandstone bed of facies F2 with planar parallel stratification and ripple cross-lamination (c), another mudstone layer of facies 4 (d), and a heterolithic deposit of facies F6 (e) capped with mudstone facies F4 (f); E – Uneven boundary between dark muddy sandstone of facies F3 with scattered mudclasts and quartz granules (a) and the underlying mudstone-marlstone debrite of facies F7 (b)

Facies F3: Non-graded or slightly inverse-graded massive sandstone

Description: Facies F3 consists of fine- to coarse-grained sandstone beds with thicknesses of 4 and 500 cm (Text-fig. 4E). The thin beds are few and are apparently erosional relics of thicker ones. Most beds are darker, richer in mud than the sandstone beds of facies F1 and F2. The lower and upper bed boundaries are sharp, flat or uneven (Text-fig. 4E), lacking sole marks. The sandstone beds are massive (non-stratified) and macroscopically non-graded or slightly coarse-tail inverse-graded. They contain scattered or patchily distributed coarse sand grains, quartz pebbles, coalified plant detritus, and intraformational clasts of mudstone, marlstone and siltstone. Thick beds contain mudclasts up to 72 cm in length. Some beds are capped with a thin layer of finer-grained sandstone showing planar or wavy parallel stratification and/or ripple cross-lamination.

Interpretation: The beds of facies F3 lack evidence of deposition from turbulent flows – such as normal grading and stratification – and are interpreted as deposits of slightly cohesive to non-cohesive sandy debris flows (cf. Shanmugham 2006, 2016b; Breien *et al.* 2010; Talling *et al.* 2012; Talling 2013; Strzeboński 2015). The non-graded beds with randomly scattered outsized clasts suggest slow-moving debris flows with a limited internal shearing (frictional regime *sensu* Drake 1990). The weak, coarse-tail inverse grading of some beds is due to the lack or sparsity of coarse clasts in the bed's lower part, which indicates slightly faster debris flows with a thicker basal shearing zone (see Nemec and Postma 1991). Only some beds have a thin finer-grained stratified capping, which supports the notion of low-speed debris flows with little or no interface turbulent entrainment of sediment by ambient water (cf. Nemec *et al.* 1984).

Facies F4: Mudstone

Description: This facies comprises mudstone beds, 1 to 25 cm thick and grey, greenish or brownish in colour (Text-fig. 4B–D). These beds have gradational, rarely sharp, lower boundaries and most often are sharply overlain by sandstone facies (Text-fig. 5A). Mudstone is mainly massive and variably calcareous, with an admixture of muscovite, pyrite, glauconite, coalified plant detritus, as well as dispersed quartz grains of very fine sand and silt. The thicker beds are partly interlaminated with silt and/or very fine sand. Biogenic component is mainly tests of benthic agglutinated and planktic calcareous foraminifers. The dark colour and weathered outcrop surface of mudstone makes bioturbation structures difficult to recognize in the field, but cut samples show *Chondrites* isp. and *Planolites* isp. The beds of facies F4 alternate with all the other facies in the studied succession, although the bulk thickness contribution of this facies is minor.

Interpretation: This mudstone facies is interpreted as deposits of a 'background' sedimentation above or close to the local lysocline. Macroscopic distinction between pelagic, hemipelagic and turbiditic mudstones is generally difficult. The mudstones of facies F4 are siliciclastic, but are also variably calcareous, which suggests a mixed hemipelagic and pelagic sedimentation. Mudstone beds richer in biogenic calcareous component may thus indicate a relatively higher contribution of pelagic sedimentation. Mudstone beds with a marked admixture of silt and sand or interlaminated with these coarser components, especially where overlying turbidite beds, are thought to represent deposition from the dilute low-density tails of turbidity currents (turbidites T_{DE} of Bouma 1962; see also Stow and Bowen 1978, 1980; McCave and Jones 1988; Talling *et al.* 2012). It is well known from laboratory experiments (e.g., Alexander and Morris 1994; Alexander and Mulder 2002) that the mobile trailing cloud of dilute suspension can spread far beyond the depositional area of turbiditic sand and silt, which may explain why the turbiditic mudstone beds – instead of capping turbidites – often overlie debrites or the other mudstone varieties of facies F4. The lamination in mudstone is probably not tractional and can be due to the rhythmic depletion of a stable density gradient of quasi-standing suspension cloud by sedimentation-driven convection (Kerr 1991). Some of the massive, non-laminated mudstone beds may represent spontaneous gravity flows of fluidal mud (Baas *et al.* 2009) unrelated directly to turbidity currents.

Facies F5: Marlstone

Description: This facies comprises isolated beds of marlstone, bluish white (locally greenish or grey to reddish) in colour, with thickness up to 30 cm, but rarely more than 5 cm (Text-figs 4B–D and 5A). The lower bed boundaries are mainly sharp, but rarely erosional, whereas the upper boundaries range from sharp (in cases of an overlying sandstone) to gradational (in cases of an overlying mudstone). The majority of marlstone beds are massive, non-laminated, and show macroscopic normal grading only where containing an admixture of sand and silt. Non-

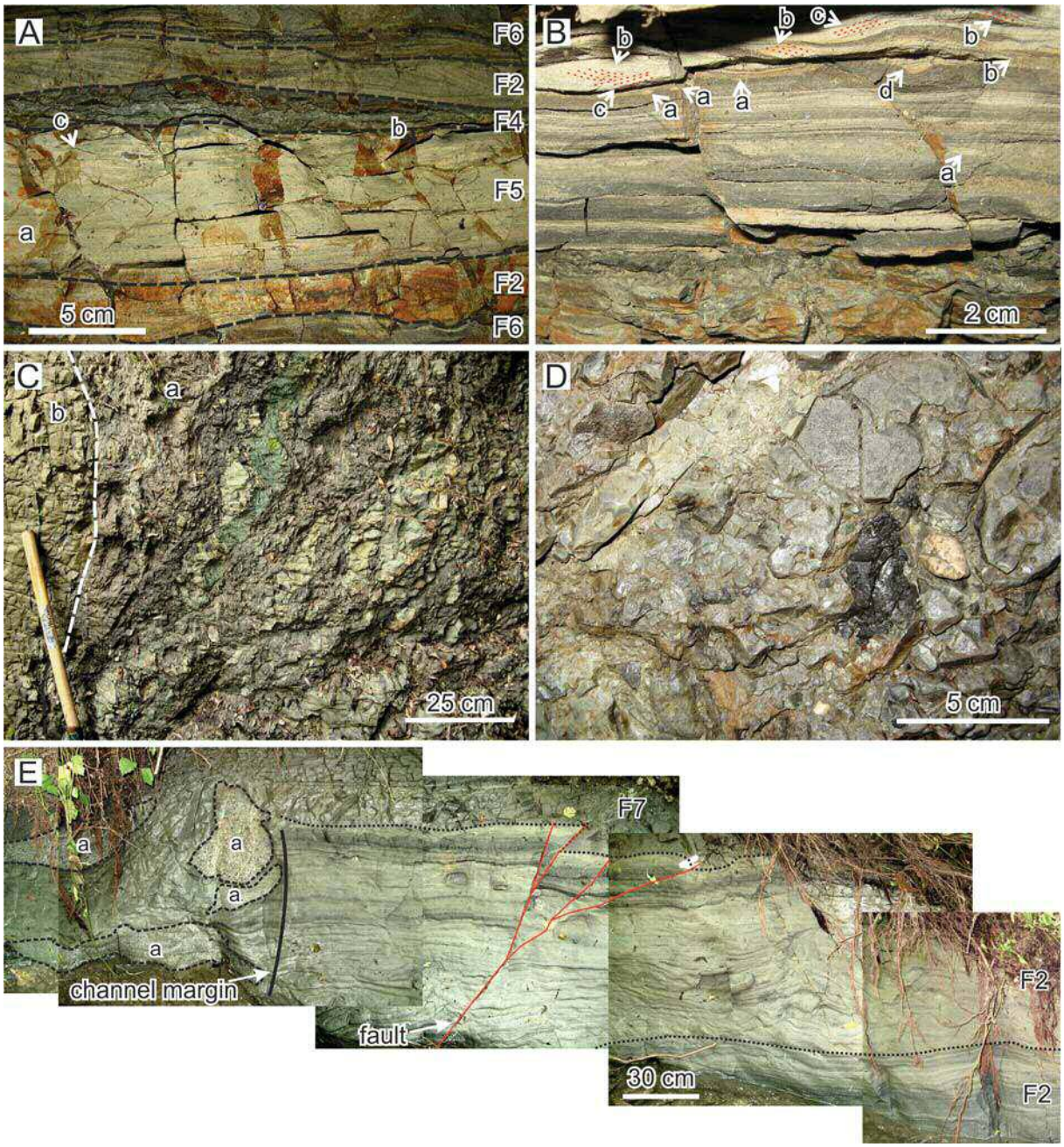

Text-fig. 5. Outcrop examples of facies F5, F6 and F7; A – Marlstone bed of facies F5 with sandy laminae (a), starved ripples (b) and starved ripples with marlstone drapes (c); note the underlying layers of facies F2 and F6 and the overlying layers of facies F4, F2 and F6; B – Heterolithic deposit of facies F6 composed of mud with planar laminae of silt and very fine-grained sand, showing burrows (a) and starved ripples with palaeotransport direction both to the right (b) and to the left (c); some ripples are loaded (d); C – Mud-rich debrite of facies F7 (a), with scattered intraformational clasts of sand, silt and mud, underlain by sandstone of facies F1 (b); beds are subvertical; D – Mud-rich debrite of facies F7 with scattered intraformational and exotic clasts; E – Outcrop photomosaic of a faulted palaeochannel margin in parallel-stratified sandstone of facies F2, buried by a debrite of facies F7 with large intraformational balls of facies F2 sandstone and facies F1 conglomerate (a)

bioturbated beds show parallel lamination or wispy lamination related to silt admixture. The thicker beds contain interlayers of quartzose very fine sandstone or siltstone, around 1 cm thick, with planar parallel lamination, ripple cross-lamination and marl-draped starved-ripple lenses (Text-fig. 5A).

Marlstone beds show abundant bioturbation structures, with burrows invariably filled with dark mud, even where such sediment is not present directly above or below the marlstone. Common are *Chondrites* isp., *Planolites* isp., *Scolicia* isp. and *Ophiomorpha* isp. Biogenic micrite consists mostly of planktic foraminifer tests, fragments of carbonate sponge spicules and shell detritus. Non-calcareous component is a variable admixture of quartz grains, coalified plant detritus, pyrite, muscovite flakes and glauconite grains. Facies F5 is difficult to distinguish from facies F4 in some poorer exposed or less accessible parts of the outcrop section, as these rocks are often similar in colour and mudstone is variably calcareous.

Interpretation: Based on the evidence of normal grading, lamination and relatively high admixture of non-calcareous sediment, the beds of facies F5 are interpreted as deposits of highly dilute, muddy calciturbiditic currents (cf. Stow and Bowen 1978, 1980). The deposits would be genetically comparably to the Bouma (1962) turbidites $T_{(B)CDE}$, but characterized by sparse sandy or silty tractional lower divisions and dominant post-tractional fallout divisions. The paucity of visible lamination is due to bioturbation, as the less bioturbated beds seem to show traces of faint parallel lamination almost throughout to the top. The lamination in marly turbidite divisions DE is unlikely to be tractional and can be due to the rhythmic depletion of a stable density gradient of quasi-standing suspension cloud by sedimentation-driven convection (Kerr 1991), whereas some of the non-laminated marlstone beds may be unrelated to turbidity currents and represent spontaneous gravity flows of fluidal mud (Baas *et al*. 2009).

Beds with multiple normal grading (Text-fig. 5A) may represent successive flows following closely one another as pulses or may reflect flow internal pulses driven by interface Kelvin-Helmholtz waves (cf. Ge *et al*. 2017). However, it cannot be precluded that the internal sandy/silty tractional divisions within a marlstone bed were inserted by the independent action of tidal or contouritic bottom currents (cf. Shanmugam 2008, 2017; Stow and Faugères 2008; Dykstra 2012).

The intense bioturbation of marlstones implies well-oxygenated seafloor conditions with an adequate supply of nutrients for benthic organisms to thrive. The mudstone facies F4, in contrast, signifies relatively dysoxic and oligotrophic conditions.

Facies F6: Heterolithic deposits

Description: Facies F6 occurs as units, up to 47 cm thick, of white, yellowish white or grey calcareous siltstone and very fine-grained sandstone intercalated with mudstone (Text-fig. 5B). Most such units are only several centimetres thick, with an uneven pinch-and-swell geometry. The thin heterolithic bedding is well pronounced, as the boundaries of the sandstone or siltstone layers and the mudstone layers are sharp, locally loaded (Text-fig. 5B), with flame structures, flute marks and bioturbation features. The sandstone and siltstone beds show internal plane-parallel lamination and climbing or non-climbing ripple cross-lamination, commonly with mud drapes or flasers, but beds are laterally discontinuous, comprised of starved and/or loaded ripple lenses. The successive ripple cross-laminae sets occasionally show significantly different or opposite palaeoflow directions (Text-fig. 5B). Recognizable trace fossils are *Ophiomorpha* isp*., Scolicia* isp. and *Planolites* isp., occurring as endichnia and hypichnia (Text-fig. 5B). Some beds are virtually homogenized by intense bioturbation. Mudstone is similar as in facies F4 and some of its layers contain parallel or wispy laminae of silty and fine sand, which makes the distinction locally difficult and somewhat arbitrary – based on the facies context.

Interpretation: Facies F6 indicates an action of short-lived or markedly pulsating, discrete tractional currents alternating with episodes of 'background' mud suspension fallout. Such depositional conditions may represent: (i) episodic incursions of the dilute tails of turbidity currents into an area of hemipelagic mud deposition; (ii) episodic spill-out of channelized turbidity currents into such an area; or (iii) episodic action of fluctuating contour currents or tidal currents (cf. He *et al*. 2008; Shanmugam 2008, 2017; Dykstra 2012). An involvement of tidal currents seems to be supported by the sharp but non-erosional bed boundaries, mud flasers in ripple cross-laminae sets and occasional evidence of palaeocurrent reversals.

Facies F7: Massive mud-rich conglomerate and pebbly or sandy

Description: This facies includes isolated and relatively thick, non-graded massive beds of mud-rich conglomerates and pebbly or sandy mudstones (Text-figs 4E, 5C–E). Conglomerate beds are a few decimetres to more than 600 cm thick, matrix-supported and containing intraformational and/or exotic clasts. Matrix is a mud-rich sand. Bed bases are sharp and often deformed by loading, but not necessarily erosional. Intraformational debris includes cobble- to boulder-sized fragments of mudstone, marlstone and siltstone (Text-fig. 5C), glauconite-rich sandstone,

as well as ball-shaped fragments of fine- to coarse-grained sandstone and granule conglomerate (Text-fig. 5E). The intraclasts are mainly subrounded and their lithological range corresponds to the associated other sedimentary facies. Some sandstone boulders are up to 40 x 100 cm in size, whereas mudstone boulders are plastically deformed and partly disintegrated, merged with the muddy matrix. Smaller clasts tend to be deformed into lenses oriented mainly parallel to bedding (Text-fig. 5C). Clasts of marlstone and mudstone are often armoured with coarse sand and granules. The intraformational conglomerate beds occur in segments E–G of the stratigraphic section (Text-fig. 3).

Conglomerate beds with exotic clasts occur only in the section's segments H and I (Text-fig. 3). They are similarly mud-rich and matrix-supported, 40 cm and to more than 350 cm in thickness, usually capped by sandstone facies F2. The bed bases are mainly flat, with no evidence of significant erosion or deformation. In addition to intraformational debris (comparable lithologically to facies F1, F2 and F3), these beds contain scattered, rounded pebble-sized exotic clasts of a Štramberk-type limestone (cf. Hoffmann *et al.* 2017), greenschist, coal, igneous and volcanic rocks, and subordinately some other sedimentary and metamorphic rocks (Text-fig. 5D). The volumetric ratio of clast to matrix is lower than in the purely intraformational conglomerates. The lithological composition of exotic clasts is similar to that reported from the conglomerates and pebbly mudstones in the Upper Cretaceous of the Silesian Nappe (Strzeboński *et al.* 2017) and from the Ropianka Formation elsewhere in the Skole Nappe (Łapcik *et al.* 2016).

The third variety of facies F7 deposits are isolated massive beds of pebbly or sandy mudstone (Text-fig. 4E), several decimetres to more than 500 cm in thickness. They are similarly non-graded, containing randomly scattered, sparse quartz pebbles and small intraclasts lithologically similar to facies F4, F5 and F6. In contrast to facies F4 and F5, the mudstones of facies F7 show little or no bioturbation. These deposits occur only in segment I of the stratigraphic section (Text-fig. 3), where they alternate with thick-bedded muddy sandstones of facies F3.

Interpretation: The deposits of facies F7 are interpreted to be debrites emplaced as highly cohesive debris flows and mudflows (cf. Crowell 1957; Prior *et al.* 1984; Mulder and Alexander 2001; Shanmugham 2006, 2016b; Talling *et al.* 2012; Strzeboński *et al.* 2017). The intraformational conglomerates, with plastically deformed sedimentary slabs and disrupted ball-and-pillow features, represent various stages of a mass-movement transformation from slump into debris flow. The preservation of intraformational clasts, which were originally soft, suggests relatively short mass-flow distances, or perhaps some longer-runout slow-moving or hydroplaned fast-moving flows with limited internal shear. The hydroplaning of mud-rich debris flows and mudflows (e.g., Mohrig *et al.* 1998; Gee *et al.* 1999; Ilstad *et al.* 2004) is particularly invoked to explain their non-erosive long runout with little or no internal shearing. The same emplacement mechanisms of slow or hydroplaned fast movement may apply to the sandy mudstones and muddy conglomerates with exotic gravel, which signify a markedly heterolithic source with sediment mixing during its gravitational collapse. The common occurrence of sandstone facies F2 with exotic gravel at the top of pebbly mudstone bed may indicate a turbiditic current triggered by retrogressive failure directly after the initial slumping and debris flow. Some of the gravel-free mudstones and sandy mudstones may be the so-called 'unifites' (e.g., Stow and Bowen 1978, 1980; Ricci Lucchi and Valmori 1980; McCave and Jones 1988; Talling *et al.* 2012), and their thickest beds may be due to amalgamation of two or more consecutive flows.

Muddy debrites comparable to facies F7 are common in basin-slope settings, and are known to occur in within the slope, at the base of slope and in more distal basin-floor areas (e.g., Gee *et al.* 1999; Tripsanas *et al.* 2008; Shanmugam 2016b). The deposits of facies F7 may then represent cohesive debris flows derived locally from the basin's adjoining northern slope or generated within the base-of-slope system by the collapses of channel cut-banks and levees. The textural variation of deposits suggests that a combination of these sources is likely. The sediment gravity movements may have been spontaneous or triggered by earthquakes, or both.

FACIES ASSOCIATIONS

Based on the stratigraphic grouping of sedimentary facies and their upward grain-size trends (Text-fig. 3), six facies associations have been distinguished – differing in their facies composition, the mean value, median and variance of bed thicknesses and the sandstone net/gross percentage (see data summary in Table 1). On the account of their component facies characteristics (depositional processes), the individual facies associations are interpreted as representing different morphodynamic sub-environments of the submarine depositional system. The

Channel-fill facies association

Package thickness: 3.8–21.1 m (mean 12.7 m)

Component facies thickness contribution:		Individual facies bed thicknesses:
F1	36.7 %	4–195 cm (mean 53.6 cm)
F2	26.6 %	3–118 cm (mean 24.1 cm)
F3	15.5 %	6–150 cm (mean 61.8 cm)
F7	7.2 %	22–219 cm (mean 108.5 cm)
F4	6.2 %	1–18 cm (mean 4.4 cm)
F6	5 %	1–30 cm (mean 6.6 cm)
F5	2.8 %	1–15 cm (mean 4.9 cm)

Sandstone bed thicknesses:
Median = 27 cm
Mean = 38.7 cm
Variance = 1408 cm^2
Standard deviation = 37.5 cm
Sandstone net/gross = 61.5–93.6 % (mean 78.1 %)

Channel-mouth lobe facies association

Package thickness: 2–8 m (mean 5.7 m)

Component facies thickness contribution:		Individual facies bed thicknesses:
F2	43.1 %	1–120 cm (mean 14.8 cm)
F1	22.4 %	12–59 cm (mean 32.6 cm)
F4	12.9 %	1–24 cm (mean 3.8 cm)
F3	9.6 %	18–50 cm (mean 26.4 cm)
F5	6.3 %	1–12 cm (mean 4.7 cm)
F6	5.7 %	1–25 cm (mean 6.2 cm)

Sandstone bed thicknesses:
Median = 12 cm
Mean = 19.3 cm
Variance = 335.1 cm^2
Standard deviation = 18.3 cm
Sandstone net/gross = 61.8–97.9 % (mean 81.7 %)

Channel-levee facies association

Package thickness: 3.8–6.1 m (mean 4.6 m)

Component facies thickness contribution:		Individual facies bed thicknesses:
F2	40 %	1–41 cm (mean 7.4 cm)
F5	21.8 %	1–15 cm (mean 5.6 cm)
F1	19.9 %	16–52 cm (mean 31 cm)
F4	13.9 %	1–15 cm (mean 2.7 cm)
F6	4.4 %	1–20 cm (mean 4.1 cm)

Sandstone bed thicknesses:
Median = 6 cm
Mean = 9.9 cm
Variance = 102.8 cm^2
Standard deviation = 10.1 cm
Sandstone net/gross = 44–67.5% (mean 58.9 %)

Interlobe basin-plain facies association

Package thickness: 0.05–5.1 m (mean 1.4 m)

Component facies thickness contribution:		Individual facies bed thicknesses:
F2	41.2 %	1–19 cm (mean 6 cm)
F5	23.8 %	1–16 cm (mean 4.8 cm)
F4	22 %	1–14 cm (mean 2.6 cm)
F6	13 %	1–30 cm (mean 6.5 cm)

Sandstone bed thicknesses:
Median = 5 cm
Mean = 5.3 cm
Variance = 11.2 cm^2
Standard deviation = 3.3 cm
Sandstone net/gross = 0–63.2 % (mean 41 %)

Crevasse-fill facies association

Package thickness: 4.8 m

Component facies thickness contribution:		Individual facies bed thicknesses:
F1	35 %	11–50 cm (mean 28 cm)
F2	34.4 %	2–18 cm (mean 7.2 cm)
F4	17.1 %	1–13 cm (mean 2.8 cm)
F5	10.8 %	1–10 cm (mean 5.2 cm)
F6	2.7 %	1–4 cm (mean 2.2 cm)

Sandstone bed thicknesses:
Median = 6 cm
Mean = 11.5 cm
Variance = 122.7 cm^2
Standard deviation = 11.1 cm
Sandstone net/gross = 69.4 %

Crevasse-splay facies association

Package thickness: 0.08–0.78 m (mean 0.32 m)

Component facies thickness contribution:		Individual facies bed thicknesses:
F1	63.7 %	7–45 cm (mean 20.3 cm)
F2	27 %	2–25 cm (mean 7.4 cm)
F3	9.3 %	14–38 cm (mean 24.7 cm)

Sandstone bed thicknesses:
Median = 12 cm
Mean = 14.5 cm
Variance = 123.4 cm^2
Standard deviation = 11.6 cm
Sandstone net/gross = 100 %

Table 1. Quantitative summary of the characteristics of facies associations in the Hucisko Jawornickie section

vertical organization of facies within their particular associations, or the time pattern of the operation of depositional processes within a particular sub-environment, has been analysed with the use of the stochastic method of embedded Markov chains (for description, see Davis 2002).

Channel-fill facies association

Description: The facies assemblages of this type are 3.8–21.1 m thick (mean ca. 13 m), have a sandstone net/gross of 62% to 94% and are dominated by facies F1 (37%), F2 (27%) and F3 (16%), with only minor contribution of the finer-grained facies F4, F5, F6 and F7 (Table 1). Facies F1, F2, F3 and F7 reach here their greatest bed thicknesses in this facies assemblage, and the overall variance of bed thicknesses is the highest, with a standard deviation (*SD*) of 37.5 cm. The mean sandstone bed thickness (M = 39 cm) is higher than the median (Md = 27 cm), which indicates a positively skewed bed-thickness frequency distribution, with an excess of thicker beds. These

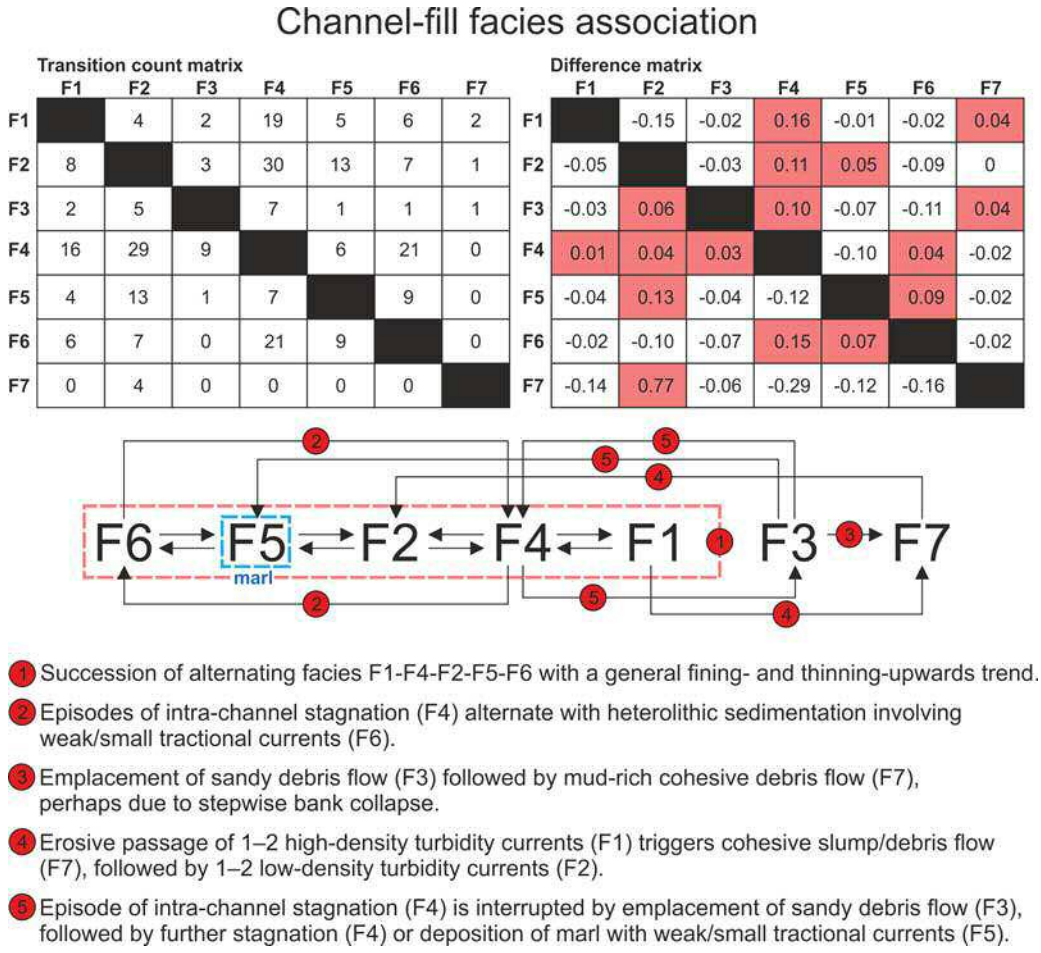

Text-fig. 6. Transition-count and difference matrices for channel-fill facies association with the corresponding Markov chain model of facies vertical organization and an interpretation of particular facies transitions. The total number of counted facies transitions is $N = 279$ and the confidence level of difference matrix is 99%. The preferential facies transitions (more frequent than random) are highlighted in colour in the difference matrix and are the basis of Markov chain model

facies assemblages show a non-systematic thinning- and fining-upwards trend, perturbed by the irregular insertion of debrite facies. The preferential pattern of upwards facies transition in this type of facies assemblages is shown as a Markov chain model in Text-fig. 6.

Interpretation: These facies assemblages – as the richest in sandstone and conglomeratic facies, with the highest amount of erosional bed amalgamation and a finning- and thinning-upwards trend – is interpreted as the infill of distributary channels (cf. Mutti and Normark 1987; Pickering *et al.* 1995; Clark and Pickering 1996; Bruhn and Walker 1997; Stow and Mayall 2000; Gardner *et al.* 2003; Mayall *et al.* 2006; Posamentier and Walker 2006; Janbu *et al.* 2007; Hubbard *et al.* 2008, 2014; Bernhardt *et al.* 2011; McHargue *et al.* 2011; Mulder 2011; Janocko *et al.* 2013; Bayliss and Pickering 2015a, b; Pickering *et al.* 2015; Shanmugam 2016a; Łapcik 2018). Submarine channels around 20 m deep would likely be only a few hundred metres wide (Clark and Pickering 1996), which supports the notion of cut-and-fill avulsive distributaries, rather than the system's longer-lived main feeder conduits. The channel-fill sedimentation dynamics, in terms of the modal upward trend of depositional processes, is interpreted in detail in Text-fig. 6.

Channel-mouth lobe facies association

Description: Facies assemblages of this type are 2–8 m thick, have a sandstone net/gross of 62% to 98% and are dominated by sandstone facies F1, F2 and F3 (jointly 75%), while lacking facies F7 (Table

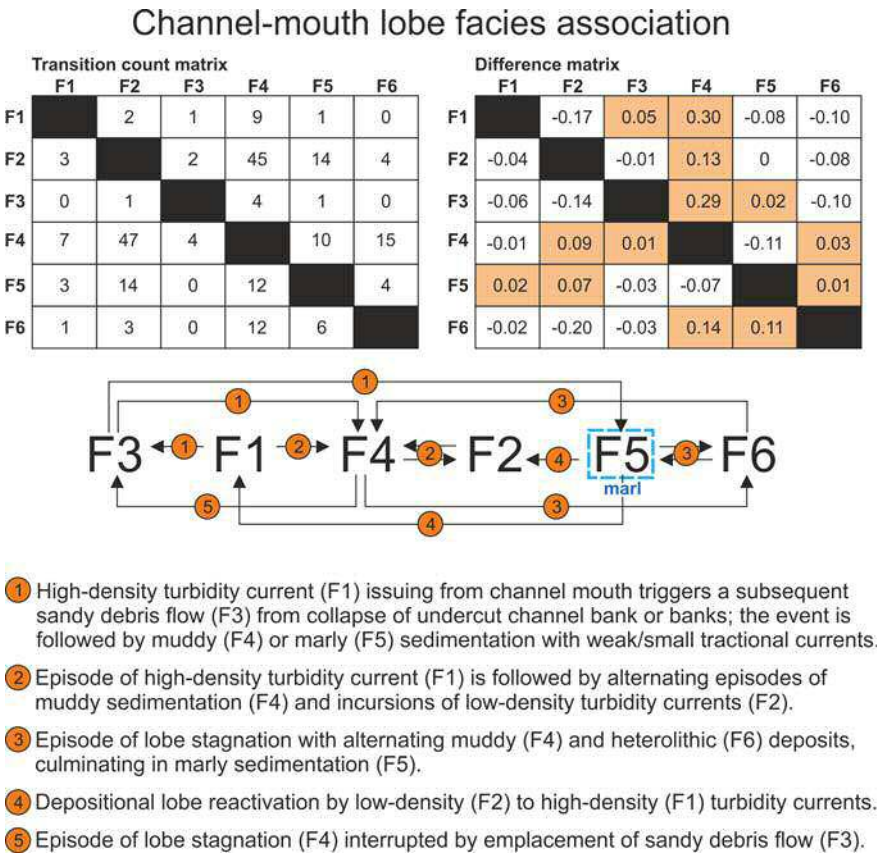

Text-fig. 7. Transition-count and difference matrices for channel-mouth lobe facies association with the corresponding Markov chain model of facies vertical organization and an interpretation of particular facies transitions. The total number of counted facies transitions is $N = 225$ and the confidence level of difference matrix is 80%. The preferential facies transitions (more frequent than random) are highlighted in colour in the difference matrix and are the basis of Markov chain model

1). Compared to the channel-fill facies association, the mean contribution of facies F2 here is higher (43%) and the contribution of facies F1 (22%) and facies F3 (10%) is lower. Significantly higher is the contribution of fine-grained facies F4 (13%) and facies F5 (6%). The sandstone beds of facies F1, F2 and F3 are much thinner and show a considerably lower thickness variance, with a standard deviation of 18 cm (Table 1). Also here, the mean sandstone bed thickness ($M = 19$ cm) is higher than the median ($Md = 12$ cm), which indicates a slightly positive skewness of the bed-thickness frequency distribution and hence an excess of thicker beds. These facies assemblages tend to show a non-systematic coarsening- and thickening-upwards trend. Their modal pattern of upward facies organization is shown as a Markov chain model in Text-fig. 7.

Interpretation: This type of facies assemblages is the second richest in sandstones, but in comparison to the previous one, it is finer-grained and thinner bedded, dominated by the tabular sandstone beds of facies F2, with much less amalgamation of beds and a higher contribution of the intervening fine-grained facies. The sandstone net/gross and bed-thickness statistics seem to reflect those of the channel-fill facies association (Table 1). This second type of facies association is thus considered to be a distal equivalent of the previous one and represent channel-mouth depositional lobes (cf. Mutti and Normark 1987; Shanmugam and Moiola 1991; Pickering *et al.* 1995; Stow and Mayall 2000; Deptuck *et al.* 2008; Prélat *et al.* 2009; Bernhardt *et al.* 2011; Mulder 2011; Grundvåg *et al.* 2014; Marini *et al.* 2015; Shanmugam 2016a; Łapcik 2017). The notion of depositional lobes is supported by the sparsity of bed erosional amalgamation and the coarsening- and thickening-upwards trend. The sedimentation dynamics of channel-mouth lobe accretion, in terms of the modal upward pattern of depositional processes, is interpreted in detail in Text-fig. 7.

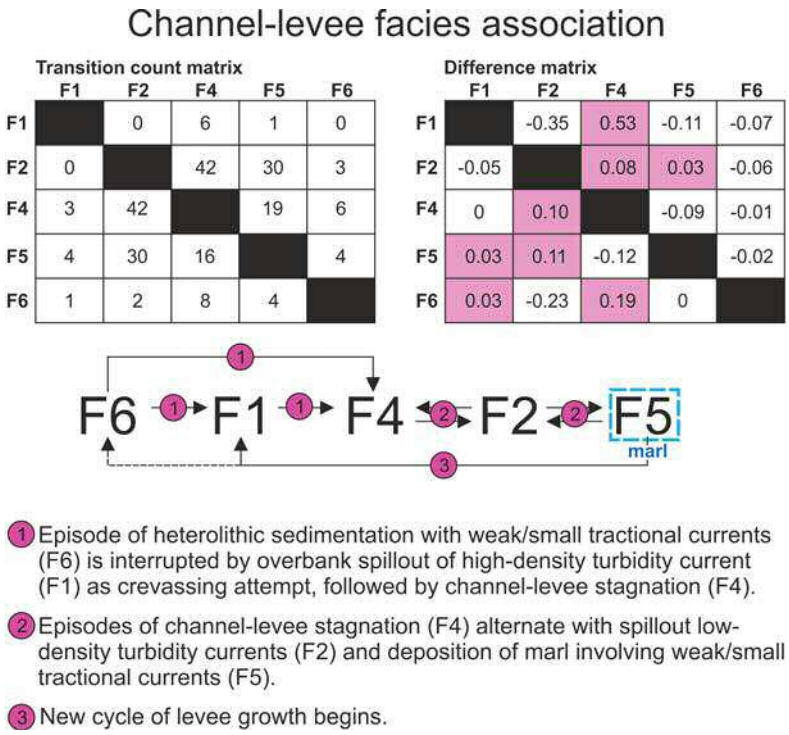

Text-fig. 8. Transition-count and difference matrices for channel-levee facies association with the corresponding Markov chain model of facies vertical organization and an interpretation of particular facies transitions. The total number of counted facies transitions is $N = 221$ and the confidence level of difference matrix is 97.5%. The preferential facies transitions (more frequent than random) are highlighted in colour in the difference matrix and are the basis of Markov chain model

Channel-levee facies association

Description: This third type of facies assemblages is 3.8–6.1 m thick (mean 4.6 m), has a sandstone net/gross of 44% to 68% and is dominated by thin-bedded sandstone facies F2 (40%) and F1 (20%), but lacking facies F3 and F7 (Table 1). The thickness contribution of fine-grained facies is similar as in the previous facies association, but the relative proportion of marlstone facies F5 (22%) is higher. Despite the apparent similarity to the previous facies association, the mean thickness of sandstone beds ($M = 10$ cm) and their median ($Md = 6$ cm) are nearly half-lower, and particularly the beds of facies F2, F4 and F6 are by comparison much thinner (Table 1). Furthermore, the bulk variance of sandstone bed thicknesses is much lower, with a standard deviation of only 10 cm. These facies assemblages show a non-systematic and often multiple coarsening- and thickening-upwards trend. Their bulk modal pattern of vertical facies organization is shown as a Markov chain model in Text-fig. 8.

Interpretation: The sedimentary characteristics of this type of facies assemblages suggest that they are like thinner-bedded imitations of the previous facies association, but with a lower sandstone net/gross, a higher proportion of marlstone facies F5 and a lack of facies F3 and F7. These facies assemblages are interpreted as levee deposits of distributary channels, a notion supported by their coarsening- and thickening-upwards trend and their direct association with inferred crevasse-fill and interlobe overbank deposits (described further below). Deposition of levees up to at least 6 m thick may indicate sinuous channels or local channel bends, where flow spill-out would be enhanced (cf. Pickering *et al.* 1995; Clark and Pickering 1996; Bruhn and Walker 1997; Posamentier and Walker 2006; Hubbard *et al.* 2008; Mulder 2011; Janocko *et al.* 2013; Bayliss and Pickering 2015a, b). The slight positive skewness of the sandstone bed-thickness frequency distribution ($M > Md$) indicates an excess of thicker beds and seems to reflect the sedimentation dynamics of channel-fill and lobe deposition. The modal pattern of depositional processes represented by facies organization is interpreted in detail in Text-fig. 8.

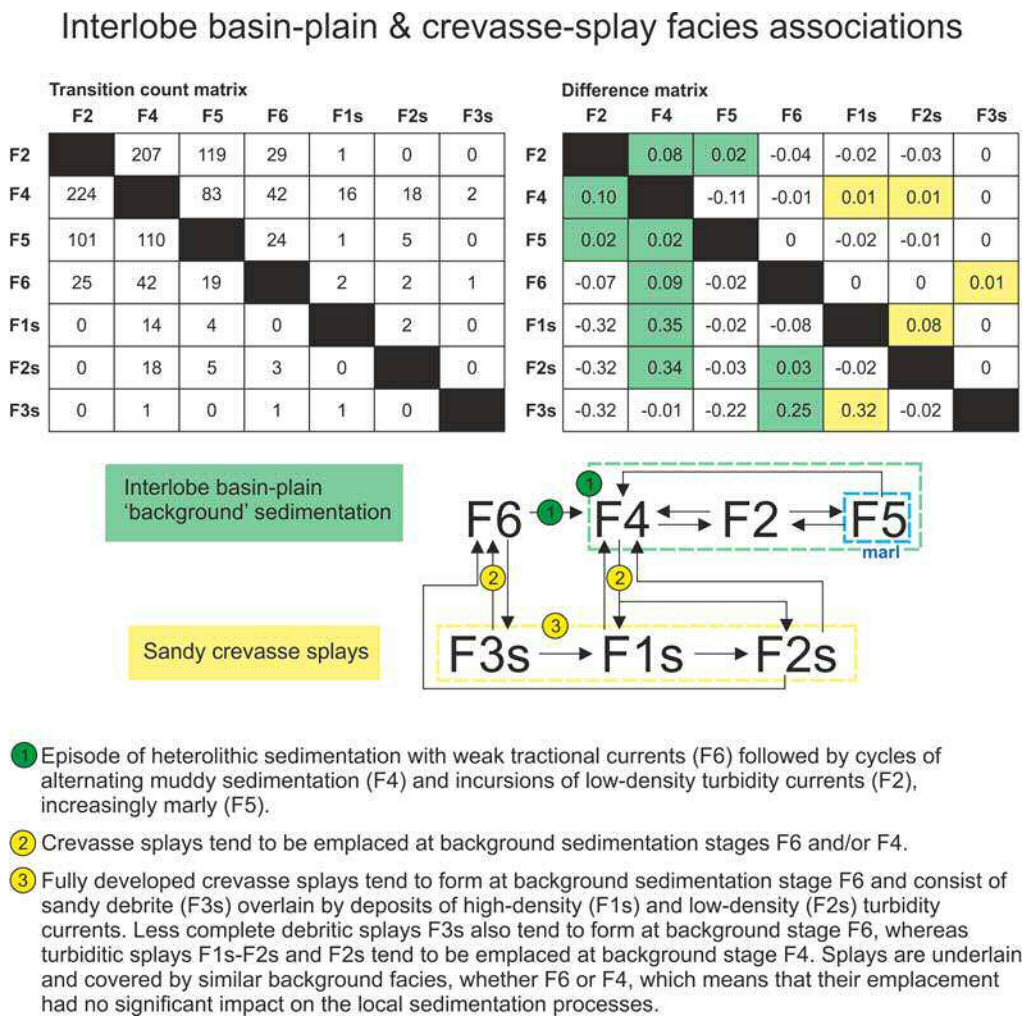

Text-fig. 9. Transition-count and difference matrices for interlobe basin-plain and crevasse-splay facies associations with the corresponding joint Markov chain model of facies vertical organization and an interpretation of particular facies transitions. The total number of counted facies transitions is $N = 1122$ and the confidence level of difference matrix is 99.9%. The preferential facies transitions (more frequent than random) are highlighted in colour in the difference matrix and are the basis of Markov chain model

Interlobe basin-plain and crevasse-splay facies associations

Description: This fourth type of facies assemblage occurs as stratigraphic intervals several tens of metres thick in the outcrop section's segments A and B (Text-fig. 3). It consists of the fine-grained packages of thinly bedded facies F2, F4, F5 and F6 intercalated with 'outsized' sandstone beds composed of facies F1, F2 and F3. The fine-grained packages are up to 5.1 m thick (mean 1.4 m), have a sandstone net/gross of 0% to 63% (mean 41%), and lack such component facies as F1, F3 and F7 (see interlobe association in Table 1). Thin-bedded sandstone facies F2 abounds (41%), the contribution of fine-grained facies F4 (22%) and F6 (13%) is higher than in the other facies assemblages, and the contribution of facies F5 (24%) is the highest in the entire succession. The beds here are thinnest, with a mean thickness ($M = 5$ cm) equal to median ($Md = 5$ cm) and a low standard deviation of 3 cm. The intervening outsized sandstone beds consist of a combination of facies F1, F2 and F3 (for details, see crevasse-splay association in Table 1). The modal upward facies organization of these associations is shown as a joint Markov chain model in Text-fig. 9 (with the facies components of outsized sandstone beds labelled with suffix 's').

Interpretation: This thinnest-bedded and fin-

est-grained facies association occurs between the sand-dominated channel-lobe assemblages and is interpreted as interlobe basin-plain deposits, variously interspersed with crevasse-splay sandstone sheets. The occurrence of crevasse splays supports the notion of interlobe areas evacuated by the lateral switching of depositional lobes, rather than distal areas of lobe 'feather-edge' termini (cf. Pickering *et al.* 1995; Deptuck *et al.* 2008; Prélat *et al.* 2009; Grundvåg *et al.* 2014; Łapcik 2017). The modal pattern of depositional processes represented by vertical facies organization is interpreted in detail in Text-fig. 9.

Crevasse-fill facies association

Description: This subordinate facies assemblage occurs only once in segment B of the outcrop section (Text-fig. 3), where it is 4.8 m thick and shows a sandstone net/gross of nearly 70%. It is dominated in equal proportion by sandstone facies F1 (35%) and F2 (34%), with some contribution of fine-grained facies F4 (17%), F5 (11%) and F6 (3%), and has a fining- and thinning-upwards trend. Facies F3 and F7 are lacking (Table 1). Beds thicknesses are comparable to those in the channel-levee assemblages, but their variance and standard deviation are slightly higher and the mean thickness of facies F6 beds is half-lower (2 cm). The mean thickness of sandstone beds (M = 11.5 cm) is higher than the median (Md = 6 cm), which indicates an excess of thicker beds – as in the channel-fill and channel-related facies assemblages (Table 1). In contrast to the channel-levee assemblages, this assemblage has an erosional base and shows an irregular fining- and thinning-upwards trend. Its modal upward facies organization is summarized as a Markov chain model in Text-fig. 10.

Interpretation: This facies assemblage resembles to some extent the channel-levee assemblages, but is markedly richer in sandstones. Its erosional base, discernible fining- and thinning-upwards trend and direct association with channel-levee deposits suggest that this facies assemblage is a crevasse-fill – the infill of a spill-out channel cut across distributary channel levee (Carter, 1988; Klaucke and Hesse 1996; Nakajima *et al.* 1998). The modal pattern of depositional processes recognized from vertical facies organization is interpreted in detail in Text-fig. 10. The notion of crevasses in the sedimentary system is

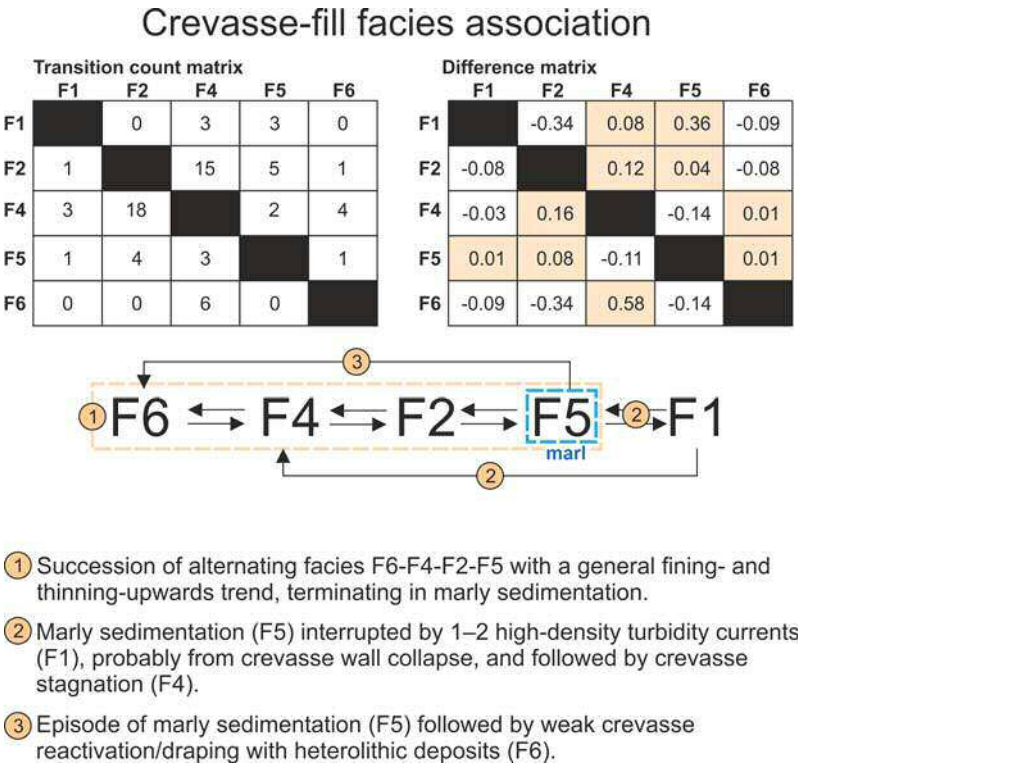

Text-fig. 10. Transition-count and difference matrices for crevasse-fill facies association with the corresponding Markov chain model of facies vertical organization and an interpretation of particular facies transitions. The total number of counted facies transitions is N = 70 and the confidence level of difference matrix is 90%. The preferential facies transitions (more frequent than random) are highlighted in colour in the difference matrix and are the basis of Markov chain model

consistent with the inferred crevasse-splay deposits (Table 1). Crevasses indicate channel propensity for avulsion and their sporadic preservation is simply a record of failed avulsion attempts.

DEPOSITIONAL MODEL

Based on the six facies associations recognized in the Hucisko Jawornickie section (Table 1), the sedimentary palaeosystem studied is envisaged as a progradational base-of-slope complex of depositional lobes fed by avulsive sinuous channels with levees, crevasses and numerous crevasse splays (Text-fig. 11A). The channel-mouth lobes and channel-fill bodies would be lenticular in transverse cross-section and hence it is reasonable to assume that only their maximum thicknesses measured in a single longitudinal outcrop section may be representative when it comes to the system dimensions. These maximum thickness are in the lowest range of values for similar features reported from elsewhere by other authors (e.g., Gardner *et al.* 2003; Mayall *et al.* 2006; Posamentier and Walker 2006; Janbu *et al.* 2007; Deptuck *et al.* 2008; Prélat *et al.* 2009; Bernhardt *et al.* 2011; McHargue *et al.* 2011; Mulder 2011; Janocko *et al.* 2013; Hubbard *et al.* 2014; Grundvåg *et al.* 2014; Bayliss and Pickering 2015a; Marini *et al.* 2015; Pickering *et al.* 2015; Shamugam 2016a). The maximum thickness of channel-fill bodies (21.1 m, Table 1), with a 20% correction for sediment compaction, would suggest distributary channels up to 21.5 m deep. The statistically expected width of such channels would be in the range of 100 m to 1000 m (Clark and Pickering 1996; Clark and Gardiner 2000). Assuming a moderate channel width of 0.5 km and a levee width around 1 km, the width of a channel-and-levee complex would be around 2.5 km, which suggests a radial length of depositional lobe around 3.5 km (Howell and Normark 1982). This estimate is similar to that made independently by Łapcik (2017) from another outcrop section of the Ropianka Formation, pointing to a relatively small size of turbiditic channels and depositional lobes in the Skole Basin (cf. global data in Howell and Normark 1982; Clark and Pickering 1996; Clark and Gardiner 2000).

The measured cumulative thickness of the sedimentary succession is more than 400 m, which means that – in addition to the build-out of depositional lobes and downstream extension of their distributary channels – the lobe complex was strongly aggrading. Therefore, a crucial component of the system morphodynamics was the lateral avulsive shifting of distributary channel within a lobe area and the lateral switching of depositional lobes due to upstream shifts of main feeder channel (Text-fig. 11B). This morphodynamic scenario is consistent with widely held concepts (e.g., Normark *et al.* 1993; Ferry *et al.* 2005; Deptuck *et al.* 2007; Cantelli *et al.* 2011; Hodgson *et al.* 2011; Hubbard *et al.* 2014) and serves to explain the stratigraphic architecture of facies assemblages stacked vertically in the sedimentary succession, as discussed in the next section.

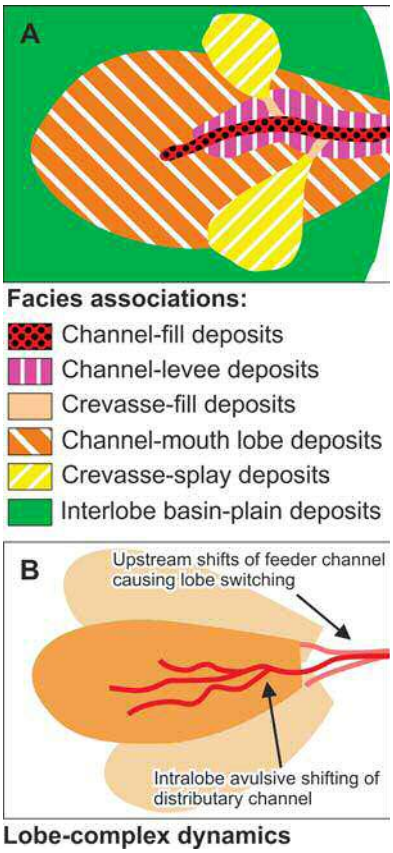

Text-fig. 11. Schematic dimensionless conceptual model for the depositional palaeosystem studied in the Hucisko Jawornickie section (for hypothetical dimensional estimates, see text); A – Spatial relationships of the depositional sub-environments (facies associations) in the system; B – The key morphodynamic factors postulated for the stratigraphic development of an aggrading system

DYNAMIC STRATIGRAPHY

The sedimentary succession in the Hucisko Jawornickie outcrop section (Text-fig. 3) is interpreted as a base-of-slope channelized lobe complex that prograded basinwards over the distal, non-chan-

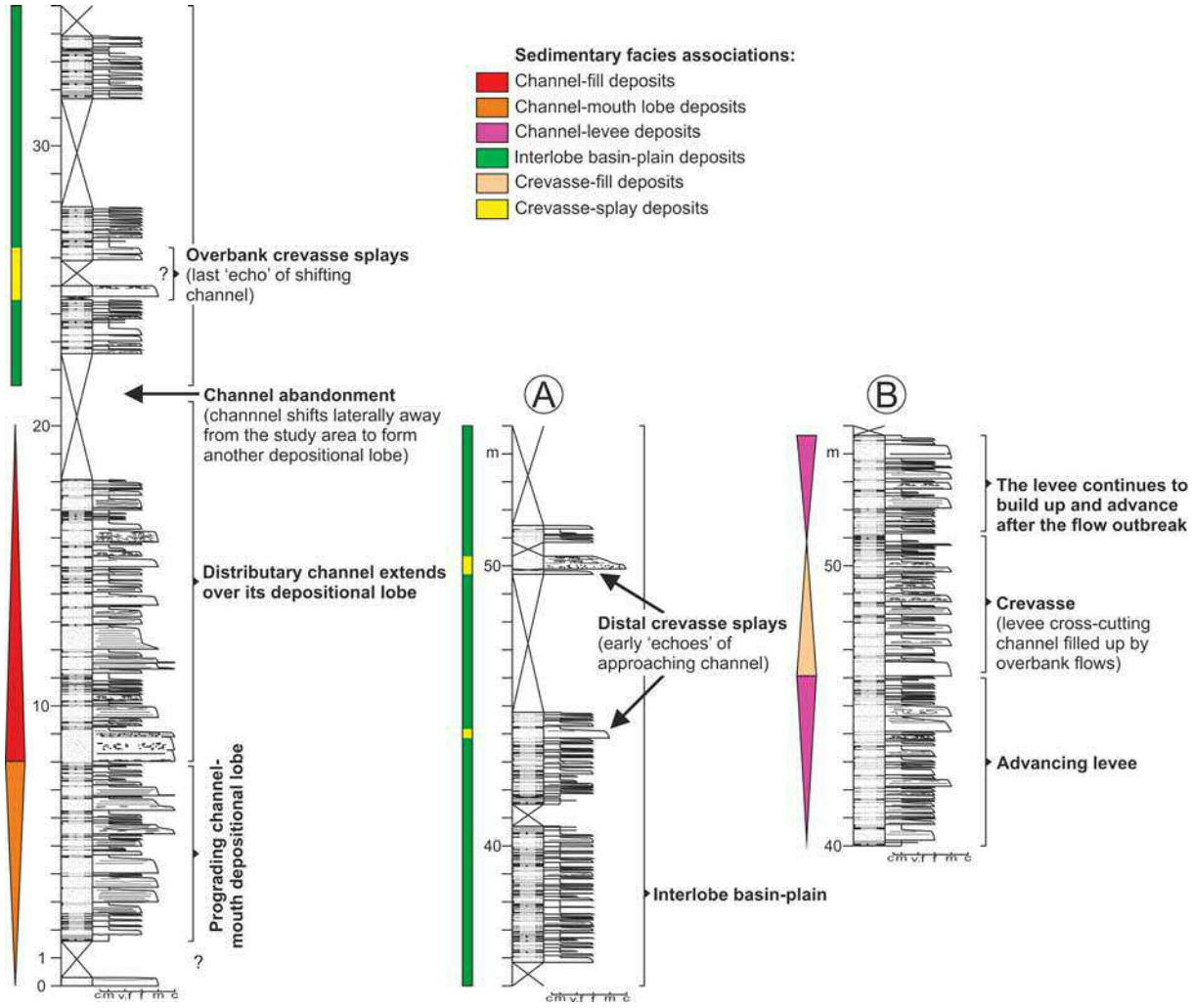

Text-fig. 12. Interpretation of the stratigraphic organization of facies associations in the Hucisko Jawornickie section (log segments A, B, C, E and G) in terms of morphodynamic evolution of the depositional system (Text-fig. 12 – continued on pp. 22–23)

nelized part of a similar earlier complex (described from another outcrop section by Łapcik 2017). The youngest, poorly exposed part of the succession (section segments H and I, Text-fig. 3) is dominated by mudstones, marlstones and mud-rich debrites and probably represents progradation of the basin-slope deposits over the base-of-slope sandy ramp system (*sensu* Reading and Richards 1994). The basinward advance of the whole system was terminated by a bulk deepening of the Skole Basin and its sediment-sourcing northern shelf zone, as indicated by the overlying Variegated Shale Formation of Paleocene–Eocene age (Text-fig. 2).

The base-of-slope system involved depositional lobes with leveed distributary channels and levee-crossing crevasses, surrounded by interlobe basin plain with channel-derived crevasse splays (Text-fig. 11A). The progradational system was strongly aggrading, which caused intralobe lateral shifting of distributary channels by avulsion as well as a bulk lobe switching by upstream shifts of the local feeder conduit (Text-fig. 11B). The sedimentation history of the system recorded in the Hucisko Jawornickie outcrop section (Text-fig. 3) can be accordingly deciphered and interpreted from the upward organization of facies associations (Text-fig. 12).

The lowermost part of the stratigraphic succession (thickness interval 0–20 m of log segment A, Text-fig. 12), corresponding to the Wiar Member of the Ropianka Formation (Text-fig. 2), shows a pro-

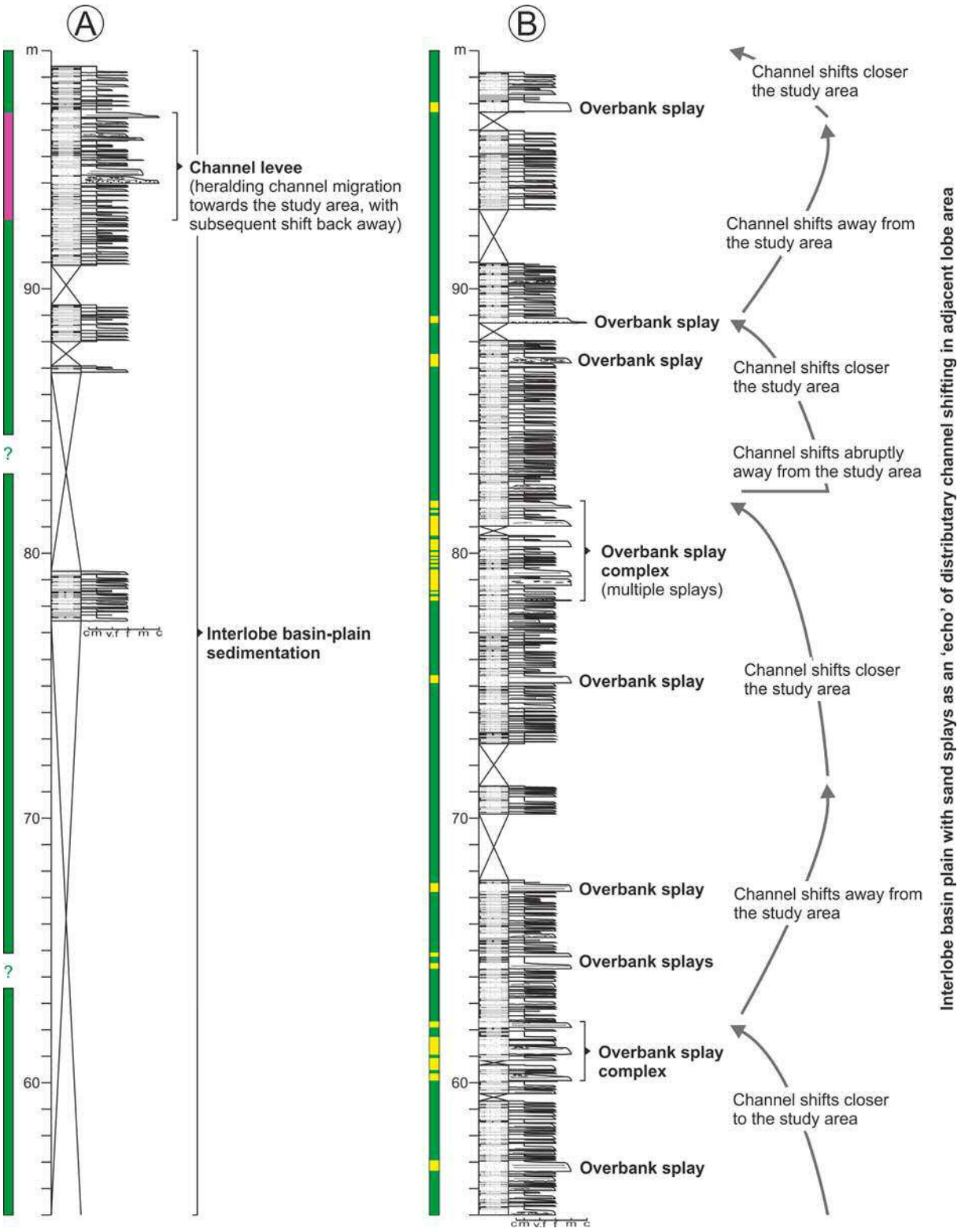
A
B
m
90
80
70
60
?
?
Channel levee
(heralding channel migration towards the study area, with subsequent shift back away)
Interlobe basin-plain sedimentation
cm v.f f m c
Overbank splay
Overbank splay
Overbank splay
Overbank splay complex
(multiple splays)
Overbank splay
Overbank splay
Overbank splays
Overbank splay complex
Overbank splay
Channel shifts closer the study area
Channel shifts away from the study area
Channel shifts closer the study area
Channel shifts abruptly away from the study area
Channel shifts closer the study area
Channel shifts away from the study area
Channel shifts closer to the study area
Interlobe basin plain with sand splays as an 'echo' of distributary channel shifting in adjacent lobe area

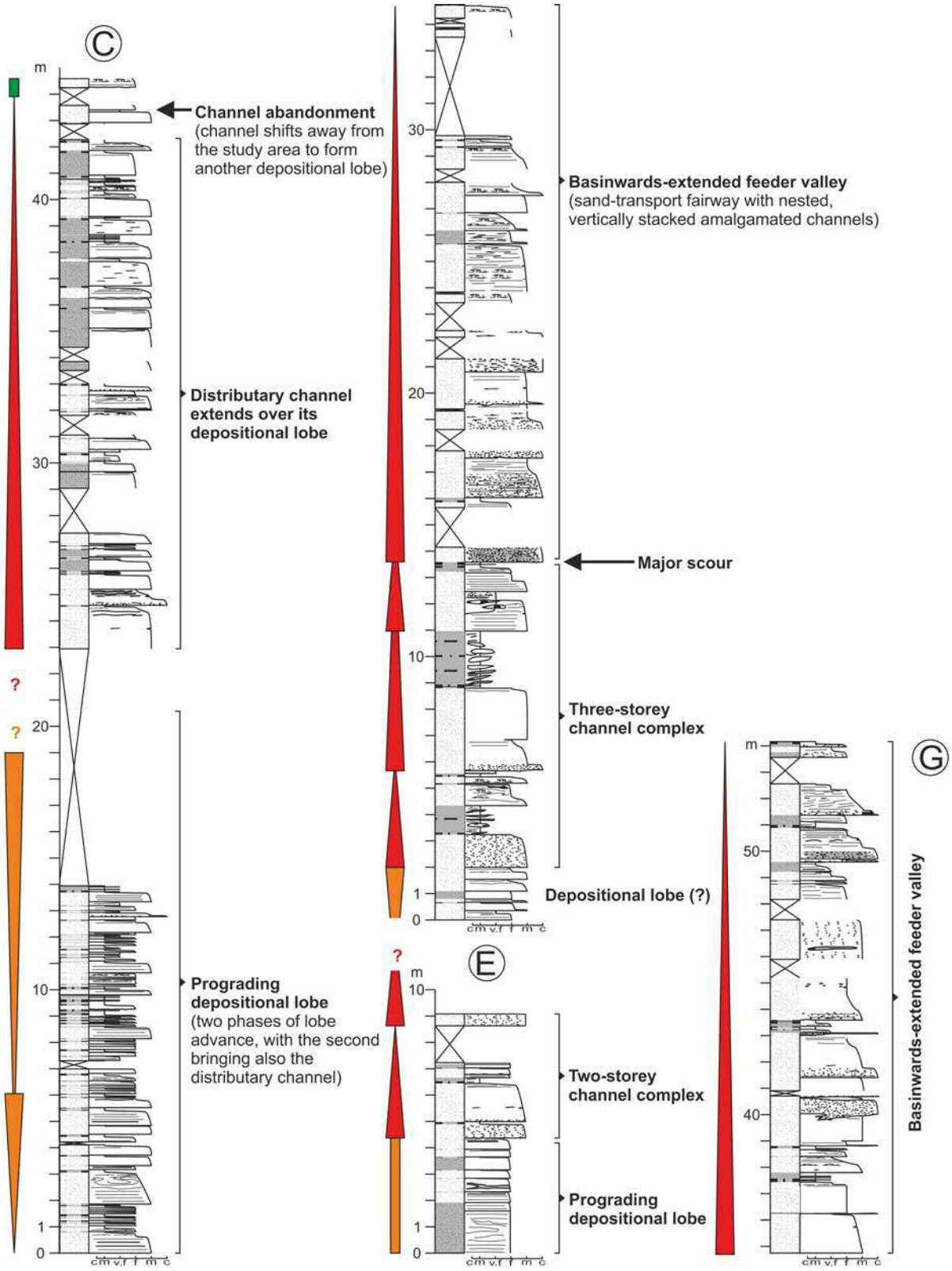
C
m
40
30
20
10
1
0
?
?
Channel abandonment
(channel shifts away from the study area to form another depositional lobe)
Distributary channel extends over its depositional lobe
Prograding depositional lobe
(two phases of lobe advance, with the second bringing also the distributary channel)
cm v.f f m c
30
20
10
1
0
Basinwards-extended feeder valley
(sand-transport fairway with nested, vertically stacked amalgamated channels)
Major scour
Three-storey channel complex
Depositional lobe (?)
E
?
m
10
1
0
Two-storey channel complex
Prograding depositional lobe
G
m
50
40
Basinwards-extended feeder valley

grading channel-mouth depositional lobe (base unexposed) overlain erosively by its parental distributary channel. The channel then shifted laterally by avulsion, leaving a trailing record of crevasse splays (log A interval 20–30 m, Text-fig. 12) and delivering sand to another sector of the depositional lobe. The bulk aggradation caused an upstream shift of the feeder channel (cf. Text-fig. 11B), whereby the lobe was abandoned and turned into a basin plain (log A interval 30–90 m, Text-fig. 12), while an adjoining new depositional lobe was probably being formed. This new lobe's distributary channel only occasionally shifted sufficiently close to the study area to leave a record of levees (log A interval 90–98 m and log B interval 40–55 m, Text-fig. 12), but otherwise was shedding there only occasional crevasse splays according with its lateral shifting. The emplacement of crevasse splays in a quasi-abandoned study area (log B interval 55–100 m, Text-fig. 12) is an important 'echo record' of the distributary channel lateral shifting in the adjacent area of a new lobe deposition, consistent with the notion of avulsive distributaries.

The feeder channel eventually switched back to the study area, forming a new prograding depositional lobe overlain erosively by its distributary channel (log C interval 0–45 m, Text-fig. 12). The distributary channel shifted briefly sideways (log C top), but soon returned by avulsion to continue its lobe-building action (log E and interval 0–13.5 m of log G, Text-fig. 12). The overlying erosive package of sand-dominated deposits (log G interval 13.5–54 m, Text-fig. 12) is probably the local feeder valley that finally extended over the base-of-slope system and was filled with vertically stacked, amalgamated channel-fill deposits. The poorly exposed deposits in the topmost part of the outcrop succession (section segments H and I, Text-fig. 3), fine-grained and rich in muddy debrites, are attributed to an advance of the basin-slope deposits over the base-of-slope ramp system.

In terms of sequence stratigraphy (Catuneanu 2006; Helland-Hansen 2009), the sedimentary succession may be considered as representing a progradational normal-regressive lowstand systems tract, turning into an increasingly aggradational transgressive systems tract – when even the feeder valley was back-filled. The transgression culminated in the deposition of the Variegated Shale Formation (Text-fig. 2) at the highstand of relative sea level.

The sedimentation occurred during a long-term eustatic sea-level fall by about 15 m from the mid-Campanian to end-Maastrichtian (Haq 2014, fig. 4), which indicates that the coeval relative sea-level rise and transgression in the Skole Basin must have been caused by local tectonics. The early tectonic contraction of Carpathian orogen had probably both deepened and narrowed the basin, as indicated by a marked advance of the basin-margin slope. However, several short-term eustatic fluctuations on the order of 30–50 m occurred during the period of sedimentation (see 3rd-order eustatic cycles KCa3–KCa7 and KMa1–KMa5 in Haq 2014, fig. 4). Their potential impact on the depositional system behaviour is difficult to assess due to the sparsity of biostratigraphic data from the sedimentary succession, but it is quite possible that the system morphodynamic development was not controlled solely by autogenic processes. For example, the evidence of multiple lobe advances (log C, Text-fig. 12) and deeply erosional amalgamation of vertically stacked palaeochannels (log G, Text-fig. 12) might well indicate an influence of short-term eustatic changes. Eustatic fluctuations would have their greatest impact on the basin-margin shelf, which might explain the alternating supply of siliciclastic mud and calcareous mud (marl) as well as the episodic delivery of plant detritus and exotic gravel from the shelf zone.

IMPLICATIONS FOR THE SKOLE BASIN

Based on a detailed sedimentological analysis of available outcrop sections (Hucisko Jawornickie, Manasterz and Słonne, Text-fig. 1A), the depositional system of the Ropianka Formation is interpreted as a base-of-slope clastic ramp supplied with coarse sediment from the basin shelf zone through incised slope valleys (Text-fig. 13). The shelf was probably narrow and controlled by short-term eustatic fluctuations, with carbonate sedimentation dominant during sea-level highstands and with deltas reaching the shelf edge during lowstands. The occurrence of a mud-accumulating slope between the base-of-slope sandy ramp and the sediment-supplying shelf zone would explain why the Ropianka Formation is increasingly dominated by marlstone and mudstone facies towards its northerly source zone.

The lateral switching of depositional lobes (Text-fig. 11B) and temporal occupation of abandoned lobe areas by fine-grained basinal sedimentation may explain further the limited lateral extent of marlstone- and/or mudstone-dominated wedges within the Ropianka Formation. These wedges were recognized by surface mapping in the lower parts of the Cisowa, Wiar and Leszczyny members (Text-fig. 2), but the steeply folded and poorly exposed formation is likely

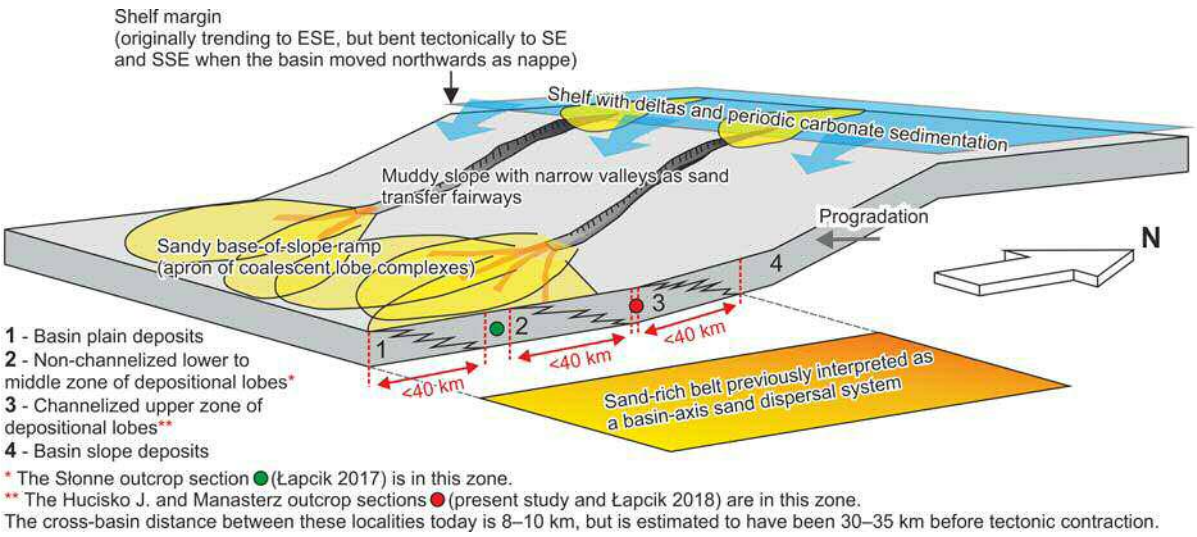

Text-fig. 13. Schematic conceptual model for the deposition of Ropianka Formation in the Skole Basin based on the Hucisko Jawornickie (present study), Manasterz (Łapcik 2018) and Słonne (Łapcik 2017) outcrop sections (see Text-fig. 1A)

to contain many more such thick local patches of fine-grained deposits (see Text-fig. 12, interval 20–100 m of log A and interval 54–100 m of log B). The hypothetical sedimentation model (Text-fig. 11) predicts that the main morphodynamic changes in the depositional system, such as lobe switching, were likely autogenic and non-synchronous, which would mean that the Ropianka Formation most probably lacks a simple layer-cake lithostratigraphy.

The channelized lobe complex studied in the Hucisko Jawornickie section, with a coeval feeder channel documented by Łapcik (2018) in the nearby Manasterz section, had prograded over the non-channelized distal part of an earlier similar lobe complex studied by Łapcik (2017) in the Słonne section (see section localities in Text-fig. 1A). The basinward distance between the Słonne section and the Hucisko Jawornickie section in the folded Skole Nappe is about 10 km (Text-fig. 1A), but is estimated to have been originally at least 35 km. If this estimate is correct, the basinward extent of the prograding base-of-slope ramp system would be around 100 km (Text-fig. 13), with the ramp evolving into a semi-continuous apron (*sensu* Reading and Richards 1994) by the lateral switching of depositional lobes and their coalescent vertical stacking. This sand-rich belt was indeed recognized by the earlier researchers from surface mapping, but was considered to represent a long-distance system of axial sand transport in the synclinal basin (e.g., Książkiewicz 1962; Bromowicz 1974; Kotlarczyk 1978). However, the measured local sediment transport directions appeared to be highly varied and hardly supporting this interpretation, indicating transport mainly from the NW, N and NE (see Łapcik 2017, fig. 1A).

The present study and related studies by Łapcik (2017, 2018) have suggested a system of transverse, rather than longitudinal, sand dispersal and indicated that the system's feeder and distributary channels were quite small by global standards (Howell and Normark 1982; Clark and Pickering 1996; Clark and Gardiner 2000), unlikely to form depositional lobes more than 3–4 km in radial length. The high variation of local transport directions is fully compatible with the present model, taking into account the avulsive channel shifting, sideways building of levees, crevassing and lateral lobe switching (Text-fig. 11) and the ultimate tectonic bending and eastward rotation of the Skole Nappe (Text-fig. 1A). Features indicative of palaeotransport direction are seldom exposed even in such relatively good outcrops as the Hucisko Jawornickie section and may have little exact meaning without being linked to specific facies association.

CONCLUSIONS

This sedimentological study of the Wiar and Leszczyny members of deep-marine Ropianka Formation in the Hucisko Jawornickie outcrop section of Skole Nappe allowed distinction of seven com-

ponent sedimentary facies representing a range of sediment-gravity flows and episodes of hemipelagic to pelagic sedimentation with possible intervention of tidal or contouritic bottom currents. The stratigraphic grouping of sedimentary facies indicated six facies associations, interpreted as representing various morphodynamic architectural elements of a base-of-slope depositional system: distributary channels, channel-mouth lobes, channel levees, interlobe basin plain, crevasses and crevasse splays. The individual facies associations have been characterized in quantitative terms of statistics, and their internal modal organization of component facies has been studied and interpreted by using Markov chain analysis.

The stratigraphic succession in the Hucisko Jawornickie section is interpreted as a complex of channelized depositional lobes, with the vertical organization of facies associations reflecting chiefly autogenic morphodynamics of an aggrading base-of-slope system. The thick erosional package of amalgamated channel-fill deposits in the uppermost part of succession is interpreted as a basinwards extended and back-filled feeder valley, buried by muddy deposits of an advancing basin slope. The slope advance over the base-of-slope ramp culminated in a strong deepening of the Skole Basin and deposition of the Paleocene–Eocene Variegated Shale Formation. This dramatic change finds no explanation in coeval eustasy and is attributed to the basin tectonics. Short-term eustatic fluctuations are thought to have had a major impact on the basin's sediment-supplying shelf zone.

The base-of-slope sandy system of the Ropianka Formation is estimated to have comprised depositional lobes with a radial length of 30–40 km and to have prograded basinwards over a distance of around 100 km, while undergoing strong aggradation. The lateral switching of lobes and their coalescent vertical stacking resulted in a base-of-slope apron, which was recognized as a sand-rich belt by previous researcher from surface mapping, but was misperceived as an axial system of sand dispersal in the synclinal basin.

The present study, as the first detailed analysis of the Hucisko Jawornickie outcrop section, is a major contribution to the sedimentological understanding of the Ropianka Formation and the Late Cretaceous–Paleocene development in the Skole Basin. Last, but not least, this sedimentological case study demonstrates that a great deal of valuable information can be derived even from a single outcrop section of a poorly exposed sedimentary formation on the basis of detailed facies analysis conducted with appropriate methods.

Acknowledgements

The study was funded by the Jagiellonian University. Alfred Uchman (Jagiellonian University) kindly offered valuable discussions and suggestions. Constructive reviews by Wojciech Nemec (Bergen University) and George Postma (Utrecht University), with editorial comments from Piotr Łuczyński (University of Warsaw), helped greatly to improve the manuscript.

REFERENCES

Alexander, J. and Morris, S. 1994. Observations on experimental, nonchannelized high-concentration turbidity currents and variations in deposits around obstacles. *Journal of Sedimentary Research*, **64**, 899–909.

Alexander, J. and Mulder, T. 2002. Experimental quasi-steady density currents. *Marine Geology*, **186**, 195–210.

Ashley, G.M., Southard, J.B. and Boothroyd, J.C. 1982. Deposition of climbing-ripple beds: a flume simulation. *Sedimentology*, **29**, 67–79.

Baas, J.H. 2004. Conditions for formation of massive turbiditic sandstones by primary depositional processes. *Sedimentary Geology*, **166**, 293–310.

Baas, J.H., Best, J.L., Peakall, J. and Wang, M. 2009. A phase diagram for turbulent, transitional, and laminar clay suspension flows. *Journal of Sedimentary Research*, **79**, 162–183.

Barwicz-Piskorz, W. and Rajchel, J. 2012. Radiolarian and agglutinated foraminiferal biostratigraphy of the Paleogene deep-water deposits on the northern margin of the Carpathian Tethys (Skole Unit). *Geological Quarterly*, **56**, 1–24.

Bayliss, N.J. and Pickering, K.T. 2015a. Transition from deep-marine lower-slope erosional channels to proximal basin-floor stacked channel-levée-overbank deposits, and syn-sedimentary growth structures, Middle Eocene Banastón System, Ainsa Basin, Spanish Pyrenees. *Earth-Science Review*, **144**, 23–46.

Bayliss, N.J. and Pickering, K.T. 2015b. Deep-marine structurally confined channelised sandy fans: Middle Eocene Morillo System, Ainsa Basin, Spanish Pyrenees. *Earth-Science Review*, **144**, 82–106.

Bąk, K., 2007. Environmental changes around the Cenomanian–Turonian boundary in a marginal part of the Outer Carpathian Basin expressed by microfacies, microfossils and chemical records in the Skole Nappe (Poland). *Annales Societatis Geologorum Poloniae*, **77**, 39–67.

Bąk, K., Bąk, M., Górny, Z. and Wolska, A. 2014. Environmental conditions in a Carpathian deep-sea basin during the period preceding Oceanic Anoxic Event 2 – a case study from the Skole Nappe. *Geologica Carpathica*, **65**, 433–450.

Bernhardt, A., Jobe, Z.R. and Lowe, D.R. 2011. Stratigraphic evolution of a submarine channel–lobe complex system

in a narrow fairway within the Magallanes foreland basin, Cerro Toro Formation, southern Chile. *Marine and Petroleum Geology*, **28**, 785–806.

Best, J. and Bridge, J. 1992. The morphology and dynamics of low amplitude bedwaves upon upper stage plane beds and the preservation of planar laminae. *Sedimentology*, **39**, 737–752.

Breien, H., De Blasio, F.V., Elverhøi, A., Nystruen, J.P. and Harbitz, C.B. 2010. Transport mechanisms of sand in deep-marine environments – insights based on laboratory experiments. *Journal of Sedimentary Research*, **80**, 975–990.

Bromowicz, J. 1974. Facial variability and lithological character of Inoceramian Beds of the Skole-Nappe between Rzeszów and Przemyśl. *Prace Geologiczne*, **84**, 1–83. [In Polish with English summary]

Bouma, A.H. 1962. Sedimentology of Some Flysch Deposits: A Graphic Approach to Facies Interpretation, 168 pp. Elsevier; Amsterdam.

Bouma, A.H. 2000. Coarse-grained and fine-grained turbidite systems as end member models: applicability and dangers. *Marine and Petroleum Geology*, **17**, 137–143.

Bruhn, C.H.L. and Walker, R.G. 1997. Internal architecture and sedimentary evolution of coarse-grained, turbidite channel-levee complexes, Early Eocene Regência Canyon, Espírito Santo Basin, Brazil. *Sedimentology*, **44**, 17–46.

Brunt, R.L., Hodgson, D.M., Flint, S.S., Pringle, J.K., Di Celma, C., Prélat, A. and Grecula, M. 2013. Confined to unconfined: anatomy of a base of slope succession, Karoo Basin, South Africa. *Marine and Petroleum Geology*, **41**, 206–221.

Burzewski, J. 1966. Baculites marls on the lithostratigraphy background of the upper Inoceramian Beds of the Skiba Carpathians. *Zeszyty Naukowe AGH, Geologia*, **7**, 89–115. [In Polish with French summary]

Cantelli, A., Pirmez, C., Johnson, S. and Parker, G. 2011. Morphodynamic and stratigraphic evolution of self-channelized subaqueous fans emplaced by turbidity currents. *Journal of Sedimentary Research*, **81**, 233–247.

Carter, R.M. 1988. The nature and evolution of deep-sea channel systems. *Basin Research*, **1**, 41–54.

Catuneanu, O. 2006. Principles of Sequence Stratigraphy, 375 p. Elsevier, Amsterdam.

Clark, J.D. and Gardiner, A.R. 2000. Outcrop analogues for deep-water channel and levee genetic units from the Grès d'Annot turbidite system, SE France. In: Weimer, P., Slatt, R.M., Coleman, J.L., Rosen, N., Nelson, C.H., Bouma, A.H., Styzen, M. and Lawrence, D.T. (Eds), Global Deep-Water Reservoirs. Gulf Coast Section SEPM Foundation 20th Annual Bob F Perkins Research Conference, pp. 175–190. Houston.

Clark, J.D. and Pickering, K.T. 1996. Architectural elements and growth patterns of submarine channels: application to hydrocarbon exploration. *American Association of Petroleum Geologists Bulletin*, **80**, 194–220.

Collinson, J.D., Mountney, N.P. and Thompson, D.B. 2006. Sedimentary Structures, 292 p. Terra Publishing; Harpenden.

Crowell, J.C. 1957. Origin of pebbly mudstones. *Geological Society of America Bulletin*, **68**, 993–1010.

Davis, J.C. 2002. Statistics and Data Analysis in Geology, 638 p. John Wiley & Sons; New York. [3rd ed.]

Deptuck, M.E., Piper, D.J.W., Savoye, B. and Gervais, A. 2008. Dimensions and architecture of Late Pleistocene submarine lobes off the northern margin of East Corsica. *Sedimentology*, **55**, 869–898.

Deptuck, M.E., Sylvester, Z., Pirmez, C. and O'Byrne, C. 2007. Migration–aggradation history and 3-D seismic geomorphology of submarine channels in the Pleistocene Benin-major Canyon, western Niger Delta slope. *Marine and Petroleum Geology*, **24**, 406–433.

Dott, R.H., Jr. 1983. Presidential address: Episodic sedimentation – How normal is average? How rare is rare? Does it matter? *Journal of Sedimentary Petrology*, **53**, 5–23.

Drake, T.G. 1990. Structural features in granular flows. *Journal of Geophysical Research*, **B95**, 8681–8696.

Dykstra, M. 2012. Deep-water tidal sedimentology. In: Davis, R.A. and Dalrymple, R.W. (Eds), Principles of Tidal Sedimentology, pp. 371–396. Springer; Berlin.

Dżułyński, S. and Smith, A.J. 1964. Flysch facies. *Rocznik Polskiego Towarzystwa Geologicznego*, **34**, 245–266.

Ferry, J.N., Mulder, T., Parize, O. and Raillard, S. 2005. Concept of equilibrium profile in deep water turbidite system: effects of local physiographic changes on the nature of sedimentary process and the geometries of deposits. In: Hodgson, D.M., and Flint, S.S. (Eds), Submarine Slope Systems: Processes and Products. *Geological Society of London Special Publication*, **244**, 181–193.

Galloway, W.E. 1998. Siliciclastic slope and base-of-slope depositional systems: component facies, stratigraphic architecture, and classification. *American Association of Petroleum Geologists Bulletin*, **82**, 569–595.

Gardner, M.H., Borer, J.M., Melick, J.J., Mavilla, N., Dechesne, M. and Wagerle, R.N. 2003. Stratigraphic process-response model for submarine channels and related features from studies of Permian Brushy Canyon outcrops, West Texas. *Marine and Petroleum Geology*, **20**, 757–787.

Gągała, Ł., Vergés, J., Saura, E., Malata, T., Ringenbach, J., Werner, P. and Krzywiec, P. 2012. Architecture and orogenic evolution of the northeastern Outer Carpathians from cross-section balancing and forward modelling. *Tectonophysics*, **532–535**, 223–241.

Ge, Z., Nemec, W., Gawthorpe, R.L. and Hansen, E.W.M. 2017. Response of unconfined turbidity current to normal-fault topography. *Sedimentology*, **64**, 932–959.

Gedl, E. 1999. Lower Cretaceous palynomorphs from the Skole Nappe (Outer Carpathians, Poland). *Geologica Carpathica*, **50**, 75–90.

Gee, M.J.R., Masson, D.G., Watts, A.B. and Allen, P.A. 1999.

The Saharan debris flow: an insight into the mechanics of long runout submarine debris flows. *Sedimentology*, **46**, 317–335.

Geroch, S., Krysowska-Iwaszkiewicz, M., Michalik, M., Prochazka, K., Radomski, A., Radwański, Z., Unrug, Z., Unrug, R. and Wieczorek, J. 1979. Sedimentation of Węgierka Marls (Late Senonian, Polish Flysch Carpathians). *Annales Societatis Geologorum Poloniae*, **49**, 105–134. [In Polish with English summary]

Gradstein, F., Ogg, J., Schmitz, M. and Ogg, G. 2012. The Geological Time Scale 2012, 1176 p. Elsevier; Oxford.

Grundvåg, S.A., Johannessen, E.P., Hansen, W.H. and Plink-Björklund, P. 2014. Depositional architecture and evolution of progradationally stacked lobe complexes in the Eocene Central Basin of Spitsbergen. *Sedimentology*, **61**, 535–569.

Gucik, S. 1963. Profile of the Lower Cretaceous from Bełwin in the Przemyśl Carpathians. *Kwartalnik Geologiczny*, **7**, 257–268. [In Polish with English summary]

Gucik, S., Paul, Z., Ślączka, A. and Żytko, K. 1980. Mapa geologiczna Polski 1:200 000, arkusz Przemyśl, Kalników. Wydawnictwa Geologiczne; Warszawa. [In Polish]

Harms, J.C., Southard, J.B., Spearing, D.R. and Walker, R.G. 1975. Depositional Environments as Interpreted from Primary Sedimentary Structures and Stratification Sequences. Lecture Notes, SEPM Short Course No. 2, 161 p. Society of Economic Paleontologists and Mineralogists; Dallas.

Haughton, P.D.W., Davis, C., McCaffrey, W. and Barker, S.P. 2009. Hybrid sediment gravity flow deposits – classification, origin and significance. In: Amy, L.A., McCaffrey, W.B. and Talling, P.J. (Eds), Hybrid and Transitional Submarine Flows. *Marine and Petroleum Geology*, **26**, 1900–1918.

Haq, B.U. 2014. Cretaceous eustasy revisited. *Global and Planetary Change*, **113**, 44–58.

He, Y., Gao, Z., Luo, J., Luo, S. and Liu, X. 2008. Characteristics of internal-wave and internal-tide deposits and their hydrocarbon potential. *Petroleum Science*, **5**, 37–44.

Helland-Hansen, W. 2009. Towards the standardization of sequence stratigraphy: Discussion. *Earth-Science Review*, **94**, 95–97.

Heller, P.L. and Dickinson, W.R. 1985. Submarine ramp facies model for delta-fed, sand-rich turbidite systems. *American Association of Petroleum Geologists Bulletin*, **69**, 960–976.

Hodgson, D.M., Di Celma, C.N., Brunt, R.L. and Flint, S.S. 2011. Submarine slope degradation and aggradation and the stratigraphic evolution of channel–levee systems. *Journal of the Geological Society of London*, **168**, 625–628.

Hoffmann, M., Kołodziej, B. and Skupien, P., 2017. Microencruster-microbial framework and synsedimentary cements in the Štramberk Limestone (Carpathians, Czech Republic): Insights into reef zonation. *Annales Societatis Geologorum Poloniae*, **87**, 325–347.

Howell, D.G. and Normark, W.R. 1982. Sedimentology of submarine fans. In: Scholle, P.A. and Spearing, D.R. (Eds), Sandstone Depositional Environments. *American Association of Petroleum Geologists Memoir*, **31**, 365–404.

Hubbard, S.M., Romans, B.W. and Graham, S.A. 2008. Deep-water foreland basin deposits of the Cerro Toro Formation, Magallanes basin, Chile: architectural elements of a sinuous basin axial channel belt. *Sedimentology*, **55**, 1333–1359.

Hubbard, S.M., Covault, J.A., Fildani, A. and Romans, B.R. 2014. Sediment transfer and deposition in slope channels: Deciphering the record of enigmatic deep-sea processes from outcrop. *Geological Society of America Bulletin*, **126**, 857–871.

Ilstad, T., Marr, J.G., Elverhøi, A. and Harbitz, C.B. 2004. Laboratory studies of subaqueous debris flows by measurements of pore-fluid pressure and total stress. *Marine Geology*, **213**, 403–414.

Janbu, N.E., Nemec, W., Kırman, E. and Özaksoy, V. 2007. Facies anatomy of a channelized sand-rich turbiditic system: the Eocene Kusuri Formation in the Sinop Basin, north-central Turkey. In: Nichols, G., Paola, C. and Williams, E.A. (Eds), Sedimentary Environments, Processes and Basins – A Tribute to Peter Friend. *International Association of Sedimentologists Special Publication*, **38**, 457–517.

Janocko, M., Nemec, W., Henriksen, S. and Warchoł, M. 2013. The diversity of deep-water sinuous channel belts and slope valley-fill complexes. *Marine and Petroleum Geology*, **41**, 7–34.

Jurkiewicz, H. and Woiński, J. 1981. Mapa geologiczna Polski, 1:200 000, arkusz Mielec. Wydawnictwa Geologiczne; Warszawa. [In Polish]

Kędzierski, M. and Leszczyński, S. 2013. A paleoceanographic model for the Late Campanian–Early Maastrichtian sedimentation in the Polish Carpathian Flysch basin based on nannofossils. *Marine Micropaleontology*, **102**, 34–50.

Kerr, R.C. 1991. Erosion of a stable density gradient by sedimentation-driven convection. *Nature*, **353**, 423–425.

Klaucke, I. and Hesse, R. 1996. Fluvial features in the deep-sea: new insights from the glacigenic submarine drainage system of the Northwest Atlantic Mid-Ocean Channel in the Labrador Sea. *Sedimentary Geology*, **106**, 223–234.

Kneller, B.C. and Branney, M.J. 1995. Sustained high-density turbidity currents and the deposition of thick massive sands. *Sedimentology*, **42**, 607–616.

Kotlarczyk, J. 1978. Stratigraphy of the Ropianka Formation or of Inoceramian beds in the Skole Unit of the Flysch Carpathians. *Prace Geologiczne, Polska Akademia Nauk, Oddział w Krakowie, Komisja Nauk Geologicznych*, **108**, 1–75. [In Polish with English summary]

Kotlarczyk, J. 1988. A Guidebook of 59th PTG Congress in Przemyśl, 298 p. Wydawnictwa AGH; Kraków. [In Polish]

Kotlarczyk, J., Jerzmańska, A., Świdnicka, E. and Wiszniowska, T. 2006. A framework of ichtyofaunal ecostratigraphy of the Oligocene–Early Miocene strata of the Polish Outer

Carpathian Basin. *Annales Societatis Geologorum Poloniae*, **76**, 1–111.

Kováč, M., Plašienka, D., Soták, J., Vojtko, R., Oszczypko, N., Less, G., Ćosović, V., Fügenschuh, B. and Králiková, S. 2016. Paleogene palaeogeography and basin evolution of the Western Carpathians, Northern Pannonian domain and adjoining areas. *Global and Planetary Change*, **140**, 9–27.

Książkiewicz, M. (ed.) 1962. Geological Atlas of Poland. Fascicle, 13 – Cretaceous and Early Tertiary in the Polish External Carpathians. Instytut Geologiczny; Warszawa. [In Polish with English summary]

Leclair, S.F. and Arnott, R.W.C. 2005. Parallel lamination formed by high-density turbidity currents. *Journal of Sedimentary Research*, **75**, 1–5.

Leszczyński, S., Malik, K. and Kędzierski, M. 1995. New data on lithofacies and stratigraphy of the siliceous and fucoid marl of the Skole nappe (Cretaceous, Polish Carpathians). *Annales Societatis Geologorum Poloniae*, **65**, 43–62. [In Polish with English summary]

Leszczyński, S. and Uchman, A. 1991. To the origin of variegated shales from flysch of the Polish Carpathians. *Geologica Carpathica*, **42**, 279–289.

Leszczyński, S. 2003. Bioturbation structures in the Holovnia Siliceous Marls (Turonian–Lower Santonian) in Rybotycze (Polish Carpathians). *Annales Societatis Geologorum Poloniae*, **73**, 103–122.

Leszczyński, S. 2004. Bioturbation structures of the Kropivnik Fucoid Marls (Campanian–lower Maastrichtian) of the Huwniki — Rybotycze area (Polish Carpathians). *Geological Quarterly*, **48**, 35–60.

Lowe, D.R. 1982. Sediment gravity flows, II. Depositional models with special reference to the deposits of high-density turbidity currents. *Journal of Sedimentary Petrology*, **52**, 279–297.

Lowe, D.R. 1988. Suspended-load fallout rate as an independent variable in the analysis of current structures. *Sedimentology*, **35**, 765–776.

Lowe, D.R. and Guy, M. 2000. Slurry-flow deposits in the Britannia Formation (Lower Cretaceous), North Sea: a new perspective on the turbidity current and debris flow problem. *Sedimentology*, **47**, 31–70.

Lowe, D.R., Guy, M. and Palfrey, A. 2003. Facies of slurry-flow deposits, Britannia Formation (Lower Cretaceous), North Sea: implications for flow evolution and deposit geometry. *Sedimentology*, **50**, 45–80.

Łapcik, P. 2017. Facies heterogeneity of a deep-sea depositional lobe complex: case study from the Słonne section of Skole Nappe, Polish Outer Carpathians. *Annales Societatis Geologorum Poloniae*, **87**, 301–324.

Łapcik, P. 2018. Sedimentary processes and architecture of Upper Cretaceous deep-sea channel deposits: a case from the Skole Nappe, Polish Outer Carpathians. *Geologica Carpathica*, **69**, 71–88.

Łapcik, P., Kowal-Kasprzyk, J. and Uchman, A. 2016. Deep-sea mass-flow sediments and their exotic blocks from the Ropianka Formation (Campanian–Paleocene) in the Skole Nappe: a case study of the Wola Rafałowska section (SE Poland). *Geological Quarterly*, **60**, 301–316.

Malata, T. and Poprawa, P. 2006. Evolution of the Skole Subbasin. In: Oszczypko, N., Uchman, A. and Malata, E. (Eds), Rozwój paleotektoniczny basenów Karpat zewnętrznych, pp. 101–110. Institute of Geological Sciences, Jagiellonian University; Kraków. [In Polish with English abstract]

Marini, M., Salvatore, M., Ravnås, R. and Moscatelli, M. 2015. A comparative study of confined vs. semi-confined turbidite lobes from the Lower Messinian Laga Basin (Central Apennines, Italy): Implications for assessment of reservoir architecture. *Marine and Petroleum Geology*, **63**, 142–165.

Mayall, M., Jones, E. and Casey, M. 2006. Turbidite channel reservoirs – Key elements in facies prediction and effective development. *Marine and Petroleum Geology*, **23**, 821–841.

McCave, I.N. and Jones, K.P.N. 1988. Deposition of ungraded muds from high-density non-turbulent turbidity currents. *Nature*, **133**, 250–252.

McHargue, T., Prycz, M.J., Sullivan, M.D., Clark, J.D., Fildani, A., Romans, B.W., Covault, J.A., Levy, M., Posamentier, H.W. and Drinkwater, N.J. 2011. Architecture of turbidite channel systems on the continental slope: Patterns and predictions. *Marine and Petroleum Geology*, **28**, 728–743.

Miall, A.D. 1973. Markov chain analysis applied to an ancient alluvial plain succession. *Sedimentology*, **20**, 347–364.

Miall, A.D. 1978. Lithofacies types and vertical profile models in braided river deposits: a summary. In: Miall, A.D. (Ed.), Fluvial Sedimentology. *Canadian Society of Petroleum Geologists Memoir*, **5**, 597–604.

Mohrig, D., Ellis, C., Parker, G., Whipple, K. and Hondzo, M. 1998. Hydroplaning of subaqueous debris flows. *Geological Society of America Bulletin*, **110**, 387–394.

Mulder, T. 2011. Gravity processes and deposits on continental slope, rise and abyssal plains. In: Hüeneke, H. and Mulder, T. (Eds), Deep-Sea Sediments. Developments in Sedimentology, Vol. 63, pp. 25–148. Elsevier; Amsterdam.

Mulder, T. and Alexander, J. 2001. The physical character of subaqueous sedimentary density flows and their deposits. *Sedimentology*, **48**, 269–299.

Mutti, E. and Normark, W.R. 1987. Comparing examples of modern and ancient turbidite systems: problems and concepts. In: Leggett, J.K. and Zuffa, G.G. (Eds), Marine Clastic Sedimentology, pp. 1–38. Graham and Trotman; London.

Nakajima, T., Satoh, M. and Okamura, Y. 1998. Channel-levee complexes, terminal deep-sea fan and sediment wave fields associated with the Toyama Deep-Sea Channel system in the Japan Sea. *Marine Geology*, **147**, 25–41.

Nelson, C.H., Maldonado, A., Barber, J.H. & Alonso, B. 1991. Modern sand-rich and mud-rich siliciclastic aprons: alternative base-of-slope turbidite systems to submarine fans.

In: Weimer, P. and Link, M.H. (Eds), Seismic Facies and Sedimentary Processes of Submarine Fans and Turbidite Systems, pp. 171–190. Springer-Verlag; New York.

Nemec, W., Alçiçek, M.C. and Özaksoy, V. 2018. Sedimentation in a foreland basin within synorogenic orocline: Palaeogene of the Isparta Bend, Taurides, SW Turkey. *Basin Research*, **30**, 650–670.

Nemec, W. and Postma, G. 1991. Inverse grading in gravel beds. Abstracts IAS 12th Regional Meeting, p. 38. International Association of Sedimentologists; Bergen.

Nemec, W., Steel, R.J., Porębski, S.J. and Spinnangr, Å. 1984. Domba Conglomerate, Devonian, Norway: process and lateral variability in a mass flow-dominated, lacustrine fan-delta. In: Koster, E.H. and Steel, R.J. (Eds), Sedimentology of Gravels and Conglomerates. *Canadian Society of Petroleum Geologists Memoir*, **10**, 295–320.

Nescieruk, P., Paul, Z., Ryłko, W., Szymakowska, F., Wójcik, A. and Żytko. K. 1995. Mapa geologiczna Polski, 1:200 000, arkusz Jasło. Polska Agencja Ekologiczna; Warszawa. [In Polish]

Nichols, G. 2009. Sedimentology and Stratigraphy, 419 p. Wiley-Blackwell; Oxford. [2nd ed.]

Normark, W.R., Posamentier, H. and Mutti, E. 1993. Turbidite systems: state of the art and future directions. *Reviews of Geophysics*, **31**, 91–116.

Olszewska, B. and Szydło, A. 2017. Environmental stress in the northern Tethys during the Paleogene: a review of foraminiferal and geochemical records from the Polish Outer Carpathians. *Geological Quarterly*, **61**, 682–695.

Pickering, K.T., Corregidor, J. and Clark, J.D. 2015. Architecture and stacking patterns of lower-slope and proximal basin-floor channelised submarine fans, Middle Eocene Ainsa System, Spanish Pyrenees: An integrated outcrop–subsurface study. *Earth-Science Review*, **144**, 47–81.

Pickering, K.T., Hiscott, R.N., Kenyon, N.H., Ricci Lucchi, F. and Smith, R.D.A. 1995. Atlas of Deep Water Environments: Architectural Style in Turbidite Systems, 334 p. Chapman and Hall; London.

Piper, D.J.W. 1978. Turbidite muds and silts on deep sea fans and abyssal plains. In: Stanley, D.J. and Kelling, G. (Eds), Sedimentation in Submarine Canyons, Fans and Trenches, pp. 163–176. Dowden, Hutchinson and Ross; Stroudsburg, Pennsylvania.

Posamentier, H.W. and Walker, R.G. 2006. Deep-water turbidites and submarine fans. In: Posamentier, H.W. and Walker, R.G. (Eds), Facies Models Revisited. *SEPM (Society for Sedimentary Geology) Special Publication*, **84**, 397–520.

Postma, G., Nemec, W. and Kleinspehn, K.L. 1988. Large floating clasts in turbidites: a mechanism for their emplacement. *Sedimentary Geology*, **58**, 47–61.

Prélat, A., Covault, J.A., Hodgson, D.M., Fildani, A. and Flint, S.S. 2010. Intrinsic controls on the range of volumes, morphologies, and dimensions of submarine lobes. *Sedimentary Geology*, **232**, 66–76.

Prélat, A., Hodgson, D.M. and Flint, S.S. 2009. Evolution, architecture and hierarchy of distributary deep-water deposits: a high-resolution outcrop investigation from the Permian Karoo Basin, South Africa. *Sedimentology*, **56**, 2132–2154.

Prior, D.B., Bornhold, B.D. and Johns, M.W. 1984. Depositional characteristics of a submarine debris flow. *Journal of Geology*, **92**, 707–727.

Rajchel, J. 1990. Lithostratigraphy of the Upper Paleocene and Eocene sediments from the Skole Units. *Zeszyty Naukowe AGH, Geologia*, **48**, 1–112. [In Polish with English summary]

Rajchel, J. and Uchman, A. 1998. Ichnological record of palaeoenvironment in the transgressive Miocene deposits of the Skole Unit in the Dubiecko region (SE Poland). *Przegląd Geologiczny*, **46**, 523–529. [In Polish with English summary]

Reading, H.G. and Richards, M. 1994. Turbidite systems in deep-water basin margins classified by grain size and feeder system. *American Association of Petroleum Ggeologists Bulletin*, **78**, 792–822.

Reineck, H.-E. and Singh, I.B. 1980. Depositional Sedimentary Environments, 549 p. Springer-Verlag; New York.

Ricci Lucchi, F. and Valmori, E. 1980. Basin-wide turbidites in a Miocene, over-supplied deep-sea plain: a geometrical analysis. *Sedimentology*, **27**, 241–270.

Salata, D. and Uchman, A. 2013. Conventional and high-resolution heavy mineral analyses applied to flysch deposits: comparative provenance studies of the Ropianka (Upper Cretaceous–Paleocene) and Menilite (Oligocene) formations (Skole Nappe, Polish Carpathians). *Geological Quarterly*, **57**, 649–664.

Salata, D. 2014a. Advantages and limitations of interpretations of external morphology of detrital zircon: a case study of the Ropianka and Menilite formations (Skole Nappe, Polish Flysch Carpathians). *Annales Societatis Geologorum Poloniae*, **84**, 153–165.

Salata, D. 2014b. Detrital tourmaline as an indicator of source rock lithology: an example from the Ropianka and Menilite formations (Skole Nappe, Polish Flysch Carpathians). *Geological Quarterly*, **58**, 19–30.

Shanmugam, G. 2006. Deep-Water Processes and Facies Models: Implications for Sandstone Petroleum Reservoirs. Handbook of Petroleum Exploration and Production, 5, 475 p. Elsevier; Amsterdam.

Shanmugam, G. 2008. Deep-water bottom currents and their deposits. In: Rebesco, M. and Camerlenghi, A. (Eds), Developments in Sedimentology, Vol. 60, pp. 59–81. Elsevier; London.

Shanmugam, G. 2016a. Submarine fans: A critical retrospective (1950-2015). *Journal of Palaeogeography*, **5**, 2–76.

Shanmugam, G. 2016b. Slides, Slumps, Debris Flows, Turbidity Currents, and Bottom Currents. Reference Module in Earth Systems and Environmental Sciences, 87 p. Elsevier online; https://doi.org/10.1016/B978-0-12-409548-9.04380-3.

Shanmugam, G. 2017. Contourites: Physical oceanography, process sedimentology, and petroleum geology. *Petroleum Exploration and Development*, **44**, 183–216.

Shanmugam, G. and Moiola, R.J. 1991. Types of submarine fan lobes: models and implications. *American Association of Petroleum Geologists Bulletin*, **75**, 156–179.

Stow, D.A.V. and Bowen, A.J. 1978. Origin of lamination in deep sea, fine-grained sediments. *Nature*, **274**, 324–328.

Stow, D.A.V. and Bowen, A.J. 1980. A physical model for the transport and sorting of fine-grained sediment by turbidity currents. *Sedimentology*, **27**, 31–46.

Stow, D.A.V. and Faugères, J.C. 2008. Contourite facies and the facies model. In: Rebesco, M., Camerlenghi, A. and Van Loon, A.J. (Eds), Contourite Research: A Field in Full Development. Developments in Sedimentology Vol. 60, pp. 223–256. Elsevier; London.

Stow, D.A.V. and Mayall, M. 2000. Deep-water sedimentary systems: new models for the 21st century. *Marine and Petroleum Geology*, **17**, 125–135.

Strzeboński, P. 2015. Late Cretaceous–Early Paleogene sandy-to-gravelly debris flows and their sediments in the Silesian Basin of the Alpine Tethys (Western Outer Carpathians, Istebna Formation). *Geological Quarterly*, **59**, 195–214.

Strzeboński, P., Kowal-Kasprzyk, J. and Olszewska, B. 2017. Exotic clasts, debris flow deposits and their significance for reconstruction of the Istebna Formation (Late Cretaceous–Paleocene, Silesian Basin, Outer Carpathians). *Geologica Carpathica*, **68**, 562–582.

Sumner, E.J., Amy, L. and Talling, P.J. 2008. Deposit structure and processes of sand deposition from a decelerating sediment suspension. *Journal of Sedimentary Research*, **78**, 529–547.

Ślączka, A. and Kaminski, M.A. 1998. A guidebook to excursions in the Polish Flysch Carpathians. *Grzybowski Foundation Special Publication*, **6**, 11–71.

Ślączka, A., Renda, P., Cieszkowski, M., Golonka, J. and Nigro, F. 2012. Sedimentary basin evolution and olistolith formation: The case of Carpathian and Sicilian region. *Tectonophysics*, **568–569**, 306–319.

Talling, P.J. 2013. Hybrid submarine flows comprising turbidity current and cohesive debris flow: deposits, theoretical and experimental analyses, and generalized models. *Geosphere*, **9**, 460–488.

Talling, P.J., Masson, D.G., Sumner, E.J. and Malgesini, G. 2012. Subaqueous sediment density flows: Depositional processes and deposit types. *Sedimentology*, **59**, 1937–2003.

Tripsanas, E.K., Piper, D.J.W., Jenner, K.A. and Bryant, W.R. 2008. Submarine mass-transport facies: new perspectives on flow processes from cores on the eastern North American margin. *Sedimentology*, **55**, 97–136.

Uchman, A., Malata, E., Olszewska, B. and Oszczypko, N. 2006. Palaeobathymetry of the Outer Carpathians Basins. In: Oszczypko, N., Uchman, A. and Malata, E. (Eds), Rozwój paleotektoniczny basenów Karpat zewnętrznych, pp. 83–102. Institute of Geological Sciences, Jagiellonian University; Kraków. [In Polish with English abstract]

Walker, R.G. 1984. General introduction: facies, facies sequences and facies models. In: Walker, R.G. (Ed.), Facies Models. *Geoscience Canada Reprint Series*, **1**, 1–9. [2nd ed.]

Wdowiarz, S. 1949. Structure géologique des Karpates marginales au sud-est de Rzeszów. *Biuletyn Państwowego Instytutu Geologicznego*, **11**, 1–39. [In Polish with French summary]

Woiński, J. 1994. Mapa geologiczna Polski, 1:200 000, arkusz Rzeszów. Polska Agencja Ekologiczna; Warszawa. [In Polish]

Wynn, R.B., Kenyon, N.H., Stow, D.A., Masson, D.G. and Weaver, P.P. 2002. Characterization and recognition of deep-water channel-lobe transition zones. *American Association of Petroleum Geologists Bulletin*, **86**, 1441–1462.

Manuscript submitted: 7th April 2018
Revised version accepted: 12th November 2018